SEISMOLOGICAL AND ENGINEERING ASPECTS OF THE 1995 HYOGOKEN-NANBU (KOBE) EARTHQUAKE
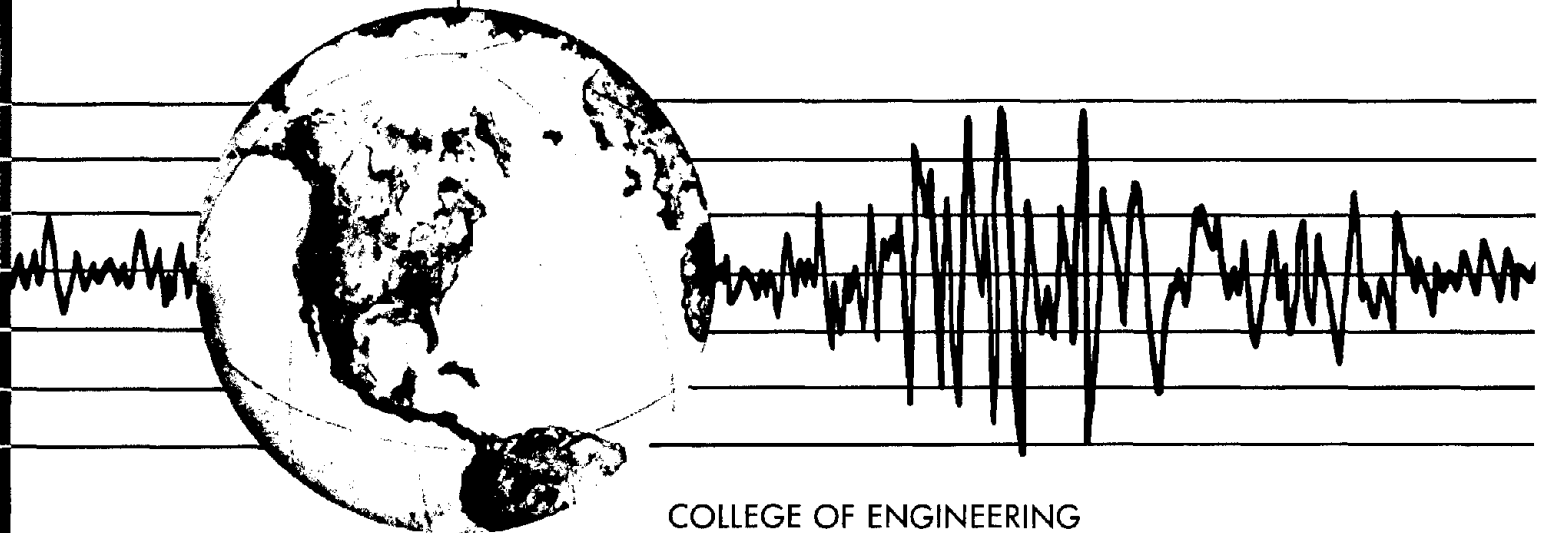
CALIFORNIA UNIV., RICHMOND
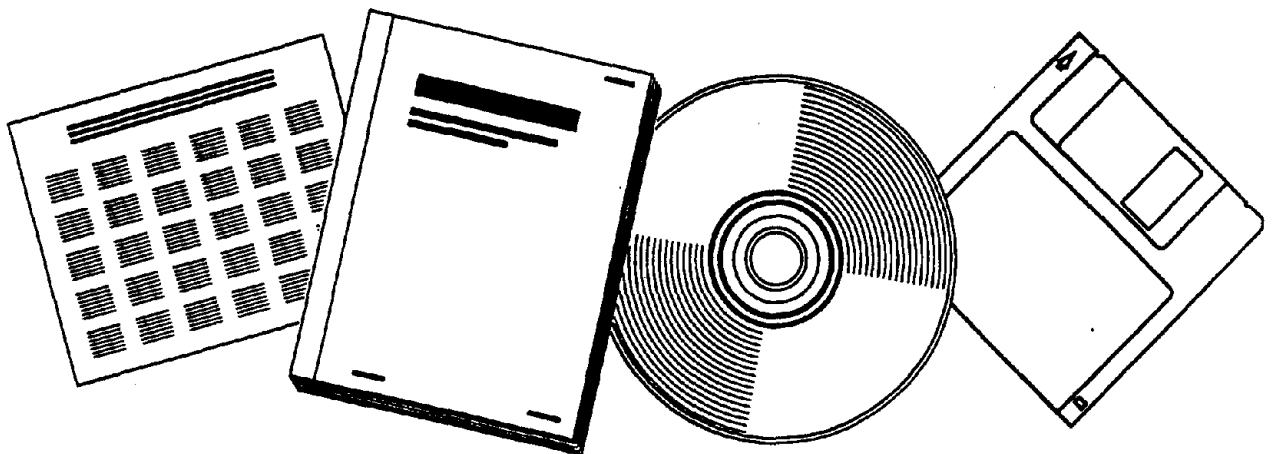
NOV 95

EARTHQUAKE ENGINEERING RESEARCH CENTER

SEISMOLOGICAL AND ENGINEERING ASPECTS OF THE 1995 HYOGOKEN-NANBU (KOBE) EARTHQUAKE

A reconnaissance report by
teams funded by

the National Science Foundation
and the Earthquake Engineering Research Center

COLLEGE OF ENGINEERING

UNIVERSITY OF CALIFORNIA AT BERKELEY

REPORT DOCUMENTATION PAGE

Form Approved
OMB No. 0704-0188

Public reporting burden for this collection of information is estimated to average 1 hour per response, including the time for reviewing instructions, searching existing data sources, gathering and maintaining the data needed, and completing and reviewing the collection of information. Send comments regarding this burden estimate or any other aspect of this collection of information, including suggestions for reducing this burden, to Washington Headquarters Services, Directorate for Information Operations and Reports, 1215 Jefferson 1302, and to the Office of Management and Budget, Paperwork Reduction Project (0704-0188), Washington, DC 20503.

PB97-186050

	2. REPORT DATE November 1995	3. REPORT TYPE AND DATES COVERED Final

4. TITLE AND SUBTITLE Seismological and Engineering Aspects of the 1995 Hyogoken-Nanbu (Kobe) Earthquake	5. FUNDING NUMBERS
6. AUTHOR(S) Vitelmo V. Bertero, et al.	

7. PERFORMING ORGANIZATION NAME(S) AND ADDRESS(ES) Earthquake Engineering Research Center University of California, Berkeley 1301 S. 46th Street Richmond, California 94804	8. PERFORMING ORGANIZATION REPORT NUMBER UCB/EERC-95/10

9. SPONSORING/MONITORING AGENCY NAME(S) AND ADDRESS(ES) National Science Foundation 1800 G. Street, N.W. Washington, D.C. 20550	10. SPONSORING/MONITORING AGENCY REPORT NUMBER

11. SUPPLEMENTARY NOTES

12a. DISTRIBUTION/AVAILABILITY STATEMENT	12b. DISTRIBUTION CODE

13. ABSTRACT (Maximum 200 words)

The Hyogoken-Nanbu earthquake struck the Hyogo prefecture of south-central Japan at 5:46 a.m. local time, Tuesday, 17 January 1995. The Seismographic Stations at the University of California at Berkeley assessed the main event at moment magnitude 6.9. According to current accounts [AIJ; 1995], the earthquake caused 5,415 deaths and over 34,500 injuries.

Immediately following the earthquake, a reconnaissance team was organized under the auspices of Earthquake Hazard Mitigation Program of the Engineering Directorate of the National Science Foundation. The mission of the team was to provide a timely, firsthand overview of the type and extent of the damage, and to provide the necessary background information for future research and for US-Japan cooperation in earthquake engineering. The research team has focused its efforts on seismology, strong ground motion, geotechnical engineering, and structural engineering. The chapters of this report provide summaries of the findings in these subject areas.

14. SUBJECT TERMS	15. NUMBER OF PAGES 250
	16. PRICE CODE

17. SECURITY CLASSIFICATION OF REPORT Unclassified	18. SECURITY CLASSIFICATION OF THIS PAGE Unclassified	19. SECURITY CLASSIFICATION OF ABSTRACT Unclassified	20. LIMITATION OF ABSTRACT

NSN 7540-01-280-5500

Standard Form 298 (Rev 2-89)
Prescribed by ANSI Std Z39-18
298-102

SEISMOLOGICAL AND ENGINEERING ASPECTS OF

THE JANUARY 17, 1995 HYOGOKEN-NANBU (KOBE) EARTHQUAKE

Principal Authors:

Vitelmo V. Bertero - University of California, Berkeley
Roger Borcherdt - U.S. Geological Survey
Peter W. Clark - University of California, Berkeley
Douglas Dreger - University of California, Berkeley
Filip Filippou - University of California, Berkeley
Douglas Foutch - University of Illinois, Urbana-Champaign
Lind Gee - University of California, Berkeley
Masahiko Higashino - Takenaka Corporation
Susuma Kono - University of Illinois, Urbana-Champaign
Le-Wu Lu - Lehigh University
Jack P. Moehle - University of California, Berkeley
Mark Murray - University of California, Berkeley
Julio Ramirez - Purdue University
Barbara Romanowicz - University of California, Berkeley
Nicholas Sitar - University of California, Berkeley
Christopher Thewalt - University of California, Berkeley
Stephen Tobriner - University of California, Berkeley
Andrew Whittaker - University of California, Berkeley
James K. Wight - The University of Michigan, Ann Arbor
Yan Xiao - University of Southern California

Report No. UCB/EERC-95/10

TABLE OF CONTENTS

Page

ACKNOWLEDGMENTS

CHRONOLOGY OF THE RECONNAISSANCE

The extent and nature of damage from the earthquake required that the reconnaissance take place over an extended period of time. The following chronology is an account of the timing of that reconnaissance.

Description	Individuals
25 Jan. - 8 Feb. 1995; Geotechnical engineering reconnaissance	J.D. Bray (UC Berkeley), R.W. Boulanger (UC Davis), J.T. Christian (Boston, MA), W.D. Liam Finn (Univ. of British Columbia), L.F. Harder, Jr. (California Dept. of Water Resources), I.M. Idriss (UC Davis), J.K. Mitchell (Virginia Polytechnic Inst.), Y. Moriwaki (Woodward-Clyde Consultants, Inc.), T.D. O'Rourke (Cornell Univ.), R.B. Seed (UC Berkeley), N. Sitar (UC Berkeley), K. Soga (Cambridge Univ., U.K.), and T.L. Youd (Brigham Young University).
26 Jan. - 2 Feb. 1995; Structural engineering reconnaissance	Douglas Foutch (Univ. of Illinois at Urbana-Champaign), Masahiko Higashino (Takenaka Corporation), Susuma Kono (University of Illinois at Urbana-Champaign), Julio Ramirez (Purdue University), Christopher Thewalt (UC Berkeley), Andrew Whittaker (UC Berkeley), James Wight (University of Michigan at Ann Arbor)
13-18 February 1995; UJNR meeting and reconnaissance.	Roger Borcherdt (USGS), Jack Moehle (UC Berkeley), M.P. Singh (Virginia Polytechnic Institute)
5-12 February 1995; ATC/SEAOC/EERI meeting and study tour with JASCA	Vitelmo Bertero (UC Berkeley), Filip Filippou (UC Berkeley), Stephen Tobriner (UC Berkeley)
24 May - 1 June 1995; 11th UJNR Bridge Research Workshop and Study Tour	Jack Moehle (UC Berkeley)
13-17 March 1995; AIJ report translation and reconnaissance	Mark Aschheim, Peter Clark, and Dawn Lehman (UC Berkeley)
9-15 June 1995; US-Japan Seminar on Reduction of Earthquake Disaster in Urban Areas	George Lee (State University of New York, Buffalo), Stephen Mahin (UC Berkeley), Jack Moehle (UC Berkeley), Mete Sozen (Purdue University), Chia-Ming Uang (UC San Diego), James Wight (U. Michigan at Ann Arbor), and Sharon Wood (University of Illinois).

v

CHAPTER 1

INTRODUCTION

The Hyogoken-Nanbu earthquake[*] struck the Hyogo prefecture of south-central Japan at 5:46 a.m. local time, Tuesday, 17 January 1995. The Seismographic Stations at the University of California at Berkeley assessed the main event at moment magnitude 6.9. According to current accounts [AIJ; 1995], the earthquake caused 5,415 deaths and 34,500 injuries. Over 150,000 houses collapsed or were severely damaged, and over 7,000 houses were burned down in subsequent fires. Current estimates of direct dollar losses are about US$150 billion. This earthquake resulted in the worst natural disaster to strike Japan since the Great Kanto earthquake of 1923. The event paints a grim picture of the potential disastrous effects of a major earthquake striking immediately beneath a modern urban region.

The epicenter of the Hyogoken-Nanbu earthquake was located approximately 5 km southwest of the city of Kobe, Japan, on the northern tip of Awaji island in Osaka Bay. The rupture appears to have comprised a main event followed by two smaller subevents located to the northeast of the epicenter, suggesting a strong component of directivity toward and directly beneath the city of Kobe. Strong ground shaking recordings illustrate effects of source rupture, wave propagation, and local geology. Peak ground accelerations exceeded 0.8g and peak ground velocities exceeded 130 cm/sec. (51 in./sec.).

The strong ground shaking associated with the earthquake caused massive damage on Awaji Island and the southern portion of the Hyogo-ken prefecture, including a major urban region with population of approximately 4 million. Extensive liquefaction of natural and artificial fill deposits caused extensive damage to port facilities and underground utilities. Collapse of more than 80,000 houses, followed by subsequent fires that consumed more than 7000 houses, was a primary cause of deaths [AIJ; 1995]. Between 1000 and 2000 reinforced concrete and steel buildings were severely damaged or collapsed completely [Okada; 1995]. Loss of main highways and rail services due to extensive damage and numerous collapses made transportation nearly impossible, and hampered emergency aid and medium-term recovery. The extent of damage to the built environment, and the long-term economic and social impacts, are as yet not fully known.

Immediately following the earthquake, a reconnaissance team was organized under the auspices of Earthquake Hazard Mitigation Program of the Engineering Directorate of the National Science Foundation. The mission of the team was to provide a timely, first-hand overview of the type and extent of the damage, and to provide the necessary background information for future research and for US-Japan cooperation in earthquake

---

[*] The Hyogoken-Nanbu earthquake of 17 January 1995 is commonly referred to as the Kobe earthquake, and the associated earthquake disaster is commonly referred to as the Great Hanshin-Awaji earthquake disaster. These terms are used interchangeably in this report.

engineering. Additional information was gathered through participation in US-Japan seminars and workshops, and through collaboration with researchers and practicing engineers in Japan. The research team has focused its efforts on seismology, strong ground motion, geotechnical engineering, and structural engineering. The following chapters of this report provide summaries of the findings in these subject areas.

The great Hanshin-Awaji earthquake disaster is one that is virtually unparalleled in modern times. Through study of this disaster, as summarized in this report, we have learned that there are in fact many parallels to similar potential disasters in the United States. Cooperative study of this disaster and its fundamental causes must continue so that the high risk associated with earthquakes in the United States, Japan, and the entire world can be more effectively mitigated.

REFERENCES

[Okada; 1995] Tsuneo Okada, "Codes We Don't Want to Crack," *Look Japan*, June 1995.

[AIJ; 1995] "Preliminary Reconnaissance Report of the 1995 Hyogoken-Nanbu Earthquake (English Edition)," Architectural Institute of Japan, April 1995.

CHAPTER 2

SEISMOLOGIC, GEODETIC AND TECTONIC ASPECTS
OF THE EARTHQUAKE

The purpose of this chapter is to provide an overview of the seismological, geodetic and tectonic observations of the January 17, 1995 Kobe earthquake (referred to in Japan as the "Hyogoken-Nanbu earthquake disaster"). The earthquake struck the port city of Kobe, Japan at 20:46:59.7 UTC, (5:56 local time) and caused approximately 200 billion dollars of damage to residential, commercial, and industrial infrastructure. It is estimated that 5,368 fatalities and 26,815 injuries were sustained, with over 300,000 people left homeless (as of February 17, 1995) [Somerville, 1995]. The geologic environment of this earthquake, particularly the proximity of the causative fault structure to an urban setting, gives this event considerable relevance in evaluating the potential effects of a large urban earthquake in the United States. For example, the type of fault motion, extent of rupture, proximity to urban development, and underlying sedimentary deposits are similar to the relationships of the San Andreas and Hayward-Calaveras faults to the communities of San Francisco Bay Area.

Japan is situated at the intersection of the North American, Pacific, Eurasian and the Philippine plates (Figure 1). As indicated by the "sawteeth" along the plate boundaries, the North American, Pacific, and Philippine plates are being subducted beneath Japan, and a number of large damaging earthquakes have occurred along these tectonic boundaries. The 1944 and 1946 Nankaido M = 8 events, south of Osaka, occurred as a result of subduction of the Philippine plate. Other major interplate events include the 1923 Great Kanto earthquake (Mw = 7.8-7.9) [Wald and Somerville, 1995], which devastated the city of Tokyo, and several large and damaging earthquakes along faults near Hokkaido, the northern island of Japan, since January 1993.

In contrast, the Kobe earthquake was an intraplate event that occurred at relatively shallow depth within the Eurasian plate. The Eurasian plate is highly fractured and several Quaternary faults in the vicinity of Kobe have been identified (Figure 2). A number of large (M · >= 6.9) intraplate events have occurred north-northeast of the Kobe-Osaka region since 1581 (Figure 1), including the 1927 M = 7.75 Tango, 1943 M = 7.4 Tottori, and the 1948 M = 7.3 Fukui earthquakes [Wesnousky et al., 1982; Kanamori, 1972, 1973; Ishikawa, 1971]. Although the Kobe region had not experienced significant local seismicity, the Research Group of Active Faults [1980] identified active faults in the region. Hashimoto and Jackson [1993] analyzed more than a century of geodetic data to study crustal deformation and plate motion in and around the Japanese islands. They estimated that faults along the Arima-Takatsuki Tectonic Line, which extends northeast from the Median Tectonic line through Awaji Island and Kobe to the Hanaore fault, have a slip rate of ~5 mm/yr and that the accumulated seismic moment over the last century along this fault system would be sufficient to produce a M = 7 event.

The epicenter of the Kobe earthquake was located approximately 5 km southwest of the city of Kobe, Japan, on the northern tip of Awaji Island in the Osaka Bay. The focal mechanism obtained by UC Berkeley from long-period surface waves indicates that the ruptured fault was

predominantly strike-slip on either a northwest striking left-lateral or northeast striking right-lateral plane, in agreement with the solutions obtained by Harvard, Caltech and NEIC. The scalar seismic moment was estimated to be 2.8 x 10**26 dyne cm, yielding a Mw = 6.9. The aftershocks delineate the northeast striking, right lateral fault plane, approximately 60 km in length and ranging in depth from 0 to 15 km (Figure 2). Surface rupture was observed on the Nojima fault on the northern tip of Awaji Island, showing 1 to 1.5 m of right-lateral and approximately 1m of vertical displacement [Somerville, 1995]. The mainshock epicenter is approximately 20 km from the southern edge of the aftershock zone, suggesting that the earthquake ruptured bilaterally. However, teleseismic body wave modeling of Kikuchi [1995] reveals a complex rupture history consisting of a primary subevent, located near the mainshock hypocenter, followed by two smaller subevents located to the northeast of the epicenter, suggesting a strong component of directivity toward the city of Kobe. The velocity seismograms recorded in Kobe are characterized by a relatively short duration, large amplitude pulse which is indicative of strong northeastward directivity [Somerville, 1995], and modeling of the strong ground motions in the vicinity of Kobe [Kojiro and Pitarka, 1995] confirm the subevents identified by Kikuchi [1995] and the rupture directivity. In addition to the source effects on the strong ground motions, substantial amplifications due to varied site conditions were observed [Kojiro and Pitarka, 1995]. Observed peak ground velocities were as large as 138 cm/s [Somerville, 1995] and are comparable to values observed in the near-field of recent California earthquakes.

The Kobe earthquake permanently deformed a broad region of the Earth's crust within 200 km of the mainshock epicenter. This deformation was measured at 18 sites using continuously monitoring Global Positioning System (GPS) receivers that had been installed in 1994 by the Geographic Survey Institute (GSI) of Japan as part of a nationwide 200-station geodetic network. Coseismic displacements of these stations (Figure 3) were determined by GSI from daily positions estimated from October 1994 to February 1995. Most of the GPS stations were horizontally displaced by more than 3 mm, and by as much as 35 mm at the stations closest to the fault. None of the stations were close enough to directly measure the 1 to 1.5 m of right-lateral surface offset found on Awaji Island. Although no significant vertical motions were detected by the continuous GPS network, preliminary analysis by GSI of a repeated leveling survey crossing the fault in southern Kobe, and of a synthetic aperture radar (SAR) interferogram of the Kobe region, have detected 10 to 30 cm vertical displacements near the fault.

Assuming simple elastic dislocation theory, the coseismic surface displacements determined by the continuous GPS network can be used to image the fault rupture at depth. We use optimized Monte Carlo techniques to simultaneously estimate the fault location, geometry, and uniform slip at depth [Murray et al., 1995]. The best-fitting fault model has many characteristics that are similar to the seismologic and geologic observations (Figure 3). Slip on the inferred fault, which dips 70 degrees to the northwest, is about 0.9 m right-lateral and 0.5 m thrust, consistent with the surface rupture observed on Awaji Island. The along-strike fault length is 35 km, the down-dip fault width is 15 km, and the fault strike is S45W, in general agreement with the aftershock locations. The fault location suggests that the majority of the slip occurred northeast of the mainshock epicenter, as indicated by the seismic directivity studies. A broad range of models are consistent with this optimal model at 95% confidence. The strike of the fault (S40-50W) and the geodetic moment (1.7-2.6 x 10**26 dyne-cm, Mw = 6.8-6.9) are well determined. However, the dip of the fault, which can vary from 60-85 degrees to the northwest and 40-70 degrees to the southeast, and the fault dimensions, which can vary from 5-

4

60 km in length and 5-30 km in depth, are more poorly resolved. Including additional geodetic observations close to the fault, such as the leveling data and SAR interferograms, should significantly improve the fault rupture model.

In summary, the Kobe earthquake was of moderate to large size and occurred on faults that had been previously identified as being active [Research Group for Active Faults, 1980] and having relatively high geodetic slip rates [Hashimoto and Jackson, 1993]. The ground motions recorded for this event are comparable to those for recent California earthquakes. The tremendous level of damage that was sustained appears to be due primarily to the location of the ruptured fault relative to urban developments. Recent California earthquakes, notably the 1992 Joshua Tree-Landers (Mw = 6.1, 7.3) and the 1994 Northridge (Mw = 6.7), produced comparable ground motions but lower levels of damage. Of these events, the Northridge earthquake was the closest to a heavily populated region; however, the closest point of the fault to the overlying cities was 8 km because the earthquake rupture was confined to depths of 19 to 8 km. In contrast, the Kobe earthquake ruptured through the downtown area of the city. The strong motion data recorded in the vicinity of Kobe reveal a pronounced directivity effect that amplified ground motions due to the focusing of energy radiated from different points on the fault in the direction of a propagating rupture [Kojiro and Pitarka, 1995; Kanamori, 1995; Somerville, 1995]. Large impedance changes in near surface materials were also likely causes of locally elevated ground motions [Kojiro and Pitarka, 1995; Somerville, 1995]. The geologic setting of Kobe, with the proximity of large strike-slip faults to an embayment and sedimentary deposits, is not unlike that of the San Francisco Bay Area. Clearly the data recorded for the Kobe earthquake should factor heavily in the characterization of near-source ground motions in California and in the design of earthquake resistant structures.

REFERENCES

[DeMets et al., 1990] DeMets, C., Gordon, R., Argus, D, and S. Stein, "Current plate motions," *Geophysical Journal International*, 101, 425478, 1990.

[Hashimoto and Jackson, 1993] Hashimoto, M., and D. D. Jackson, Plate tectonics and crustal deformation around the Japanese Islands, *Journ. Geophys. Res.*, 98, 16149-16166, 1993.

[Ishikawa, 1971] Ishikawa, M., "Reanalyses of mechanisms of earthquakes which occurred in and near Japan, and statistical studies on the nodal solutions obtained," *Geophysical Mag.*, 35, 207-274, 1971.

[Kanamori, 1972] Kanamori, H., "Tectonic implications of the 1944 and the 1946 Nankaido Earthquakes," *Phys. Earth Planet Int.*, 5, 129-139, 1972

{Kanamori, 1973] Kanamori, H., "Mode of strain release associated with major earthquakes in Japan," *Ann. Rev. Earth Planet. Sci.*, 1, 213-239, 1973.

[Kanamori, 1995] Kanamori, H., The Kobe (Hyogoken-Nanbu), Japan, Earthquake of January 16, 1995, *Seism. Res. Lett.*, 66, 6-10, 1995.

[Kikuchi, 1995] Kikuchi, M., "The mechanism of the Hyogoken-Nanbu earthquake of January 17, 1995," in Yokohama City University Seismology Report No. 38, 1995.

[Kojiro and Pitarka, 1995] Kojiro, I. and A. Pitarka, "Some aspects of the strong ground motions from the January 17, 1995 Hyogoken-Nanbu Earthquake," SSA annual meeting 1995 special session on the Kobe earthquake, 1995.

[Murray et al., 1995] Murray, M. H., G. A. Marshall, M. Lisowski, and R. S. Stein, "The 1992 M=7 Cape Mendocino, California, earthquake: Coseismic deformation at the south end of the Cascadia megathrust," submitted to *Journ. Geophys. Res.*, 1995.

[Research Group of Active Faults, 1980] Research Group for Active Faults, "The active faults of Japan," University of Tokyo Press, Tokyo, 1-380, 1980.

[Somerville, 1995] Somerville, P., The January 17, 1995 Hyogo-Ken-Nanbu (Kobe) Earthquake: Geoscience and strong ground motion aspects, SSA annual meeting 1995 special session on the Kobe earthquake, 1995.

[Wald and Somerville, 1995] Wald, D. J., and P. G. Somerville, Variable-slip rupture model of the Great 1923 Kanto, Japan, Earthquake: Geodetic and Body-Waveform Analysis, Bull. Seism. Soc. Am., 85, 159177, 1995.

[Wesnousky et al., 1982] Wesnousky, S. G., C. H. Scholz, and K. Shimazaki, Deformation of an island arc: Rates of moment release and crustal shortening in intraplate Japan determined from seismicity and Quaternary fault data, Journ. Geophys. Res., 87, 6829-6852, 1982.

6
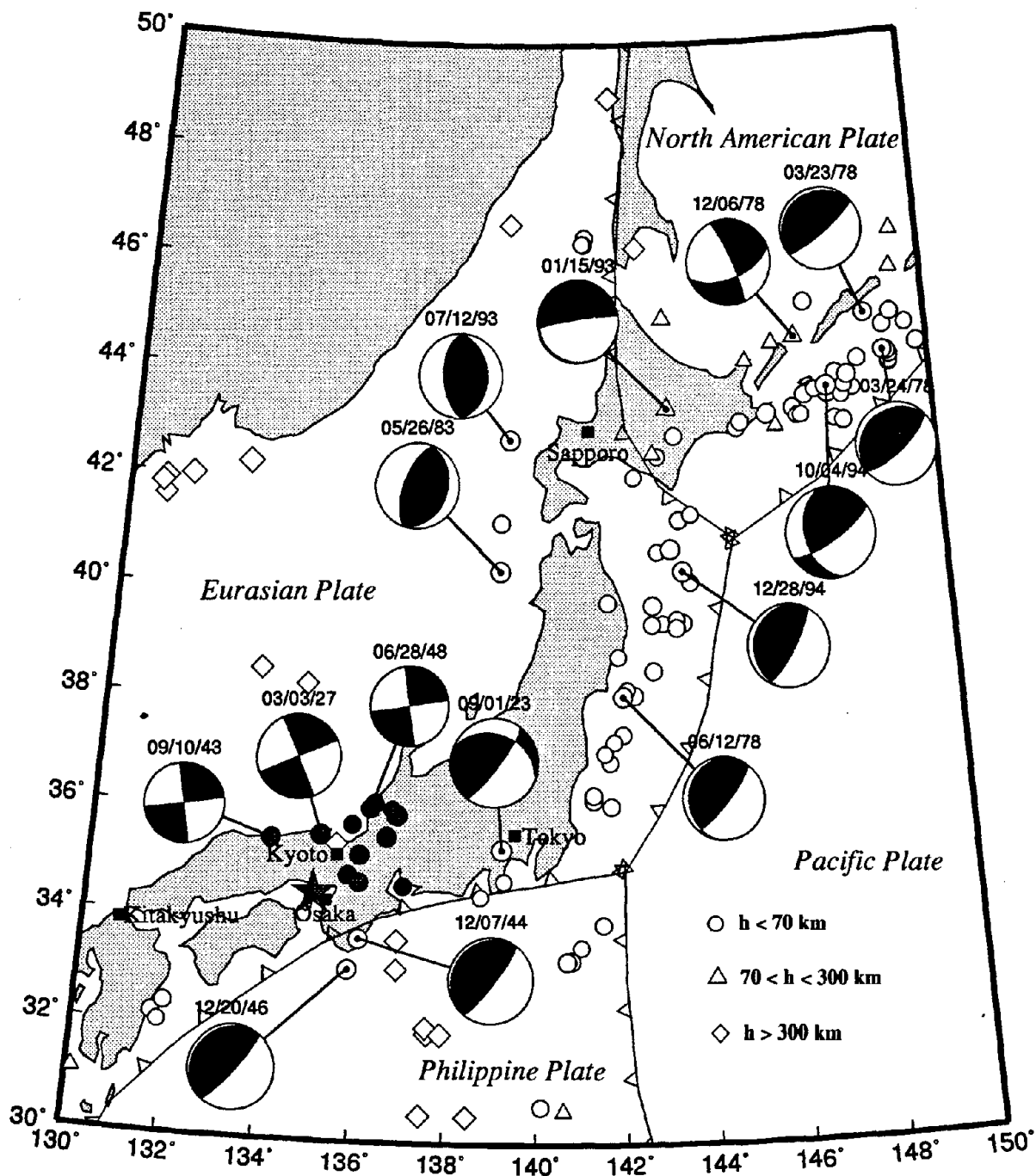
Figure 1: Japanese earthquakes of magnitude 6.5 and larger, with source depth indicated by symbol type. Open symbols are interplate events from 1927-1994; shaded symbols denote intraplate events in the Kobe-Osaka region from 1891-1994 (NEIC; Ishikawa, 1971; Kanamori, 1972, 1973; Wesnousky et al., 1982). Earthquake focal mechanisms for events with moment magnitude greater than 7.5 are displayed from the Harvard centroid moment tensor catalog and from Kanamori (1972, 1973). Boundaries of the four places that converge in Japan from the NUVEL-1 model (DeMets et al., 1990) are plotted with solid lines. The epicenter of the Kobe earthquake is indicated with a star.

7
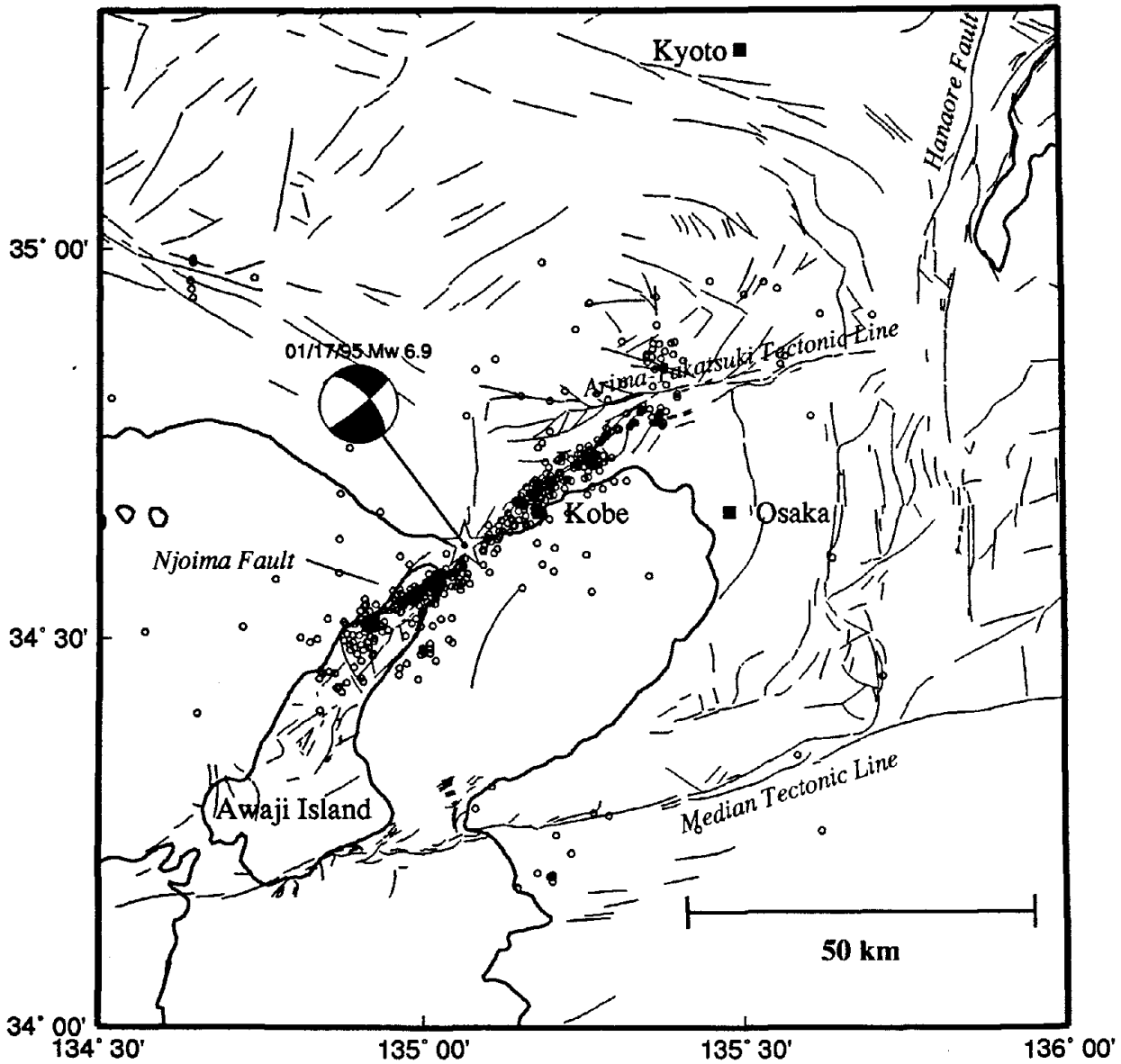
Figure 2: Detailed map of the epicentral region, illustrating the location of the mainshock (star) and aftershocks from the automatic hypocenter location system at the Earthquake Research Institute, University of Tokyo based on data from the seismic networks of the Earthquake Research Institute, the Disaster Prevention Research Unit of Kyoto University, and the Faculty of Science, Kochi University. The focal mechanism obtained at UC Berkeley from the inversion of long-period surface waves indicates a right-lateral strikeslip event.
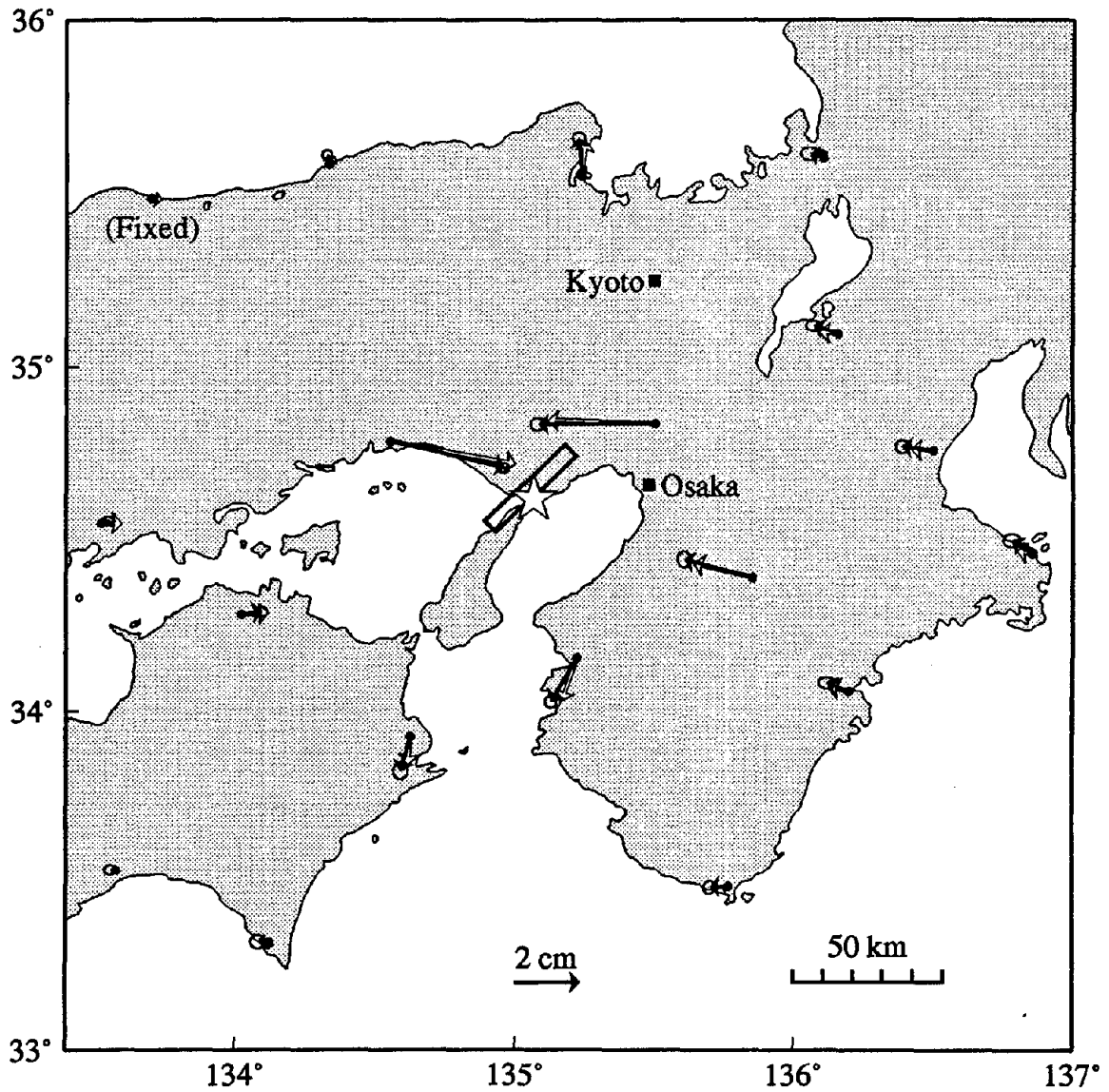
Figure 3: Coseismic displacements of continuous monitoring GPS stations caused by the Kobe earthquake (epicenter at star). Observed horizontal displacements (solid vectors with 95% confidence ellipses) are relative to a fixed station northwest of the epicenter. Predicted displacements (open vectors) are calculated assuming uniform slip occurred on a rectangular fault embedded in an elastic halfspace with a rigidity of 30 GPa. The inferred fault is shown near epicenter, with the southeast edge at the surface and the northwest edge at 15 km depth.

CHAPTER 3

STRONG-GROUND SHAKING GENERATED BY THE EARTHQUAKE

3.1 INTRODUCTION

Understanding the nature of the strong ground shaking radiated by the crustal rupture process is fundamental to understanding the damaging effects of this earthquake and the effects of similar earthquakes in other densely urbanized areas. The strong-motion recordings were obtained with instrumentation installed and maintained by a variety of private, government, and university-affiliated agencies in Japan. Data assimilation and distribution is provided by each agency with coordination provided for some agencies by The National Research Institute for Earth Science and Disaster Prevention of the Science and Technology Agency, Japan. All of the data and results reported here have been derived from preliminary information supplied by the various agencies, the "Prompt Report on Strong Motion Accelerograms No. 46", and principal investigators and colleagues in Japan. A conscious effort has been made to report the results accurately with appropriate credit to the agencies, which made this outstanding data set possible. Any omissions or inaccuracies are not intentional, but some are sure to exist due to language translation difficulties.

This report provides a preliminary summary of the strong-motion data set known to the author as of this writing. Preliminary analyses of the peak acceleration data regarding attenuation and the effects of local geologic deposits are provided. These results are reproduced from Borcherdt (1995).

3.2 STRONG MOTION RECORDINGS

Locations for the strong-motion stations, superimposed upon the geologic map for Japan and the seismicity for a two day interval are shown in Figure 3.1 as reproduced from Wentworth, et al. (1995). A detailed description of the map layers shown in Figure 3.1 is provided by Borcherdt and Wentworth (1995). The geologic map was derived from the digital version of the Geologic Map of Japan (Geological Survey of Japan). The geologic units shown in Figure 3.1 differentiate the Holocene and Pleistocene "soil" units, the Pliocene, Miocene, and Pre-Miocene sedimentary "rock" units, and one generalized unit of igneous and metamorphic "rocks". The boundaries for these units include those that approximately coincide with the boundaries for the site classes with distinct seismic response characteristics proposed for NEHRP code changes (BSSC 1994).

Seismicity for a two-day time period including the occurrence time of the main shock also is shown in Figure 3.1. The location of the main-shock epicenter is that reported in the "Prompt Report on Strong Motion Accelerograms No. 46". The seismicity distribution was derived from aftershock locations reported via ftp by the Earthquake Research Institute, University of Tokyo, Observation Networks of Disaster Prevention Research Institute, Kyoto University, and Faculty of Science, Kochi University. The seismicity suggests a rupture surface about 46 km long extending from about 19 km southwest of the epicenter to about 27 km northeast of the epicenter. The seismicity suggests the rupture zone increases slightly in average depth to the northeast beneath downtown Kobe City. No surface rupture associated with the fault system had been confirmed in Kobe City as of this writing.

Preceding page blank

Coordinates for the strong-motion stations are tabulated in Table 3.1. Coordinates for some stations were provided by the agencies and coordinates for others were inferred from page-sized maps projected to a common scale. The locations inferred from these maps (shown in italics in Table 3.1) are considered least accurate and should be updated, when additional information becomes available. Projection of available maps is expected to have introduced location errors in general less than 100 m; however, other sources of error may have contributed to larger uncertainties for some sites whose coordinates are shown in italics.

The peak amplitudes shown in Figure 1 were measured using different types of instrumentation and reported in different ways by some agencies. Measurements reported by the Committee on Earthquake Research and Observation in the Kansai region were detected with velocity transducers. Peak accelerations reported by the Railway Technical Research Institute (JR publication No. 23a) and Osaka Gas represent the maximum value of the vectorial sum of the two perpendicular horizontal components. Other agencies report the maximum value of the three orthogonal components, while others report the maximum value of only the horizontal components. An effort has been made to tabulate peak horizontal values (PGA in Table 3.1) as reported by the individual agencies. It is not possible at this writing to resolve all of the differences in reported values; however, resolution of these differences as additional information becomes available is needed to reduce uncertainty. These differences should be considered in deriving conclusions from the data.

Station identification, various measures of distance and peak amplitude data, and geologic classifications of the sites are tabulated (Table 3.1). The measurements exceeding full scale at two stations are indicated. Measures of distance shown in Table 3.1 are 1) distance to epicenter (E-Dist), 2) distance to hypocenter (H-Dist), 3) distance to projected rupture surface (Surf-Dis), and 4) distance to seismogenic rupture (SR-Dis; depth below surface, 4 km). Distances to the surface projection of the fault rupture surface were approximated as the closest distance to the straight line implied by the seismicity and determined by endpoints defined by coordinates [34° 29.4`N, 134 53.2E] and [34 45.7N, 135 16.3E].

Acceleration contours, derived from the peak acceleration values tabulated in Table 3.1, are shown in Figure 3.1. The contours were derived from a grid of values interpolated at a spacing of 0.5 km (Wentworth, et al., 1995). The contours are shown with a contour interval of 50 gals. Inadequate station spacing in some areas contributes to generalized grid values and hence generalized contours. The contours suggest a linear zone of intense ground shaking underlain by Holocene soil deposits parallel to the surface projection of the crustal rupture zone. The suggested zone of intense ground shaking includes the zone mapped as JMA intensity 7.

Record sections showing the north-south, east-west, and vertical components of motion as recorded at stations located at increasing distance from the fault are shown in Figure 3.2. These recordings, shown with the same amplitude scale, indicate a well-defined velocity pulse near 1 second period. They suggest that the peak amplitude of ground velocity decreases rapidly within the first few kilometers of the projected surface rupture, with the duration of shaking extending from about 11-15 seconds for a site on Pleistocene deposits (KC-KBU) near the source to more than 60 seconds at several sites on Holocene soil deposits (see e.g. sites KC-FKS, KC-YAE, KC-SAS).

Acceleration, velocity and displacement time histories as derived by Nakamura (1995) for four locations are reproduced in Figures 3.3a through 3,3e. These analyzed versions illustrate effects of source rupture, wave propagation and local geology on the resultant motions. Corresponding response spectra are provided by Nakamura (1995).

Ground motions recorded at the Kobe Ocean Meteorological Station (JM-KBM) within 1 km of the surface projection of the rupture surface are of special note. The peak acceleration amplitude of 818 gal on the north-south component is one of three recording sites near the source region for which motions exceeded 0.8g. The measurements at the JM-KBM site were obtained using accelerometers and 16 bit digital recorders (K. Ohtani, pers. commun., 1995). These recordings were obtained on a concrete pier inside a single story concrete building. The building is located atop a hill with a steeply dipping slope near the building. The station is located near the boundary of Holocene and Pleistocene deposits. Inspection of the site revealed a collapsed brick wall outside the instrument structure, but relatively minor amounts of damage to structures located at the base of the hill. Detailed studies to infer the role of topographic amplification at this site are needed.

Response spectra were provided by the Building Research Institute for several significant earthquake recordings (Figure 3.4a, 3.4b, and 3.4c). They show that the JM-KBM spectra are greater than the other spectra in the period band 0.8 to 2.0 seconds. Comparison of the spectrum with those used for tall building design in Japan (Figure 3.4c) shows that the JM-KBM spectra exceed the design spectra in the period band 0.25 to 2.0 seconds by about a factor of 2 at periods near 1 second. (Note that the El-Centro, Tuft, and Hachinohe earthquake records, all scaled to a peak ground velocity of 50 cm/sec. (Kine) are commonly used for design of tall buildings in Japan.)

Measurements obtained from a three-component vertical borehole array of sensors located on Port Island at a distance of about 4 km from the projected surface rupture are of special importance. They provide measurements of shaking at the ground surface and at depths of 12, 27, and 79 meters. With liquefaction occurring at this site, these measurements provide an exceptionally important data set for inferring the *in-situ* response characteristics of soils at ground-motion levels sufficient to induce failure. Some preliminary observations follow.

Ground motion measurements obtained on the vertical array located on Port Island are shown in Figure 3.5. The simplified geologic log and velocity profiles for the site are shown in Figure 3.6. The site is underlain by about 13 m of fill, which in turn is underlain by at least two thick layers of clay and several layers of interbedded sands and clays. Depth of bedrock at the site is thought to exceed 100 m.

Peak acceleration, velocity and displacement values inferred at the various depths (Figures 3.5a, 3.5b, and 3.5c) reveal several effects of the soil deposits on resultant ground motions. Horizontal motions at the surface above the liquefied layer show a marked reduction in high frequencies, but a significant amplification of low frequency motion. The peak horizontal accelerations increase slightly as they propagate upward toward the bottom of the liquefied layer, but are reduced by factors of 1.7 and 1.9 in the north-south and east-west directions, respectively, upon reaching the surface. Peak horizontal velocities atop the liquefied layer are comparable to those at the bottom of the layer, which are larger than those at depth by factors of 1.7 and 1.3. Peak displacement values inferred at the surface are about 1.5 and 1.9 times larger than corresponding values measured at a depth of 79 m.

Each measure of vertical motion (acceleration, velocity and displacement) is larger at the surface than at depth. The vertical motions probably are predominantly dilatational energy. The various measures of vertical motion are amplified by the liquefied layer by factors of 1.0 for acceleration, 1.9 for velocity, and 1.6 for displacement.

The shear-wave velocity profile shows that the velocity of the near-surface fill, clay, and interbedded sands and clays within the first 30 m of the surface range between 170, 210 and 245m/s, resulting in an average shear velocity to a 30 m depth of 196 m/s. These velocities clearly illustrate that the

13

upper shear-wave velocity limit of 183 m/s as it has currently evolved for consideration in the proposed NEHRP and UBC site definitions should be reinstated at a minimum of 200 m/s as initially proposed (Borcherdt, 1994). Otherwise, soft-soil sites with interlayered sands and clays with a high failure potential, such as this site, will be inappropriately classified.

3.3 ATTENUATION OF GROUND MOTION

Peak horizontal accelerations as reported for the Hyogoken-Nanbu earthquake (Table 3.1) are plotted versus the closest distance to seismogenic rupture approximated to be at a depth of about 4 km beneath Kobe City (Figure 3.7). Peak horizontal accelerations from the Northridge earthquake with a minimum depth to seismogenic rupture of 6 km are superimposed. Also superimposed are attenuation curves developed by Boore et al. (1994) and Campbell and Borzognia (1994).

The peak values for the Hyogoken-Nanbu earthquake tend to be less than those for the Northridge earthquake for sites within 4 to 20 km of the seismogenic source, but greater at distances exceeding about 30 km. These differences in amplitude are roughly consistent with differences in source mechanism and types of geologic site conditions. The source mechanism for the Northridge earthquake is predominantly vertical movement on a thrust fault. Such source mechanisms typically generate higher peak accelerations near the source than comparable sized strike-slip mechanisms. The geologic conditions beneath a majority of the recording sites for the Hyogoken-Nanbu earthquake are soft-soil (Holocene) deposits with higher amplification capabilities for ground motions near one second period than the stiff Pleistocene deposits beneath many of the recording sites for the Northridge earthquake. Consequently, the high frequency motions near the source might be expected to be larger for the Northridge earthquake, but the longer period motions at some distance from the source might be expected to be larger for the Hanshin Awaji earthquake.

The peak acceleration values plotted as linear function of distance (Figure 3.8) emphasize the rapid decrease in peak acceleration values with distance. The recent attenuation curves derived by Boore, et al., 1994 when extrapolated to soft soils using an average shear-wave velocity of 200m/s fit the data quite well. Peak values observed at sites in a ± 22.5 degree window centered along strike with apex at the epicenter are superimposed on those observed in a ± 67.5 degree window centered at the epicenter perpendicular to strike. Similar trends in each data set suggests that a significant directivity effect is not apparent in these two samples of peak acceleration values. However, a similar comparison of peak velocity values reflecting the mid-period characteristics of the ground motion might be expected to yield a different result.

Comparison of the peak vertical acceleration recorded at each of the sites with the peak horizontal (Figure 3.9) shows that on the average the peak vertical accelerations are about 62% or 2/3 of the corresponding horizontal values. Peak vertical accelerations that exceed the peak horizontal values are most evident for sites near or on Port Island (MC-PRI, MC-PIA). These larger vertical accelerations are consistent with larger amplification factors observed for vertical motion above the liquefied layer on the Port Island array.

3.4 AMPLIFICATION EFFECTS OF SOFT-SOIL DEPOSITS

The geologic classification of the sites shown in Table 3.1 provides a basis for a preliminary evaluation of the effect of local site conditions on recorded peak accelerations. The geologic classification was inferred from superposition of the strong-motion station coordinates on the 1:1,000,000 scale geologic

14

map of Japan. The resultant classification is dependent on both the accuracy of the station coordinates and the published map scale. Consequently, the geologic classification for sites inferred from map projections and associated results must be regarded as preliminary.

Site-specific amplification factors were computed for each site by normalizing the peak values by corresponding peak values observed at the nearest station on rock or firm alluvium at seismogenic-rupture distances (SR-Dis, Table 3.1) of about 4, 25, 50 and 75 km in 45 degree azimuthal windows centered along strike of the fault with apex at the epicenter. The amplification factors also are normalized by the reciprocal ratio of the seismogenic-rupture distances for each site. Sites for normalization were chosen from those for which coordinates had been provided by owner agencies. If chosen normalization sites were not on rock (SC-Ib, Borcherdt, 1994), then corresponding average amplification factors were used to adjust resultant amplifications to rock.

The mean and standard deviation for amplification factors inferred for Holocene sites in the azimuthal window of 45 degrees centered along strike are 1.8 and 1.5, respectively. Corresponding values inferred for the azimuthal window of ± 67.5 degrees perpendicular to strike are 1.7 and 1.5. The Holocene sites are thought to be categorized as soft-soil sites as defined by Borcherdt, 1994, that is the sites are classified as SC-IV or as D sites as initially proposed for the NEHRP code revisions (BSSC, 1994). The preliminary 1.8 value is slightly smaller than the 2.0 value for SC-IV sites as initially inferred from the Loma Prieta strong-motion for input ground motion levels near 0.1g (Borcherdt and Glassmoyer, 1992).

As a preliminary attempt to quantify the response characteristics of the Holocene deposits at high input ground motion levels near the source, amplification ratios were computed with respect to the Shin-Kobe site (JR-SNK) for which a peak acceleration of 0.57 g was recorded at a distance of about 0.8 km from the surface projection of the crustal rupture zone. The geologic map and site coordinates imply that the site is underlain by geologic unit QP3 (gravels, sands, and clays of Late Pleistocene age). The amplification ratios, normalized by the reciprocal ratio of the seismogenic-rupture distance, are plotted for sites along strike at distances less than 22 km (Figure 3.10). The mean and standard deviation for the amplification factors are 2.0 and 1.1, respectively. The linear trend fit to the data do not show a tendency to decrease with increasing peak acceleration level. Liquefaction induced ground failure is known to have reduced the amplification at only the Port Island vertical array station. These preliminary observations suggest that the amplification factors for these Holocene sites do not decrease with increasing peak amplitude. Confirmation of this important result with further analyses would suggest that amplification factors currently being suggested for the NEHRP and UBC code revisions should be modified so as to reduce the influence of nonlinearity on site factors at sites for which the potential for ground failure is low.

3.5 SUMMARY

The strong ground motion measurements of the Hyogoken-Nanbu earthquake provide an important new near-source strong-motion data set. The data set provides an unprecedented set of measurements on soft soils at high input ground motion levels near the causative crustal rupture. Horizontal ground acceleration exceeded 500 gal at ten sites and 800 gal at two sites near the surface projection crustal rupture zone. Measurements at ten other sites within distances of 20 km were between 200 and 500 gal. About sixty percent of the measurements are located on "soft-soil" deposits of Holocene age. These deposits are comprised of interbedded sand, clay, and gravel layers, with a majority of the interval shear-wave velocities for the deposits between about 100 and 350 m/s (Iwasaki, et al., 1991).

Acceleration contours for the higher levels of motion (>400 gal) show a linear southwest-northeast trend roughly parallel to and inclusive of the surface projection of the crustal rupture zone. Preliminary compilations of the peak acceleration data suggest that the peak levels decrease rapidly with increasing distance from the surface projection of the implied fault rupture. This rapid attenuation, is apparent on plots of peak acceleration with distance compiled with linear scales and the generalized acceleration contours. This attenuation rate is anticipated well by recently derived empirical attenuation curves for peak acceleration extrapolated to sites with mean shear velocity of 200 m/s (Boore, et al., 1995). Input ground motion levels of 0.3 to 0.4g implied by the recording at KC-KBU are less than 0.5 to 0.6 g inferred for the Northridge, CA earthquake of January 17,1994 (Borcherdt, 1994). This difference is consistent with ground motion variations that might be expected for differences in source mechanisms for the two earthquakes, namely, strike-slip versus thrust.

Preliminary amplification factors derived for the Hyogoken-Nanbu earthquake are in general agreement with those derived from the Loma Prieta earthquake. This agreement suggests that site amplification and proximity to the crustal rupture zone contributed to the high levels of ground acceleration measured at sites near the source. The area of most intense motion as indicated by generalized acceleration contours for levels greater than 400 gal includes the zones of most intense damage mapped with JMA intensity level 7. This correspondence emphasizes the severity of the ground motion observed on soft soil near the surface projection of the fault rupture. These high levels of shaking confirm the significance of "near-source" factors currently being considered for U.S. building codes and the need to evaluate *in-situ* amplification factors at high input ground-motion levels.

3.6 ACKNOWLEDGMENTS

REFERENCES

[Boore, et al., 1994] Boore, D.M., Joyner, W.B., and Fumal, T., 1994, Estimates of response spectra and peak accelerations from western North American earthquakes; an interim report part 2 (with insert), *U. S. Geological Survey Open File Report 94-127*, 1994, 39 pp.

[Borcherdt, 1994a] Borcherdt, R.D., "Simplified site classes and empirical amplification factors for site-dependent code provisions," *Proceedings*, NCEER, SEAOC, BSSC workshop on site response during earthquakes and seismic code provisions, University of Southern California, Los Angeles, California, November 18 - 20, 1992, publ. 1994.

[Borcherdt, 1994b] Borcherdt, R.D., "Estimates of site-dependent response spectra for design (Methodology and Justification)," *Earthquake Spectra*, **10**, 1994, pp. 617-653.

[Borcherdt, 1995] Borcherdt, R.D., "Seismology, geology, and geotechnical issues," National Institute of Science and Technology, U. S. Geological Survey, Reports, 1995, *in preparation*.

[Borcherdt and Wentworth, 1995] Borcherdt, R. D. and Wentworth, C.W., "Preliminary map of peak horizontal ground acceleration for the Hyogoken-Nanbu earthquake of January 17,1995," Japan, Part II of 2 - Description of mapped data sets, *U. S. Geological Survey Open File Report No. ____, 1995, ____ pp.

[Borcherdt and Glassmoyer, 1992] Borcherdt, R.D., and Glassmoyer, G., "On the characteristics of local geology and their influence on ground motions generated by the Loma Prieta earthquake in the San Francisco Bay region, California," *Bulletin of the Seismological Society of America*, 82, 1992, pp. 603-641.

[Borcherdt and Glassmoyer, 1993] Borcherdt, R.D. and Glassmoyer, G., "Influences of local geology on strong and weak ground motions in the San Francisco Bay region, California and their implications for site-specific code provisions, in The Loma Prieta earthquake of October 17, 1989 — strong ground motion," R. D. Borcherdt, ed., *U.S. Geological Survey Professional Paper 1551-A*, 1993, 655 pp.

[Campbell and Borzognia, 1994] Campbell, K. W. and Bosorgnia, Y., "Near-source attenuation of peak acceleration from worldwide accelerograms recorded from 1957 to 1993," *Proceedings*, Fifth U.S. National Conference on Earthquake Engineering, Chicago Illinois, 1994.

[Comartin, Greene, and Tubbesing, 1995] Comartin, C.D., Greene, M, and Tubbesing, S.K., eds., "The Hyogoken-Nanbu earthquake great Hanshin earthquake disaster January 17, 1995," Preliminary Reconnaissance Report 95-04, Earthquake Engineering Research Institute, 1995, 116 pp.

[Geological Survey of Japan] Geological Survey of Japan, *Geological Map of Japan*, CD-ROM Version, Third Edition, CD-ROM series of Earth Science Databases, CDGSJ92010, 1992, Map Scale 1:1,000,000.

[JR publication No. 23a] Maximum accelerations observed by JR, *JR Earthquake Information No. 23a*, Internet.

[Kikuchi, 1995] Kikuchi, M., "The Mechanism of the Hyogoken-Nanbu earthquake of January 17,1995," in YCU (Yokohama City University) Seismology Report No. 38, 1995.

[Kuribashi, 1995] Kuribashi, E., "The Japan's earthquake in Kobe of January 17,1995, The Hyogoken-Nanbu earthquake, a reconnaissance report," Toyohashi University of Technology, 1995, Research Report No. 95-1.

[Nakakita and Watanabe, 1977] Nakakita, U., and Watanabe, Y., "Soil stabilization by preloading in Kobe Port Island," in *Proceedings*, 9th International Conference on Soil Mechanics and Foundation Engineering, Tokyo, Case History Volume, 1977, pp. 611-622.

[Nakamura, 1995] Nakamura, Y., "Waveform and its analysis of the 1995 Hyogoken-Nanbu earthquake," *JR Earthquake Information No. 23c*, 1995, 46 pp.

[Nakamura, et al., 1995] Nakamura, Y., Kazutoshi, H., Saita, J., and Sato, S., "Strong Accelerations and damage of the 1995 Hyogoken-Nanbu earthquake," *JR Earthquake Information No. 23b*, 1995, 25 pp.

[NEHRP, 1991] NEHRP Recommended Provisions for the Development of Seismic Regulations for New Buildings, 1991 edition, Prepared by Building Seismic Safety Council for Federal Emergency Management Agency, Washington D.C., vol. I, 199 pp.

[Oka, et al., 1995] Oka, F., Sugito, M., Yashima, A., and Bardet, J.P., "The Great Hanshin Earthquake Disaster (The 1995 South Hyogo Prefecture Earthquake)," Preliminary Investigation Report, Gifu University, Gifu, Japan, 1995, 71 pp.

[Prompt report on strong-motion accelerograms No. 46, 1995] Prompt report on strong-motion accelerograms No. 46, The National Research Institute for Earth Science and Disaster Prevention, Science and Technology Agency, 1995, 42 pp.

[Wentworth, et al., 1995] Wentworth, C.W., Borcherdt, R. D., and Mark, R., "Preliminary map of peak horizontal ground acceleration for the Hyogoken-Nanbu earthquake of January 17,1995," Japan, Part I of 2, *U. S. Geological Survey Open File Report No. ____, 1995, ___ pp.*
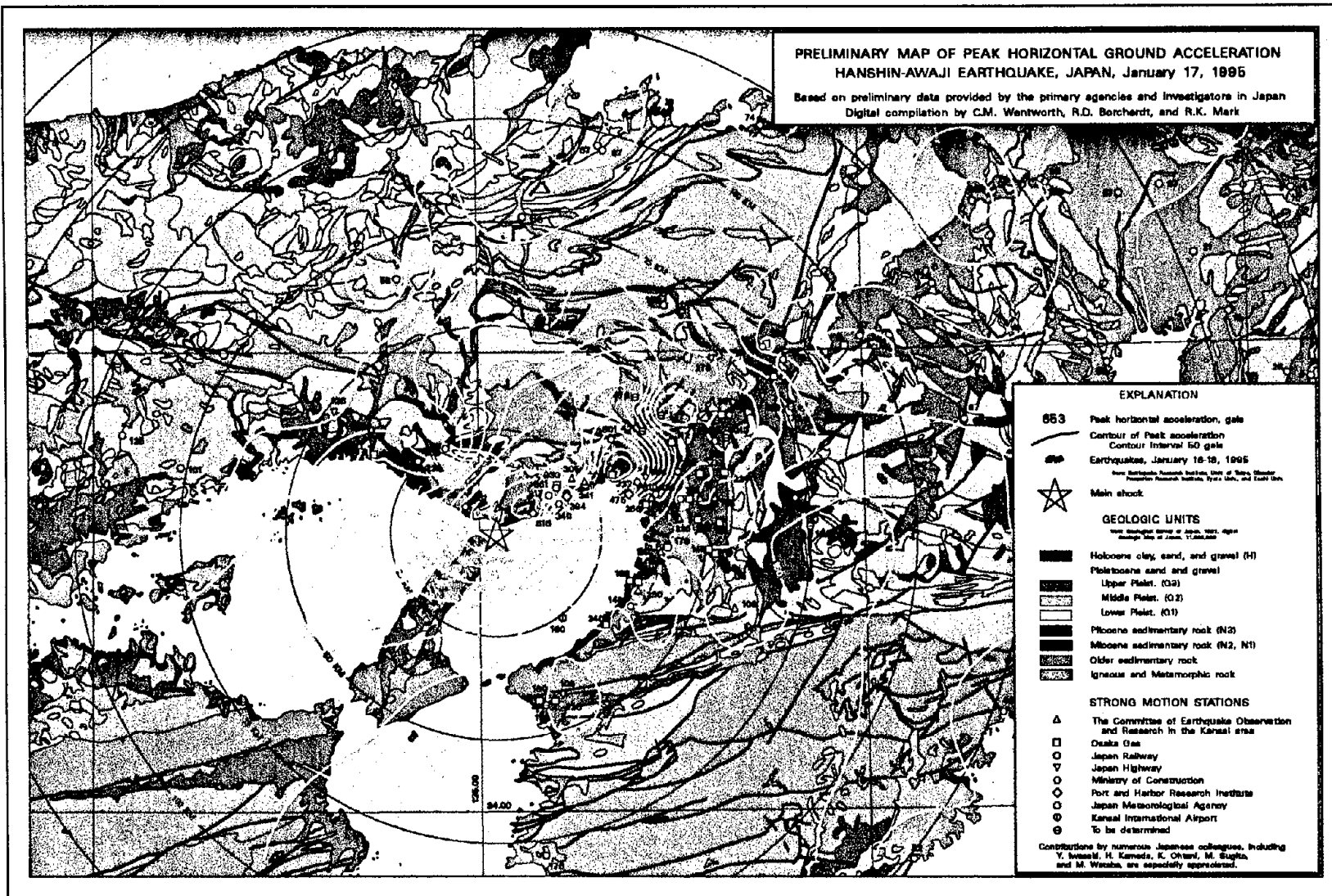
Figure 3.1 Preliminary map showing geologic units, strong-motion stations, peak horizontal acceleration, and approximate contours of acceleration (from Geologic map of Japan, scale 1:1,000,000, CD-ROM; Strong motion information courtesy of agencies and colleagues indicated).

NS

TIME (sec.)

| | 0.00 | 25.00 | 50.00 | 75.00 | 100.00 |

KOBE-UNIV — 55.109 (cm/s)

KOBE — 40.000 (cm/s)

AMAGASAKI — 40.000 (cm/s)

FUKUSHIMA — 30.981 (cm/s)

MORIGAWACHI — 27.056 (cm/s)

YAE — 21.207 (cm/s)

SAKAI — 15.865 (cm/s)

TADAOKA — 24.437 (cm/s)

CHIHAYA — 5.182 (cm/s)

ABENO — 21.370 (cm/s)
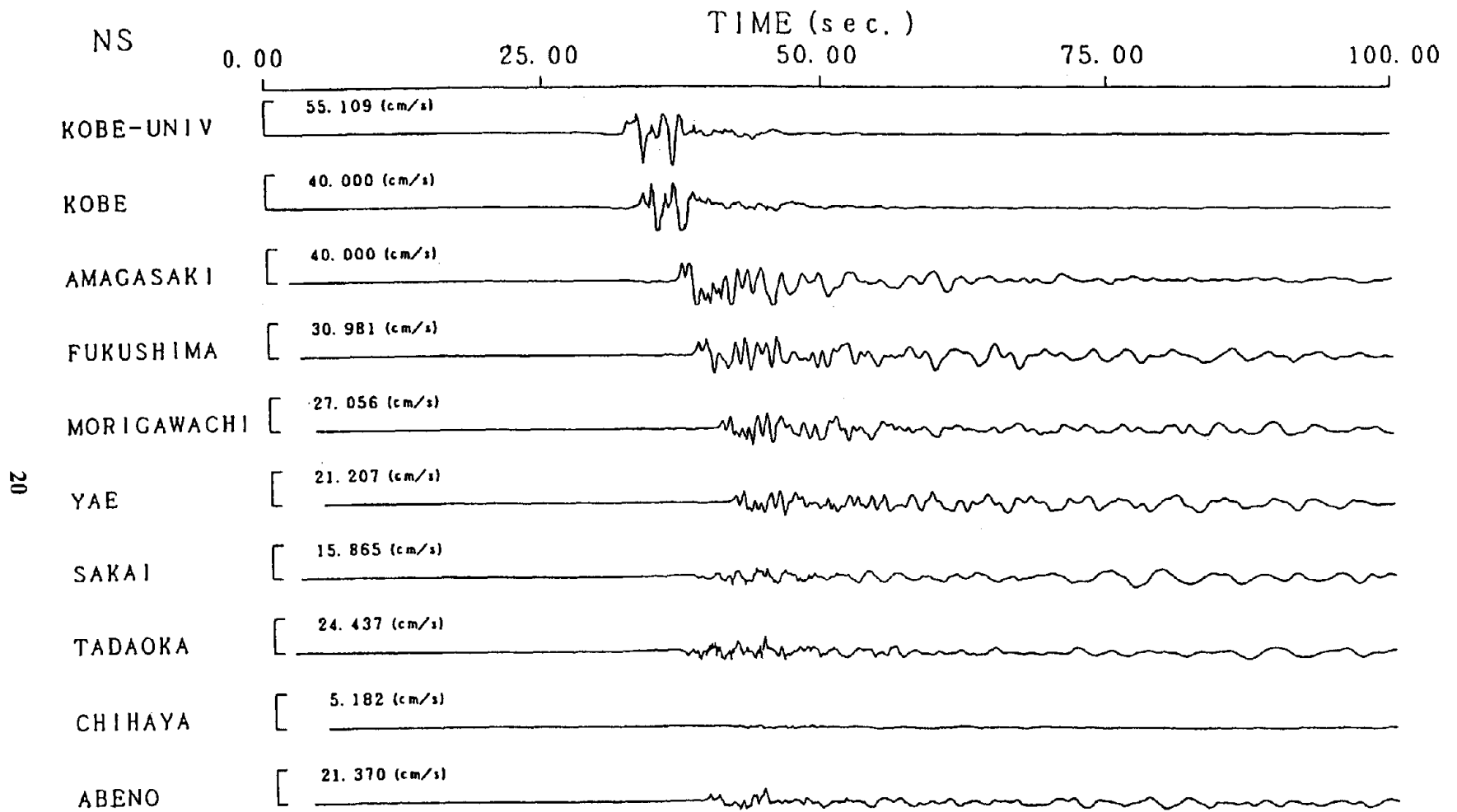
(a)

Figure 3.2a Record section showing ground velocity in the NS (a), EW (b), and UD (c) directions (from The Committee on Earthquake Observation and Research in the Kansai Area, CEORKA).

EW

TIME (sec.)

0.00   25.00   50.00   75.00   100.00

KOBE-UNIV   31.042 (cm/s)

KOBE   40.000 (cm/s)

AMAGASAKI   40.000 (cm/s)

FUKUSHIMA   29.811 (cm/s)

MORIGAWACHI 24.673 (cm/s)

YAE   21.817 (cm/s)

SAKAI   15.664 (cm/s)

TADAOKA   14.713 (cm/s)

CHIHAYA   4.861 (cm/s)

ABENO   24.889 (cm/s)

(b)

Figure 3.2b

21

UD

TIME (sec.)

0.00   25.00   50.00   75.00   100.00

KOBE-UNIV   33.173 (cm/s)

KOBE   40.000 (cm/s)

AMAGASAKI   26.095 (cm/s)

FUKUSHIMA   9.607 (cm/s)

MORIGAWACHI   6.106 (cm/s)

YAE   6.979 (cm/s)

SAKAI   6.597 (cm/s)

TADAOKA   5.923 (cm/s)

CHIHAYA   2.466 (cm/s)

ABENO   6.277 (cm/s)
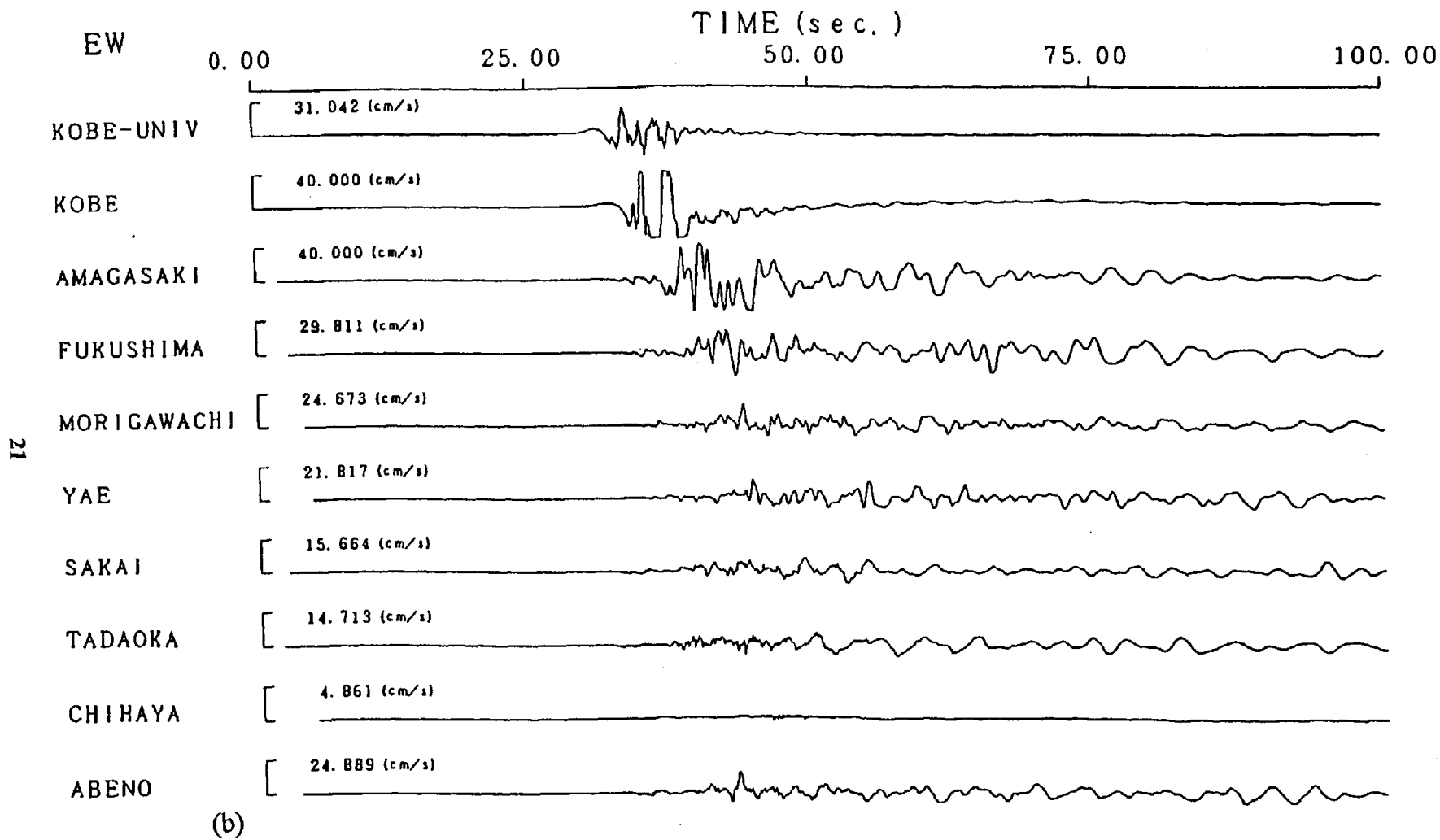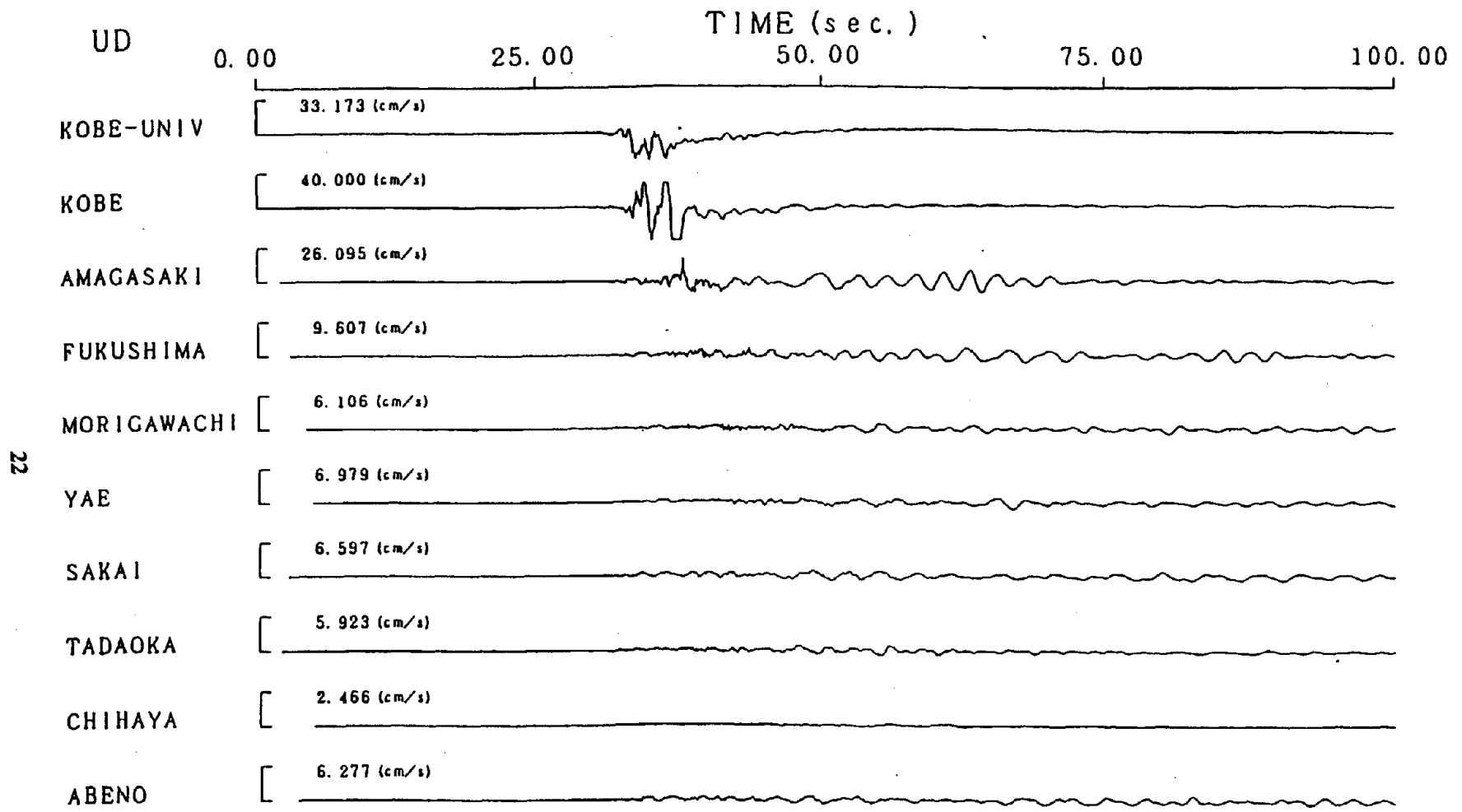
(c)
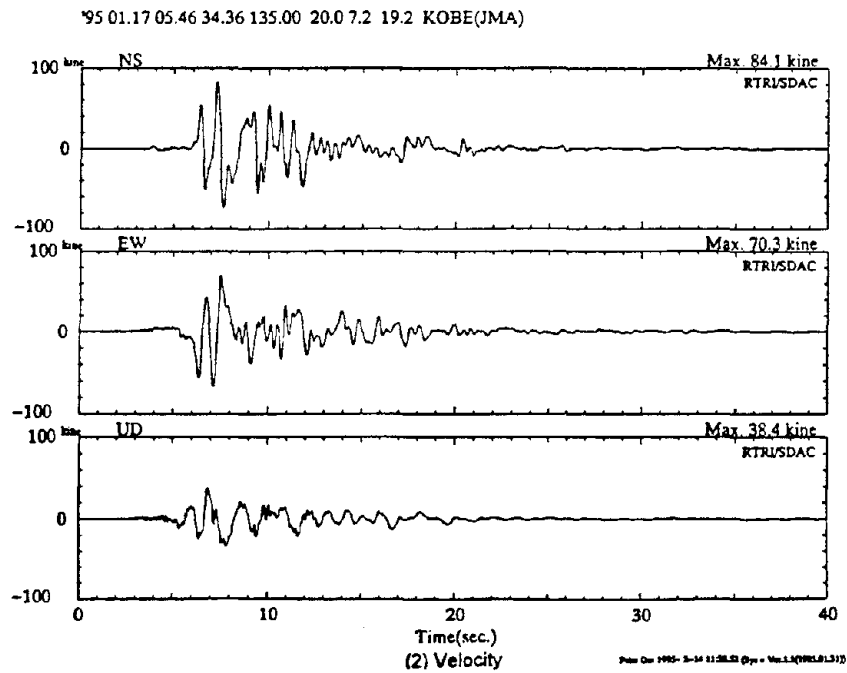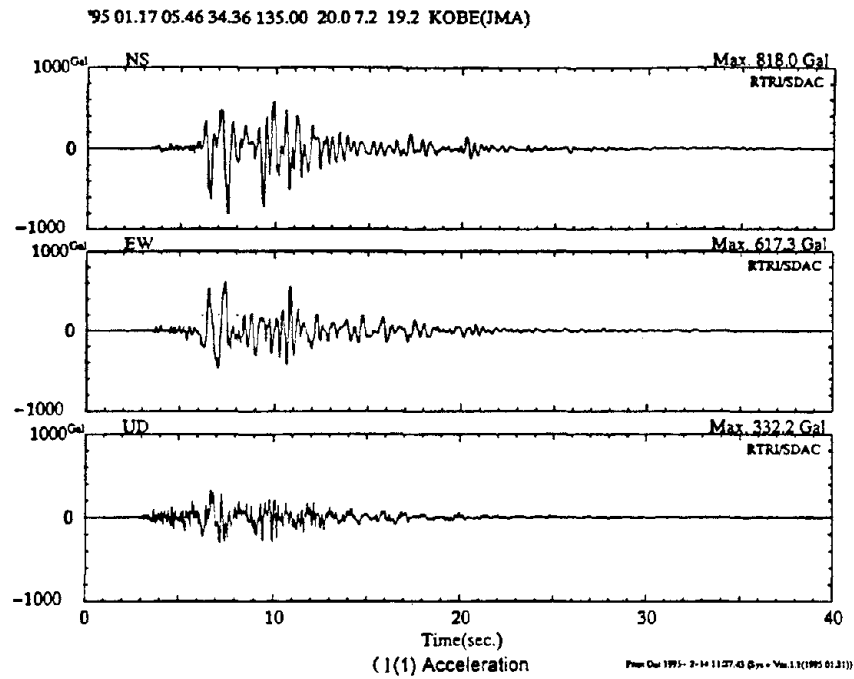
Figure 3.2c

Figure 3.3 Three-component (1) acceleration, (2) velocity, (3) displacement, and (4) displacement loci inferred by Nakamura (1995) from strong-motion recordings at site (a) Kobe Marine (JM-KBM), (b) Takatori (JR-TKT), (c) Takarazuka (JR-TKD), and (d) Nishi-Akashi (JR-NSA).

'95 01.17 05.46 34.36 135.00 20.0 7.2 19.2 KOBE(JMA)

(3) Displacement

(4) Loci of Displacement

(UNIT: cm)

神 戸 (JMA)
KOBE

Figure 3.3a continued

'95 01.17 05.46 34.36 135.00 20.0 7.2 13.8 TAKATORI

(1) Acceleration

'95 01.17 05.46 34.36 135.00 20.0 7.2 13.8 TAKATORI

(2) Velocity

Figure 3.3b

25
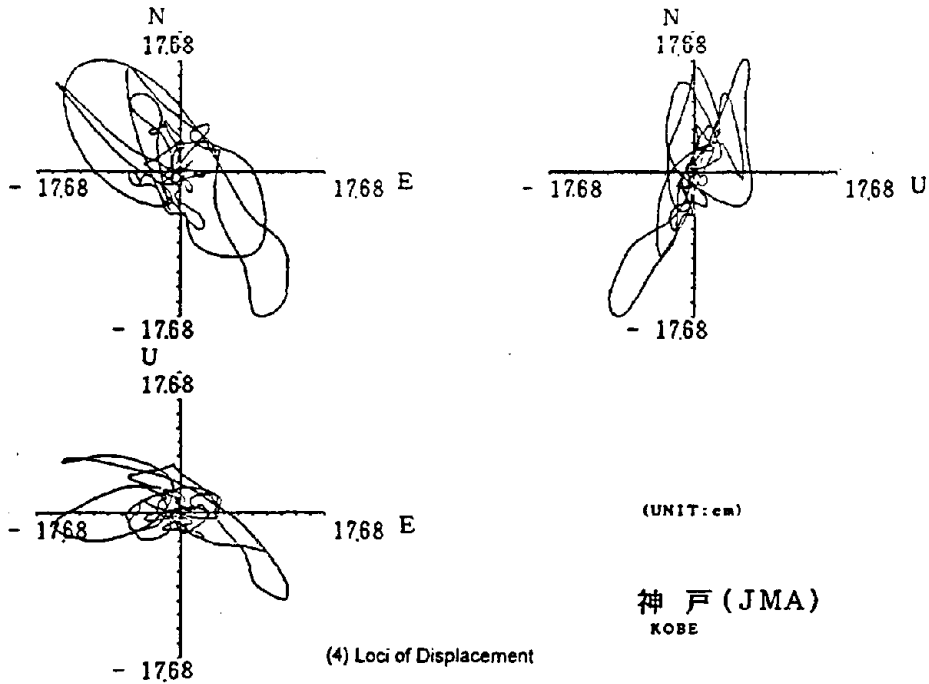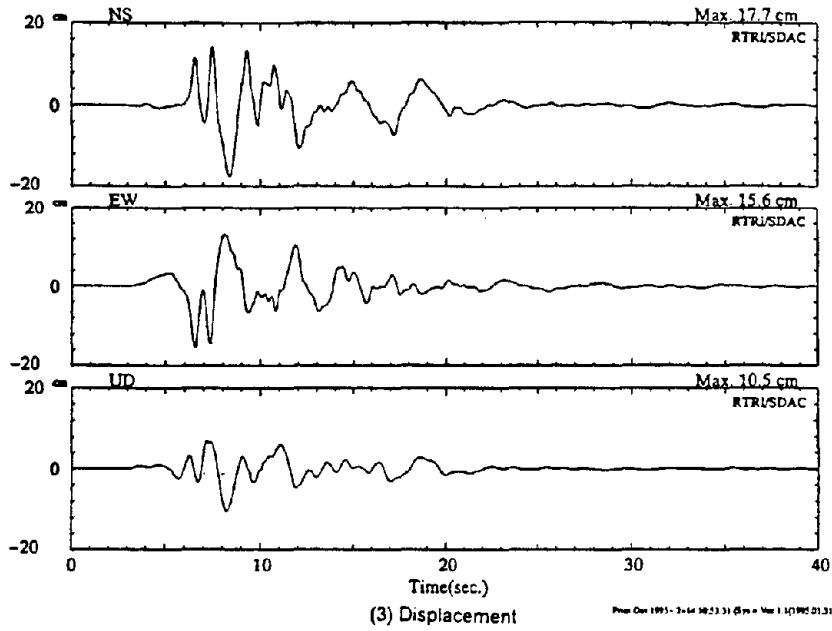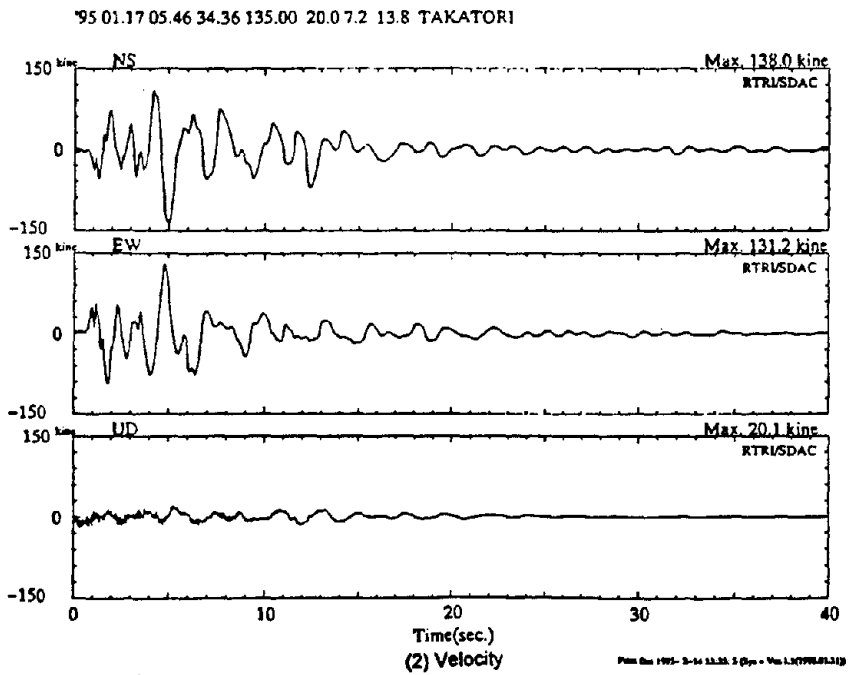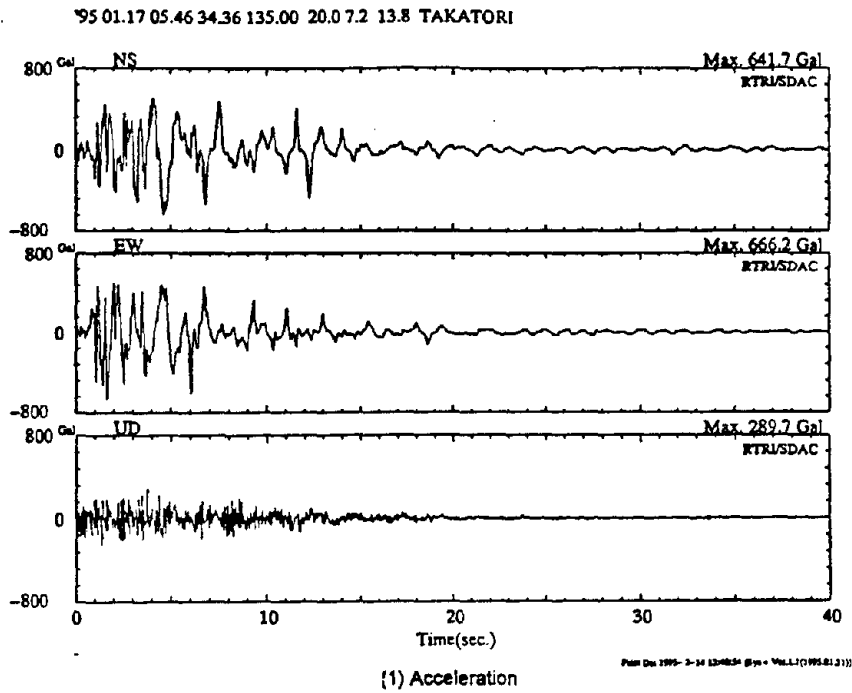
'95 01.17 05.46 34.36 135.00 20.0 7.2 13.8 TAKATORI

(3) Displacement

(4) Loci of Displacement

(UNIT : cm)

震 取
TAKATORI

Figure 3.3b continued

'95 01.17 05.46 34.36 135.00 20.0 7.2 39.2 TAKARAZUKA
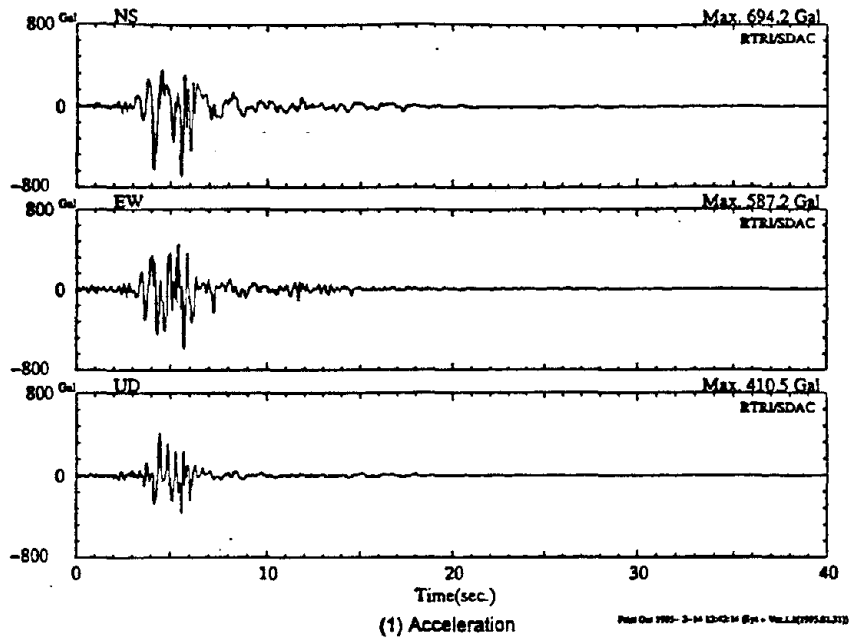
(1) Acceleration

'95 01.17 05.46 34.36 135.00 20.0 7.2 39.2 TAKARAZUKA

(2) Velocity

Figure 3.3c

27

'95 01.17 05.46 34.36 135.00 20.0 7.2 39.2 TAKARAZUKA

NS   Max. 24.6 cm
RTRI/SDAC

30

0

-30

EW   Max. 26.5 cm
RTRI/SDAC

30

0

-30

UD   Max. 12.5 cm
RTRI/SDAC

30

0

-30

0   10   20   30   40

Time(sec.)

(3) Displacement

N
26.52

- 26.52   26.52   E

- 26.52

N
26.52

- 26.52   26.52   U

- 26.52

U
26.52

- 26.52   26.52   E

- 26.52

(UNIT:cm)

宝 塚
TAKARAZUKA
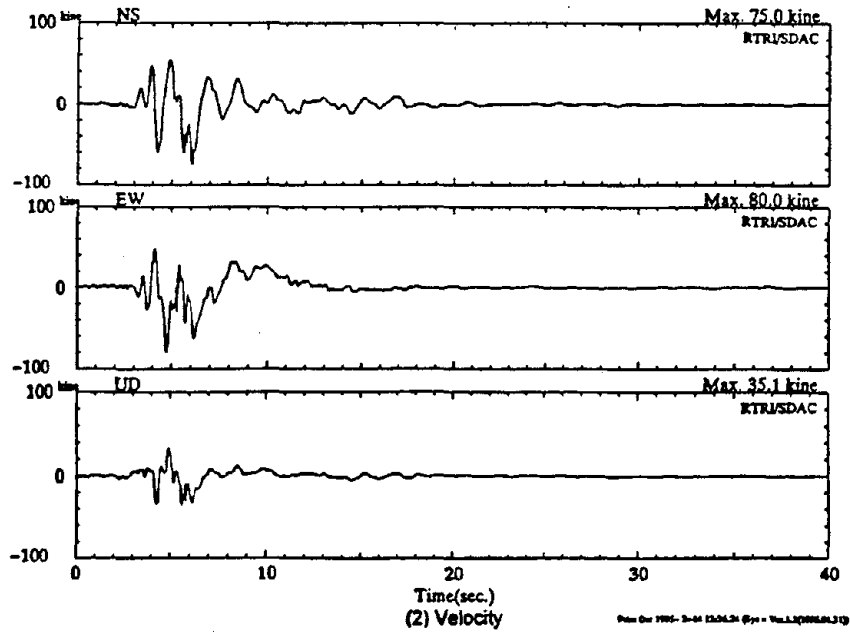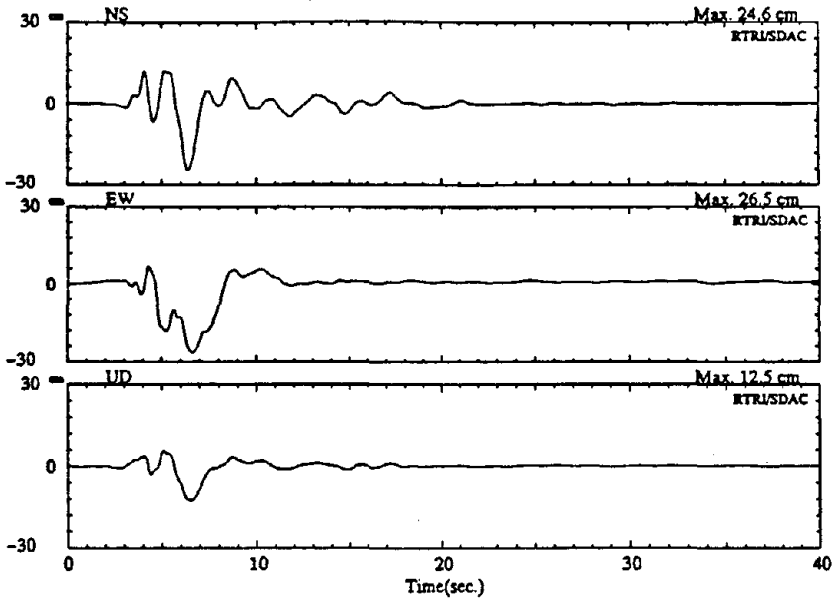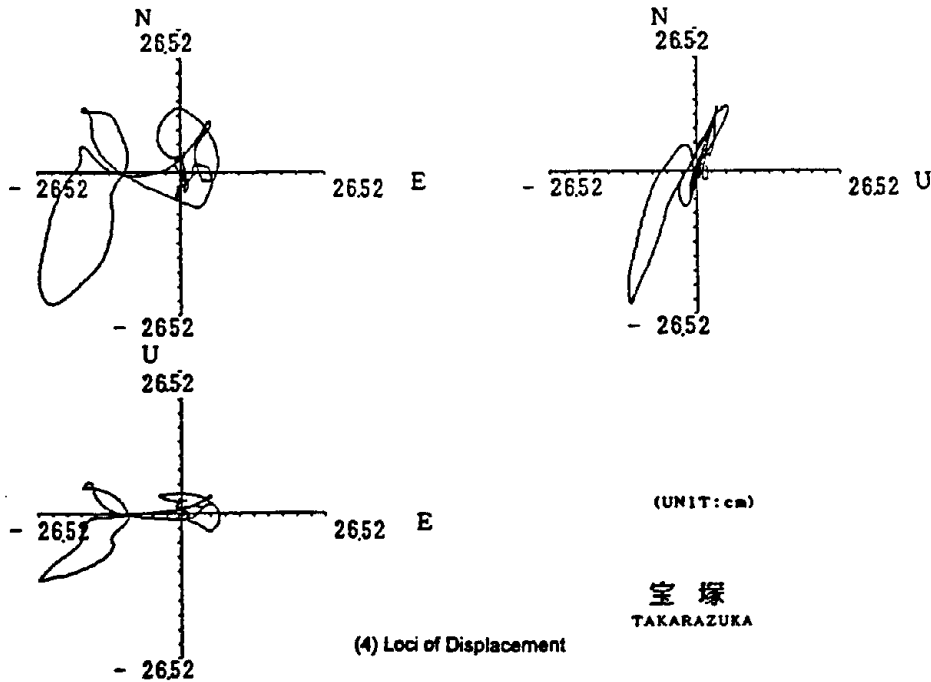
(4) Loci of Displacement

Figure 3c continued

28

'95 01.17 05.46 34.36 135.00 20.0 7.2 8.0 NISHI-AKASHI

NS   Max. 397.3 Gal
                                                                 RTRI/SDAC

EW   Max. 381.5 Gal
                                                                 RTRI/SDAC

UD   Max. 318.9 Gal
                                                                 RTRI/SDAC

Time(sec.)

Figure 3.3c continued   (1) Acceleration

'95 01.17 05.46 34.36 135.00 20.0 7.2 8.0 NISHI-AKASHI

NS   Max. 39.2 kine
                                                                 RTRI/SDAC

EW   Max. 33.7 kine
                                                                 RTRI/SDAC

UD   Max. 18.0 kine
                                                                 RTRI/SDAC

Time(sec.)

(2) Velocity

Figure 3.3d

(3) Displacement

(4) Loci of Displacement

(UNIT:cm)

西 明 石
NISHI-KASHI

Figure 3.3d continued
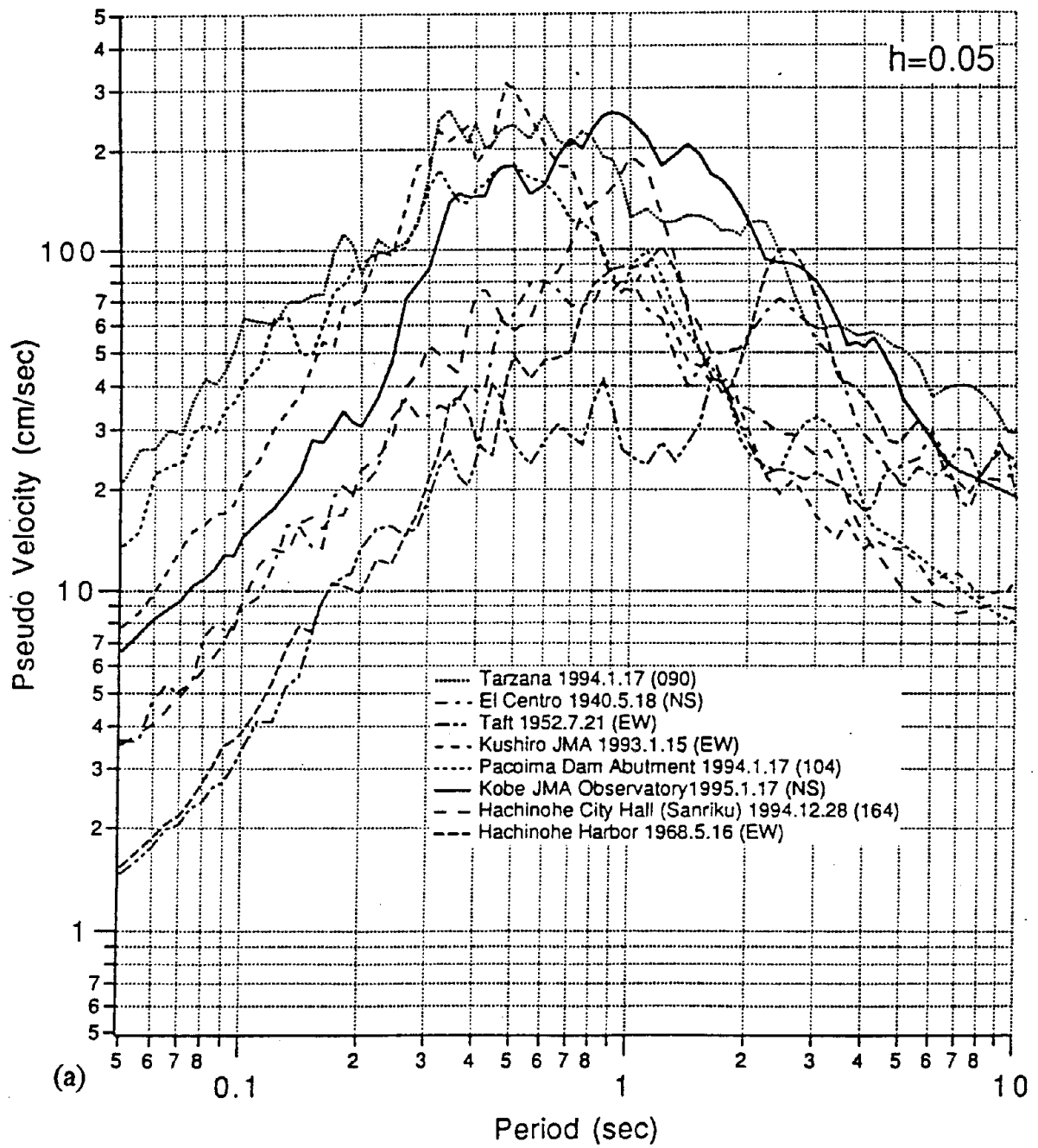
Figure 3.4. Pseudo Velocity Response Spectra for recent devastating earthquakes for the horizontal components (a), the UD component (b), and for design spectra for tall buildings (c), (from Building Research Institute, courtesy M. Watabe).

31

Figure 3.4b.

Figure 3.4c.

100 200 300 400   0   1000 2000

Depth Below Low Water Level (m)

10

0 — L.W.L

-10 — Fill (gravel)

-20 — Alluvial Clay

-30

-40 — Interlayered Sand & Clay

-50

-60

-70 — Diluvial Clay

-80 — Interlayered Sand & Clay

-90

Shear-Wave Velocity (m/s)   P Wave Velocity (m/s)   Boreholes

34
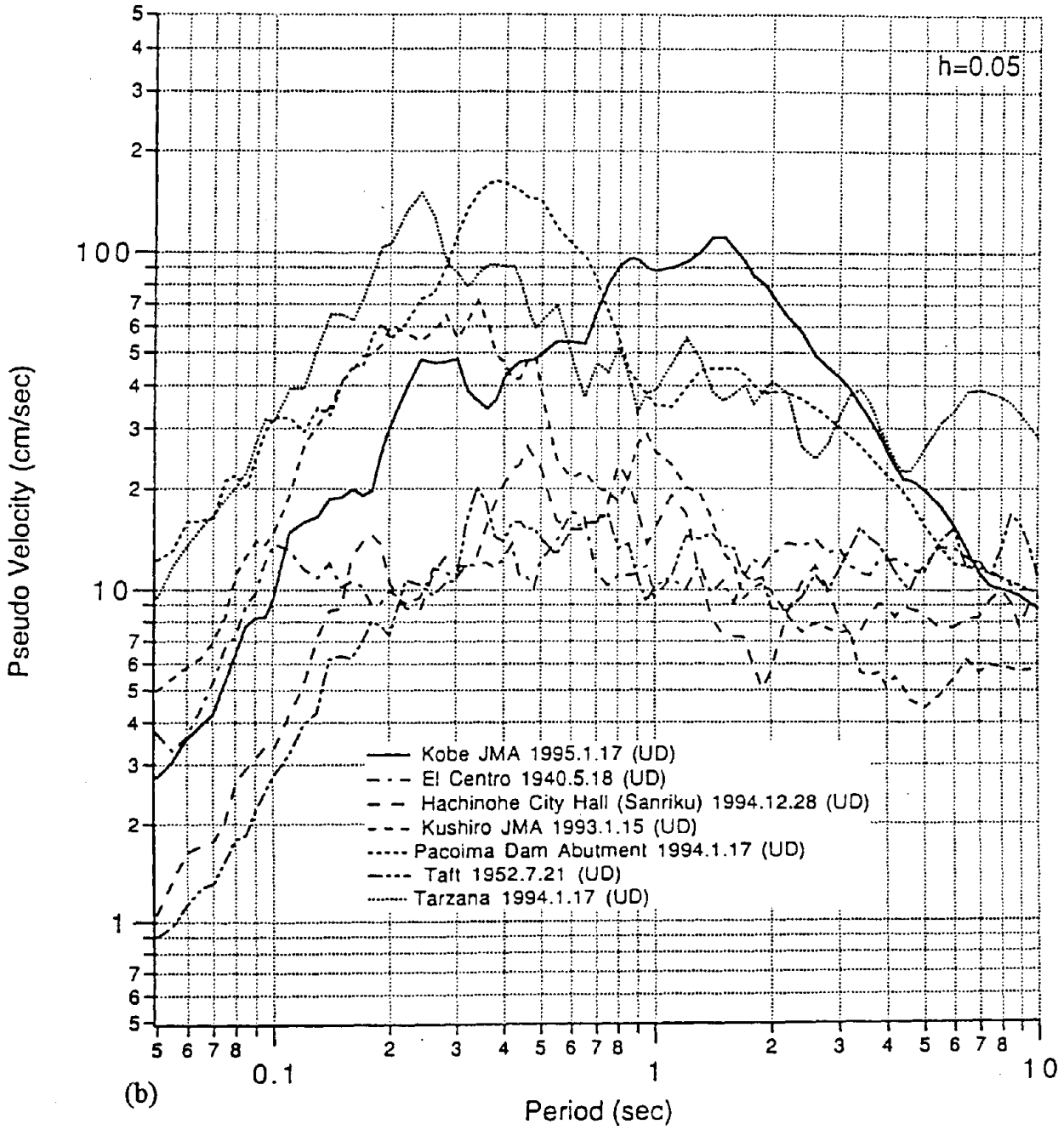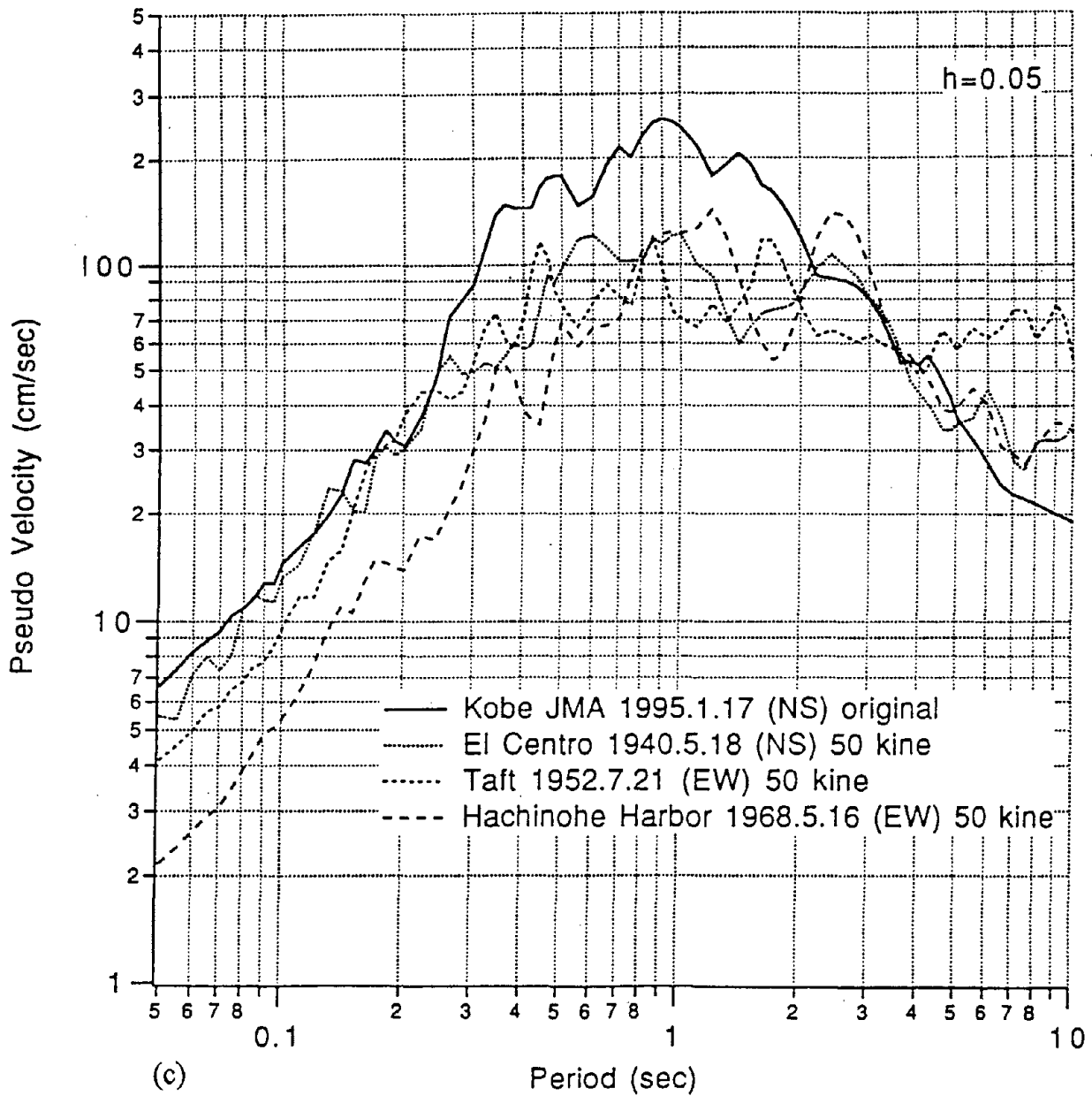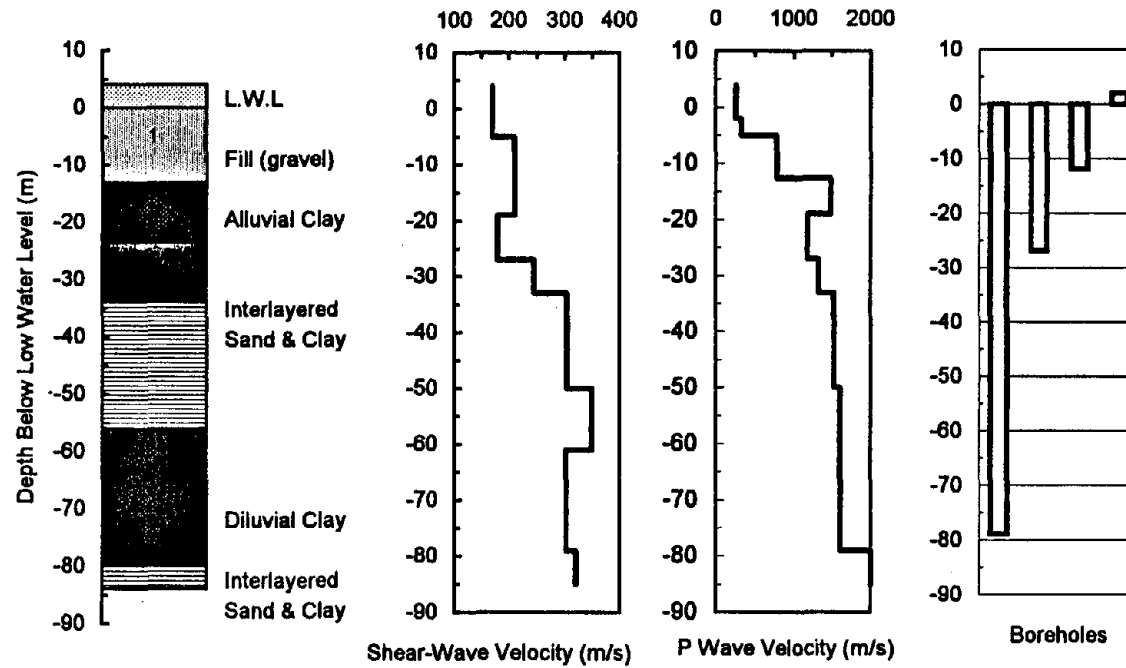
Figure 3.5 Geologic and seismic logs for the Port Island vertical array site (modified from logs provided by The Committee on Earthquake Observation and Research in the Kansai Area, CEORKA, courtesy Y. Iwasaki).
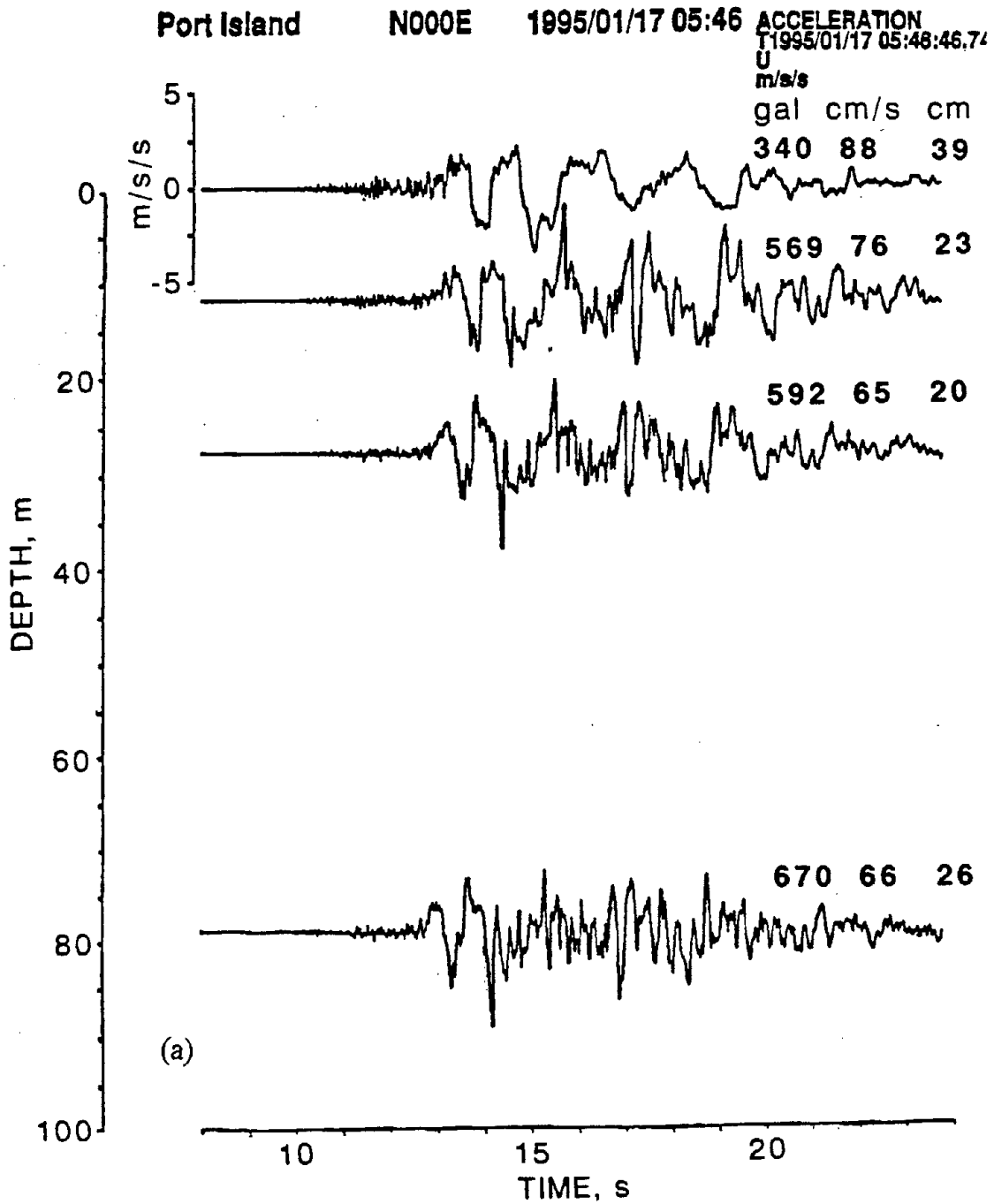
Figure 3.6. Strong motion recordings obtained on the Port Island vertical array at the surface and at approximate depths of 12, 27, and 79 m for the NS (a), EW (b), and UD (c) components (from The Committee on Earthquake Observation and Research in the Kansai Area, CEORKA, courtesy Y. Iwasaki).

Figure 3.6b

Port Island   UP   1995/01/17 05:46 ACCELERATION
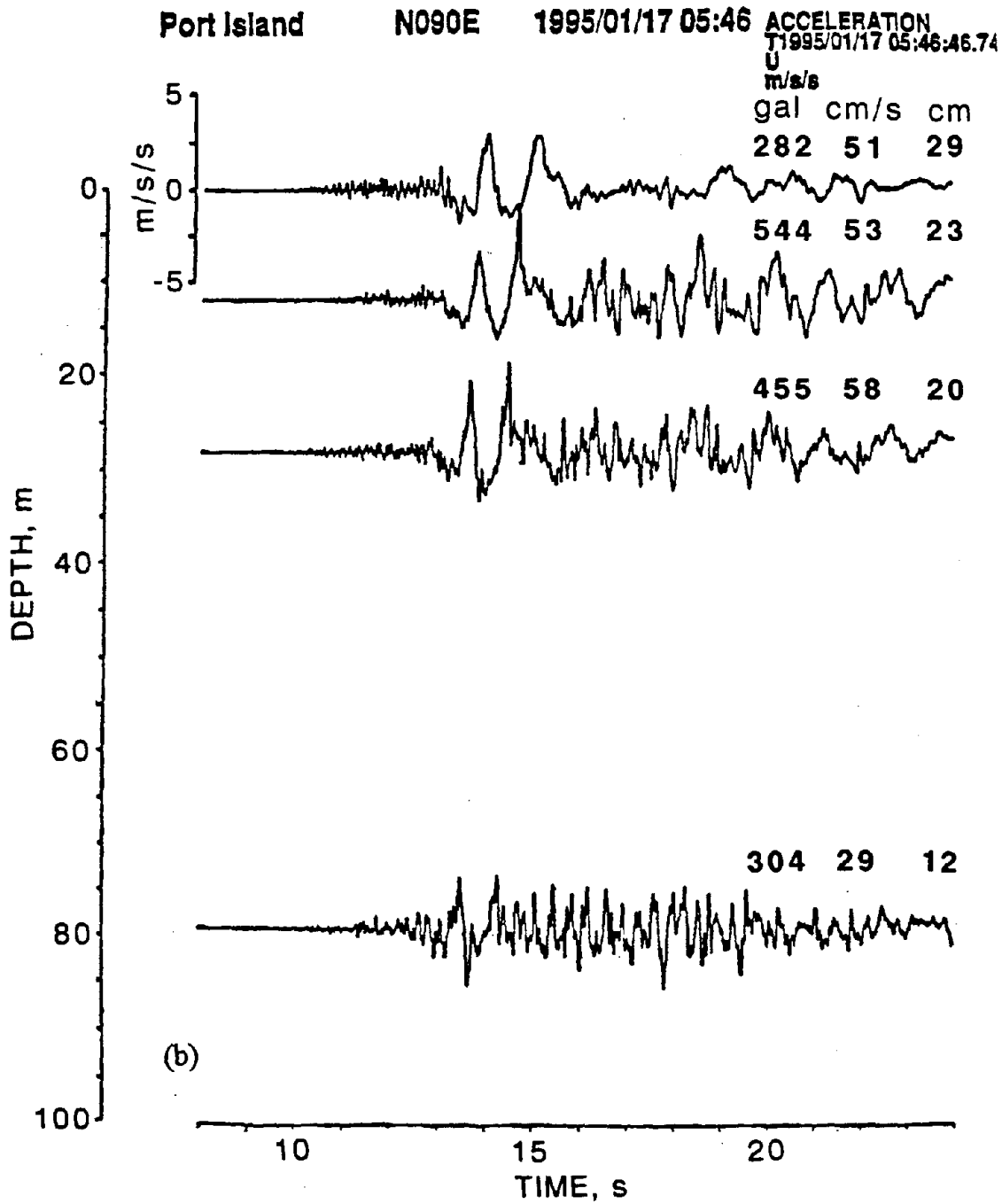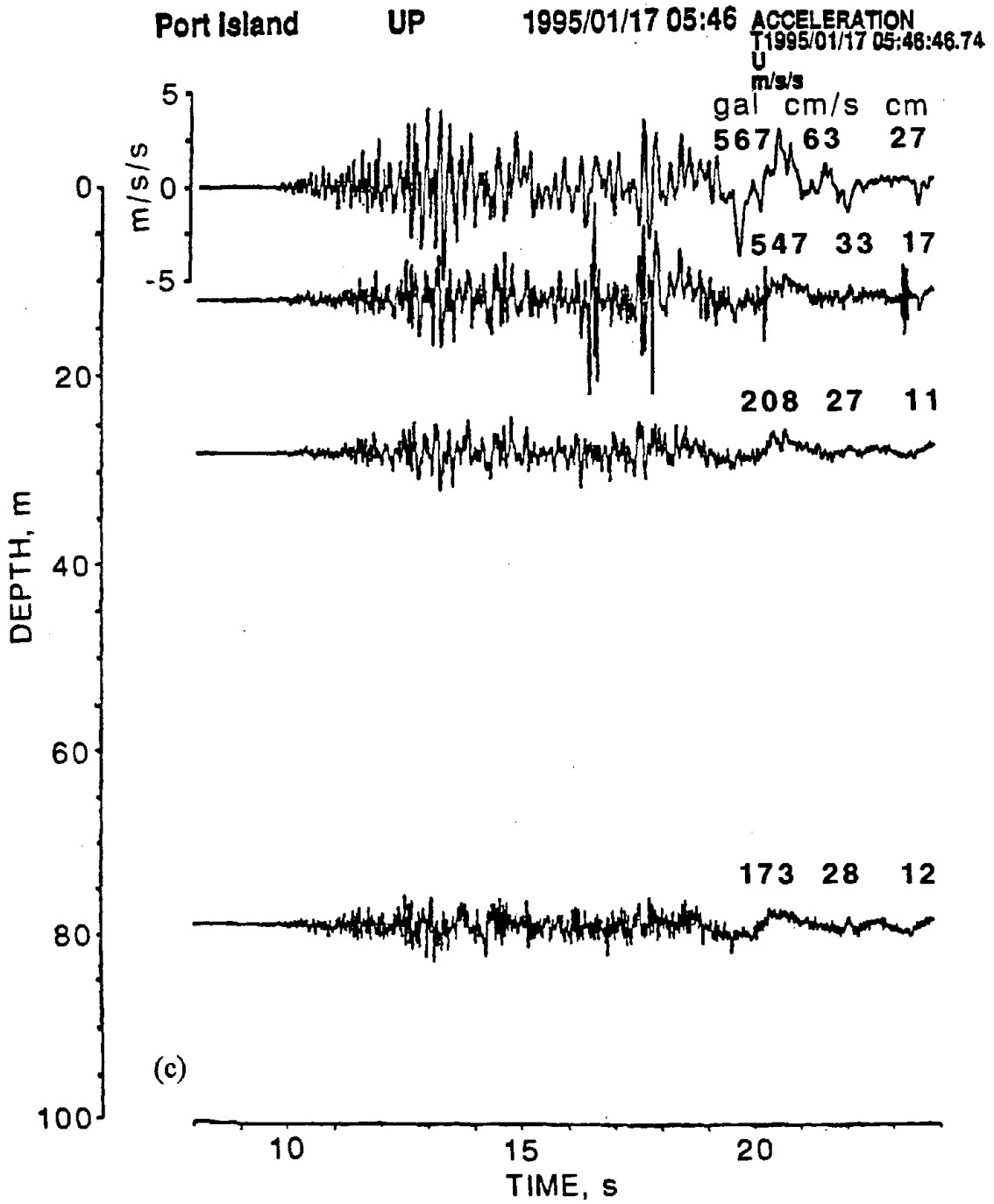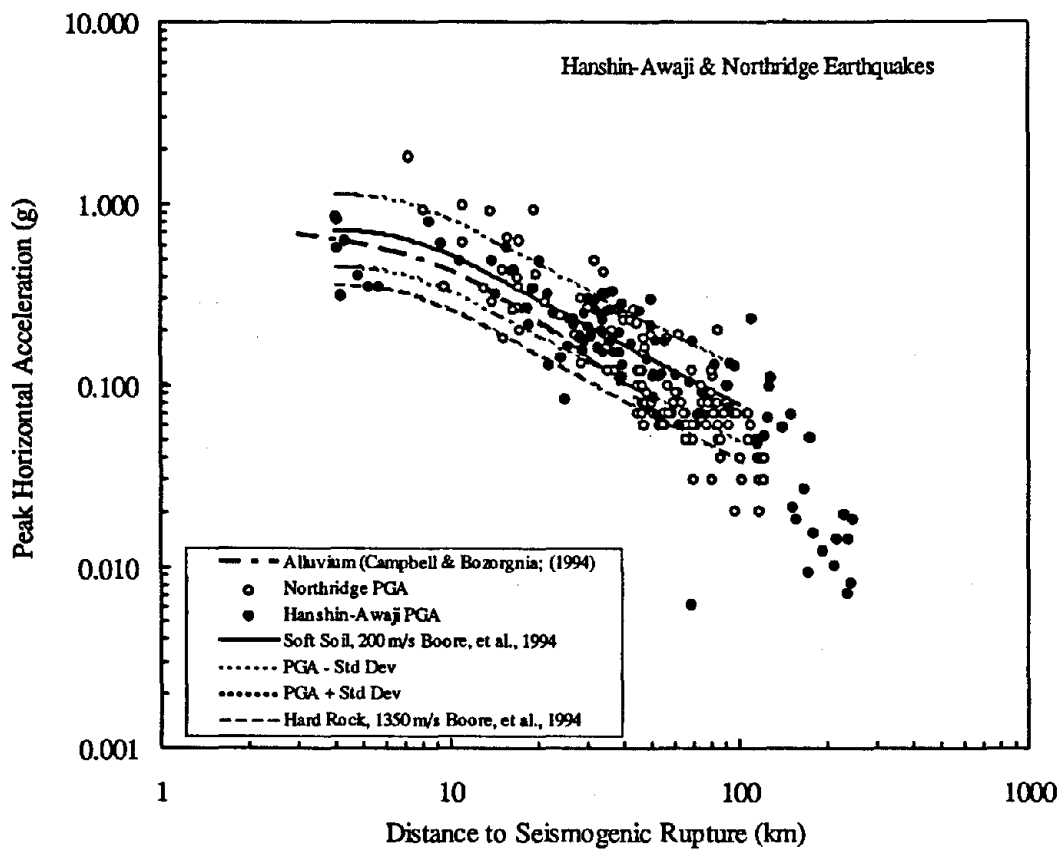
Figure 3.6c

Figure 3.7. Preliminary compilation of peak horizontal acceleration as a function of closest distance to seismogenic rupture for the Northridge and Hyogoken-Nanbu earthquakes (attenuation curves courtesy of K. Campbell and D. Boore).
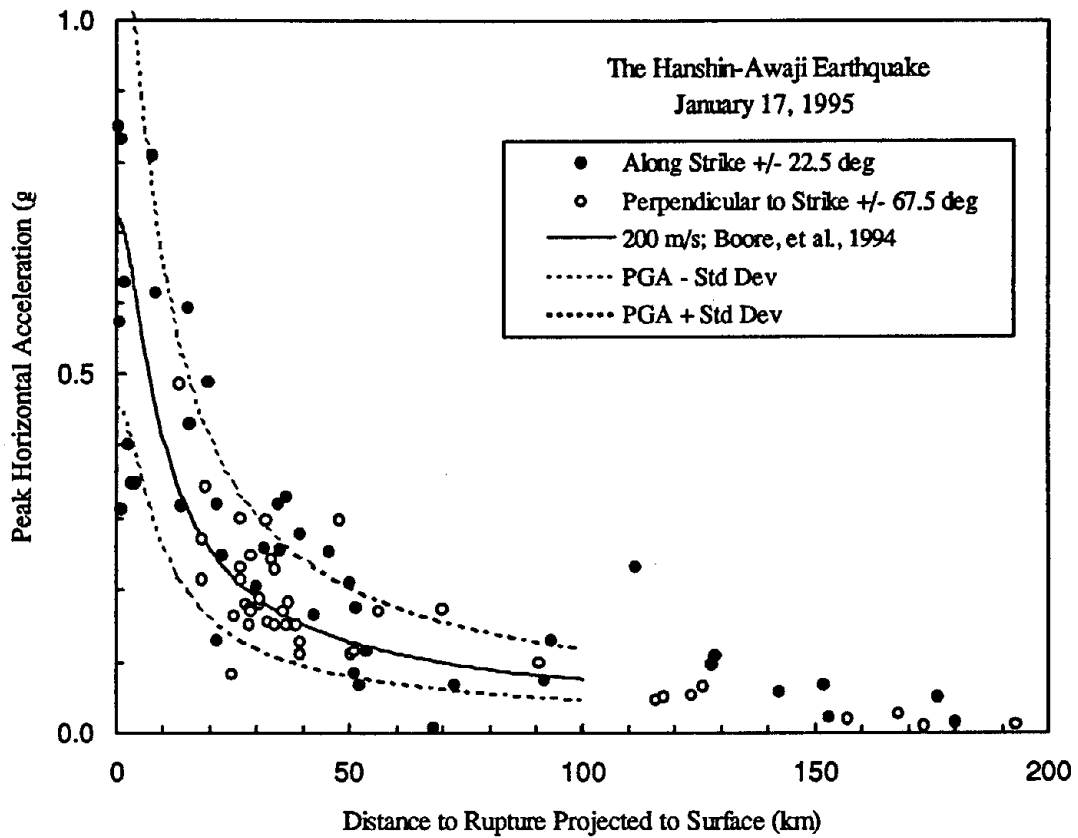
Figure 3.8. Preliminary compilation of peak horizontal acceleration compiled along strike (± 22.5 degree) and perpendicular to strike (± 67.5 degrees).
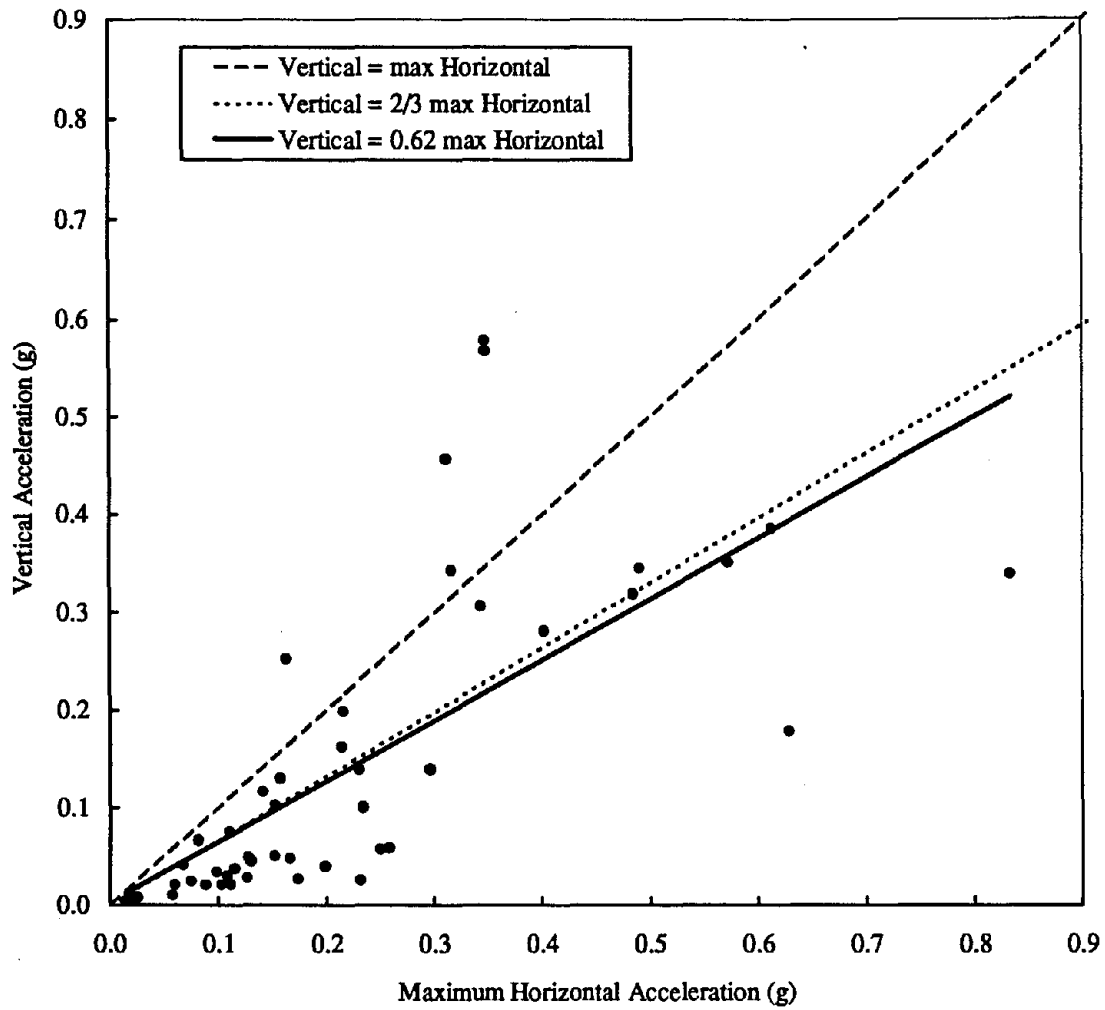
Figure 3.9. Preliminary compilation of peak vertical and peak horizontal acceleration.
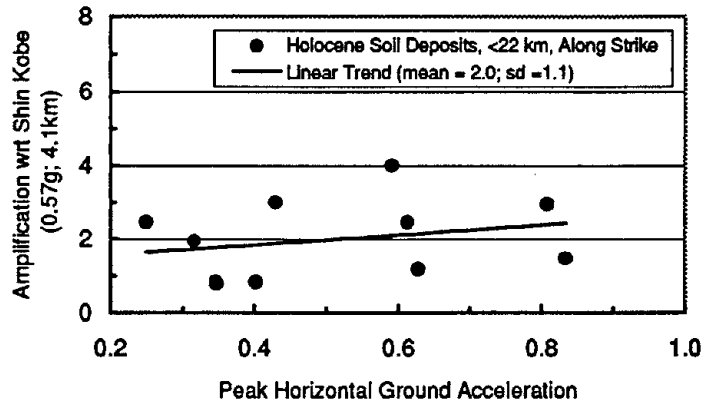
Figure 3.10. Amplification of peak horizontal acceleration with respect to corresponding value at Shin-Kobe station (0.57g) as normalized by the reciprocal ratio of respective distances to seismogenic rupture for sites within a +/- 22.5 degree azimuthal window of fault strike (51⁰).

Table 1 A preliminary list of strong motion stations for the Hanshin-Awaji earthquake

Station Name	Sta Code	Geol.	Site Class	N. Lat. (deg)	E. Long. (deg)	Azm (deg)	E-dist (km)	H-dist (km)	Surf-Dis (km)	SR-Dis (km)	PGA (gal)	Sta Azm	H1 (gal)	H2 (gal)	UD (gal)
Fuklai	OG-FUI	Qp-Q3	III	34.710	135.202	52	18.5	23.4	0.4	4.0	833				
Shin-Kobe	JR-SNK	Qp-Q3	III	34.704	135.200	53	18.0	22.9	0.8	4.1	561	NS	-530	-267	-344
Kobe Marine	JM-KBM	Qh	IV	34.688	135.180	54	15.4	21.0	0.9	4.1	817	NS	817	617	332
Kobe University	KC-KBU	Qp-Q3	III	34.725	135.240	54	22.3	26.4	1.3	4.2	305	NS	270	305	447
Takatori	JR-TKT	Qh	IV	34.649	135.139	62	9.9	17.4	1.7	4.3	616	NS	635	553	175
PHRI Kobe	PH-KOB	Qh	IV	34.697	135.225	59	19.4	24.1	2.7	4.8	394	NS	394	169	275
Port Island	MC-PRI	Qh	IV	34.691	135.226	61	19.1	23.9	3.3	5.2	341	NS	341	284	557
Kobe Motoyama	KC-KOB	Qh	IV	34.718	135.273	60	24.4	28.2	3.8	5.5	775?	NS	421?	775?	379?
Port Island Array	MC-PIA	Qh	IV	34.669	135.206	65	16.4	21.8	4.0	5.6	340	NS	340	282	567
Nishinomiya	OG-NSM	Qh	IV	34.732	135.346	63	31.0	34.1	7.5	8.5	792				
Takaraduka	JR-TKD	Qh	IV	34.809	135.344	51	35.5	38.2	8.5	9.3	601	NS	595	530	377
Nishi-Akashi	JR-NSA	Qh	IV	34.664	134.964	311	9.7	17.2	10.1	10.8	481	NS	481	-389	338
Amagasaki 1	KC-AMG	Qh	IV	34.718	135.408	70	35.6	38.3	13.4	14.0	>321	NS	271	322	328
PHRI Amagasak	PH-AMG	Qh	IV	34.689	135.388	74	32.9	35.8	13.4	14.0	475	NS	475	320	312
Amagasaki 2	MC-AMG	Qh	IV	34.715	135.410	70	35.7	38.4	13.7	14.3	310	TR	310	274	336
Amagasaki 3	JH-AMO	Qh	IV	34.724	135.432	70	37.9	40.4	15.3	15.8	580	NS			
Inagawa River	TD-OKI	Qh	IV	34.826	135.426	55	42.6	44.9	15.8	16.3	421				
Hokko	OG-HOK	Qh	IV	34.666	135.432	80	36.2	38.9	18.1	18.5	266				
Fukushima	KC-FKS	Qh	IV	34.681	135.446	78	37.8	40.3	18.3	18.8	212	NS	180	212	195
Yodo R (Ooyodo	MC-YRO	Qh	IV	34.688	135.458	77	39.0	41.5	18.9	19.3	336	TR	150	200	300
Hitokura Dam	TD-HTD	sed	I	34.900	135.408	46	46.7	48.7	19.8	20.2	478				
Toyonaka	KC-TYN	Qp-Q1	III	34.800	135.492	62	46.3	48.4	20.6	21.0		NS			
Senri	OG-SEN	Tp-N3	I	34.801	135.501	63	47.1	49.2	21.4	21.8	312				
Minoogawa Dam	TD-MND	sed	I	34.860	135.475	55	48.5	50.5	21.6	21.9	127				
Shin-Osaka(SS)	JR-SNO	Qh	IV	34.737	135.516	72	45.6	47.7	22.5	22.8	245	NS	-218	-217	56
Kakogawa Ozeki	MC-KGO	Qh	IV	34.791	134.913	330	23.8	27.7	23.9	24.2	139	TR	136	139	114
Osaka	JM-OSK	Qp-Q3	III	34.678	135.522	80	44.5	46.7	24.7	25.0	80	NS	80	66	-65
Kansai Int'l. Airport	KA-KIA	Qh	IV	34.421	135.212	143	25.8	29.5	25.2	25.6	160				247
Kakogawa	JR-KKG	Qh	IV	34.764	134.843	314	25.3	29.0	25.7	26.0	229	NS	165	262	98
Abeno	KC--ABN	Qp-Q3	III	34.636	135.519	86	43.7	45.9	26.6	26.9	226	NS	217	226	136
Morikawachi	OG-MKW	Qh	IV	34.678	135.545	80	46.5	48.6	26.6	26.9	210	NS	210	123	159
Kawachi	OG-KAW	Qh	IV	34.732	135.574	74	50.5	52.4	27.8	28.1	177				
Sakai S	KC-SAS	Qh	IV	34.564	135.469	97	39.3	41.7	28.4	28.7	150	NS	150	125	100
Sakai N	OG-SKN	Qh	IV	34.573	135.487	95	40.8	43.2	28.8	29.0	173				
Fujiidera	OG-FU2	Qh	IV	34.501	135.387	111	33.6	36.5	28.9	29.2	168				
Shin-osaka	KC-AHN	Qh	IV	34.679	135.572	81	49.0	51.0	28.9	29.2	243	NS			
Minami-Osaka	JH-MNO	Qh	IV	34.755	135.600	72	53.5	55.3	30.0	30.3	202				
Izumi	OG-IZ1	Qh	IV	34.498	135.409	110	35.6	38.4	30.5	30.7	178				
Iwasaki	OG-IWS	Qh	IV	34.632	135.567	87	48.1	50.1	30.6	30.9	185				
Yodo River (Hirakata)	JR-HRH	Qh	IV	34.803	135.614	67	56.6	58.3	31.6	31.9	253	TR	144	253	57
Tadaoka	KC-TAD	Qp-Q3	III	34.480	135.408	113	36.3	39.0	31.9	32.2	290	NS	290	190	137
Yae	KC-YAE	Qh	IV	34.680	135.612	81	52.7	54.5	32.4	32.6	155	NS	155	145	127
Izumi 2	OG-IZ2	Qp-Q3	III	34.406	135.324	131	34.0	36.9	33.2	33.4	240				
Sasayamaguchi	JR-SMG	sed	I	35.053	135.180	14	51.2	53.0	33.5	33.7	195	NS	139	-177	39
Higashi-Kishiwada	JR-HGK	Qp-Q3	III	34.445	135.388	120	36.3	39.0	33.7	33.9	149	NS	-110	-144	49
Shirahama	OG-SHR	Qh	IV	34.779	134.729	304	34.5	37.3	33.7	34.0	189				189
Shijonawate	OG-SHJ	Qh	IV	34.734	135.639	76	56.3	58.0	33.8	34.0	224				
Yodo River, Hirakata City	OG-HRH	Qh	IV	34.810	135.645	68	59.5	61.1	34.5	34.8	313				
Hashiramoto	OG-HSM	Qh	IV	34.860	135.634	63	60.9	62.5	34.8	35.1	251				
Onji	OG-ONJ	Qh	IV	34.625	135.624	88	53.2	55.0	35.6	35.9	169				
Fujiidera	OG-FJ3	Qp-Q3	III	34.567	135.594	95	50.6	52.5	36.5	36.7	149				
Shin-Takatsuki(SS)	SNT	Qh	IV	34.859	135.654	63	62.5	64.0	36.6	36.8	323	NS			
Matsuo	OG-MTS	Qh	IV	34.241	135.150	167	41.8	44.2	36.7	36.9	180				
Shikama	KC-SHM	Qh	IV	34.799	134.691	304	38.7	41.2	37.7	37.9	253				
Fujiidera	OG-FU1	Qp-Q3	III	34.558	135.611	96	52.3	54.1	38.4	38.6	149				
Kino-Kawa Ohashi	TD-KKO	Qh	IV	34.231	135.167	165	43.3	45.6	38.6	38.8	150				

Table 1 continued

Name	Code			Lat	Long										
Himeji	KC-HIM	volc	I	34.835	134.723	311	38.8	41.3	38.9	39.1	189				
Nakanoshima	OG-NKS	Qh	IV	34.240	135.191	162	43.0	45.3	39.3	39.5	126				
Wakayama Br	JH-WKY	Qh	IV	34.254	135.211	159	42.2	44.5	39.3	39.5	109				
Oimosaka-Kamex	JH-OMK	Qp-Q2	III	34.983	135.609	51	66.5	67.9	39.4	39.6	273				
Sonobo	JR-SNB	Qh	IV	35.100	135.487	37	68.2	69.6	42.4	42.6	163	NS	-102	163	-47
Keiji Bypass	JH-KJB	Qh	IV	34.898	135.741	63	71.5	72.8	45.4	45.6	249				
Tatsuno	JH-TSN	volc	I	34.871	134.626	308	48.2	50.2	47.7	47.9	136				
Fushimi	OG-FUS	Qh	IV	34.941	135.772	61	76.2	77.4	49.8	49.9	206				
Chihaya	KC-CHY	ig/meta	I	34.439	135.659	108	59.4	61.1	50.4	50.6	109	NS	91	109	74
Nijo	JR-NJO	Qh	IV	35.007	135.744	55	77.9	79.1	51.0	51.1	84	NS			
Nara	JR-NRA	Qh	IV	34.677	135.821	84	71.6	72.9	51.1	51.2	113	NS	112	104	-36
Amagase Dam	TD-AMD	Qp-Q1	III	34.875	135.815	67	76.6	77.8	51.2	51.3	172				
Kyoto	OG-KYO	Qh	IV	35.012	135.755	55	79.1	80.2	52.1	52.3	67				
Higashiyama	JR-HGY	sed	I	34.978	135.797	59	80.3	81.4	53.6	53.8	113	NS			
Shirakawa Dam	TD-SKD	TmN1/2	II	34.615	135.858	90	74.6	75.9	56.1	56.2	169				
Fukuchiyama	JR-FHY	Qh	IV	35.293	135.121	5	76.7	77.8	60.7	60.8	110	NS	72	107	21
Ikuno	JR-IKN	volc	I	35.160	134.792	339	65.7	67.1	62.1	62.2	59	NS	-36	53	20
In	JR-IN	volc	I	34.750	134.227	282	76.3	77.6	66.9	67.0	101	NS	-36	53	20
Kusatsu	OG-KUS	Qh	IV	35.008	135.956	62	94.5	95.5	68.2	68.3	6				
Gobo	JR-GBO	sed	I	33.904	135.162	172	78.9	80.1	69.9	70.0	170	NS	-111	132	26
Ritto	JR-RTO	Qh	IV	35.028	135.996	62	98.8	99.7	72.4	72.5	67	NS			
Nishi-Maiduro	JR-NSM	sed	I	35.438	135.333	16	96.1	97.0	75.4	75.5	87	NS	-60	79	-20
Maizura	JM-MAZ	ig/meta	.	35.448	135.320	15	96.9	97.8	76.4	76.5	67	NS	-67	-52	-40
Himeji	JR-HMJ	volc	I	34.821	134.075	285	91.7	92.7	82.9	83.0	125	NS	82	125	48
Tsuge	JR-TSG	Tp-N3	III	34.843	136.259	77	114.2	114.9	90.6	90.7	97	NS	77	-67	33
Obama	JR-OBM	Qh	IV	35.488	135.749	33	117.2	117.9	91.7	91.8	74	NS	70	-57	-24
Gokasou	JR-GOK	volc	I	35.139	136.184	61	119.7	120.4	93.1	93.2	128	NS	-125	119	-44
Toyooka	JR-TYK	TmN1/2	II	35.541	134.800	348	106.2	107.0	96.7	96.8	124	NS	103	-90	-27
Shin-Malbara(SS)	JR-SNM	Qh	IV	35.316	136.293	56	138.5	139.1	111.6	111.6	227	NS	217	135	-25
Kji-Nagashima	JR-KNG	sed	I	34.205	136.342	111	127.2	127.9	116.0	116.1	46	NS			
Matsuzaka	JR-MTZ	Qh	IV	34.573	136.538	92	136.9	137.5	117.7	117.8	49	NS			
Kumancshi	JR-KUM	volc	I	33.889	136.105	130	126.1	126.8	123.5	123.6	52	NS			
Yokkaichi	JR-YKC	Qh	IV	34.960	136.633	75	150.4	150.9	126.2	126.2	65	NS			
Sekigahara	JR-SKH	Qh	IV	35.360	136.472	58	154.8	155.2	127.9	128.0	95	NS			
Shin-Sekigahara(	JR-SNS	Qh	IV	35.354	136.483	58	155.3	155.7	128.4	128.5	106	NS	106	72	-29
Hashima	JR-HSM	Qh	IV	35.326	136.575	62	168.8	169.2	142.3	142.4	57	NS	57	-31	10
Kisogawa	JR-KIS	Qh	IV	35.343	136.783	63	178.4	178.8	152.0	152.1	67	NS			
Biwajima(SS)	JR-BWJ	Qh	IV	35.195	136.867	69	178.7	179.1	153.1	153.2	21	NS	-21	18	-7
Odaka(SS)	JR-ODK	Tp-N3	III	35.066	136.953	74	181.6	182.0	157.0	157.1	18	NS	-17	-14	-7
Anjo(SS)	JR-ANJ	Qp-Q3	III	34.929	137.099	80	191.2	191.5	167.8	167.8	26	NS	-22	-19	-7
Okazaki	JR-OKZ	Qp-Q3	III	34.920	137.160	80	196.5	196.8	173.2	173.3	9	NS			
Mino-Ota	JR-MNO	Qh	IV	35.443	137.022	63	202.8	203.0	176.3	176.4	50	NS			
Tajimi	JR-TJM	TmN1/2	II	35.330	137.122	68	205.8	206.0	179.9	180.0	15	NS			
Toyohashi	JR-TYH			34.760	137.385	86	214.8	215.0	193.1	193.1	12	NS			
Gero	JR-GRO			35.802	137.242	57	239.9	240.1	213.0	213.0	10	NS			
Nakatsugawa	JR-NKT			35.495	137.505	67	244.9	245.0	218.9	218.9	14	NS			
Nagiso	JR-NGS			35.596	137.612	66	258.3	258.3	232.1	232.1	19	NS			
Takayama	JR-TKY			36.138	137.254	50	263.0	263.0	235.9	236.0	7	NS			
Shin-Iwata(SS)	JR-SHI			34.723	137.901	88	261.7	261.8	240.3	240.3	14	NS	10	13	-4
Hiraoka	JR-HRK			35.271	137.857	75	266.9	267.0	242.2	242.2	8	NS			
Ida	JR-IDA			35.517	137.825	69	272.7	272.7	246.9	246.9	18	NS			

KC - Kansai Committee for Earthquake Observation and Research
OG - Osaka Gas
JR - Japan Railway
JH - Japan Highway
MC - Ministry of Construction

PH - Port and Harbor Research Institute
JM - Japan Meterological Agency
KA - Kansai International Airport
TD - To be Determined
Bold faced coordinates provided by agencies.
Italicized coordinates inferred from maps

CHAPTER 4

GEOTECHNICAL ASPECTS

4.1 INTRODUCTION

Immediately following the earthquake, a geotechnical reconnaissance was organized under the auspices of the Siting and Geotechnical Systems Earthquake Hazard Mitigation Program of the Engineering Directorate of the National Science Foundation. Only the some of the most significant findings are reviewed here, since a detailed discussion of the main findings is presented in a separate report No. UCB/EERC 95-01.

A combination of factors contributed significantly to the severity of much of the damage: the area had previously been considered to have relatively low seismic risk, the projected location of the release of energy along the earthquake fault was almost immediately below a densely developed urban area, and the geologic setting of the region, on the shores of a large embayment, provided for a substantial thickness and areal distribution of liquefiable sediments and fills. Most importantly, from a geotechnical standpoint, the area affected by the 1995 Hyogoken-Nanbu earthquake has many similarities to other locations around the world, in terms of geologic setting, types of sedimentary deposits, and the level and the type of development.

4.2 LIQUEFACTION AND RELATED EFFECTS

Extensive liquefaction of natural and artificial fill deposits occurred along much of the shoreline on the north side of Osaka Bay. Probably the most notable were the liquefaction failures of relatively modern fills on Rokko and Port Islands. On the Kobe mainland, evidence of liquefaction extended along the entire length of the waterfront, east and west of Kobe, for a distance of about 20 km (12 miles) (Figure 4.1).

Overall, liquefaction was a principal factor in the extensive damage experienced by the port facilities in the affected region, as illustrated in Figure 4.2. Most of the liquefied fills were constructed of decomposed granite soil. This material was transported to the fill sites and loosely dumped in water. Compaction was generally only applied to materials placed above water level. As a result, liquefaction occurred within the underwater segments of these fills, causing settlement in their interior regions and lateral spreading along their margins (Figure 4.3).

Typically, liquefaction led to pervasive eruption of sand boils and, on the islands, to ground settlements on the order of as much as 0.5 m (Figure 4.4). The ground settlement caused surprisingly little damage to high- and low-rise buildings, bridges, tanks and other structures supported on deep foundations. These foundations, including piles and shafts, performed very well in supporting superstructures where ground settlement was the principal effect of liquefaction (Figure 4.5). Where liquefaction generated lateral ground displacements, such as near island edges and in other waterfront areas, foundation performance was typically poor. Lateral displacements fractured piles (Figure 4.6) and displaced pile caps, causing structural distress to several bridges (Figure 4.7). In a few instances, such as the Port Island Ferry Terminal, strong foundations

Preceding page blank

withstood the lateral ground displacement with little damage to the foundation or the superstructure.

There are numerous tank farms in the area most severely affected by the earthquake. Some of the tank farms are associated with the port facilities, while others provide storage for refineries, fossil fuel power plants, and chemical manufacturing facilities. Most of the tanks surveyed from the air appeared to have performed well, and there were no reports of widespread damage to tanks even within port areas disturbed by severe liquefaction effects. The generally good performance of tanks may be due to the apparent practice of placing tanks on pile foundations (Figure 4.8). However, there were a few exceptions to the generally good performance; these few instances of poor performance may have been due to use of mat foundations in areas where liquefaction occurred (Figure 4.9).

Shallow foundations consisting of a grid of interconnected perimeter-wall footings and grade beams performed well in several areas subjected to liquefaction (Figure 4.10). Where foundation elements were not well tied together, differential ground displacements pulled apart overlying structures at points of weakness, such as joints and doorways.

4.3 IMPROVED GROUND SITES

The earthquake provided an opportunity to evaluate the performance of several improved ground sites in the Kobe area. All cases involved loosely dumped hydraulic fill placed over soft alluvial clay. The treatment method was to construct sand compaction piles in-situ by vibro-rod probes or using the casing method with introduction of additional material from above ground. The post-treatment SPT N-values were typically 20 to 25 blows per 30 cm (75 inches), as opposed to about 10 to 15 blows per 30 cm (75 inches) before treatment. The ground surface settlements as a result of the treatment were on the order of 20 to 40 cm (50 to 100 inches), with the largest values being reported for the Portopialand Park area. In comparison, the liquefaction-induced surface settlements of adjacent untreated ground were on the order of 50 cm (125 inches). Overall, the observations show that improved ground sites on land sustained significantly less deformation and damage than did the untreated ground. Figure 4.11 shows the ground surface in the treated area of the Portopialand Park, with a Ferris wheel in the background. The ground deformations were limited to minor cracking, and the amusement ride was fully operational once power was restored.

4.4 DAMS AND LEVEES

In general, most dams performed well with little or no damage noted. The principal exception was the failure of the relatively small Upper and Middle Niteko Dams (Figure 4.12), together with significant damage sustained at the Lower Niteko Dam. The earthquake was estimated to have induced peak ground accelerations of approximately 0.3 to 0.5g in this area. All three dams are reported to have been constructed over 100 years ago with minor additions and modifications made to them in more recent times. Of the three dams, the Lower Niteko Dam performed the best. Nevertheless, the dam sustained major cracking and slumping in the middle of the embankment, losing as much as 2 meters (6.2 feet) of height. The Upper and Middle Niteko Dams experienced flow failures with the material traveling as much as 70 m (220 feet) downstream

(Figure 4.13). This mode of failure strongly suggests that liquefaction was responsible, despite the fact that sediment boils were not observed.

The rivers in the area are commonly confined by gravity and cantilever retaining walls. In some places, armored earth embankments are also used as levees. In several locations major damage to these structures occurred, apparently as a result of liquefaction and associated settlement and lateral spreading. While as much as 3 m (9.3 feet) of settlement was observed in the most seriously affected area, much of the damage consisted of vertical and lateral deformations in the range of 10 to 20 cm (25 to 50 inches) (Figure 4.14).

4.5 LIFELINE SYSTEMS

Extensive damage to lifeline systems occurred throughout the epicentral area of the earthquake. Liquefaction appears to have been a major factor involved in the failures of lifeline systems due to geotechnical causes, such as the damage to port facilities, underground transit, and underground utilities. There was pervasive disruption of underground utilities caused by ground deformations. In some locations, pipe joints were simply pulled apart due to ground displacement. However, most common failures occurred due to differential movements between foundation elements and the surrounding soil at points of entry to buildings and other structures (Figure 4.15).

Particularly notable was the damage to several underground stations of the Kobe Rapid Transit Railway. These stations were constructed using the cut and cover method of construction, and soil-structure interaction appears to have been responsible for the observed failures and distress (Figure 4.16).

4.6 SLOPES, RETAINING STRUCTURES, AND LANDFILLS

Seismically induced landslides were generally limited to shallow slips and raveling of boulders, with the exception of one large flow slide which killed 34 people. In addition to landsliding on natural slopes and occasional rockfalls (Figure 4.17), structural fills for roads and house pads experienced cracking and lateral deformations in the hills above Kobe (Figure 4.18). In many cases, this form of distress caused disruption of underground utilities as well as structural damage to houses and retaining walls. Large retaining structures for roads and railroads generally performed well. In particular, mechanically stabilized walls performed very well (Figure 4.19).

Waste fills located on reclaimed land experienced distress which can be directly attributed to the liquefaction of the loosely-dumped fill. Liquefaction-induced lateral spreading resulted in cracking in the covers and in lateral displacements of the side slopes (Figure 4.20). The overall impact of these deformations on the integrity of the containment has yet to be established.

4.7 CONCLUSIONS

In conclusion, it is important to note that many of the observed effects of the January 17, 1995, Hyogoken-Nanbu earthquake are similar to those observed in the recent urban earthquakes

such as the Northridge and Loma Prieta earthquakes in California. Moreover, while many of the observations will provide an opportunity to further improve and refine our methods of analysis and design, much of the observed phenomena and effects could have been predicted and avoided with currently available methodologies.
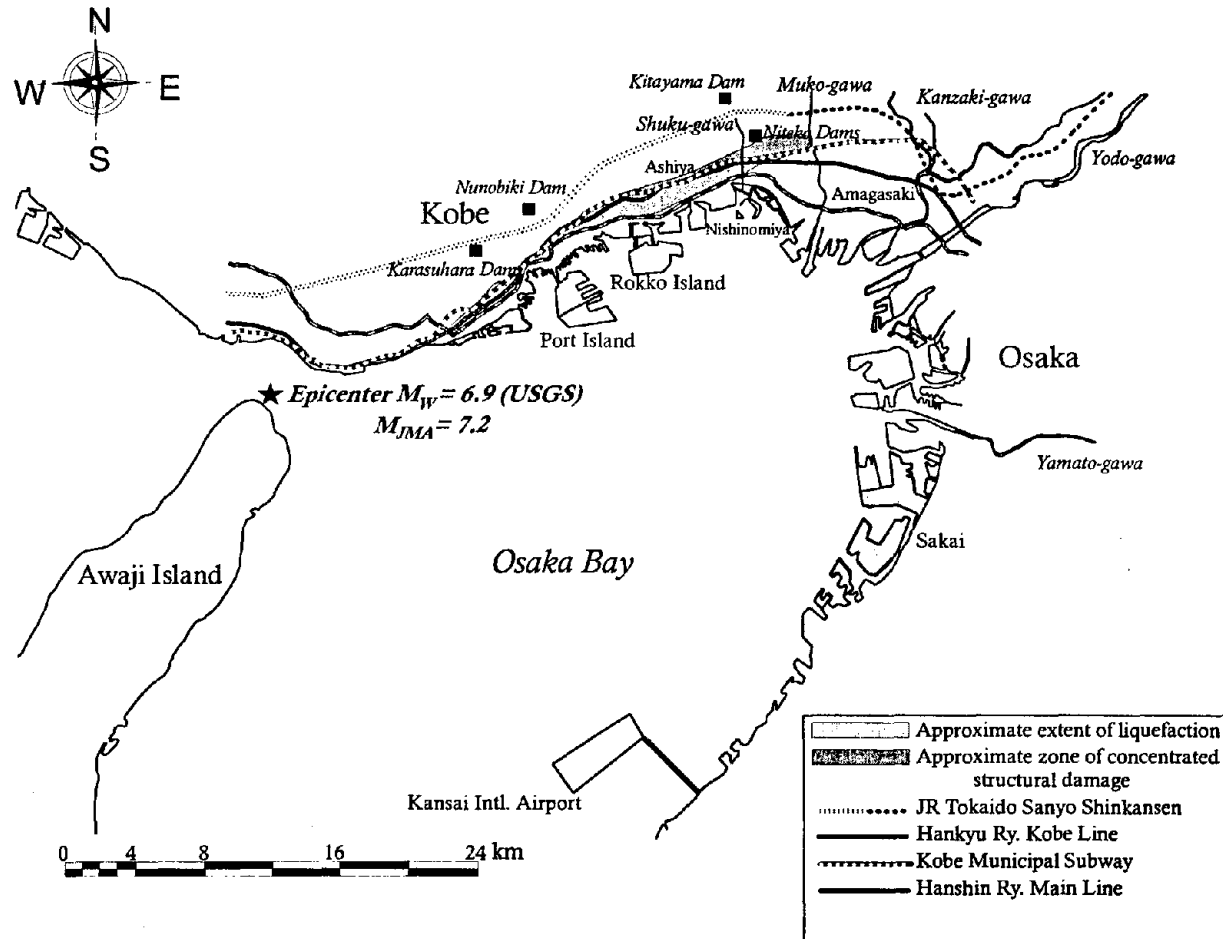
Fig. 4.1 Map of the Osaka Bay region, showing the principal areas of interest and the approximate extent of the areas which experienced liquefaction and structural damage.

Fig. 4.2   Crane collapsed due to outward lateral movement of the quay wall on Rokko Island.
The depth of the resulting graben is ≈2 m.
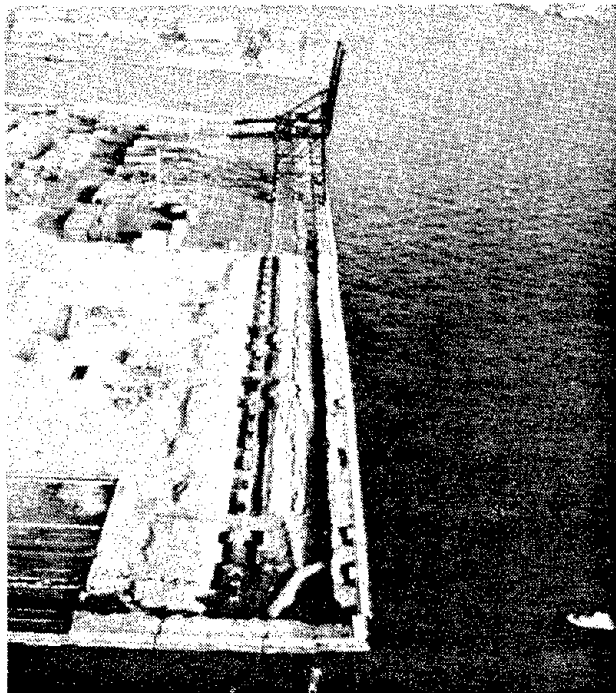
Fig. 4.3   Aerial view of the longitudinal cracking and graben along the outboard edge of Rokko
Island.

Fig. 4.4　Liquefaction-induced differential settlement ($\approx$40 cm) next to a pile-supported pier of the elevated railway on Port Island.

Fig. 4.5　Apparently undamaged pile-supported building. The magnitude of liquefaction-induced differential settlement at the site is $\approx$30 cm.

Fig. 4.6 Sheared and translated hollow tube pile.

Fig. 4.7 Tilted pier of the Rokko Island causeway.

52
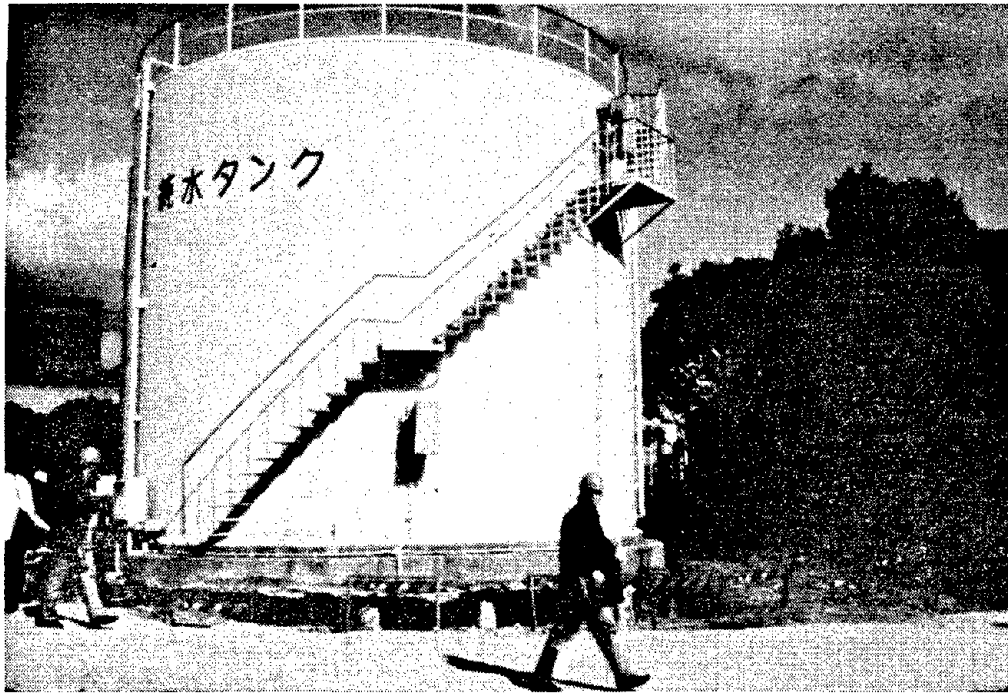
Fig. 4.8 Pile-supported tank showing no apparent damage.

Fig. 4.9 Listing tank in the Nippon Gatx tank farm.

Fig. 4.10 No significant structural damage was evident in this modern residential development in spite of extensive ground deformation due to liquefaction.
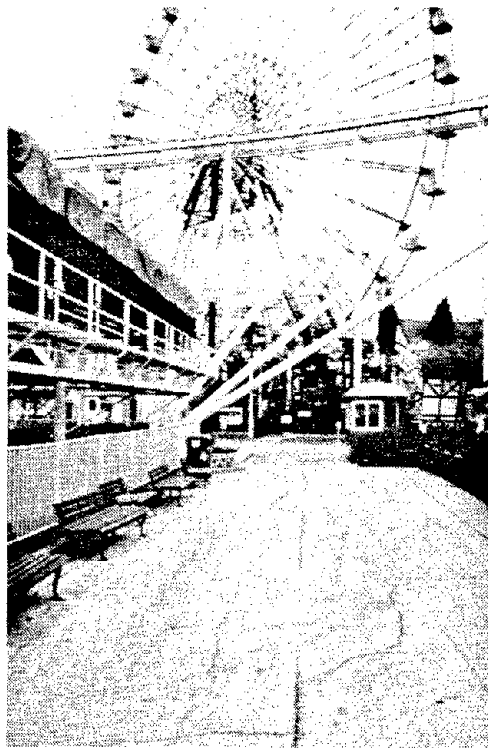
Fig. 4.11 Minor ground cracking, but no significant displacement occurred on improved ground at the Protopialand Park on Port Island.

Fig. 4.12 Aerial view of the Niteko Dams.
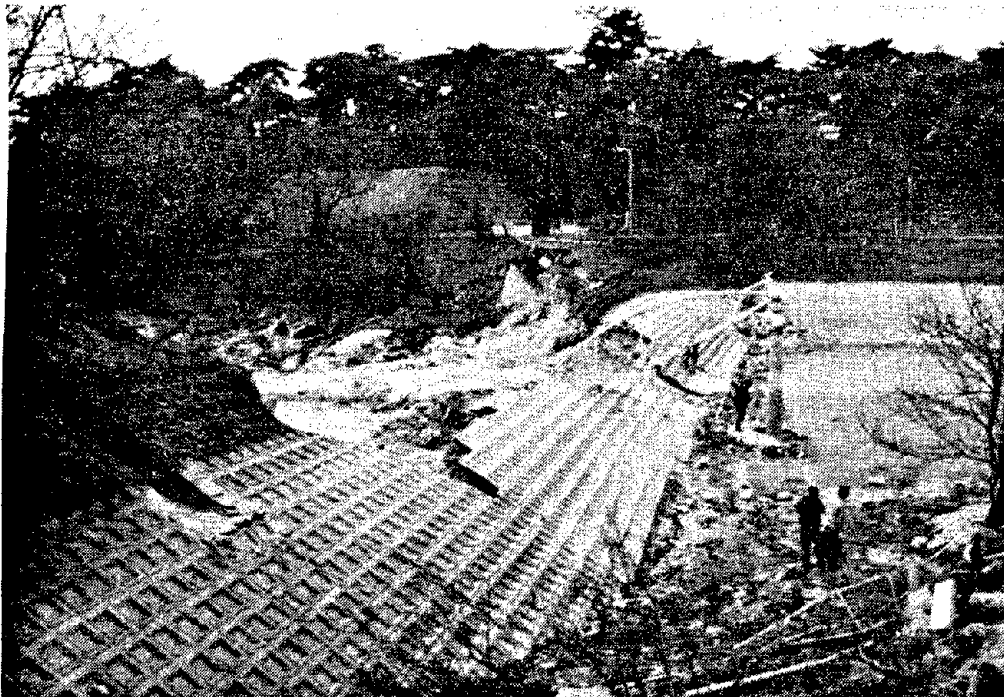
Fig. 4.13 A view of the Middle Niteko Dam showing the loss of the downstream part of the embankment and a breach in the middle.

Fig. 4.14 Longitudinal separation of a levee in Ashiya.
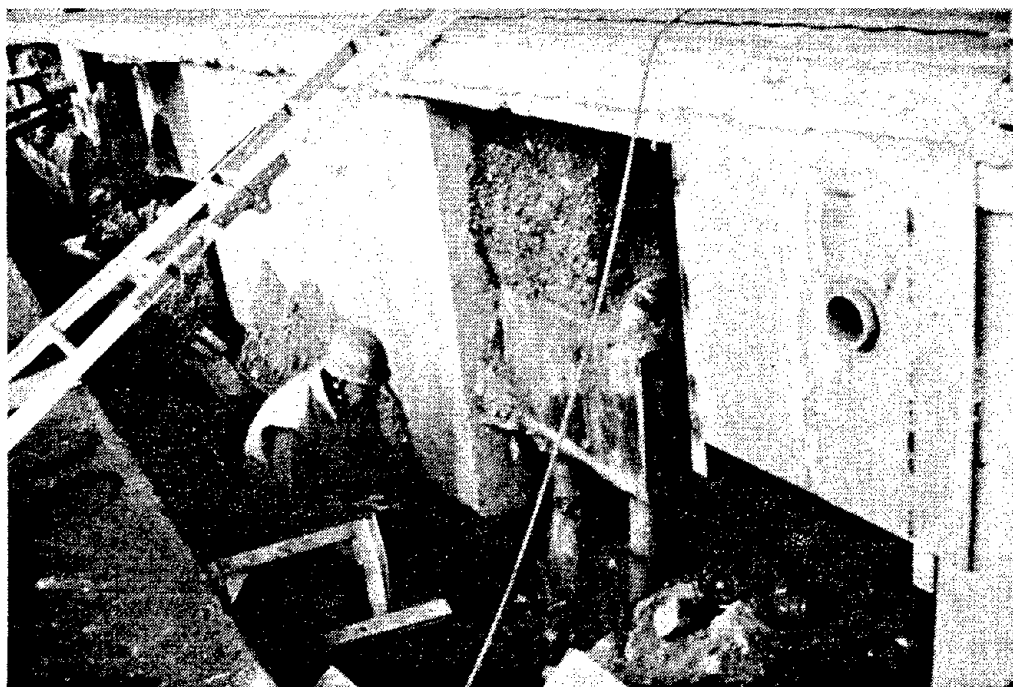
Fig. 4.15 Utility lines broken along a graben formed around the perimeter of a foundation.

Fig. 4.16 Collapsed street surface over Dakai Station.

Fig. 4.17 Car crushed by a fallen boulder ~3 m in diameter.

Fig. 4.18 Road embankment deformed by lateral and vertical displacements.

Fig. 4.19 This mechanically stabilized wall experienced only minor deformation in contrast to the extensive damage to the residential structures in the vicinity.
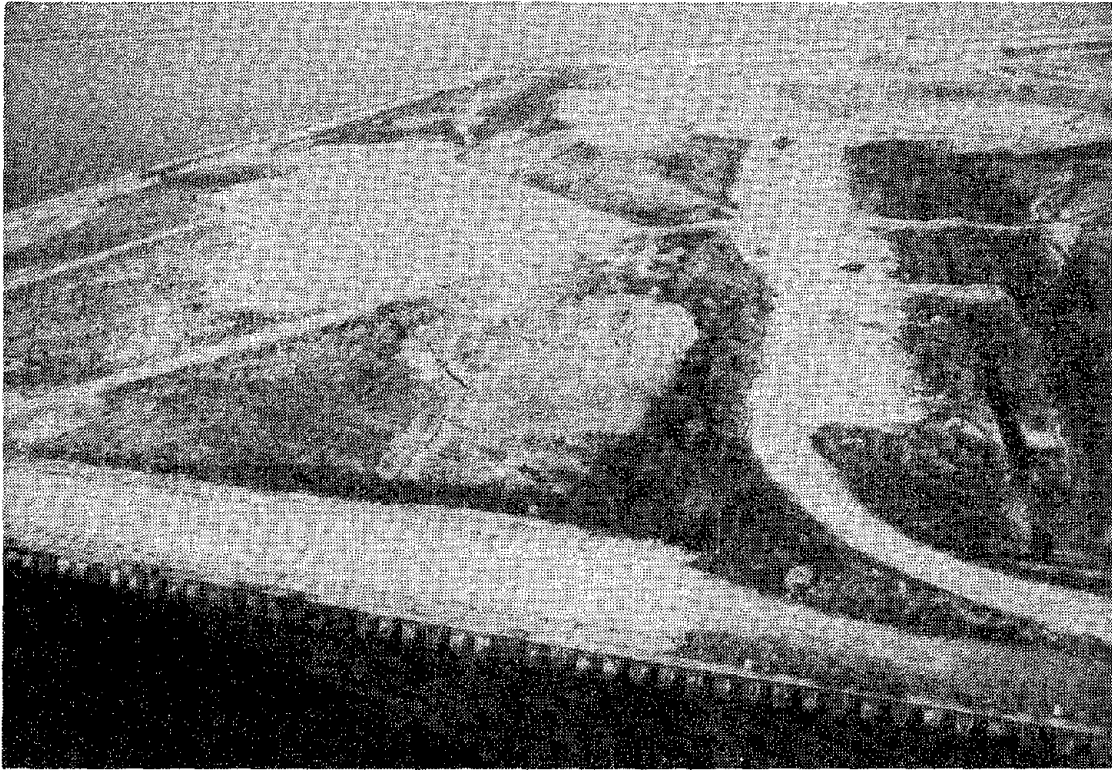
Fig. 4.20 Aerial view of ground cracking at a waste fill site west of Osaka.

CHAPTER 5

RESPONSE OF TRADITIONAL WOODEN JAPANESE CONSTRUCTION

5.1 INTRODUCTION

One of the surprises of the January 17, 1995, Hyogoken-Nanbu earthquake was the extent of the poor performance of traditional Japanese wood residences and rowhouse-stores. Although the construction system and design of these buildings differ greatly from structures in the United States, their inclusion in this report is important because their performance illustrates problems inherent in timber construction and poses crucial questions about whether people incorporate the observations of past seismic disasters in traditional building practice. These vernacular structures encode Japanese cultural and design values which are not being reincorporated in the "two-by-four" and prefabricated steel and wood structures which are replacing them.

Traditional Japanese buildings have been crucial to the development of modern architecture in the West. Gropius, Mies van der Rohe, and Wright have all been influenced by the spare beauty of these structures supported on elegant posts, whose plans, regulated by the module of the tatami mat incorporate varied symmetrical and asymmetrical spaces made even more flexible by removable shoji screens and shutters. The indoor-outdoor permeability of these elegant and seemingly ephemeral structures, the manner in which they combine interior design with exterior views of controlled landscaping and near vistas, made a deep impression on modern American architects.

Traditional residences are primarily of two types: the detached upper-class residences, and, less well know in the West, the traditional city rowhouses or machiya, which incorporate spaces for living and selling [Tingey, 1981; Durston, 1987; Shimamura and Suzura, 1993]. These wooden structures have narrow street frontages of about 24 feet in which the store or restaurant is located, often entered through a toriniwa or stone walkway which leads both to the shop and back into the more private areas of the house which include rooms usually facing a rear garden. The construction system of the machiya is nearly identical to that of traditional residences. Many traditional machiya and updated Meiji (1867-1912) versions still stood in the Kobe area before the 1995 earthquake.

Behind both types of structures at the end of the lot often stands a kura, a special storehouse to be used when earthquakes, fires, or hurricanes threaten [Itoh, 1974; Treib, 1976]. Built to be stronger than the Japanese house, the storehouse was intended to serve as a receptacle for the transfer of valuables when disasters were imminent. Several different types of kura can be found in Japan. In this area the kura is of the dozo type. a two story gabled storehouse with an interior framework of heavy timber coated with clay and covered with a fine plaster finish. The deep clay walls, tile roofs and shutters protected contents from fire. The heavy timber construction lashed or pieced together with complex joinery and encapsulated in deep clay walls could resist hurricanes as well. But these stout heavy structures could not resist seismic damage and failure.

Preceding page blank

5.2 GENERAL OBSERVATIONS ON THE PERFORMANCE OF TRADITIONAL STRUCTURES

A large number of traditional structures in downtown Kobe, and in Ashiya, Nishinomiya, and Nagata collapsed during the earthquake causing loss of property and death. Traditional construction accounted for the vast majority of the fifty-five thousand wooden buildings that collapsed and the thirty-two thousand partially destroyed in the earthquake [AIJ, 1995]. Rowhouses, residences, and stores performed poorly, causing most the five thousand earthquake casualties [AIJ, 1995]. The cause of this poor performance of traditional wooden construction lay in both the design of the structures and their deteriorated condition.

It appears that the aesthetic virtues of traditional Japanese structures praised by Western architects are the very features that undermine their structural integrity and make them vulnerable in earthquakes: delicate post and lintel construction, flexible plans and indoor-outdoor permeability created by screens and shutters. Many suffered major cracks in exterior walls and appeared out of plumb. All had some form of damage to their roofs. The heavy tile roof in which tiles are bedded in two or three in inches of loose sand is designed to mitigate against fires and hurricanes. But it rests upon a structure which cannot resist the lateral forces such a weight generates. Further, if the roof is asymmetrical it often has little lateral integrity to work as diaphragm in distributing forces.

The heavy roof rests on a structure which may itself be "light", composted of 3 5/12 inch posts at 3 1/2 or 6 or 9 or 12 foot intervals with mortise and tenon joinery secured by wedges and/or toe-nailing. While many joints held others did not have the strength either to resist, or the ductility to transmit, lateral forces. They either disassembled or shattered.

The wooden post and lintel system, the "moment frame" of these structures, is not assisted by any shear walls and diagonal bracing is rarely present. When diagonal braces occur they are usually found at the corners of a building, attaching the corner posts to the floor plate. Commonly walls are constructed of a lath which is applied a light armature of tied bamboo over which a fine mud plaster is applied. This kind of wall, while it looks beautiful, can develop no shear. The very few walls are useless in earthquakes.

The supporting posts often sit on a brick foundation or simply on the ground secured by the force of gravity alone. Traditional Japanese houses are often raised above the ground several feet to promote the flow of air under the ground floor. Continuous foundations are therefore rarely present. In the instances I saw there were no continuous foundations nor were there anchor bolts or brackets to secure the posts to the foundation. As at the roof level, the buildings were not tied together.

The earthquake appeared to have shaken the buildings back and forth until the weight of the roof acting on the joinery caused it to break and to settle out of plumb or to fall apart. In the worst cases the structure either collapsed straight down in a telescope fashion or more commonly fell to the side where it either hit a neighboring structure or dropped to the ground.

The stores in central Kobe, because of their narrow, open first floors could be said to have collapsed because of a soft story problem. But in truth one could say that all traditional Japanese construction suffers from potential soft stories because of its design characteristics. In the case of

many buildings no diaphragms were incorporated in floors or roofs. There was no way to distribute the unequal torsional loads often generated by asymmetrical plans.

The dozo style kuras fared little better than the residences and machiya. The kura walls formed a mass which was too heavy for its wooden framework to stabilize. The narrow two story kuras rocked back and forth shedding their clay and plaster covering. Many stood out of plumb and I found several had collapsed entirely.

In several of the collapses surveyed it was obvious that the connections had rotted or had extreme termite damage. Whatever strength the structural system has depends upon its connections. Compromised by rot or insect infestation these structures have no capacity to resist earthquakes. A number of the rowhouses in downtown Kobe and in other areas were occupied by low-income tenants and owners, undoubtedly factors in why these structures were poorly maintained. However, as previously stated, the connections themselves were suspect, even without rot and insect infestation.

5.3 THE TAKAHASHI/KAWAI HOUSE IN ASHIYA

The Takahashi/Kawai house (hereafter the Takahashi house) illustrates how a traditional Japanese house failed in the earthquake. Like many badly damaged traditional structures the house has since been demolished leaving photographs as the only records of how it fared.

The Takahashi house was located on alluvial soil one block east of the Miyagawa River between the Hanshin highway on the south and the Kokudo National Route 2 highway on the north in the Uchidekozuchi-cho neighborhood of eastern Ashiya. The wooden house had a garden on south and east sides. To the north, adjoining the wooden house, is a post-war reinforced concrete house also owned by the family which suffered little damage in the earthquake and still exists. To the west an apartment building, which also suffered no damage in the earthquake, hovers just beyond the property line. Between the Takahashi house and the apartment building is a concrete wall erected by the apartment house owners over the objections of the Takahashis.

The Takahashi house was an adaptation of the shoin style. Shoin literally means writing desk and first appeared during the Muromachi period in reference to study areas used by abbots in Zen monasteries. These study areas broke down the formality of the earlier shinden style halls. In the shoin style the proportions of the dwelling were based on the tatami mat, which covered the entire floor. The Takahashi house incorporates characteristic shoin style features: the decorative alcove (tokonoma) in the formal main room with its staggered shelves (chigaidana) and built in desk (tsukeshoin); the structure supported by square posts; and the coved, decorated ceiling of the formal room. Interior spaces can be divided by pulling shut plain or shuttered screens (fusuma) while the garden vista can be closed by shoji screens or heavy wooden panels (amando), the last of which are now shut in as can be seen in the photographs of the house illustrated here. The main room is flanked by two rooms to the north. There is a second story above the main room and a second story addition overlooking the garden to the east of the main room. On the northwest corner of the property is the family kura.

The construction system of the house was traditional post and beam with unreinforced mud and bamboo walls. The beautifully crafted posts and beams were joined by mortise and tenons and

were spaced to support maximum spans to provide the open areas so vital to the shoin style dwelling. At the time of the earthquake the joinery was in excellent condition showing no signs of insect infestation or dry root. Terra-cotta tiles typically found in the Kyoto-Osaka area were placed in a bed of sand on the roof.

During the earthquake the building oscillated in the east-west direction. As it fell in an apparent final collapse to west the entire back wall hit the contested concrete wall on the property line. The wall arrested the collapse saving the matriarch of the family sleeping on the first floor, but utterly shattering the walls of both the house and its kura. Mortise and tenons seem to have completely separated, wall joints toe nailed in place or secured with wedges uncoupled. The mud, sand and bamboo walls shattered. Every connection in the house was badly strained or broken, not a wall or floor remained plumb. The kura shook loose its mud covering laying bear the heavy timber construction.

Before condemning the traditional construction of the Takahashi house it is important remember that there were high accelerations in this area: the box girders of several modern steel and concrete megastructures at Wakaba-cho just a kilometer south snapped apart. A block north the bottom floor of a reinforced concrete apartment building collapsed. Also within a kilometer to the east the Hanshin elevated highway collapsed. Yet across the street from the Takahashi home several steel and wood prefabricated residences survived unscathed.

After examining the poor performance of traditional wooden buildings we might ask why they were not constructed to be more seismically resistant. The building practices in the Kobe area are not so different from those throughout Japan. In this country where earthquakes are so common why has traditional architecture apparently failed to respond? The answer to this question is complex and multifaceted, cultural as well as technological. I present only a few preliminary observations here which I hope to investigate in more depth.

5.4 DISCUSSIONS OF TRADITIONAL ARCHITECTURE

The literature on the seismic resistance of traditional wooden construction is scarce. Two representative commentaries on traditional Japanese architecture mention natural disasters like earthquakes in their discussions of climate: "Japanese architecture came into being under a feudal regime, in damp climate; it makes use of perishable and replaceable materials, which have to be light in weight on account of the earthquakes" writes André Corboz [Corboz]. Heinrich Engel in his fundamental text, The Japanese House---A Tradition for Contemporary Architecture, argues that since earthquakes "afflict man and his buildings in a manner similar to that of the seasonal storms, that are, in an architectural sense, of the same environmental nature." Engel lists earthquakes along with typhoons, heavy precipitation, snowfall and humidity as problems [Engel, 1964].

Adaptation to climate makes traditional Japanese architecture very dangerous in earthquakes. The structures are often raised on stilts to avoid humidity. The interiors have as few walls as possible to provide maximum ventilation during insufferably hot summers. Shoji screens can be shifted or removed to provide visual privacy while causing little impediment to the circulation of air. In the winter the shoji screens and shutters can be remounted providing some insulation, but certainly not the kind of warmth westerners might expect. Heat is provided by

portable charcoal braziers and kerosene and electric space heaters which were so deadly in starting fires during the Hyogoken-Nanbu earthquake.

Engel points out that Japanese residential construction is as delicate as it seems and not adapted to either typhoons or earthquakes: "The entire framework, owing to the lack of any diagonal bracing members, is susceptible to the slightest horizontal stress, the danger of which is aggravated by a fatally high point of gravity due to the overly heavy roof. Indeed, the Japanese house in a typhoon is like a house of cards in a draft." Similarly Engel finds an absence of any measures to counteract the effects of earthquakes and doubts whether the Japanese even considered the elasticity of wood in relation to seismic resistance.

> [The] lack of lateral stability in the framework certainly must raise doubts as to whether the Japanese chose wood material because they realized its advantages in the face of earthquakes. Rather, it seems that the Japanese actually were never really aware of the structural advantages of wood...In spite of continuously recurring earthquake damage, the over-dimensioned roof construction and heavy roof load of clay tics and clay joinery have been maintained, without any visible attempt to reduce the dangerous top weight or to increase the dimensions of the undersized vertical members, or to brace the latter by rigid diagonal members. Even minor horizontal earthquake shocks, thus, may easily become fatal..." [Engel, 1964]

Japanese authors also discuss earthquake resistance in traditional structures summarily and fatalistically. Teiji Itoh uses the example of the great Kyoto earthquake of 1830 to illustrate a Japanese attitude toward seismic disaster. So forceful was the earthquake that it collapsed the wood and mud storehouses (or kura) of the rich prompting the common people to write comic epitaphs on the broken walls ridiculing the structures and their owners. Itoh concludes:

> This no doubt would not have happened if such destruction from earthquakes had been a common occurrence. It is precisely because the earthquake was of unprecedented violence that people felt moved to joke about the fallen storehouses. Perhaps we may see in this an example of the Japanese attitude toward earthquakes: They are unpredictable catastrophes that must be coped with by the human spirit, not by the structure of buildings [Itoh, 1974].

5.5 SAFETY IN TRADITIONAL JAPANESE ARCHITECTURE

The extent of the incorporation of consciously anti-seismic features in traditional wooden buildings is an unresolved question As early as the late 18th century the Jishin-den, or Jishin-goten, the Earthquake Palace or Earthquake House, was constructed in the gardens of the Kyoto-Gosho, the Imperial Palace of Kyoto [Fujioka, 1956]. There is no doubt that whoever designed this structure wanted to make it earthquake resistant. It lacks the raised floor and heavy roof which are dangerous in earthquakes and incorporates a continuous foundation and oversized timbers for strength and continuity. During the Meiji period an active group of engineers and seismologists tried to design earthquake resistant buildings, among them John Milne and F. Omori [Milne, 1886; Lawson, 1910]. Milne experimented with base isolation and Omori with brick structures incorporating parabolic curves. After the Yokomana earthquake of 1880 Milne formed the Seismological Society of Japan and another temblor, the earthquake of 1891 spawned the

Earthquake Investigation Committee. This committee published guidelines for seismically resistant wooden buildings [BEIC, 1900]. Some authors have proposed that even before the 18th century and 19th century wooden buildings had been built to incorporate seismically resistant features [Tanabashi, 1960]. For example, Japanese pagodas are often built around a tall interior mast which hangs in the center supported by chains. As the pagoda oscillates in an earthquake the mast does not, acting like a damper to counteract drift. Sometimes the masts are fixed in the ground, helping to control excessive drift through their natural elasticity. Authors have also argued that the bracketing system imported from China helps distribute earthquake forces [Shiping, 1991]. But it is still unclear whether vernacular Japanese stores and residences were ever consciously designed to resist earthquakes.

Fire was a more urgent problem than earthquakes and fire-resistance added to the weight of Japanese roofs. As in the United States where brick buildings built to resist fires have become an enormous seismic problem, so in Japan where the mitigation of one danger has accentuated another. The Great Tenmei fire of 1864 destroyed nearly eighty percent of Kyoto, a city of wooden buildings. The wooden dwellings and stores in present-day Kyoto, the most historic of all Japanese cities, are no more than 120 years old. The great Ginza fire of Tokyo in 1872 illustrated the danger of wood and spawned the brick Ginza district. The cities of Osaka and Kobe developed their own fire regulations which stipulated terra-cotta roofing in 1909 and 1912 respectively [Ohashi, 1992]. Fire was still a major problem in Tokyo after the earthquake of 1923 which burned through the traditional structures of that city. The almost universal use of terra-cotta roof tiles bedded in sand in the Kyoto-Osaka area seems a sound fire mitigation method but the flammable screens, mats, and small wooden members in building interiors could provide highly combustible fuel.

Only comparatively recently have regulations and codes been enacted to protect wooden buildings in earthquakes. The use of braces in new wood houses was first required in the Building Standards Act of 1950. Code provisions for bearing walls and minimum ratios of wall areas to plan were introduced in 1960 and increased in 1981. Most likely the 1995 earthquake will spawn stricter more comprehensive codes.

5.6 FURTHER RESEARCH

This survey of earthquake damage to traditional Japanese stores and residences raises questions that call for further research. More historical research is necessary to be done to clarify the Japanese attitude toward earthquakes and to study how this attitude effected the design and construction of traditional structures. More testing of Japanese traditional houses and stores is necessary to understand their weaknesses and to suggestion retrofit strategies. Even after the imposition of new code requirements in 1981, present-day construction could still be improved by the addition of more tiedowns straps and stirrups, better floor and roof diaphragms, and better lateral bracing systems. I saw many failures of recently constructed buildings. A careful retrofit strategy using artfully designed metal connections would improve the performance of the frame by securing joinery. Perhaps a lighter roofing system which had the beauty and fire-resistance of terra-cotta tiles could be invented to reduce the weight of roofs. It is clear that in order to save lives in the future traditional Japanese construction techniques must adapt to modern anti-seismic technology. The challenge is to propose solutions that will not prejudice the aesthetics of traditional buildings and that will not increase their already high cost. Hopefully a retrofit strategy

can be devised before these traditional buildings, so much a part of the Japanese architectural heritage, are lost.

REFERENCES

[Tingey, 1981; Durston, 1987; Shimamura and Suzura, 1993] William R. Tingey, "The Principal Elements of Machiya Design," *Process: Architecture* (Tokyo, 1981), 25, pp. 83-102.
Diane Durston, *Kyoto; Seven Paths to the Heart of the City* (Kyoto, 1987).
Noboru Shimamura and Yukio Suzura's *Machiya of Kyoto* (Kyoto, 1993).

[Itoh, 1974; Treib, 1976] Teiji Itoh, *Kura, Design and Tradition of the Japanese Storehouse* (Seattle, 1974), pp. 31-35.
Treib, Marc, "The Japanese Storehouse," *Journal of the Society of Architectural Historians*, May 1976, Vol. 35, No. 2, pp. 124 -137.

[AIJ, 1995] *Preliminary Reconnaissance Report of the 1995 Hyogoken-Nanbu Earthquake* (English ed.), The Architectural Institute of Japan (April 1995), pp. 53-56.

[Corboz] André Corboz in Henri Stierlin and Tomoya Masuda, *Architecture of the World: Japan*, (Lausanne, nd), p. 5

[Engel, 1964] Heinrich Engel, *The Japanese House—A Tradition for Contemporary Architecture*, 1964, pp. 356-357.

[Itoh, 1974] Teiji Itoh, p. 35

[Fujioka, 1956] Michio Fujioka, *Kyoto-Gosho* (Tokyo, 1956), pp. 169-170.

[Milne, 1886; Lawson, 1910] John Milne, "On Construction in Earthquake Countries," *Minutes of Proceedings of the Institution of Civil Engineers* (London, 1886) 83, pp. 278-291.
Lady Lawson, *Highways and Homes of Japan* (London, 1910), pp. 250-258.

[BEIC, 1900] "Condensed Statement on the Construction of Earthquake-proof Wooden Buildings," *Bulletin of the Earthquake Investigation Committee in Foreign Languages* (Tokyo, 1900), 4, pp. 1-12.

[Tanabashi, 1960] Ryo Tanabashi, "Earthquake resistance of traditional Japanese wooden structures," *Proceeding of the Second World Conference on Earthquake Engineering at Tokyo and Kyoto, July, 1960* (Tokyo, 1960), pp. 151-163.

[Shiping, 1991] H. Shiping, "The earthquake-resistant properties of Chinese traditional architecture," *Earthquake Spectra*, (1991), 7, pp. 355-389.

[Ohashi, 1992] Yuji Ohashi, *The History of Structural Codes of Buildings in Japan* (Tokyo, 1992), pp. 51-52.
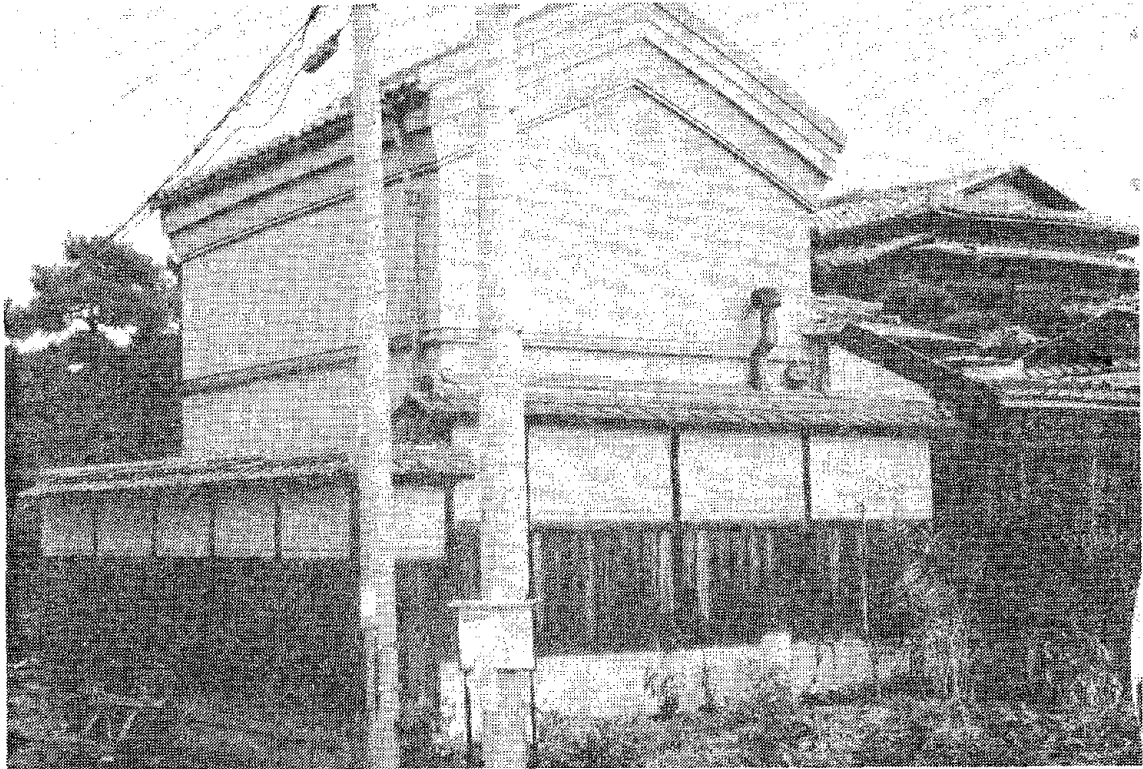
Fig. 5.1   Residence in Nishinomiya. The kura is in tact while the residence itself is damaged although remains standing. Note the disturbed roof tiles.
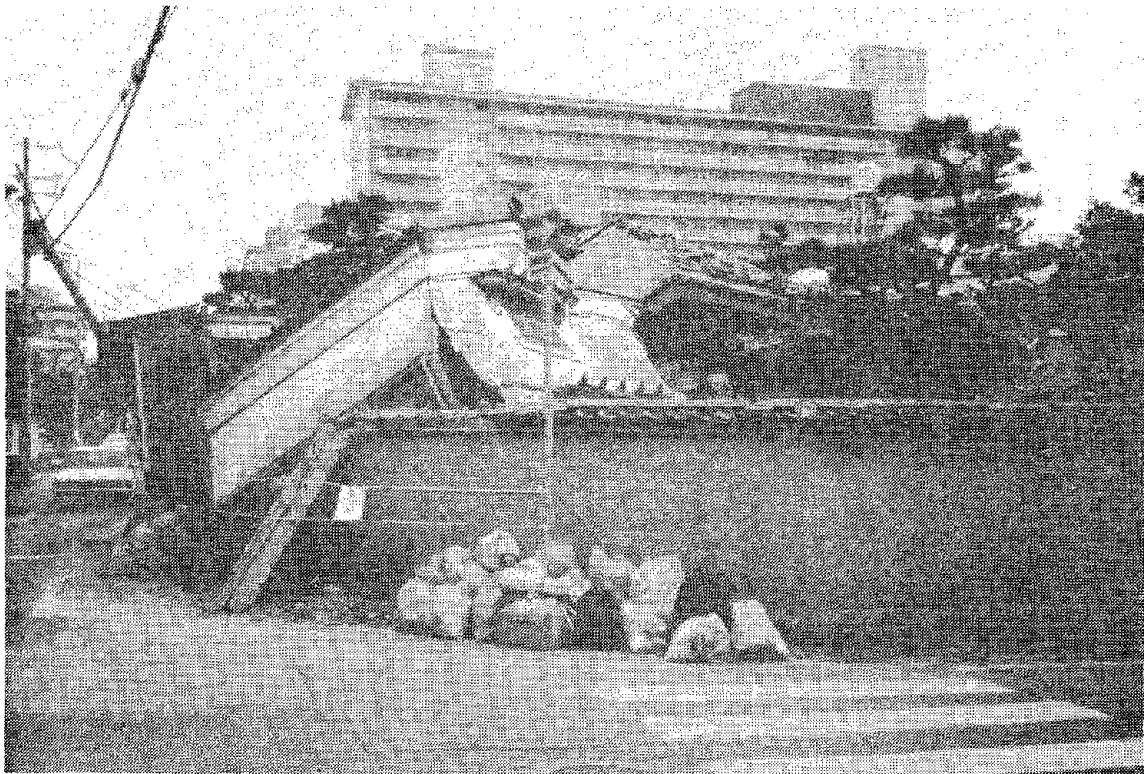

Fig. 5.2   Residence in Ashiya. The kura and residence have both collapsed in a northerly direction.

Fig. 5.3   The collapse of machiyas along the Kokudo route 2 in Ashiya. Note the collapses
seem to have occurred as buildings twisted under the weight of the tile roofs. (ill.:
Asahigraph, Special edition on Kansai Earthquake, February 1, 1995)

Fig. 5.4   Traditional machiyas in Tsuna-cho, on the northern part of the island of Awaji-shima.
Note the lack of diaphragms in the roofs. The machiya at the bottom left resembles a
classic Kyoto machiya. The one in the central illustrates the long narrow lot with
residence behind. (ill. *Asahigraph, Special edition of Kansai Earthquake*, February
1, 1995)
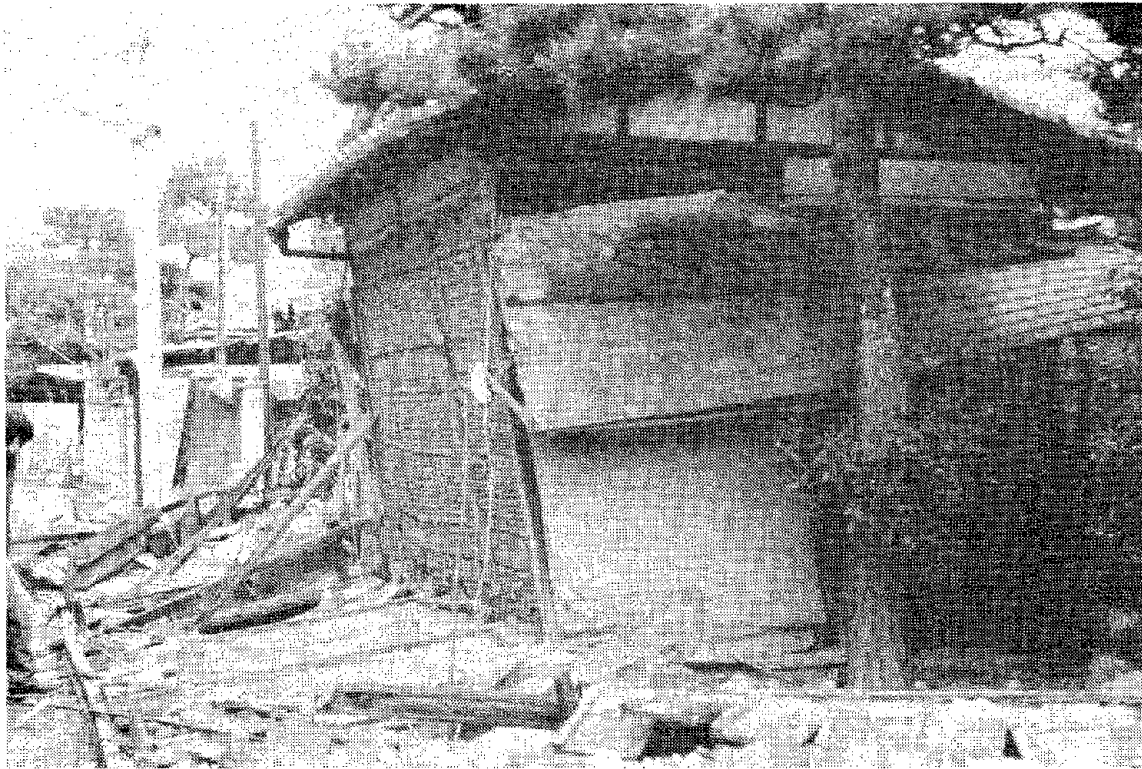
Fig. 5.5   Residence in Nishinomiya. The collapsed wall of this teahouse illustrates typical frame and wall construction.
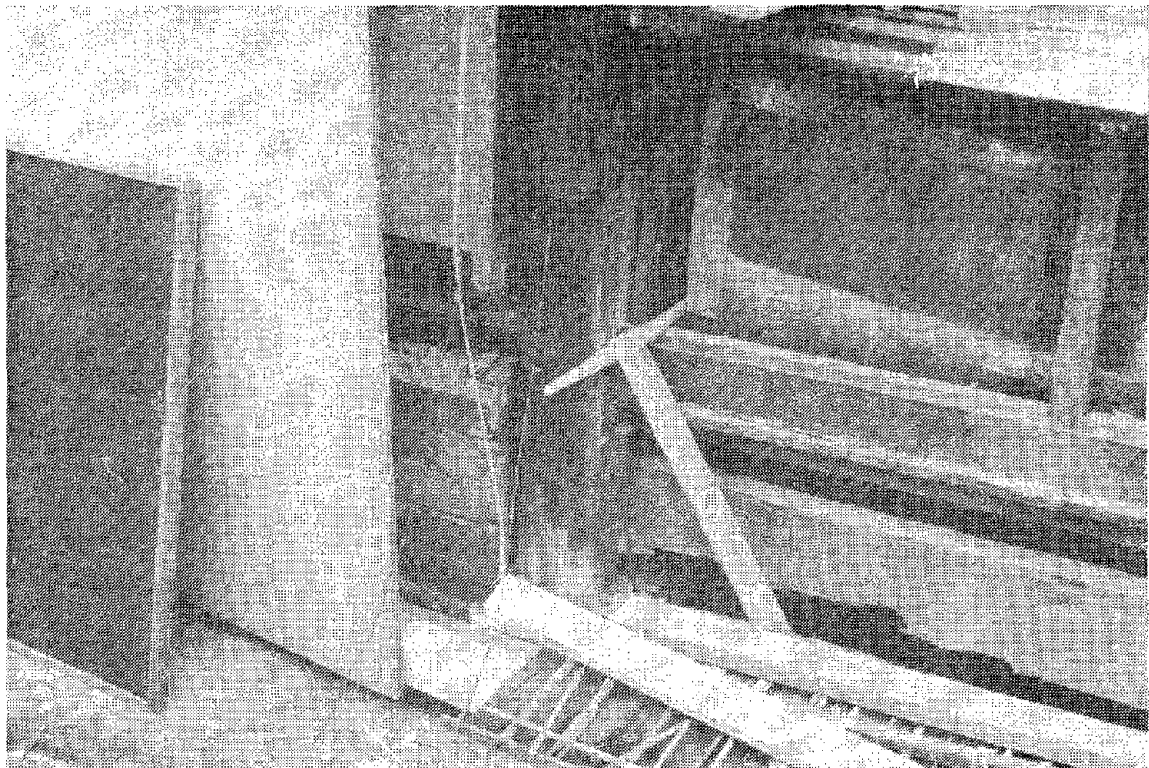
Fig. 5.6   Residence in Nishinomiya. Detail of post illustrating lack of ties between foundation and post.

70

Fig. 5.7   Machiya ruins in Ashiya. The lack of metal fasteners, plywood and plastic and the
abundance of small pieces of wood, sand, and terra-cotta make these structures
completely recyclable.

Fig. 5.8   Machiyas still standing but gravely damaged in Ashiya. Each demonstrates the effects
of soft stories.

71
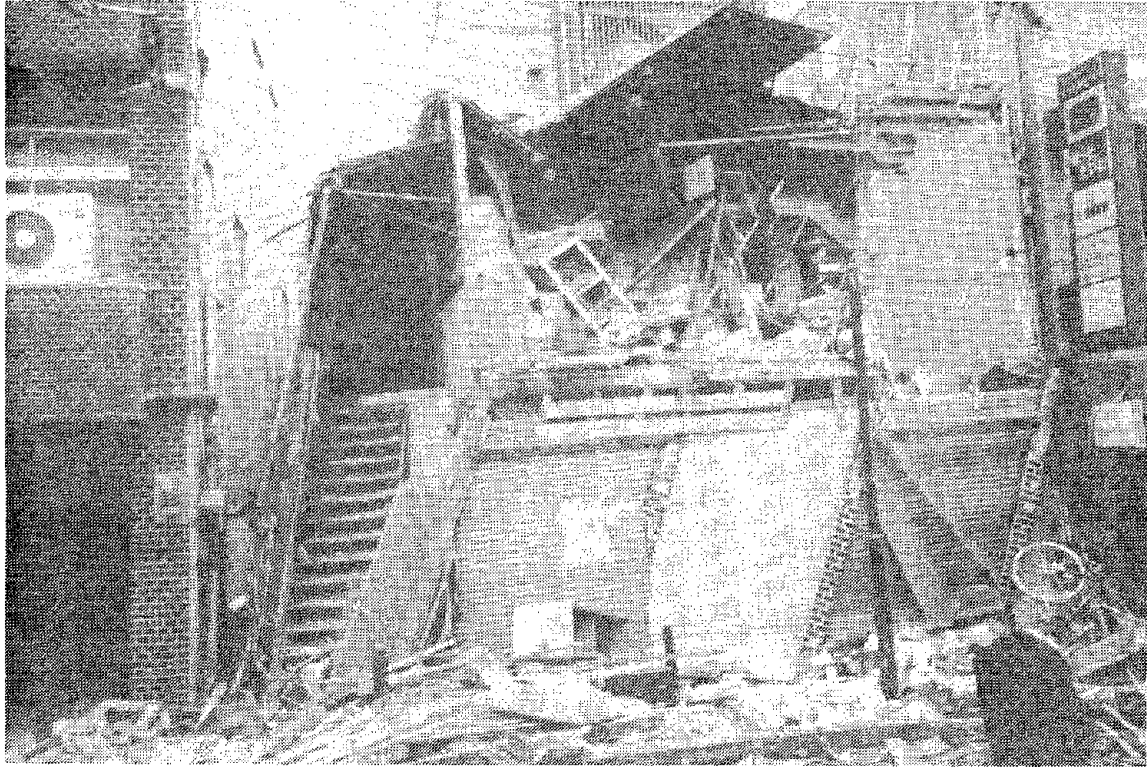
Fig. 5.9   Modernized machiya of traditional construction in downtown Kobe. Soft story collapse.
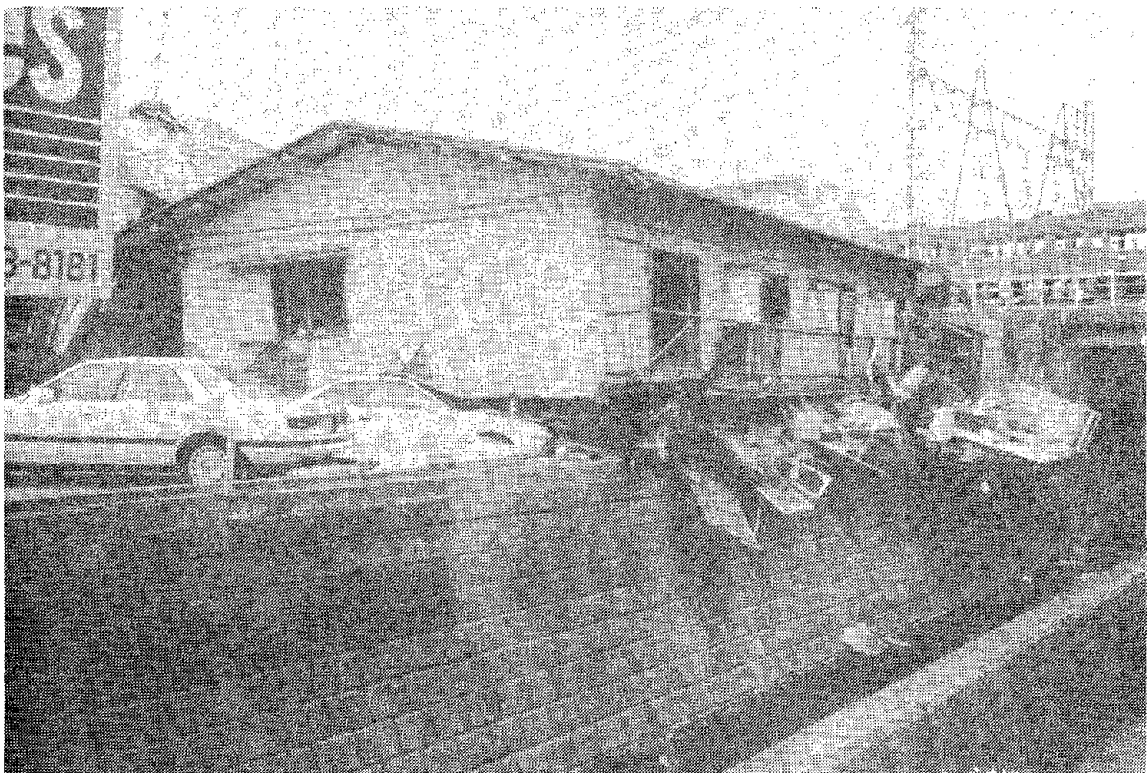
Fig. 5.10   Soft story failure in Ashiya.
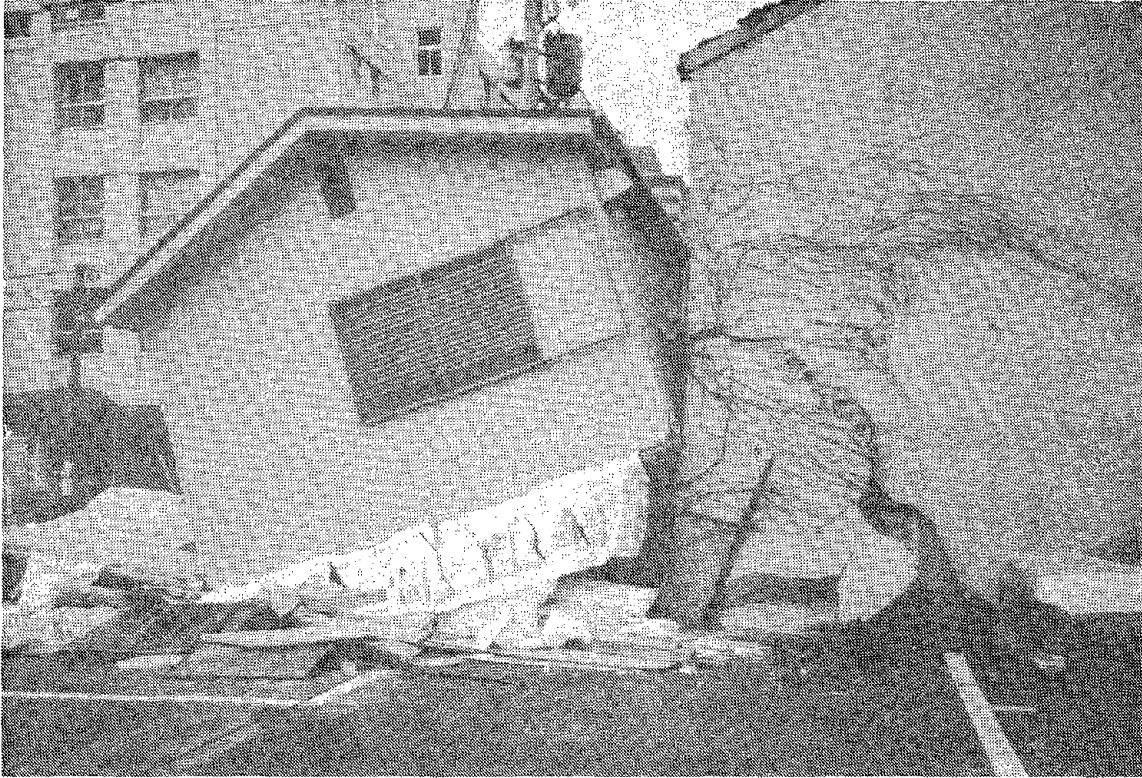
Fig. 5.11   Soft story collapse of newly constructed building in Ashiya which slammed into older structure next door.

Fig. 5.12   Detail of Fig. 11 illustrating the uncoupling of mortise-tenon. The system could not sustain the lateral forces and the mortise detached from the tenon although it was extensively nailed.

Fig. 5.13   Machiya in downtown Kobe. Detail of termite-damaged connection.
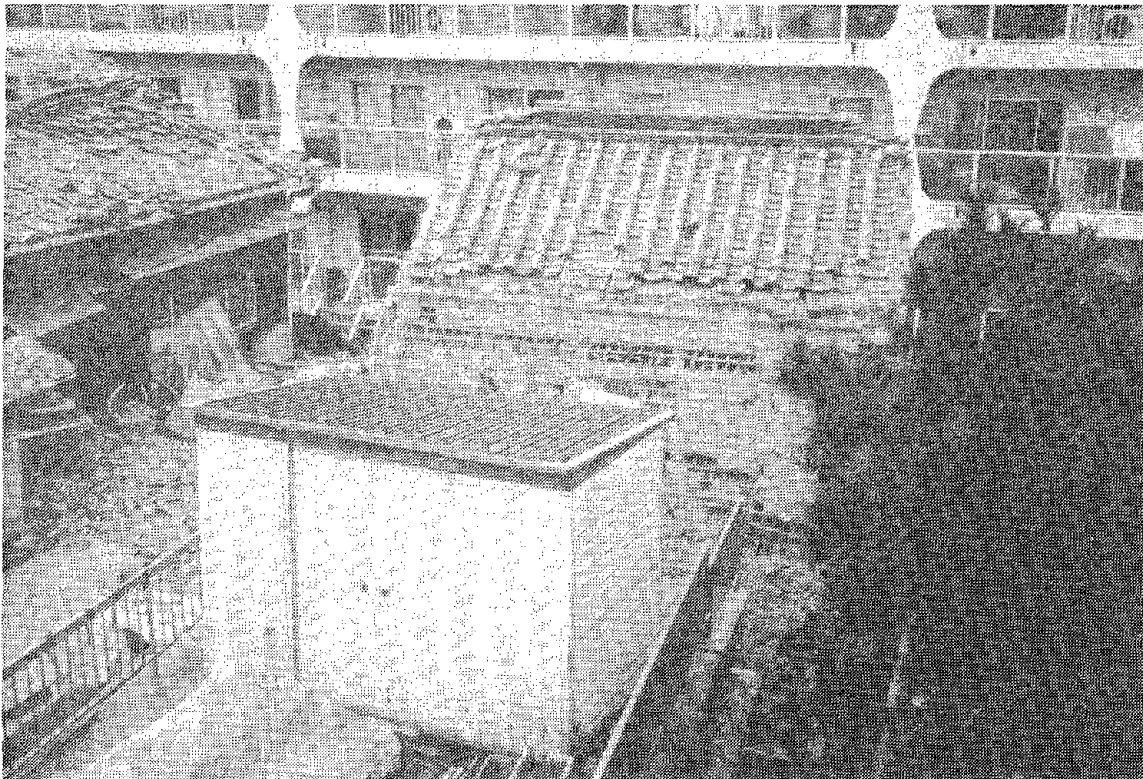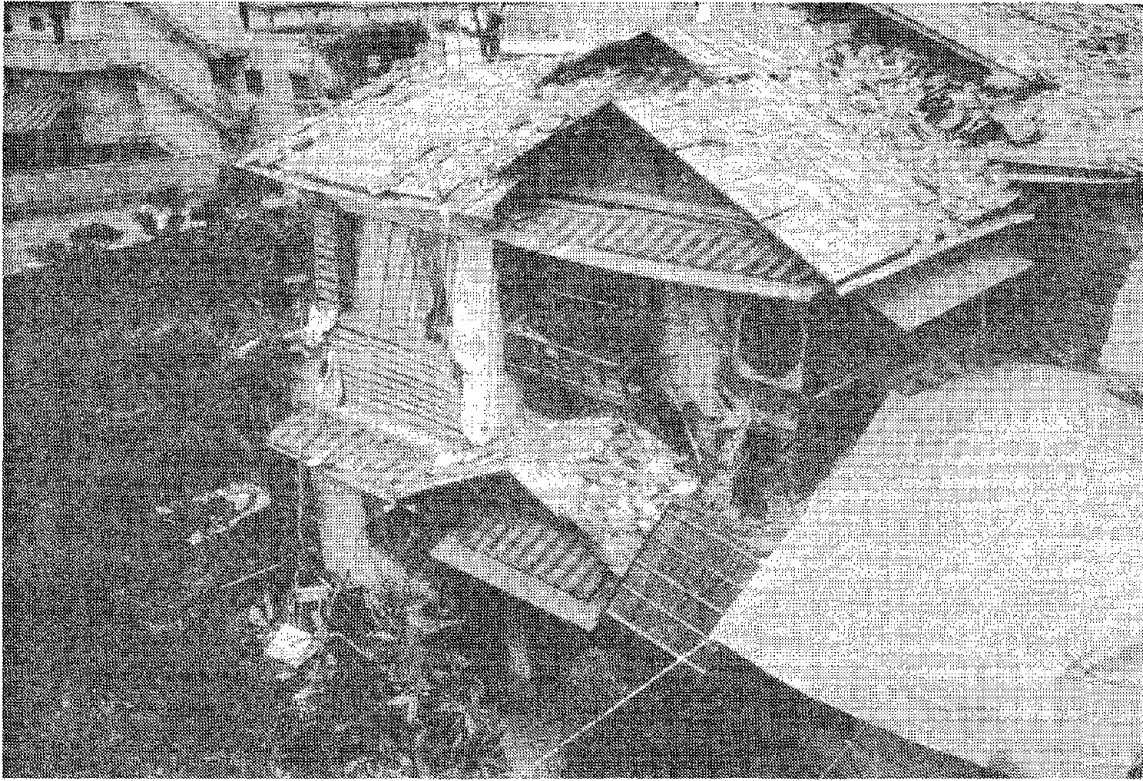
Fig. 5.14 and 5.15 Takahashi/Kawai house in Ashiya. View from the roof of the reinforced concrete house looking west. The traditional residence is on the left, the *kura* on the right.
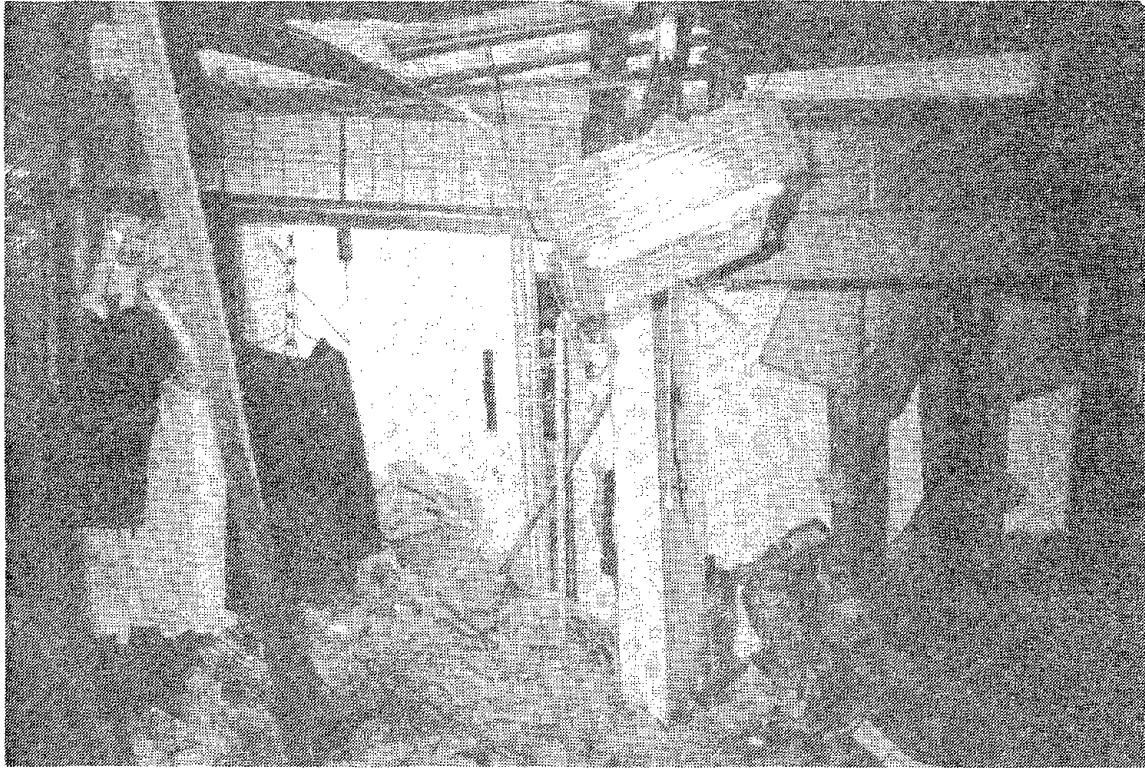
Fig. 5.16   Takahashi/Kawai house. View of northeastern room on ground floor.
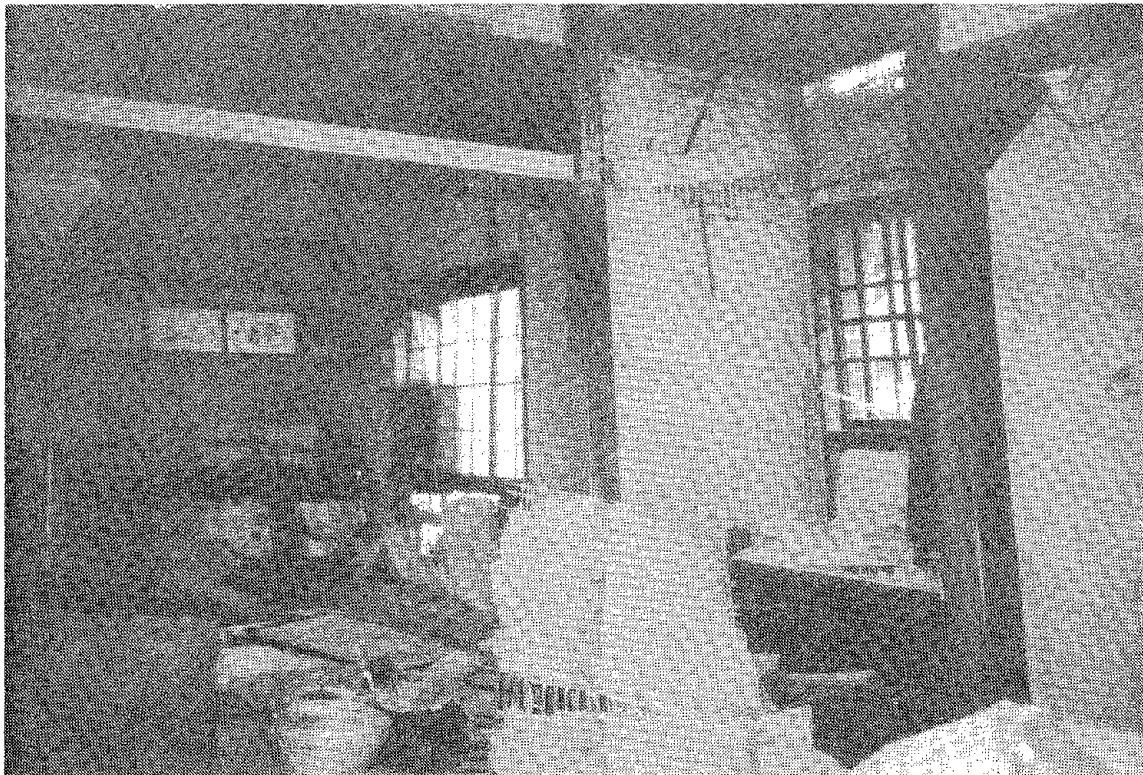
Fig. 5.17 and 5.18 Takahashi/Kawai house. View of second floor.
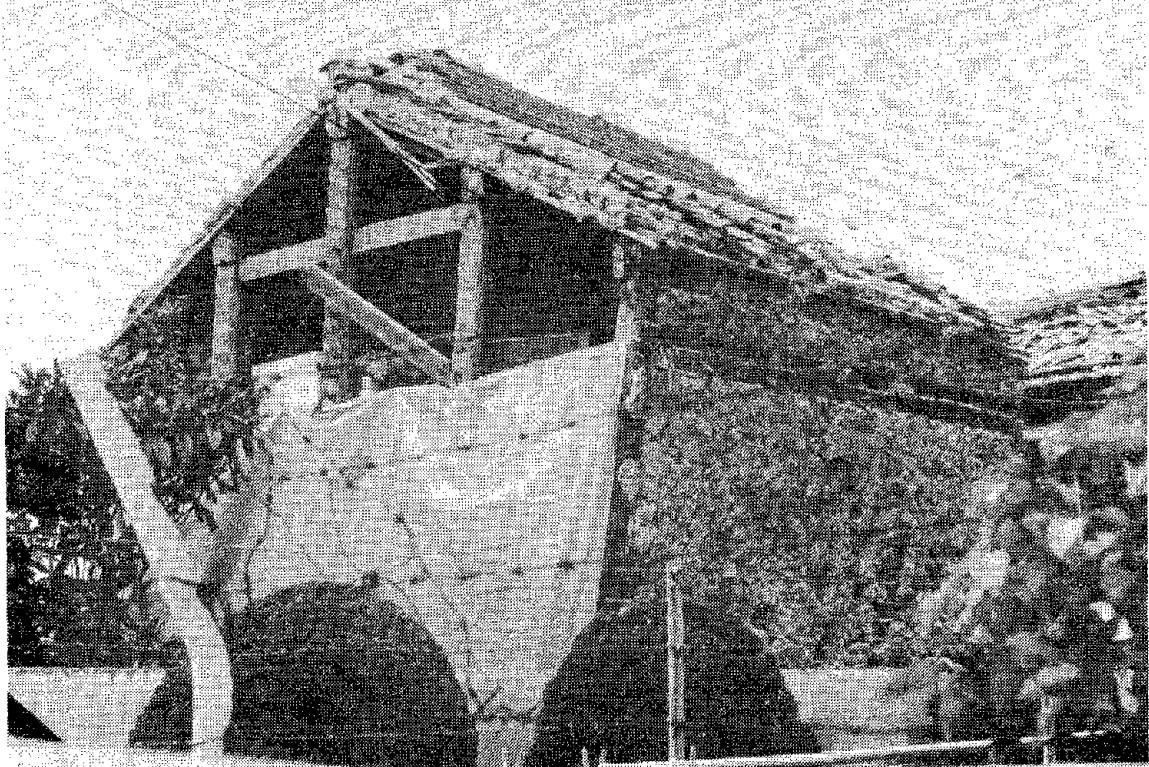
Fig. 5.19   Takahashi/kawai house. Ruined *kura* from adjacent property looking south.
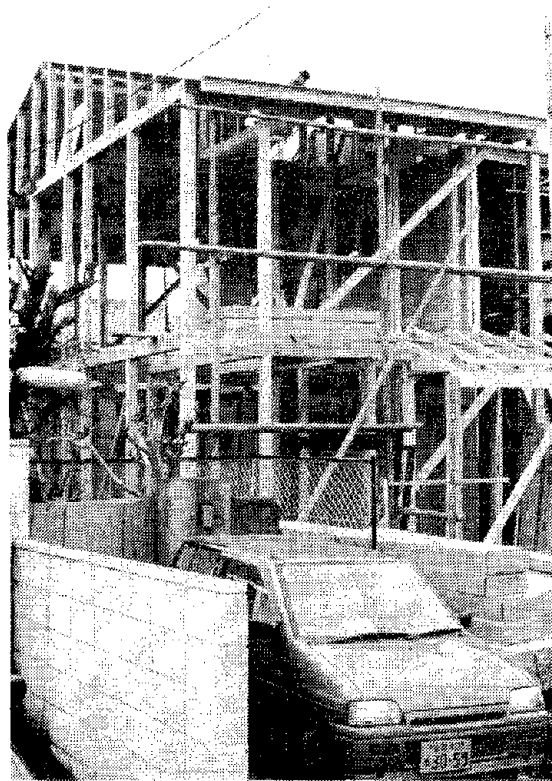
Fig. 5.20   Wooden house under construction. Some diagonal bracing will probably be installed later.
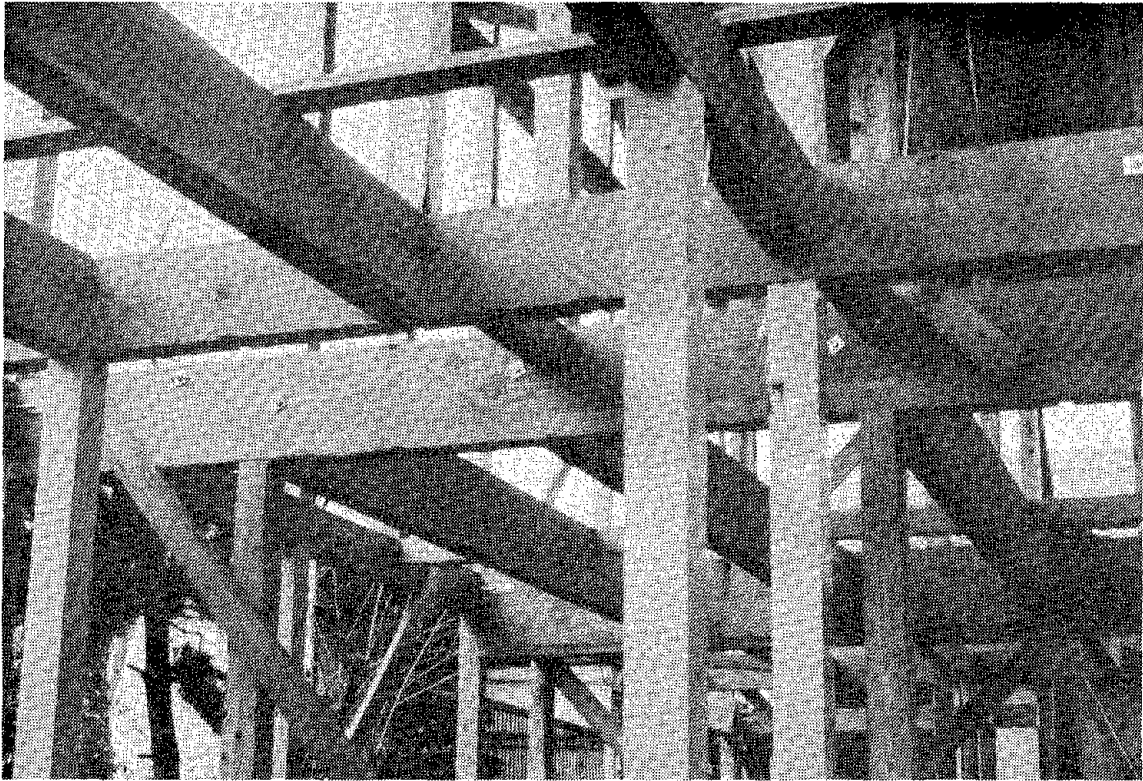
Fig. 5.21　Wooden house under construction. Connections could be made more secure with greater use of metal fasteners.
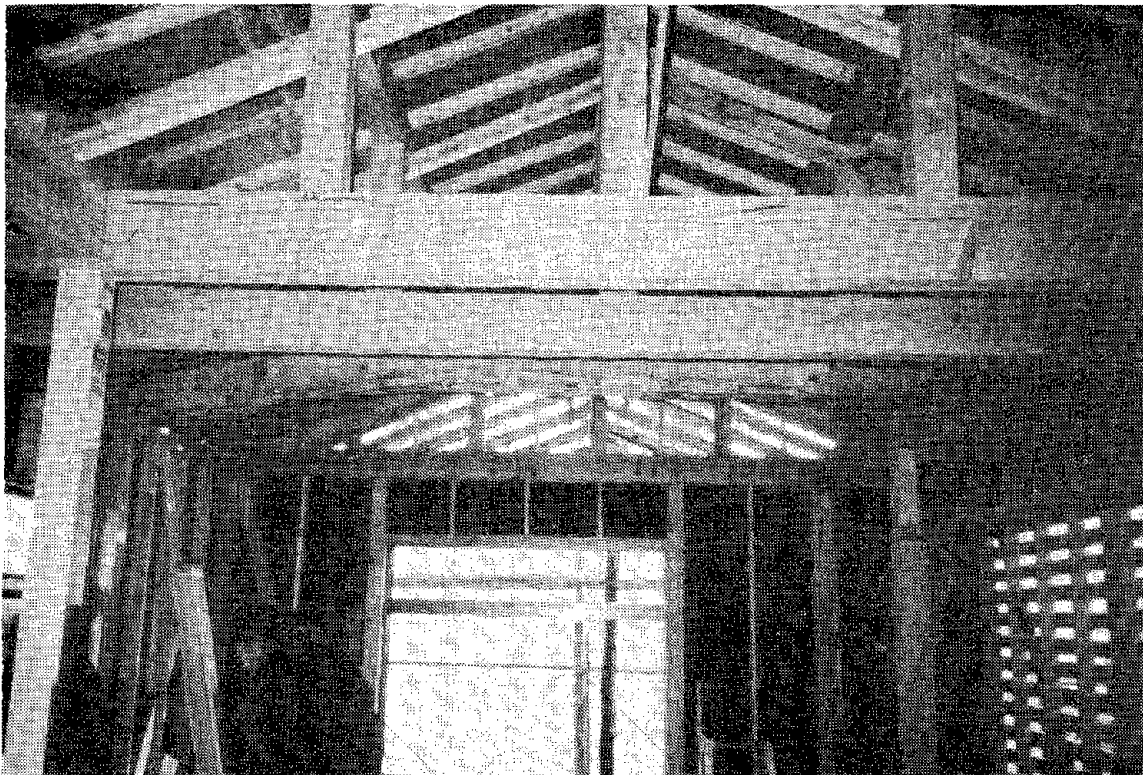
Fig. 5.22　Wooden house under construction. Could metal fasteners and plywood sheathing be added to this structure without sacrificing its aesthetics?

CHAPTER 6

ENGINEERED BUILDINGS

6.1 INTRODUCTION

The widespread destruction of the built environment in and around Kobe was unexpected by many design professionals, academicians, and researchers, both in Japan and the United States. The goals of this chapter are to (a) describe the distribution of damage to engineered buildings in the Kobe region, and (b) detail the observed behavior (response) of prevalent seismic framing systems.

The information presented in this chapter was collected in the field by the members of the NSF buildings reconnaissance team, and from a number of other sources including Professor Nakashima at Kyoto University, the Building Research Institute, and the report on the Kobe earthquake prepared by the Architectural Institute of Japan (AIJ) [AIJ, 1995a]. The NSF buildings reconnaissance team made three trips to Japan between late January and mid March, 1995. Because the damage to buildings was so widespread, the reconnaissance teams concentrated their efforts in the Hyogo, Chuo, and Nada Wards in Kobe City, and in the cities of Ashiya and Nishinomiya (see Figure 6.1 [RMS, 1995] for details). Detailed descriptions of building damage in the Tarumi, Suma, Nagata, and Higash-Nada Wards in Kobe City, and in the cities of Takarazuka and Amagasaki, are available in [AIJ, 1995a; AIJ, 1995b].

Damage and collapse of buildings in California due to earthquakes have often been described in terms of the codes of practice enforced at the time of construction. Similarly, damage to engineered buildings in the Kansai region is described and categorized as a function of Japanese design standards. To facilitate the discussion of the type, degree, and demographic distribution of the damage, an overview of the development of both Japanese seismic codes and seismic building construction is presented in Section 6.2.

Engineered buildings were most heavily damaged in the narrow zone adjacent to the JR railway line running through Kobe and along the edge of Osaka Bay. The distribution of the building damage is described in Section 6.3.

For the purposes of this chapter, buildings are classified in terms of one of two construction materials, namely, reinforced concrete and structural steel. Reinforced concrete construction is assumed to comprise moment frames, structural walls, frame-walls, and steel reinforced concrete (SRC) construction. Structural steel construction is composed of moment frames and braced frames. In Sections 6.4 and 6.5, typical failure modes, seismic deficiencies, and the response of a select number of buildings composed of reinforced concrete and structural steel, respectively, are described. Response of the selected buildings is examined in terms of the design and construction standards enforced at the time of their construction and the probable levels of ground motion experienced by the building. Failure modes of selected components in these

Preceding page blank

buildings are identified wherever possible; speculative causes for building collapse are not presented in this report.

Two seismically isolated buildings are located approximately 35 km (21 miles) from the epicenter of the Hyogoken-Nanbu earthquake. The behavior of these buildings during the earthquake, and the efficacy of the seismic isolators in reducing the response of these two buildings, are reported in Section 6.6.

Section 6.7 presents information on the behavior of nonstructural components, including cladding, and elevated intra-building walkways (also referred to as air-bridges). Much of the damaged construction in and around Kobe was not engineered for seismic resistance. Damage to this class of construction is summarized in Section 6.8 with specific reference to light-steel framed and masonry construction.

Section 6.9 summarizes the damage to engineered buildings in Kobe, makes recommendations regarding the need to retrofit nonductile construction in both the United States and Japan, and draws preliminary conclusions in regard to the likely impact of this devastating earthquake on seismic design and construction in both countries.

6.2 DEVELOPMENT OF JAPANESE CODES AND BUILDING CONSTRUCTION

6.2.1 DEVELOPMENT OF JAPANESE BUILDING SEISMIC REGULATIONS

The modern era of Japanese building construction (chronicled in Table 6.1) can be considered to have had its origin with the end of the Edo Period and the Meiji Restoration in 1868. At this time, Japan was eager to embrace foreign culture and sciences, including adoption of some foreign building construction practices. The AIJ (Architectural Institute of Japan) was formed in 1886, and by 1888, the first city planning legislation was in place. Formation of the Earthquake Investigation Committee following the 1891 Nobi earthquake was an early step toward developing modern earthquake resistant construction technology in Japan [Ishiyama and Ohashi, 1990].

Observations on building performance in earthquakes during this period strongly influenced development of modern earthquake engineering construction [Otsuki, 1956]. Masonry construction, introduced in the British form to reduce fire hazards associated with traditional wood construction, suffered many collapses in 1891 and 1894 earthquakes, slowing development of this construction form. Following the 1923 Great Kanto earthquake, engineers noted that steel frames withstood earthquake loads but did not withstand the subsequent fires, contributing to development of SRC construction in which reinforced concrete encloses structural steel sections. In the same earthquake, observations of poor performance of reinforced concrete construction without hooks at ends of reinforcement led to abandonment of this practice. Generally good performance of wall buildings in the Kanto earthquake contributed to development of this construction form.

Table 6.1 - Some Events in the History of Japanese Seismic Code Development

Date	Event	Code Change
1868	Meiji Restoration - Japan sets course of modernization.	
1886	AIJ founded.	
1888		First city planning legislation in Japan.
1891	Nobi earthquake (M7.9) causes extensive damage.	
1892	Earthquake Investigation Committee founded.	
1894	Earthquake shakes Tokyo and causes damage.	
1906	San Francisco earthquake (M8.3).	
1915	Sano proposes concept of seismic coefficient.	
1919		City Planning Law and Urban Building Law enacted for six major cities. First structural standards.
1923	Great Kanto earthquake (M7.9) and fire.	
1924		Urban Building Law adds article to require seismic coefficient of 0.1. Height limit of 100 ft unchanged.
1925	Earthquake Investigation Committee re-chartered as the Earthquake Research Institute.	
1933	Muto proposes D-value method to calculate stresses under horizontal forces.	
1943		Urban Building Law suspended except for some fire restrictions. Relaxation of allowable stresses due to wartime shortage of construction materials. Dual allowable stresses introduced.
1948		Urban Building Law restored.
1950		Building Seismic Law replaces Urban Building Law. Seismic coefficient increased to 0.2, allowable stresses under temporary loads set at twice the allowable stress under permanent loads.
1958		First standard for SRC.
1963		Height limit of 100 ft abolished. Ministry of Construction recommends use of SRC for buildings over 6 stories in height.
1964	Nigata earthquake (M7.5).	
1968	Tokachi-Oki earthquake (M7.9) causes heavy damage to RC buildings. First high-rise building constructed in Japan.	
1970		Steel code revised.
1971	San Fernando earthquake (M6.4).	Concrete code revised to require closer spacing of transverse reinforcement.
1972-77	Ministry of Construction project for development of new seismic design method, resulting in 1977 proposal.	
1978	Miyagiken-Oki earthquake (M7.5).	
1981		Building Standard Law changed. Main features include seismic coefficient that varies with period and two-level design.

In 1915, Toshikata (Riki) Sano introduced the concept of the seismic coefficient, which defines a lateral force for seismic design (V) as the product of a seismic coefficient (C) and the structure weight (W), that is,

$$V = CW$$

At this time, no specific guidance was provided on the value for the seismic coefficient [Otsuki, 1956]. The 1923 Great Kanto earthquake led to the addition of an article in the Urban Building Law to require that all buildings be designed for a seismic coefficient of 0.1.

The use of a seismic coefficient of 0.1, in conjunction with a materials safety factor of 3 on ultimate stress, was deemed sufficient for a building to withstand a major earthquake such as the 1923 event. The Urban Building Law, which applied to certain urban districts, was a landmark in seismic code development worldwide.

Introduction of the Muto D-value method in 1933 provided a means of calculating internal stresses for buildings under horizontal forces [Ishiyama and Ohashi, 1990]. The D-value method is similar to the portal method of analysis widely used in the United States prior to the advent of computers for structural analysis.

Wartime activities in the first half of the twentieth century had an important impact on building construction in all of Japan [Ishiyama and Ohashi, 1990]. Whereas World War I provided opportunities for rapid economic development in Japan, war conditions in the 1930's and 1940's had more adverse effects. During part of this period, because of a shortage of construction materials, allowable stresses were increased. In 1943, the Urban Building Law was suspended entirely, except for some fire restrictions. Bombing during World War II took a grim toll on many Japanese cities, and Kobe was not spared significant losses. As a consequence, the majority of medium- and high-rise building construction in Kobe dates from after this war.

Following World War II, the Urban Building Law was briefly restored, but was replaced when the new constitution mandated the use of the Building Standard Law. This law applied to building construction throughout Japan, as opposed to limited districts, and increased the seismic coefficient increased from 0.1 to 0.2. The net effect on proportioning materials was minimal, as there was a simultaneous increase in allowable stresses for materials. However, the increase in design lateral forces represented a significant change in overturning moment requirements. This effect was especially notable in the postwar building boom when many buildings were proportioned to be more slender than prewar buildings [Otsuki, 1956].

Later changes of significance included the abolishment in 1963 of the height limit of 100 ft. At the same time, the ministry of construction recommended that buildings over six stories in height should be constructed of SRC [Naka, Wakabayashi, and Murata, 1972].

A very significant change in the reinforced concrete code to require closer spacing of column transverse reinforcement was imposed in 1971 in response to heavy damage to reinforced concrete buildings in the 1968 Tokachi-Oki earthquake [Aoyama, 1993].

84

In the period from 1972 to 1977, the Ministry of Construction directed a project for development of a new seismic design method, resulting in a proposal in 1977 [Ishiyama and Ohashi, 1990]. The 1978 Miyagiken-Oki earthquake, which caused serious damage in Sendai and demonstrated the effects of a strong earthquake on an urban area, led to accelerated implementation of the Building Standard law in 1981. The Building Standard Law includes a seismic coefficient that varies with structural vibration period, and introduced a two-level design procedure. The first level design, which is similar to the design method used in earlier codes, is intended as a strength check for frequent, moderate events. The second level design, which had not been included in previous codes, is intended as a check for strength and ductility in a maximum capable event. This code was in effect at the time of the Hyogoken-Nanbu earthquake.

6.2.2 TYPES OF CONSTRUCTION IN JAPAN

Figure 6.2 [Aoyama, 1993] shows types of construction common in Japan and the number of stories typically used for each type. Not shown is masonry building construction, which is not widespread in Japan. As indicated, wood frame construction, commonly one or two stories in height, is the predominant form of traditional house construction. Reinforced concrete bearing wall construction is the most common form for apartment house construction; typical heights are from three to five stories, although it may be used up to eight stories. Reinforced concrete frames, with or without shear walls, are used for a variety of structures, with typical heights up to seven stories but recent examples exceeding 20 stories. Steel reinforced concrete (SRC) is common for a wide range of construction, and is most common for medium-rise structures above six stories in height. Steel structures may be used throughout the height range and are the most widely used form of construction for modern high-rise buildings.

Figure 6.3 plots the relative use of construction materials in building construction between 1953 and 1987 [Chiba, 1989].

Each of these construction forms and materials has its own development history. In many cases, the history is unique to Japan. Some key aspects of each are described in the following sections. The discussion emphasizes aspects that were predominant in the period from the end of World War II to the present, and therefore had most significance for construction in and around Kobe.

The growth in the Japanese economy was rapid in the 1960's. Two major international events held in Japan during this period were the 1964 Tokyo Olympics and the 1970 Osaka World Exposition. Significant infrastructure and commercial construction preceded these events, with the Tokyo-Osaka Expressway and the Shinkansen Railway Line being completed before the Tokyo Olympics, and the Hanshin Expressway and many commercial buildings in the Kansai region being opened before the World Exposition. Much of this construction in Kobe was damaged during the Hyogoken-Nanbu earthquake.

6.2.2.1 Wood Frame Construction for Traditional Houses

Traditional wood-frame construction for houses was relatively unchanged from the beginning of this century until the 1970's. Two forms were in widespread use, the older being Shinkabe and the more recent being Ohkabe. Prefabricated timber houses have lately become more popular [EERI, 1995].

Shinkabe construction uses a post-and-beam framing, with lateral resistance provided by a mud-filled lattice of bamboo in the walls. The need for additional bracing was recognized by the AIJ, although the specification merely recommended that such bracing, having dimension not less than half the column dimension, be placed wherever it would not impair the external appearance of the dwelling [AIJ, 1970]. In Ohkabe construction, the bamboo is replaced with a narrow-plank lathe, preferably placed on both sides of the wall, nailed to the posts, and covered with stucco. Diagonal bracing was also recommended. Connections between posts and beams is often by wood joinery rather than nailing or connectors. Roofs commonly consist of relatively heavy tile set in a thick mud mortar.

Information on the response of wood frame construction during this earthquake is presented in Chapter 7.

6.2.2.2 Reinforced Concrete Bearing Wall Construction

Observations of building performance following the 1923 Great Kanto earthquake revealed the value of constructing low-rise buildings with reinforced concrete bearing walls. Figure 6.4 depicts a typical example of bearing wall construction.

As described by the AIJ [1970], the design emphasis in bearing wall construction is on proper layout and proportioning of the structural system, as opposed to structural calculations. Minimum wall thicknesses were required to range from 120 mm (4.8 inches) or $h/25$ for one-story construction to 180 mm or $h/22$ for four-story construction. The required ratio of wall length (parallel each principal direction) to floor area was 15 cm/m^2 for the first story in four-story construction, and 12 cm/m^2 for all other floors. Web reinforcement ratios of 0.15%, 0.20%, and 0.25% were required for the top story, the second-from-top story, and all other stories, respectively.

Studies of building damage following the 1968 Tokachi-Oki earthquake suggested that bearing wall construction provides reliable protection against severe damage [Aoyama, 1981; Aoyama, 1993] (Figure 6.5). The abscissa in Figure 6.5 is the *wall area index* defined as the ratio of the total wall area (ΣA_w) in each principal direction of the building, to the total floor area (ΣA_f). The ordinate in Figure 6.5 is the *average shear stress* assuming 1g response; W is the reactive weight calculated using a floor weight of 10 KPa (209 psf); and ΣA_c is the total column area. The damage studies following the Tokachi-Oki earthquake suggested that (a) buildings falling outside the shaded rectangle bounded by a wall area index equal to 0.003 and an average shear stress equal to 1.2 MPa (8.3 ksi) would suffer slight to no damage, and (b) buildings falling

within the rectangle would suffer moderate to major damage. Aoyama [1993] reported that this proposal closely predicted damage to bearing wall construction in the 1978 Miyagiken-Oki earthquake.

The curves plotted in this figure correspond to limits defined in the 1981 Building Standard Law for bearing wall construction. Buildings with regularly configured walls whose parameters fall within the curve need not be checked for ultimate lateral strength (see Section 6.2.3.2 for additional information).

6.2.2.3 Reinforced Concrete Frame and Frame-Wall Construction

Reinforced concrete frame construction in Japan is commonly taken to include both pure frame construction and combined frame-wall construction. Although both types are prevalent, observations of the performance of reinforced concrete frames has led to recommendations to combine frames and walls [AIJ, 1970]. Wall construction may include solid walls framed by beams and columns, or walled frames that consist of deep girders and wide columns (Figure 6.6).

Concrete may include normal weight aggregate concrete or lightweight aggregate concrete [AIJ, 1970]. Apparently in the 1960's, the lower mass associated with lightweight aggregates led to some applications in seismic zones much as occurred in the U.S. at the same time. The AIJ Structural Standards of the time specified minimum strengths of not less than 135 kg/cm^2 (1920 psi) for normal weight aggregate concrete and 120 kg/cm^2 (1710 psi) for lightweight aggregate concrete. In the Osaka-Kobe area, builders began to use crushed stone for aggregate around 1970, and have used it exclusively since 1975. During the transition period, both crushed stone and river gravel were used [AIJ, 1995a].

Both plain (smooth) and deformed reinforcement have been used in Japan. Starting around 1960, builders in the Osaka-Kobe region began to use deformed bars for longitudinal reinforcement, and these became compulsory after 1970. Deformed transverse reinforcement was implemented about 6 to 7 years after the introduction of deformed longitudinal reinforcement [AIJ, 1995a]. Five grades of reinforcement were used in the 1960's, having minimum yield stresses of 24 kg/mm^2 (34 ksi), 30 kg/mm^2 (43 ksi), 35 kg/mm^2 (50 ksi), 40 kg/mm^2 (57 ksi), and 50 kg/mm^2 (71 ksi) [AIJ, 1970].

Some typical recommended details of pre-1971 construction are in Figures 6.7 and 6.8. These details include haunched beams with maximum transverse reinforcement spacing not to exceed 300 mm (12 inches) and either two-thirds or three-quarters of the beam depth (depending on the level of shear stress). Columns were required to have hoops with maximum spacing not exceeding (a) 300 mm (12 inches), (b) the minimum column depth, and (c) 15 times the diameter of the main reinforcement. Column reinforcement typically consisted of smooth longitudinal rebar with diameters ranging between 20 mm (0.8 inch) and 25 mm (1 inch), and smooth hoop rebar 10 mm (0.4 inch) in diameter. Walls were required to have minimum thickness of 120 mm (4.8 inches), and two layers of reinforcement were required where the wall thickness exceeded 200 mm (8 inches). The maximum spacing of wall reinforcement was 300 mm (12 inches). The maximum allowable shear stress was one-eighth of the concrete compressive strength [AIJ, 1970].

Common practice was to hook the ends of all reinforcement, although a trend away from the use of hooks was reported by Otsuki [1956]. In the 1960's, hooks were only required for plain bars, except that deformed bars required hooks in high stress areas and in stirrups and hoops [AIJ, 1970]. Reinforcement could be spliced either by lapping or welding. In recent decades, rebar splices have almost always been made by gas pressure welding [AIJ, 1995a]. In this process, bars are aligned, butted together, and fused by a combination of heat and pressure applied by mechanical devices, causing the bars to flare out at the splice.

In 1971, following damage to reinforced concrete construction in the 1968 Tokachi-Oki earthquake, there was a partial revision of the Building Standard Law and a large scale revision of the AIJ Standards incorporating ultimate strength design in shear of reinforced concrete [Aoyama, 1993]. Perhaps the most notable change in reinforced concrete construction was the reduction of the maximum spacing of hoops in columns to 150 mm (6 inches), except in column end regions where the maximum spacing was further reduced to 100 mm (4 inches). The requirement for 135° hooks on column hoops was also introduced at this time.

6.2.2.4 Steel Reinforced Concrete Construction

Steel reinforced concrete (SRC) construction in Japan grew out of observations of performance during the 1923 Great Kanto earthquake [Naka, Wakabayashi, and Takada, 1960]. Bare steel frame construction, while highly resistant to earthquake forces, was less resistant to fire. In steel frames encased in bricks, the bricks commonly failed, exposing the steel. Steel frames with concrete casing, or with walls, performed well. This led to an ascendance of SRC construction using steel encased in reinforced concrete — albeit for improving fire resistance rather than seismic resistance.

The original form of SRC construction, known as the full web form, used steel "I" or "H" sections. Later, in the interest of maximizing section modulus and minimizing rolled section consumption, built-up members composed of small steel sections became more common. The trend toward decreasing the amount of steel in SRC construction is shown in Figure 6.9 [AIJ, 1970].

Some examples of SRC construction details from the 1950's and 1960's are shown in Figures 6.10 and 6.11. The need for continuity of the steel framing members at joints was well established, and was provided using welded or riveted plates. Splice plates were commonly riveted or welded. Butt welds were considered unsuitable for field work at the building site [AIJ, 1970]. Two types of connection were common at the foundation level: a non-embedment type, where a steel base plate was anchored using anchor bolts, and an embedment type, where the steel extends into the reinforced concrete foundation with special detailing. In 1963, when the height limit of 100 ft (31 meters) was eliminated, the Ministry of Construction recommended the use of SRC for buildings over six stories in height. While it is unclear whether this recommendation led to a practice of using SRC for the first seven stories, with either reinforced concrete or steel used for the remaining stories, it was reported that many buildings over five stories had reinforced concrete in the upper floors supported by SRC in the lower stories [AIJ, 1995a].

The 1958 *AIJ Standard for Structural Calculation of SRC Structures* was the first standard for SRC in Japan. Until that time, many different types of SRC were built [Naka, Wakabayashi, and Murata, 1972]. Subsequent revisions were published in 1963, 1975, and 1987. The standard approach is to calculate allowable loads on SRC members as the sum of the allowable loads for the steel and the concrete sections, with the reinforced concrete component designed according to the reinforced concrete standard, and the steel component designed according to the steel standard except for less stringent requirements for width-to-thickness ratios. Because of observed superior behavior of full web construction in the laboratory, the 1975 revision to the SRC building code recommended full steel webs [AIJ, 1995a]. The 1987 revision recommends use of the embedment type steel base [AIJ, 1995a]. It also provides a method to evaluate lateral load resisting capacity as required by the 1981 Building Standard Law [Morino, Nishiyama, and Sakaguchi, 1994].

6.2.2.5 Steel Construction

Applications of steel in building construction grew rapidly in the years following World War II. According to Chiba [1989], early steel products were light gauge steel. The next developments took place around 1961 when rolling mills began to produce standard column and beam sections. Developments in welding technology enabled production of welded box sections beginning in 1969. Square hollow steel sections were first produced in Japan around 1977. Figure 6.12 shows annual production of various steel components.

With the introduction of higher strength steels (SS55, SM53, and SM58) by the mid-1960's, a wide range of steels was available for building construction. The building code defined allowable stresses as a function of a nominal stress limit (F), defined as the lesser of (a) the nominal yield stress, and (b) 70% of the nominal ultimate stress. The nominal stress limit ranged between 2.4 tonnes/cm^2 (35 ksi) for normal grade steel and 4.1 tonnes/cm^2 (60 ksi) for high strength steel for welding applications [AIJ, 1979]. Allowable stresses in tension, bending, and compression (with due allowance for slenderness effects) were typically $F/1.5$, and for shear they were $F / (1.5\sqrt{3})$. Allowable stresses in welds were generally equal to those of the base metal. Width-to-thickness ratios for flanges supported along one edge were limited to $24 / \sqrt{F}$, and for elements stiffened along both edges (including rectangular box sections) the ratio was limited to $74 / \sqrt{F}$. These limits are similar to those of the American Institute of Steel Construction (AISC) during the same time period.

A wide range of structural details was used over the period of interest. Figure 6.13 displays some typical details for a small building during the 1950's [AIJ, 1960]. Figure 6.14 shows a variety of connection details from the 1960's [AIJ, 1970]. In the 1970's and 1980's, steel box sections became increasingly popular. These were produced directly for use as columns starting in the mid-1970's, but were also fabricated by welding together light gauge steel sections, rolled parallel flange channel sections, or thick steel plates. Some examples are in Figure 6.15 [Chiba, 1989]. It was typical to shop weld the connections at the beam-column joint and to make bolted connections in the field.

Three details for beam-to-box column connections are shown in Figure 6.16 [AIJ, 1995b]. These details are identified by AIJ as (a) through-diaphragm, (b) interior-diaphragm, and (c) exterior-diaphragm. Of these three details, the through-diaphragm is the most popular — in this connection, the column panel zone is a short section of the box column that is welded to the upper and lower continuity plates.

6.2.3 LATERAL FORCE AND DESIGN REQUIREMENTS

In 1915, Sano introduced the seismic coefficient concept, which offered an earthquake resistant design approach in which the structure was designed for a lateral force equal to the product of a coefficient and the weight. No specific value was assigned to the seismic coefficient, and the procedure was not part of law, until after the 1923 Great Kanto earthquake. In 1924, the Urban Building Law added an article to require a seismic coefficient of 0.1. The height limit of 100 ft (31 meters) remained unchanged from earlier times. This law governed construction in major cities until 1943, when it was suspended due to the war. The law was reinstated in 1948, and replaced by the Building Standard Law in 1950 [Otsuki, 1956]. This law, and the 1981 revision, governed lateral force requirements for the majority of buildings in the Kobe region that were affected by the 1995 Hyogoken-Nanbu earthquake. Some aspects of these two laws are detailed in the following paragraphs.

6.2.3.1 The Building Standard Law from 1950 through 1980

The basic seismic coefficient during this period was set at 0.2, or double the value that had been used since 1924. As described by Otsuki [1956], the doubling of the seismic coefficient caused problems in design related to overturning, and this was the subject of great debate among engineers. The outcome was not a decrease in the overturning moment, but instead an increase in the seismic coefficient for portions of the building more than 16 meters (53 ft) above ground. The Building Standard Law was modified in 1955 to include reductions to account for seismicity of the region and site subsoil.

According to the 1955 Building Standard Law [AIJ, 1970], the design horizontal seismic coefficient (K) for the superstructure must be at least equal to the quantity:

$$K = K_o \alpha \beta$$

where the product $\alpha\beta$ must not be less than 0.5; K_o is 0.2 for the first 16 meters (53 ft) above the foundation and is increased by 0.01 for each additional 4 meters (13 ft); α is a modification factor for ground condition and type of construction; and β is a modification factor for seismicity of the region, equal to 1.0 for the Kobe region. The distribution of K_o with height is shown in Figure 6.17. Story shear forces were calculated by summing the product of K and the story weight, for all stories above the level under consideration. Values of α are listed in Table 6.2, with simplified descriptions of relevant conditions.

90

Table 6.2 - Values of α

Soil	Wood	Steel	RC and SRC
Rock, hard sandy gravel	0.6	0.6	0.8
Sandy gravel, sandy hard clay, loam, classified as diluvial	0.8	0.8	0.9
Alluvium	1.0	1.0	1.0
Bad or soft ground	1.5	1.0	1.0

An abbreviated listing of allowable unit stresses is in Table 6.3 [AIJ, 1970]. For steel, the allowable stresses for temporary loading are equal to the nominal yield value. For concrete, the allowable compressive stress under temporary load is two-thirds of the design compressive strength.

6.2.3.2 The Building Standard Law of 1981

In the period 1972-1977, the Ministry of Construction conducted a project aimed at establishing a new seismic design method. The method was released in 1977, and generally accepted by 1978 [Ishiyama, 1989]. The 1978 Miyagiken-Oki earthquake provided momentum for implementation of this proposal, which was adopted in June 1981 as part of the Building Standard Law [Aoyama, 1993].

The design method features a two-level procedure. The first phase design follows the traditional allowable stress design approach, with steel allowable stress equal to the yield stress, and concrete allowable stress equal to two-thirds of the specified compressive strength. The second phase design is a direct and explicit evaluation of strength and ductility, and may be regarded as a check of whether these are sufficient for severe ground motions [Aoyama, 1993]. A flowchart of the design process is in Figure 6.18.

Timber structures and low-rise structures satisfying rigidity, eccentricity, and detailing limitations need not be checked using the second phase design. Other structures, including all structures of height between 31 m (100 ft) and 60 m (198 ft), must be checked by both phases. Structures over 60 m (198 ft) in height are subject to special approval.

In the first phase design, the seismic coefficient (formerly K in the 1955 Building Standard Law) at each floor level is determined as:

$$C_i = Z R_t A_i C_o$$

In the Kobe region, Z is equal to 1.0. Except for wood structures on soft subsoil, C_o is equal to 0.2. Variables R_t and A_i vary as shown in Figures 6.19 and 6.20. For the first phase design, member proportions are computed at the strength level (similar to the *NEHRP Provisions* [BSSC, 1994]) using design actions based on unreduced seismic forces. In the second phase design, the engineer checks story drift, eccentricity, and ultimate lateral load carrying capacity. If checked,

the ultimate lateral load capacity is computed using plastic analysis, and seismic demands are estimated using C_o equal to 1.0 and a framing system-dependent *ductility* factor D_s. Typical values of D_s range between 0.3 and 0.5. Details of this innovative design procedure are summarized by Aoyama [1981, 1993] and Whittaker, Moehle, and Higashino [1995]. The 1981 Building Standard Law was the current edition of the law at the time of the Hyogoken-Nanbu earthquake.

Table 6.3 - Abbreviated List of Allowable Stresses Under Permanent Loads [AIJ, 1970]

Material	Designation	Tension	Compression	Bending	Shear	Factor for Temporary Loading
Structural Steel	Common Steel	1.4	1.4	1.4	0.8	1.5
Structural Tubular	STK 41	1.4 - 1.6	1.4 - 1.6		0.8 - 0.9	1.5
Steel	STK 50	2.0 - 2.2	2.0 - 2.2		1.2 - 1.3	
Concrete	Normal Weight	$F_c/30$	$F_c/3$		$F_c/30$	2.0
Reinforcing Bar	Common Steel	1.4	1.4			1.5

Note: 1. All values in tonnes/cm^2; 1.0 tonne/cm^2 = 14.5 ksi

2. F_c is the compressive strength of concrete

6.2.3.3 Modifications to Lateral Force Profiles

As described in Sections 6.4 and 6.5, many older reinforced concrete buildings suffered mid-height failures in the earthquake. Early reports attributed this type of damage to the lateral force profile used for the design of older construction.

Lateral force profiles and story shear distributions for three generations of Japanese seismic codes, namely, pre-1950, 1950-1981, and post-1981, are presented in Figures 6.21 through 6.23. The data presented in these figures are based on an analysis of a 32-meter (105 ft) tall, 8-story reinforced concrete building located in Kobe. It is clear from Figures 6.22 and 6.23 that the lateral strength and stiffness of the upper stories of the subject building, if designed prior to 1981, would be substantially smaller than if it had been designed per the 1981 Building Standard Law.

If it is further assumed that the lateral force profile defined by the 1981 Building Standard Law is correct, consider the story shear demands per the 1924 Urban Standard Law and 1950 Building Standard Law, normalized to the demands of the 1981 Building Standard Law and presented in Figure 6.23. Demand-to-capacity ratios in the upper stories of the subject building would likely have been much higher than in the lower stories had the building been designed prior

to 1981. Recognizing that minimum structural dimensions and other code requirements often result in constant-sized framing in the upper stories of buildings, the data presented in these three figures may provide a partial explanation for the mid-height collapses observed in older mid-rise construction in Kobe — all assuming that the force profile defined in the 1981 Building Standard Law is correct.

6.3 EARTHQUAKE DAMAGE DISTRIBUTION

6.3.1 INTRODUCTION

The fault ruptures extended northeast from the northern end of Awajishima Island through downtown Kobe. Surface rupture was limited to less than 10 km (6 miles), all at the northern end of Awajishima Island. The greatest damage to the built environment was concentrated in a 10 km (6 mile) wide corridor centered immediately above the line of rupture, and traversing the densely populated center of Kobe.

Earthquake shaking caused much of the damage to engineered buildings. The collateral earthquake hazard of liquefaction, observed to be widespread near buildings and other civil facilities sited on soft alluvial soil and fill, also contributed to the degree of building damage. Only minimal damage to modern construction on piled foundations, due to ground failure, has been reported.

6.3.2 INTENSITY OF EARTHQUAKE SHAKING

The intensity of the ground motion shaking in the epicentral region, estimated by the Japanese Meteorological Agency (JMA), varied between 5 and 7 on the Shindo scale. (The maximum value on the Shindo scale is 7.) The extent of the intensity 7 shaking in the wards in and around the city of Kobe is shown in dark shading in Figure 6.24 [AIJ, 1995b].

6.3.3 BUILDING INVENTORY

The 10 km wide corridor of greatest damage (assigned intensity 7 on the Shindo damage scale) corresponds to the zone of most intense shaking. This zone lies directly above the fault trace, and atop either alluvial deposits or fill; the northeast trending longitudinal axis of the zone loosely follows the Japan Railway (JR) railway line.

Kobe was devastated during World War II. In the late 1940's and early 1950's, much reconstruction work was concentrated in a narrow corridor on both sides of the JR railway line. In the late 1950's and 1960's, engineered buildings were constructed on both sides of this corridor. From observations of building facades, the reconnaissance team concluded that the engineered buildings between the JR corridor and the harbor were generally older than the buildings to the north of the corridor. Unfortunately, the zone of greatest shaking coincided with the greatest concentration of older, more vulnerable buildings in the epicentral region, namely, along the JR corridor.

6.3.4 DAMAGE DISTRIBUTION

Three primary factors determined the distribution and degree of damage to engineered buildings in and around Kobe.

First, the line of fault rupture passed directly under the cities of Kobe, Ashiya, and part of Nishnomiya. Heavy damage to older engineered construction is expected in the near field (defined by many in the United States as a 10 km wide corridor centered over the line of fault rupture) in moderate-to-severe earthquake shaking. The zone of intensity 7 shaking as determined by JMA fell within the near field of this earthquake. This concentration of damage in the near field was observed by the reconnaissance team, and is also reported elsewhere [AIJ, 1995a].

Second, the line of rupture lay beneath deposits of alluvium and fill, likely resulting in significant local amplification of ground motion. Ground motion amplification was a hallmark of the 1989 Loma Prieta earthquake in California. Although there are no ground motion records available from adjacent rock and soil sites in the zone of heaviest damage, analysis of earthquake records [AIJ, 1995a] from sites 1.85 km (1.1 miles) apart in the Ikoma Mountains (rock site) and on the Osaka Plain (soil site), both approximately 50 km (30 miles) from the epicenter, showed significant amplification of ground motion and spectral response as noted in Table 6.4 below. Spectral velocity has been used by a number of researchers to estimate damage potential in past earthquakes, and is used herein to compare likely damage on adjacent rock and soil sites.

Table 6.4 - Response Amplification on Soil Sites

Input/Response Quantity	Period (sec.)	Rock Site	Alluvium Site	Amplification
Peak Ground Acceleration	N.A.	110 gals	152 gals	1.5
Spectral Velocity	0.5	20 cm/sec.	45 cm/sec.	2.3
Spectral Velocity	1.0	15 cm/sec.	60 cm/sec.	4.0
Spectral Velocity	2.0	12 cm/sec.	50 cm/sec.	4.0

The data presented in Table 6.4 clearly suggest that the likelihood of damage is much greater for buildings on soil sites than for adjacent buildings on rock sites.

In the region of heaviest damage, extensive liquefaction was observed. Although the liquefaction of founding material will reduce the intensity of shaking experienced by a building, it is noted that most engineered buildings are supported by piles driven to refusal below the liquefiable stratum. As such, the degree to which the ground motion intensity was reduced by liquefaction is a matter of speculation at this time, and detailed studies are needed to quantify the likely reduction. The data presented in Table 6.4 provide valuable insight into the likely areas of heaviest damage given a uniform age distribution of the building stock, namely, those areas underlain by soft to moderately firm soils. In Kobe, the areas of greatest damage were all located

on the Osaka Plain. Damage to older construction, close to the edge of the plain near the Rokko Mountains, was minimal in comparison to the widespread damage on the plain proper.

The third factor contributing to the observed damage relates to the age of much of the building stock in the epicentral region and the codes and standards of design practice used to design these buildings. In Section 6.2, the evolution of Japanese seismic codes and construction practice was described in some detail — modern Japanese seismic codes for buildings are among the most advanced of any enforced in the world. To illustrate the impact of the revisions to the Building Standard Law on the extent of damage to engineered buildings in Kobe, consider the data presented in Table 6.5. These data [AIJ, 1995a] were collected in the Chou Ward by members of the AIJ reconnaissance teams following investigation of approximately 100 buildings. The Chou Ward is the district to the east of Flower Road, the arterial road running south from the Shin Kobe railway station to the harbor. The buildings in the Chuo Ward are categorized by material type (steel reinforced concrete building data are included under the heading of reinforced concrete) and year of construction (rather than year of design). The major revisions to the codes define the transition dates in the table, namely, 1971 (steel and reinforced concrete code changes enforced) and 1982 (1981 Building Standard Law enforced).

Table 6.5 - Damage Statistics in the Chuo Ward

		Age of construction		
Material	Degree of damage	pre-1971	1971 - 1982	post-1982
Reinforced concrete	None	7	6	6
	Slight	3	3	4
	Moderate	8	2	3
	Severe/Collapse	18	2	0
Structural steel	None	0	5	7
	Slight	2	3	1
	Moderate	0	0	0
	Severe/Collapse	5	0	0

The data presented in Table 6.5 provide clear evidence of the impact of substantial improvements in the Japanese codes of practice. Many pre-1971 reinforced and steel reinforced concrete buildings in the Chou Ward collapsed or were severely damaged, but no such damage was observed in buildings designed per the 1981 Building Standard Law. A similar trend is evident for steel buildings.

6.4 RESPONSE OF REINFORCED CONCRETE CONSTRUCTION

6.4.1 INTRODUCTION

In this section, three types of reinforced concrete framing systems are defined, namely, reinforced concrete bearing wall construction, reinforced concrete frame and frame-wall construction, and steel reinforced concrete. Pertinent information and historical data on these three types of framing systems were presented in Section 6.2.

The members of the reconnaissance team often had difficulty differentiating between reinforced concrete construction and steel reinforced concrete construction. In many instances, often when the building damage was minor to moderate, it was not possible to assign a construction type to a building. For the purposes of this report, older damaged concrete frame or frame-wall buildings of unknown construction type are assumed to be of steel reinforced concrete construction.

Three stages in reinforced concrete code development in Japan were identified in Section 6.2: pre-1971, 1972-1981, and 1982 to present. These stages are used to help categorize damage to reinforced concrete buildings in this section.

In reviewing the response of reinforced concrete construction, the following factors should be considered:

1. Steel reinforced concrete was the preferred seismic framing type prior to 1970 because of its perceived good performance during the 1923 Kanto earthquake.

2. Prior to 1963, the building height limit was 100 ft (31 meters); the limit was abolished in 1963.

3. Following the Tokachi-Oki earthquake of 1968, the building code for reinforced concrete was amended to require closer spacing of transverse reinforcement in columns.

Accordingly, much of the older reinforced concrete building stock is composed of low- to medium-rise, non-ductile, steel reinforced concrete construction. Given experience and knowledge of non-ductile concrete construction, it is not surprising that this class of building fared poorly in the Hyogoken-Nanbu earthquake.

Much damage to reinforced concrete buildings was observed and documented by the reconnaissance team. Most of this damage was to buildings built before 1982, although moderate damage was documented for buildings constructed after 1982. Whether the damage to the post-1982 buildings was the result of (a) non-compliant code designs and non-typical construction details, (b) ground motions much greater than those assumed for design, (c) shortcomings in the codes and standard detailing practice, or (d) some combination of the above, was not determined by the reconnaissance team.

General observations regarding the damage follow in Section 6.4.2. A review of the behavior of a selected number of reinforced concrete buildings follows in Section 6.4.3. The reader is referred to the report by AIJ [1995a] for additional information.

6.4.2 GENERAL OBSERVATIONS AND REMARKS

6.4.2.1 Failure of Weak and Soft Stories

Numerous total and partial collapses of buildings were recorded. Collapses were observed in both the first story and mid-height stories.

Weak (insufficient strength) and soft (insufficient stiffness) story failures were widespread in Kobe, Ashiya, and Nishinomiya. Such failures were often a result of geometric changes in the seismic framing system to accommodate changes in building occupancy, with examples of the latter including (a) retail occupancy to residential occupancy, and (b) parking to residential occupancy. Other failures have been attributed to (a) mid-height changes in the type of framing system, typically a transition from steel reinforced concrete to reinforced concrete [AIJ, 1995a], and (b) the use of now outdated design lateral force profiles (see Section 6.2.3.3).

Examples of weak and soft story failures in older reinforced concrete structures, at both first and mid-height stories, are presented in Figures 6.25, 6.26, 6.27, and 6.28. The exact causes of failure in these buildings are not known.

6.4.2.2 Failure Due to Irregularity

Vertical and plan irregularity in stiffness and/or strength has been cited as the main cause for collapse of many buildings in past earthquakes. Likewise, the Hyogoken-Nanbu earthquake led to severe damage or collapse of many buildings of irregular configuration.

Buildings located on street corners are prime candidates for plan (torsional) irregularity. Often these buildings are composed of moment frames (and windows) on the street frontages, and stiff infill masonry or concrete walls supported by moment frames on the remaining faces — likely resulting in a large eccentricity of the centers of mass and stiffness, and significant torsional response in the event of an earthquake. Examples of building failures, most probably attributable in part to irregularity, are presented in Figures 6.29 and 6.30.

Aesthetic requirements and architectural constraints can often result in vertical irregularity, namely, a large change in strength and stiffness in a seismic framing system between two adjacent stories. An apparent example of vertical irregularity in a building can be seen in Figure 6.31 — a modern reinforced concrete building incorporating structural walls. Note the transition from regular framing in the upper levels of the building to irregular framing in the lower levels of the building, and the degree of structural damage immediately below the regular framing.

97

6.4.2.3 Failure Due to Overturning

Partial overturning of many reinforced concrete buildings was documented by the reconnaissance team, but many of the dramatic failures in downtown Kobe reported by the media had been removed by the time the NSF reconnaissance team arrived in Kobe. Two buildings that overturned in the earthquake are described below. No evidence of building overturning resulting from foundation failure was found; the response of foundation systems in this earthquake was in general excellent, despite widespread soil failures.

A nine-story reinforced concrete building (Figure 6.32) overturned onto Flower Road in downtown Kobe during an aftershock to the 17 January, 1995, main shock. It is reported that this building was severely damaged in the main shock, causing it to lean into Flower Road. The lateral load resisting system in this building was composed of reinforced concrete frames and bearing walls. Inspection of the foundation of the building (by others) indicated that the lightly reinforced concrete bearing walls (Figure 6.33) failed in sliding shear. A photograph of the foundation following removal of the building is presented in Figure 6.34.

A six-story reinforced concrete framed building (Figure 6.35) partly overturned following failure of its first and second stories. On the eastern side of the building, the exterior columns failed in combined shear and compression; the columns and piers on the western face of the building apparently failed in tension (Figure 6.36). The behavior of this building is described in more detail in Section 6.4.4.

6.4.2.4 Failure of Columns in Shear

Numerous column shear failures in older, pre-1971, buildings were observed. These columns were typically lightly reinforced to resist shear forces. Poor performance of similar shear-critical columns in the 1968 Tokachi-Oki earthquake led to major changes in the Building Standard Law — see Section 0. The column rebar detailing in pre-1971 construction is clearly seen in the failed column shown in Figure 6.37. Note the paucity of shear reinforcement in the column — smooth ties at 300 mm (12 inches) on center, 90° hooks and short extensions of the hooks on the shear reinforcement, and smooth longitudinal rebar with 180° hooks. As noted in Section 6.2.2, current detailing requirements for shear and confinement in reinforced concrete are much more stringent (Figure 6.38) than the requirements enforced prior to 1971.

One notable example of column shear failures resulting in the partial collapse of a building is shown in Figure 6.39. This building, an older seven-story hospital, failed in the fifth story — perhaps due in part to its pounding on an adjacent, stiff, lower-rise modern addition to the hospital. A view of three failed columns in the fifth story is presented in Figure 6.40.

The consequences of column shear failure were not surprising, with building damage ranging from severe local damage, through story collapses, to complete collapse. Given the large inventory of non-ductile reinforced concrete framed buildings, the widespread damage and collapse due to shear failure was not unexpected.

The good behavior of modern reinforced concrete framed buildings was in stark contrast to that of the pre-1971 buildings. The reconnaissance team saw little evidence of shear-related damage or failure in modern reinforced concrete construction; notable exceptions included (a) severe damage to the short (shear-critical) columns in a ten-story building (Figure 6.41), (b) significant shear cracking in the short columns in a multi-story parking structure (Figure 6.42), and (c) complete failure of selected bottom story columns (Figure 6.43) in a nine-story apartment block (Figure 6.44) — the ties in this column were placed at approximately 4 inches (100 mm) on center. Close inspection of the damaged facade shown in Figure 6.41 revealed that (a) the beams framing into the column (Figure 6.45) were likely stronger than the columns framing into the joint, (b) the shear reinforcement in the column (Figure 6.46) was likely insufficient to develop the flexural strength of the short column, and (c) no cross-ties were present in the column to confine the concrete at the mid-depth of the column.

6.4.2.5 Failure of Beam-to-Column Joints

Poor performance of beam-to-column joints was evident in older construction and was also observed in a limited number of newer buildings. It was not possible to attribute the collapse of any non-ductile concrete building frames to the failure of beam-to-column joints — generally those collapses that involved joint failure also involved shear failure of the adjacent column(s).

In older construction, beam-to-column joints were poorly detailed by modern standards. (Note that beam-to-column joints in reinforced concrete framed buildings of the same vintage in the United States were detailed and constructed in a similar manner.) The deficiencies in the joint included (a) insufficient or no horizontal shear and confinement reinforcement, (b) congestion of longitudinal column and beam rebar, and (c) insufficient development length of longitudinal column and beam rebar in the joint. Examples of damaged beam-to-column joints are presented in Figures 6.47 (a partially collapsed building in the Chuo Ward), 6.48 (haunched beam-to-column connections), and 6.49 (a failure mode similar to that seen in the Oakland and San Francisco double-deck viaducts following the 1989 Loma Prieta earthquake).

Beam-to-column joints in modern construction performed well overall. One notable exception can be seen in Figure 6.45 — a modern ten-story reinforced concrete building in which column shear failures were also observed. The beam-to-column joint pictured in Figure 6.45 suffered moderate damage, although transverse joint reinforcement at approximately 4 inches (100 mm) on center was provided over the height of the joint. Another example of poor joint behavior can be seen in Figure 6.50 — a multi-story apartment building in the same complex as the building pictured in Figure 6.44. Note in Figure 6.50 (a) the use of closely spaced transverse ties at the top of the column, and (b) the lack of transverse ties within the joint region — and the consequent buckling of the longitudinal reinforcement. One notable difference between construction practice in the United States and Japan is evident by close inspection of Figures 6.45 and 6.50, namely, the absence of transverse cross ties in columns and joints.

6.4.2.6 Damage to Precast Concrete Cladding Elements

Damage to precast concrete facade or cladding elements was observed in numerous instances. Although failure of such elements rarely leads to building collapse, the consequence of failure can be substantial loss of life if heavy cladding elements fall from the building into the street below. One example of the failure of precast concrete cladding elements is presented in Figure 6.51 — if the earthquake had struck during daylight hours in Kobe, the failure of these cladding elements would likely have led to substantial loss of life.

The causes of failure of the precast cladding shown in Figure 6.51 are unknown, but external inspection of the building, and close inspection of the damaged precast panels lying in the street, would suggest that (a) the primary seismic framing system was not sufficiently stiff to protect the cladding elements from excessive deformation, and (b) the strength and deformation capacity of the panel restraint connections was insufficient to prevent the panels dislodging from the building.

6.4.2.7 New Construction Details

An example of column rebar detailing for a ten-story reinforced concrete building, under construction at the time of the Hyogoken-Nanbu earthquake, is shown in Figures 6.52 and 6.53. There is a high percentage of longitudinal rebar in the column, likely a result of the short plan dimensions of the building. The longitudinal rebar is spliced using gas pressure welds — a line of weld nodes is clearly visible in Figure 6.52 at the midheight of this column. Further, the transverse reinforcement in the column, although closely spaced, consists of only perimeter ties with 90° hooks; there are no cross-ties in the short direction of the column. The lack of cross-ties, use of non-staggered splices in longitudinal rebar, and 90° hooks on the perimeter ties would not be permitted in special ductile moment frame construction in the United States. Ninety degree hooks on perimeter ties are also not permitted in Japan.

6.4.3 REINFORCED CONCRETE BEARING WALL BUILDINGS

Section 6.2.2.2 describes the construction requirements for non-engineered bearing wall buildings in Japan. The response of bearing wall buildings during the earthquake was generally good with only limited foundation damage reported [Otani, 1995].

6.4.4 REINFORCED CONCRETE FRAME AND FRAME-WALL BUILDINGS

Reinforced concrete buildings constructed prior to 1971 fared poorly in this earthquake. Many instances of total collapse (Figure 6.54) and partial collapse (Figures 6.25, 6.26, 6.27, 6.28, and 6.55) were documented. The causes of failure in older frame and frame-wall buildings, along with descriptions of damage to a number of buildings are outlined in Section 6.4.2 above.

Reinforced concrete frame and frame-wall buildings constructed after 1971 fared reasonably well during the earthquake. The damage to modern reinforced concrete construction documented by the reconnaissance team was generally consistent with the intent of the Building

100

Standard Law, namely, (a) to dissipate energy in predetermined plastic hinge zones, and (b) prevent building collapse. Damage to a building incorporating reinforced concrete structural walls is shown in Figures 6.56 and 6.57.

Damage to four reinforced concrete buildings, namely, two older buildings and two modern buildings, is described in more detail below.

In the city of Nishinomiya, many older reinforced concrete buildings were damaged, and numerous collapses were recorded. One of the badly damaged buildings, an eleven-story structure on Route 2 near the JR Nishinomiya Station, is shown in elevation in Figure 6.58, and in part elevation in Figure 6.59. Figure 6.58 is a south (part east) elevation of the building, and Figure 6.59 is a part west elevation of the building. This building is irregular, U-shaped in plan above the fourth-floor level, and composed of both reinforced concrete frame-walls and steel reinforced concrete framing [AIJ, 1995a]. It was constructed in 1971. The northern segment of the eastern and western wings of the building are eleven-story apartment blocks; the southern wing of the building (fronting Route 2) and the southern segment of the eastern and western wings of the building are composed of seven stories of apartments atop three stories of retail space. Schematic plan views of the building at the second and fourth floors of the building are shown in Figure 6.60 to illustrate the plan irregularity of the building. The height of the three stories of retail space equals that of four stories of apartments, resulting in a vertical irregularity in the lower stories of this building (Figure 6.61). The structural framing in the retail spaces and the apartments likely differed widely, with conventional beam and column framing used in the retail space, and bearing walls used in the apartments. The strength and stiffness of the lateral framing in the apartments was likely much greater than that of the framing in the retail space. Given that it is most probable that the bearing walls in the seven stories of apartment framing were discontinued in the third story of the retail space, it is most likely that the third story of the retail space was both weak and soft by comparison with the fourth story.

The building suffered a partial collapse of the third story of the retail space. The collapsed framing can be clearly seen in Figures 6.58 and 6.59. A view of the eastern face of the collapsed building is shown in Figure 6.62; the junction of the retail space and the eleven-story apartment block that defines the extent of the story collapse can be seen near the right hand edge of this figure. Above the retail space, the apartments looked in on a courtyard. A photograph of the damaged building taken from inside the courtyard is shown in Figure 6.63. Note the stiff pier and spandrel framing typical of the upper six stories of apartment framing. The heavy damage to the structural framing evident in this figure is most likely a consequence of the collapse of the third story of the retail space. A photograph of structural damage inside the line of the exterior wall is presented in Figure 6.64. Note the use of deformed longitudinal rebar and smooth transverse rebar in both the beams and the columns; the tie spacing of approximately 300 mm (12 inches) in the column likely confirms that this building was constructed prior to 1972. The damage to the first story of apartment framing above the retail space, shown in Figure 6.64, is typical of that observed in this building.

Many older reinforced concrete buildings in the Chuo Ward were severely damaged. One such building is shown in Figure 6.35 — a six-story building composed of moment frame and

frame-wall construction. This corner building overturned as described in Section 6.4.2.3 above. The framing system was irregular in plan: moment frames on each of the two faces of the building fronting a street (see Figure 6.35) and frame-wall construction on the other two faces of the building (see Figure 6.36). The first and second stories of the eastern segment of this building collapsed. The frame-wall construction on the western face of the building failed in net tension. The quantity of debris and level of damage made it impossible to identify the cause(s) of failure with certainty. A possible cause of failure is that combined translational and torsional response in the building (as evinced by the at-rest position of the building after the earthquake) resulted in shear failure in the columns of the moment frame; the torsional response resulted from the eccentricity of the centers of mass and stiffness in the building.

The extensive damage to the western frame-wall made it possible to identify the rebar details used for its construction, namely, 20 mm (0.8 inch) diameter smooth longitudinal rebar (180° hooks) and 6 mm (0.25 inch) diameter smooth ties (90° hooks) at 450 mm (18 inches) on center in the column; 6 mm diameter rebar in the walls/piers; and 20 mm diameter smooth longitudinal rebar and 6 mm diameter ties at various spacings in the beam.

There is much modern construction on Port Island, including numerous reinforced concrete frame-wall apartment buildings (Figure 6.65). Most of the frame-wall buildings on Port Island inspected by the reconnaissance team suffered no visible exterior damage. One exception to this observation was shear cracking in short wall piers in one apartment building (Figure 6.66).

The reinforced concrete framing system in the recently completed Hankyu shopping complex (Figure 6.67) near Kobe Harborland suffered significant damage. The framing system appeared to be composed of structural walls and moment frames. There was a series of plan-elevation steps in one exterior wall (Figure 6.68), and significant damage (Figure 6.69) was observed at the 90° corners in the wall. There was no apparent boundary rebar in the corners of the wall, rather just the typical vertical and horizontal wall reinforcement. The distribution of the large cracks in this wall is atypical, suggesting that either (a) construction joints played an overly important role in the response of the wall, or (b) the wall was not assumed to be part of the seismic framing system, and as such was not detailed appropriately. Damage to some first-story columns (Figure 6.70) in this building was also documented. The subject columns were supporting a structural wall above the first story. Plastic hinges developed at each end of the column shown in Figure 6.70. The spacing of the transverse ties in this column was approximately 100 mm (4 inches); no cross-ties were present in the column.

6.4.5 STEEL REINFORCED CONCRETE BUILDINGS

Steel reinforced concrete (SRC) construction has been used for mid-rise and high-rise building construction since the 1923 Great Kanto earthquake. Given the average age of the inventory of SRC buildings in the Kobe area, it is not surprising that this framing system suffered extensive and widespread damage. Systemic damage to SRC buildings constructed after the introduction of the 1981 Building Standard Law was not observed. The embedment-type baseplate connections, recommended for use in the 1987 SRC building code (see Section 6.2.2.4),

102

performed well in the earthquake — no damage to this type of connection was observed (or reported by other reconnaissance teams).

Six examples of damage to SRC buildings are presented herein. The first building, shown in Figure 6.71, is the five-story Kobe-Chuo Post Office. The seismic framing system in this building was composed of moment frames in the north-south direction and frame-walls in the east-west direction. The northern wall of the post office is shown in Figure 6.71. A detailed view of the heavy damage to the northern wall is shown in Figure 6.72. Note the sliding shear failure in the eastern panel of the structural wall, and the diagonal tension failure in the western panel of the structural wall. Damage to the three steel reinforced columns in the wall was also severe. Figure 6.73 shows the failed central SRC column in the wall — with failure likely due to a combination of compression and shear. The steel sections in this column are clearly visible in the photograph. Failure of the western column or boundary element in the wall is shown in Figure 6.74. The shear crack in the wall was not arrested at the boundary element, but propagated through the column as seen in the figure.

The Kobe City Hall complex is composed of two buildings: a modern 34-story steel moment frame and steel shear wall building, and an older eight-story SRC structure built in the 1960's. The two structures were joined by air-bridges at the fifth and eighth stories. The modern high-rise building suffered no apparent damage in the earthquake. The sixth story in the older structure collapsed in the earthquake, and the air-bridge (Figure 6.75) joining the two buildings at the eighth level failed during the earthquake. An aerial view of the partially collapsed building is shown in Figure 6.76; part of the undamaged high-rise City Hall building can be seen in the upper left hand corner of the figure. The seismic framing system in the older building (hereafter referred to as the City Hall) was composed of four stories of reinforced concrete framing above four stories of steel reinforced concrete framing [Nikkei, 1995]. The steel columns (part of the SRC construction) terminated near the mid-height of the fifth story columns — one story below the partial collapse.

The sixth story of the City Hall building, the lowest story of reinforced concrete framing, collapsed in the earthquake. Photographs of the damaged building are presented in Figures 6.77 and 6.78 — the collapsed story is evident in each figure. Although the causes of failure in this building are still being investigated, it is likely that the sixth story was a weak and/or a soft story [Nikkei, 1995]. Preliminary review and analysis of the building [Nikkei, 1995] suggests that the lateral strengths and stiffnesses of each of the three stories of reinforced concrete construction were equal, because framing sizes were driven by nonstructural concerns. Such a distribution of strength and stiffness, combined with an abrupt transition to a stiffer and stronger steel reinforced concrete framing system in the lower five stories, likely resulted in the concentration of damage in the sixth story.

The third building, a ten-story SRC moment frame building, suffered significant damage in its first story. Permanent displacements in the first story are evident in Figure 6.79. Reinforcement details in the first story columns can be seen in Figure 6.80. The transverse reinforcement is placed at approximately 100 mm (4 inches) on center with 90° hooks.

103

A modern SRC building in the Chou Ward suffered significant damage. The eleven-story building, shown in elevation in Figure 6.81, suffered damage in its reinforced concrete walls and steel reinforced boundary elements. Damage to a boundary element in the third story is seen in Figures 6.82 (exterior view) and 6.83 (interior view). Closely spaced transverse ties in the boundary element and diagonal cracking in the web of the structural wall are evident in Figure 6.83. The spliced connection in the steel boundary element failed during the earthquake — repair details in the form of welded steel fins can be seen in Figure 6.84. A view along the damaged wall is presented in Figure 6.85. The safety helmet on the floor in this photograph provides a scale by which the deformation in the rebar can be estimated. For the vertical rebar in the wall to buckle as shown, the crack in the wall would have had to open at least 3 to 4 inches (75 to 100 mm).

The two SRC buildings shown in Figure 6.86 both suffered damage, albeit to differing degrees. The 10-story building in the center of the photograph (also seen in Figure 6.30) collapsed in the third story; this building was constructed prior to 1971. The building to the immediate left of the 10-story building in Figure 6.86, a post-1981, 13-story SRC building suffered little external damage. However, further investigation by members of the AIJ reconnaissance team revealed significant damage to the reinforced concrete structural walls in the building (Figure 6.87).

6.5 RESPONSE OF STRUCTURAL STEEL CONSTRUCTION

6.5.1 INTRODUCTION

The 1994 Northridge earthquake focused the attention of the earthquake engineering community in Japan and the United States on the probable seismic response of steel moment and braced frames. Special attention was paid by the earthquake reconnaissance team to the performance of modern steel construction in the epicentral region to ascertain if the damage patterns observed in steel buildings in Los Angeles in 1994 had been repeated.

The use of structural steel in building construction in Japan became popular after World War II with the production of light gage steel sections. Construction of structural steel framing systems of the type used in the United States commenced in earnest in the early 1960's with the local production of rolled column and beam sections. Structural steel frames for high-rise buildings were implemented following the development of techniques to fabricate large welded rectangular and square hollow sections. Much of the older structural steel building stock is composed of low- to medium-rise braced steel frames. It is this class of steel framing system that appears to have suffered the most damage in the Hyogoken-Nanbu earthquake. Note that the braces in older construction were typically slender, but that in newer (post-1970) construction, the braces are relatively stocky.

In this section, two categories of steel framing systems are assumed, namely, steel braced frames and steel moment frames. Pertinent information and historical data on these two framing systems are presented in Section 6.2.

6.5.2 GENERAL OBSERVATIONS

Damage to older steel construction was widespread. Although only limited damage to newer steel moment and braced frame buildings was observed and documented by the reconnaissance team, more recent investigations by AIJ reconnaissance teams have uncovered significant damage to newer steel construction.

General observations regarding the damage to steel construction are presented first, followed by a review of the behavior of a selected number of steel buildings. The reader is referred to the reports by the Architectural Institute of Japan [AIJ, 1995a; AIJ, 1995b] for much additional information. The AIJ is currently conducting more detailed studies of lightly damaged steel buildings to determine the extent of damage to critical connections — a somewhat similar effort to that conducted by engineers in California following the 1994 Northridge earthquake.

6.5.2.1 Failure of Weak and Soft Stories

There was little evidence of the failure of steel buildings due to either weak or soft stories. The three-story steel moment frame building shown in Figure 6.88 could be considered to have failed due to either a soft first story or a weak first story — the first story is soft with respect to the infilled masonry frame in the second and third stories and weak with respect to the lateral strength of the infilled frame in the upper two stories.

The lessons to be learned from this example are well understood by design professionals, namely, (a) irregular vertical distributions of lateral stiffness and lateral strength are problematic, and (b) nonstructural cladding elements, although not considered part of the seismic framing system, can dramatically influence the load path for seismic forces, and indeed control the seismic response of a building.

6.5.2.2 Failure Due to Overturning or Excessive Sway

Overturning is generally a consequence of the failure of one or more framing members, components, and connections in a building. Overturning due to failure of a foundation system was not observed by the reconnaissance team. Many of the commercial buildings in Kobe have high aspect ratios (height-to-plan dimension) and are more likely to suffer damage due to overturning than buildings with low aspect ratios. Examples of such high aspect ratio buildings are presented in Figure 6.89. The tallest of the three buildings in this figure (an automated parking garage) suffered permanent lateral and torsional deformation in the earthquake (see Figure 6.90).

Complete overturning and failure due to excessive sway (Figure 6.91) of steel framed buildings was documented by the reconnaissance team, and determined to be the result of one or more of the following:

- Fracture of a column-to-beam continuity plate connection — typically a fillet welded connection (Figure 6.92)

- Fracture of a beam connection to the column (Figure 6.93)

- Failure of the bolted baseplate-to-pedestal connection (Figure 6.94)

- Fracture of flat bar and rod bracing elements (Figure 6.91)

In the building shown in Figure 6.91, the column-to-beam connections were effectively pinned through the use of web shear (non-moment) connections. Failure of the slender braces led to a dramatic reduction in the lateral strength and stiffness of the building, and the resulting excessive sway of the building.

6.5.2.3 Failure of Braces and Connections

Concentrically braced and cross-braced frame buildings suffered damage in the Hyogoken-Nanbu earthquake ranging from minor to severe. No eccentrically braced frames were identified by the reconnaissance team.

The damage observed in bracing elements in buildings in Kobe was similar to that seen in previous earthquakes in both Japan and the United States. Damage in the form of buckled braces, failed brace-to-gusset plate connections, and failed brace-to-column connections was documented. Examples of this damage are presented in Section 6.5.4 below.

6.5.2.4 Failure of Columns, Beams, and Beam-to-Column Joints

Failure of columns, both through the cross-section and at welded splices, was documented. The failure of 500 mm (20 inches) square box columns in the Ashiyahama development in Ashiya is described in detail in Section 6.5.4.3 below.

Another notable column failure was observed in the modern steel cross-braced building shown in Figure 6.95. In the ground story of this parking garage, the diagonal brace framed into a 400 mm (16 inch) by 400 mm (16 inch) by 25 mm (1 inch) box column (Figure 6.96) at the ground floor level; damage to the box column approximately 800 mm (32 inches) above the floor level is also evident in this figure. The subject column also buckled globally and locally, indicating that it was subjected to high axial compression during the earthquake. The box column fractured immediately above the reinforced concrete foundation located more than 500 mm (25 inches) below the ground floor level. The 75 mm (3 inch) wide through-section crack in the box column is clearly seen in Figure 6.97. The cause of the column failure is likely the eccentricity in the brace-to-column-to-foundation connection detail.

No beam failures, in either flexure or shear, exclusive of connection-related failures or damage, were observed. Likewise, there are no reports of such failures published by other reconnaissance teams.

Numerous beam-to-column joints suffered damage. Some of this damage is documented in Section 6.5.3. Typical moment-resisting beam-box column joint details are presented in Figures 6.15 [Chiba, 1989] and 6.16 [AIJ, 1995b]. Such joints are generally constructed with horizontal continuity plates in the column at the level of the incoming beam flanges. Vertical continuity in the column is provided by welding a stub section of column between the two continuity plates. The beam-to-column connection is typically fabricated by welding the beam flanges to the continuity plates, and the beam web directly to the column stub located between the horizontal continuity plates. The failures in beam-to-box column connections included fracture of the fillet weld connection of the column to the lower continuity plate, and fracture of the fillet weld connection of the beam to the column. Damage to moment-resisting joints composed of wide-flange beams fillet welded to wide-flange columns was also observed (Figure 6.97); this connection detail is seldom used in the United States.

Damage to steel beam-to-column connections was widespread in the epicentral region following the 1994 Northridge earthquake. Similar types of damage, namely, (a) tension failure of full penetration groove welds, (b) tension failure of beam flanges, (c) cracking and fracture in column flanges and webs, and (d) pullout of flange nuggets, were not observed by the reconnaissance team but have been documented in detail by AIJ [1995b] following surveys of more than 1,000 buildings. The AIJ report documents damage similar to that observed following the Northridge earthquake including (a) weld fractures, (b) beam flange failures, and (c) cracking, fracture, and buckling of box steel columns.

6.5.3 MOMENT-RESISTING FRAMES

Modern steel moment frame construction generally performed well in this earthquake. The systemic, widespread damage to new steel moment frame construction reported in Los Angeles following the 1994 Northridge earthquake was not observed by the reconnaissance team in Kobe after the Hyogoken-Nanbu earthquake.

A detailed investigative effort by AIJ to expose beam-to-column connections in buildings with little visible damage has led to the discovery of damage in more than 20 buildings. It is reported that such failures followed significant yielding and/or local buckling in the beam flanges — something not observed following the Northridge earthquake. A summary of the observed failure modes is presented in Figure 6.98 (reproduced from [AIJ, 1995b]): a Type 1 crack denotes flange fracture; Types 2 and 3 cracks denote failure in the heat affected zone; and a Type 4 crack denotes fracture of the continuity plate. Figure 6.99 (courtesy of the Steel Committee of the AIJ Kinki Branch) shows a Type 1 fracture of the beam bottom flange. Flaking of paint on the underside of this beam was a result of significant local buckling of the beam flange.

The 36-story steel moment frame building shown in Figure 6.100 suffered no visible (exterior) damage during the earthquake. This building is located above Shin-Kobe railway station, and was likely subjected to ground motions with peak accelerations on the order of 0.22g.

Considerable damage to low-rise steel moment frames composed of square hollow section columns was observed in the zones of greatest likely shaking. Three types of damage were commonly observed, namely, failure of the column-to-continuity plate weld at the underside of the rolled steel floor beam, failure of the beam-to-column weld at the interface of the beam and column, and damage and failure of the column baseplate connections.

Failure of the column baseplate-to-pedestal connection in a high aspect ratio building (Figure 6.101) located in the Chuo Ward was likely a result of large seismic shear forces and overturning moments (causing large axial forces in the columns) being resisted by either four or six seismic connections. The failed column baseplate connection, shown in Figure 6.94, shifted laterally 24 inches (600 mm), and dropped 12 inches (300 mm) off the reinforced concrete pedestal, after shearing off the light reinforced concrete encasement around the base of the column.

The damage to the baseplate connection shown in Figure 6.102 provides clear evidence of the high axial forces that can be developed in columns during earthquake shaking. The framing system above the damaged connection was composed of perimeter braced frames in the north-south direction, and perimeter moment frames in the east-west direction; the six-story open steel structure was a fire egress route for a department store. The nuts on the holding down bolts that connected the baseplate to the footing displaced approximately 6 inches (150 mm) during the earthquake.

The overturning of the steel framed building shown in Figures 6.103 and 6.104 appeared to have been a result of the failure of baseplate connections. The failed building was prevented from collapsing completely by the reinforced concrete building directly across the lane. A photograph of a failed baseplate connection in the building is presented in Figure 6.105, along with two members of the reconnaissance team. Note that the four holding-down bolts through the baseplate are missing, and that there is no visible damage to the column-to-baseplate connection. The beam-to-column connections at the first level of this building also suffered gross damage. The framing system was composed of all-welded beam-to-column connections and moment splices in the beams away from the connections. The welded beam-to-column connections shown in Figures 6.106 and 6.93 are similar to those depicted in Figures 6.15 and 6.16, with continuity plates at (or about) the level of the beam flanges enclosing a short length of column section. The amount of welding required to construct this type of beam-to-column joint is significant, and the residual strains in the steel components in and around the joint were likely extremely high. In the failed connection shown in Figure 6.93, the fillet welds at the top and bottom of the lower continuity plate failed. (In both Japan and the United States, complete penetration groove welds are typically required for this type of connection.) The welds were observed to be of poor quality with much slag inclusion and limited fusion between the plate and the columns above and below the plate.

Similar damage to beam-to-column connections was observed in a number of buildings. The six-story steel moment frame building shown in Figure 6.107 suffered significant damage. A failed perimeter moment connection is presented in Figure 6.108. The damage to this connection was a result of the partial fracture of the fillet weld connection of the column to the continuity

plate at the level of the beam bottom flange. Complete failure of an exterior perimeter connection is shown in Figure 6.93. In this connection, the fillet-welded connection of the beam to the column fractured.

6.5.4 BRACED FRAMES

For the purposes of this report, braced frames have been categorized as either (a) concentrically braced, (b) cross braced, or (c) mega-braced. No eccentrically braced frames were identified by the reconnaissance team. The section on mega-frames refers to the complex of 52 high-rise residential buildings on reclaimed land in Ashiya, close to Osaka Bay.

6.5.4.1 Concentrically Braced Frames

The behavior of both modern and older concentrically braced steel frames varied widely. Damage to both modern and older construction was observed by the reconnaissance team.

The six-story parking structure shown in Figure 6.109 performed well during the earthquake. This building was composed of concrete fill on metal deck slabs, concrete encased beams and columns, and rolled H-section concentric braces (Figure 6.110). Minor shear yielding in some stiffened gusset plate connections (Figure 6.111) was observed; some brace buckling was reported by AIJ [1995b]. Note that the use of a large number of bays of vertical bracing in this parking structure is very different from construction practice in the United States, where the emphasis is often placed on minimizing the number of bays of seismic framing.

Damage to an older four-story concentrically braced parking structure (Figure 6.112) is documented in Figure 6.113. In Figure 6.113, the gusset plate connection of the braces to the floor beam fractured at the brace-to-gusset junction (Figure 6.114). The concentric braces in this building are encased in concrete, likely leading to a substantial increase in the strength of the bracing member. Whether the concrete encasement forced the failure out of the brace and into the unreinforced connection is unknown. Note in Figure 6.113 the temporary repair in place at the time of the visit of the reconnaissance team, namely, circular steel braces, running parallel to the encased concentric steel braces, welded to the underside of the floor beam above.

A modern ten-story concentrically braced parking structure (Figure 6.115) suffered significant structural damage in the earthquake. Only framing members in the north-south axis of the building were damaged. However, because of the large number of bays of vertical seismic framing in this building, there was no apparent danger of collapse. This building is composed of a concrete fill on metal deck floor slab, 460 mm (18 inch) deep fire-sprayed steel beams, 400 mm (16 inch) by 400 mm (16 inch) box columns, and 200 mm (8 inch) by 200 mm (8 inch) by 12 mm (0.5 inch) tubular steel braces. A photograph of one damaged bay of framing, on the eastern face of the building at the second floor level, is presented in Figure 6.116. Note in the photograph (a) the failure of the floor beam-to-column connection (Figure 6.117) at the upper left hand side of the photograph in Figure 6.116, (b) the damage to the floor beam in the vicinity of the brace-to-beam-to-brace gusset plate connection (Figure 6.118), and (c) the lack of lateral (torsional) restraint to the brace-to-beam-to-brace gusset plate connection. A photograph of the left hand

buckled brace shown in Figure 6.116, looking north along the eastern face of the building, is presented in Figure 6.119. The buckled bottom flange shown in Figure 6.118 likely resulted from minor plastic hinging in the beam — a consequence of brace buckling.

The damage to the bay of concentric framing evident in Figure 6.116 can be used to illustrate the importance of good detailing in seismic construction. First, laboratory studies have demonstrated the need to provide lateral torsional restraint to brace-to-beam connection points in braced frames. Such restraint is typically provided in braced steel frames in California; it was not provided in the subject building, and the lack of restraint likely contributed to the failure of the bay of bracing. Second, floor beams in concentrically braced frames, immediately adjacent to the brace-to-beam-to-brace gusset plate connection, have a tendency to form plastic hinges after brace buckling, requiring the floor beams to be detailed to accept large local strains and curvatures. In Figure 6.118, the plastic hinge formed outside the gusset plate which served to strengthen and stiffen the connection zone. The yielding in the web of the floor beam, and the antisymmetric buckling of the beam's flange outstands, clearly identify the plastic hinge. Improved detailing practice would involve providing lateral-torsional restraint to the potential hinging zones.

6.5.4.2 Cross Braced Frames

Cross- or X-braced frames were common steel bracing systems in Japan in the 1950's and 1960's. Typically, the cross braces were only designed to resist tension forces. As such, relatively slender bracing elements, such as rods, flats, and angles, were used in these frames.

It is well known that this type of framing system exhibits poor hysteresis. Laboratory tests have demonstrated the shortcomings of cross braced frames. As demonstrated below, the poor behaviors seen in the laboratory were replicated in buildings incorporating cross braced frames.

The slender braces in the seven-story building shown in Figure 6.91 failed during the earthquake, likely causing the building's large permanent displacement. The axial strength of the failed braces (ignoring the important issues associated with the likely hysteresis of the braces) is small, and there is no doubt that the pre-earthquake seismic strength of the building was insufficient for the building to survive moderate or severe earthquake shaking.

A photograph of the front elevation of an eight-story building incorporating rolled steel cross-braces in the north-south direction, and moment frames in the east-west direction, is presented in Figure 6.120. A part elevation of one wall of braced framing, taken from the roof of the adjacent parking garage, is shown in Figure 6.121. Note the large number of bays of cross bracing used in this building; the redundancy in this building is substantially greater than that typically found in steel braced frame buildings in the United States. Failure of the cross braced frames in this building took a number of forms, namely, brace buckling (Figures 6.122 and 6.123), brace-to-brace gusset plate connection failure (Figure 6.124), and brace-to-column gusset plate connection failure (Figure 6.125). The connection failures, and the loss of the facade cladding, can likely be attributed to the displacements associated with the brace deformations.

110

6.5.4.3 Mega-Frames

Fifty-two buildings, ranging in height from 14 to 29 stories, comprise the Ashiyahama Seaside Town development in Ashiya, on the shore of Osaka Bay (Figure 6.126). The 52 high-rise steel buildings, completed in 1979, are built on steel piles driven through hydraulic fill to depths ranging from 25 to 35 meters; the typical building footprint is approximately 29 m (96 ft) by 12 m (40 ft). The Ashiyahama megaframes were designed in the mid- to late-1970's using the dual level design procedure that was adopted by the 1981 Building Standard Law. A photograph of one building in the complex is presented in Figure 6.127. The housing units evident in this figure are prefabricated precast concrete units. Soil failures, in the form of lateral spreading, liquefaction, and settlement, were both widespread and extensive throughout the development, with the most significant failures observed close to the shore line.

The steel mega-frames are composed of two, three-dimensional vertical braced towers, each with a plan dimension of approximately 2.3 m (8 ft) by 9.5 m (31 ft). The orientation of these towers can be seen in Figure 6.128. The two towers, 14.2 meters (47 ft) apart center-to-center, support 3230 mm (10 ft) deep transfer trusses on the outside lines of the frames. The towers are each composed of eight columns; four exterior box columns — 500 mm (20 inch) by 500 mm (20 inch) in the first story, and four interior rolled H columns. The center line of the H columns is 2,750 mm (9 ft) inboard of the center line of the box columns. Shown in elevation in Figure 6.129, the transfer trusses act as coupling girders, transferring longitudinal seismically induced overturning moments in the building into axial forces in the two supporting towers. The transfer trusses are located at the 7th, 12th, 17th, 22nd, and 27th levels of the high-rise buildings. The highest transfer truss in each building is typically located three stories below the roof line. In the transverse (short) direction of the building, each tower is composed of two frames of concentric circular tube steel bracing.

The most pronounced damage in the mega-frames was associated with the transfer trusses and their supporting box columns; the damage was concentrated in the box columns located between the lowest transfer truss and the ground level. The AIJ [1995b] reported that box column failures were found in 21 of the 52 buildings and that 57 columns were damaged. Of the 57 fractures, 13 were located in the base material (cross section failure), 7 initiated at the junction of the column-to-brace connection — with the fracture typically propagating into the brace, and 37 were documented in welded column splice connections. Cross section tension failures were observed in 500 mm (20 inch) by 500 mm (20 inch) box columns with wall thicknesses of approximately 50 mm (2 inches). All 57 fractures occurred in the lower 14 stories of the buildings. Most of the fractures were observed in the 19- and 24-story buildings. No fractures were documented in the 29-story buildings.

The causes of the observed damage are unclear at this time. It is believed that the steel box columns were composed of two rolled, high strength (F_y = 410 MPa or 59 ksi) H sections, each with one pair of flange outstands removed, welded together toe-to-toe to form an enclosed box section. The resulting box columns, with wall thickness of up to 500 mm (2 inches), were supported in the lowest level by pedestals approximately 500 mm high composed of welded bent steel plates.

Many of the failures [AIJ, 1995b] were located within 200 mm (8 inches) of the welded junction of the pedestal and the box column (Figures 6.130 and 6.131). Note that in the lowest level of the vertical towers (Figure 6.132), the heavy longitudinal braces were eliminated, thus changing the framing system from braced to moment-resisting.

Significant damage to brace-to-beam-to-column connections was observed by the reconnaissance team. Photographs of damaged connections are presented in Figures 6.133, 6.134, and 6.135. Figure 6.135 illustrates the fracture of a horizontal member in one of the vertically braced towers.

Figures 6.133 and 6.134 illustrate the degree of damage observed in one connection in Block 6-1 at Level 6; the level immediately below the lowest transfer truss. Note that the section failure in this box column is level with the top of the gusset plate connection to the transverse concentric brace. Although the cause of the damage to this connection is unknown, it is likely that the axial forces in the subject gusset plate contributed to the damage. It is most probable that the 50 mm (2 inches) of lateral movement of the column shown in Figure 6.133 caused the observed fracture in the rolled steel H brace. For reference, the depth, breadth, and flange thickness of the torn brace are 320 mm (12.5 inches), 320 mm, and 32 mm (1.25 inches), respectively.

Some damage in the form of local yielding was observed in the longitudinal transfer trusses. A photograph of a truss connection, at the quarter point (see Figure 6.129) in a seventh-story transfer truss, is presented in Figure 6.136. The fire spray has been removed from this connection. Significant yielding in the web and flanges of the horizontal chord member, and yielding in the webs of the diagonal members, are clearly seen in this figure. No evidence of weld failure was observed in this connection.

Although some of the precast concrete panels cladding the building exhibited signs of distress (Figure 6.137), there was no systemic damage to the cladding. This observation suggests that the interstory drifts in the building were likely small.

6.6 RESPONSE OF BASE ISOLATED BUILDINGS

Over the past decade, the use of seismic isolation in Japan has proliferated, with more than 75 isolated buildings constructed to date. While the majority of these applications are in the Tokyo area, two recently completed structures in the northern part of Kobe near the city of Sanda were moderately shaken by the Hyogoken-Nanbu earthquake. One of these is the largest isolated building in Japan, a six-story steel reinforced concrete computer center with a total floor area of 505,000 square feet (47,000 square meters). The other, on a site approximately one-third of a mile (500 meters) away, is a three-story reinforced-concrete laboratory with a total floor area of 5,200 square feet (486 square meters). These structures are supported on relatively stiff soil approximately 22 miles (35 km) northeast of the epicenter of the earthquake, and because of their proximity to one another, it can be assumed that both experienced similar levels of ground motion.

The smaller of the two structures is part of the Technical Research Institute of the Matsumura-Gumi Construction Company. It was completed in March 1994 and is used as a laboratory and conference area. The superstructure is a reinforced concrete space frame with a total height of 42 feet (12.8 meters) and is supported on eight high-damping rubber bearings. The fixed-base period of the superstructure is 0.24 second, and the target period of the isolation system varies with displacement from 1.2 seconds at 0.5 inch (1.35 cm) to 2.3 seconds at 8.0 inches (20.3 cm). Adjacent to the isolated structure is a four-story steel moment frame with a rigid foundation, and the two buildings are connected via sliding joints. An exterior view of the fixed-base (left) and isolated (right) buildings is presented in Figure 6.138.

The peak ground accelerations observed at the Matsumura-Gumi site were approximately 0.27 g in both the longitudinal and transverse directions of the building, with a duration of strong motion of approximately seven seconds. Although digital data is not yet available, Table 6.6 shows the peak response accelerations, indicating that while there was some attenuation of the horizontal input, it was not as great as anticipated for this level of excitation. There was no damage in the isolated structure, but at the roof of the adjacent fixed-base structure there were reports of dropped ceiling tiles and a crack in a ventilation duct. The accelerations at the roof of this steel frame peaked at 0.98 g. Based on scratches in the stainless steel sliding joint at the first floor of the isolated building, the relative bearing displacement was almost five inches (125 mm), which would imply a vibration period of approximately two seconds. However, the measured period was closer to 1.5 seconds, perhaps because the earthquake struck early in the morning when the temperature in the basement of the building was about 0° C (32° F), leading to a slight stiffening of the rubber isolators.

Table 6.6 - Floor Accelerations in the Base-Isolated Matsumura-Gumi Laboratory

Floor Level	East-West	North-South	Vertical
Roof	0.274 g	0.200 g	0.343 g
First	0.256 g	0.148 g	0.273 g
Foundation	0.266 g	0.279 g	0.238 g

The West Japan Postal Savings Computer Center (Figure 6.139) is owned by the Ministry of Post and Telecommunications and serves as the computer center for all of the financial transactions of this Ministry in western Japan. It was occupied in late 1994, and since that time has been closed to the public for security reasons. The lateral force-resisting system in the superstructure consists of braced frames, while the isolation system is a hybrid of several different types of devices including 54 lead-rubber bearings, 66 natural rubber bearings, and 44 steel coil dampers. The fixed-base period of the superstructure is 0.68 second, and the target period of the isolation system varies with displacement from 2.8 seconds at 4.7 inches (120 mm) to 3.3 seconds at 9.4 inches (240 mm). Although detailed records of the response of this building to the earthquake are not yet available, peak response quantities have been reported (Table 6.7). These data indicate that the isolation system was very effective. The input accelerations can be assumed to be equivalent to those at the Matsumura-Gumi site, but the bearings in the Postal Center are

not exposed to the environment. The peak displacement of the isolators in this building was reported to be approximately 4 inches (100 mm).

Table 6.7 - Floor Accelerations in the Base-Isolated West Japan Postal Center

Floor Level	X-direction	Y-direction	Vertical
Sixth	0.105 g	0.076 g	0.380 g
First	0.108 g	0.058 g	0.197 g
Foundation	0.306 g	0.268 g	0.217 g

6.7 RESPONSE OF OTHER STRUCTURAL AND NONSTRUCTURAL COMPONENTS

6.7.1 NONSTRUCTURAL DAMAGE DUE TO EXCESSIVE DRIFT AND/OR ACCELERATION

Extensive damage to exterior cladding and interior nonstructural components was recorded by the reconnaissance team and others, following the earthquake.

Numerous instances of damage or collapse of exterior concrete and lath-mortar cladding were recorded. Examples of collapsed precast concrete cladding are reported in Section 6.4.2.7. Failure of the lath-mortar cladding shown in Figure 6.140 could be attributed to: in-plane and/or out-of-plane motion of the building; brittleness of the mortar-based cladding; inadequate anchorage of the cladding to the floor framing; out-of-plane motion of the cross bracing; or any combination of the above.

It was generally quite difficult to determine the extent of damage to interior nonstructural components because access into buildings was often either impossible or prohibited. However, buildings known to have little or no structural damage were evacuated because of extensive damage and failure of interior nonstructural elements and components. Such damage is often due to excessive interstory drift and/or high floor accelerations.

6.7.2 DAMAGE AND COLLAPSE DUE TO POUNDING AND DIFFERENTIAL DISPLACEMENT

There was significant evidence of structural damage due to pounding of buildings (i.e., adjacent buildings impacting on each other). However, no collapses could be attributed solely to pounding, although the damage (collapse) was so extensive in many buildings that the cause of failure will likely never be known.

Damage and collapse of intra-building air-bridges (elevated walkways connecting buildings) was observed in a number of instances. The failure of the eighth-story air-bridge between the low-rise and high-rise buildings that comprise the Kobe City Hall has received much

114

attention (Figure 6.75). In the absence of structural drawings and earthquake response data for the two buildings, it is not possible to determine the cause of its failure. The plausible causes of failure for this air-bridge include (a) excessive relative displacement between the two buildings, and (b) inertia forces in the corridor exceeding the seismic strength of the walkway [AIJ, 1995a].

Damage and near-collapse of an air-bridge located near Kobe Harborland was documented (Figures 6.141 and 6.142). There is clear evidence tracing the damage to differential displacement of the buildings, namely, the gravity load tension brace and compression struts, adjacent to the connection of the walkway to the wall of the building, both buckled during the earthquake — only a small relative displacement of the buildings toward one another is necessary to cause buckling in these steel braces.

Air-bridges linking apartment blocks (Figure 6.44) also failed and collapsed in the earthquake (Figure 6.143) — likely due to differential movement of the buildings supporting the air-bridges.

6.8 RESPONSE OF NON-ENGINEERED BUILDINGS

6.8.1 LIGHT-STEEL FRAMED BUILDINGS

Many of the older low-rise buildings that collapsed in and around Kobe were composed of light steel frames. Typical construction details for such frames are presented in Figure 6.13. Light steel framing composed of built-up sections was popular immediately following World War II — due primarily to the shortage, and thus high cost, of steel framing. It is likely that many of these older buildings were not designed for seismic forces.

6.8.2 UNREINFORCED MASONRY BUILDINGS

Masonry construction was relatively popular in Japan in the late 18th Century and early 19th Century. However, as a result of (a) the poor performance of masonry buildings during the 1923 Great Kanto earthquake (resulting in a near-suspension of masonry construction), and (b) the extensive bombing of Kobe during World War II, only a few examples of masonry construction remained in Kobe in January 1995. The seismic performance of unreinforced masonry buildings ranged from limited damage through complete collapse.

6.9 SUMMARY

6.9.1 GENERAL OBSERVATIONS

Modern construction, assumed herein to be composed of buildings constructed in accordance with the 1981 Building Standard Law, generally performed well. Based on the reconnaissance work of the NSF team and others, there is no evidence to date that any modern engineered buildings collapsed during this earthquake. Given the high intensity of earthquake shaking in the Kobe region, one can conclude that building framing systems designed to meet the requirements of the 1981 Building Standard Law will likely perform well during severe earthquake shaking.

115

Interior nonstructural damage can profoundly influence the perceived performance of a building: large interstory drifts will likely damage story height partitions, and large floor accelerations can wreak havoc with building contents that are not secured. Significant nonstructural damage in buildings suffering no apparent structural damage has been reported.

The Building Standard Law, similar to the Uniform Building Code, pays limited attention to the behavior of nonstructural components and building contents. After the 1994 Northridge earthquake, engineers in the United States began to take a more holistic approach to assessing building performance — a move away from considering the building frame as isolated from the remainder of the building. The damage wrought to nonstructural components and building contents by the Hyogoken-Nanbu earthquake has reinforced the need to consider a more comprehensive approach to seismic design that explicitly considers nonstructural elements and components.

The devastation to older construction in Kobe is a clear reminder of the seismic vulnerability of much of the building stock in both the United States and Japan, especially those buildings located in regions of high seismic hazard. Further, the loss of life in older construction will generally be much greater than that recorded in Kobe if a large magnitude earthquake strikes a major urban area in either country during regular business hours. The exposure to huge fiscal losses and immense societal disruption in both the United States and Japan is extremely high. Comprehensive retrofit programs are likely the only means by which to mitigate these risks to acceptable levels.

6.9.2 IMPLICATIONS FOR SEISMIC DESIGN OF BUILDINGS IN THE UNITED STATES

In order to draw implications from the observed damage to the built environment for seismic design practice in the United States, it is important to recognize the importance of (a) the intensity of earthquake shaking in the epicentral region, (b) the age of the building stock in the affected region, and (c) differences in design and construction practice between the United States and Japan.

The peak ground accelerations and velocities measured in the near field to the Hyogoken-Nanbu earthquake were consistent with those anticipated for the design earthquake in regions of high seismicity. However, the measured duration of strong motion, less than 10 seconds [Teran-Gilmore; 1995], for the north-south component of the Kobe Marine record described in Chapter 3 is arguably much less than that anticipated for M7.5+ events. That is, more damage to a given inventory of buildings would likely be expected for a M7.5+ event than that caused by the Hyogoken-Nanbu earthquake.

Japanese seismic design practice was substantially changed in the early 1970's, and in 1981, with the introduction of the Building Standard Law. As demonstrated in Table 6.5, changes in design practice for steel (1970) and reinforced concrete construction (1971) led to substantial improvements in building behavior. A decade later, the comprehensive overhaul of the Building Standard Law (1981) produced a seismic code of practice the equal of any in the world.

116

The timeline for changes in seismic design practice in the United States somewhat mirrors the changes in Japan, with the advent of ductile detailing requirements for steel and reinforced concrete in the late 1960's and the publication of ATC-3 in 1978. Given these similarities in the code development process, it is not unreasonable to draw conclusions from the Japan experience regarding likely damage to buildings in a design earthquake in the United States.

Nonductile steel and concrete buildings, that is, those buildings constructed prior to 1970, performed poorly in the Hyogoken-Nanbu earthquake. This result is not in the least surprising given the state of the knowledge regarding nonductile construction. Similar damage to nonductile construction in the United States must be anticipated in a design earthquake.

Modern steel and reinforced concrete buildings, that is, those constructed after 1982 in accordance with the 1981 Building Standard Law, generally fared well in the Hyogoken-Nanbu earthquake. Damage to these buildings was documented by the reconnaissance teams, but the levels of damage were consistent with that expected for a large earthquake. In order to gauge the implications of this observation on seismic design practice in the United States, consider the data presented in Table 6.8: a comparison of design base shears for regular buildings constructed in Japan per the 1981 Building Standard Law, and buildings constructed in the United States per the 1991 *NEHRP Provisions* [BSSC, 1991]. The data presented in Table 6.8 are computed assuming (a) a story height of 12 feet, (b) the buildings are located on rock sites in the regions of highest seismicity ($Z = 0.4$ in the United States, $Z = 1.0$ in Japan), and (c) "excellent ductility" for the calculation of D_s in the Building Standard Law. In this table, MRF $\equiv$ ductile moment frame, Wall $\equiv$ structural wall, and BF $\equiv$ concentrically braced frame. Per the requirements of both the *NEHRP Provisions* and the Building Standard Law, the design base shears for braced frames in Table 6.8 have been increased by 50%.

The design base shear is calculated at the strength level in the *NEHRP Provisions*. In the Building Standard Law, two base shear forces are calculated, namely, Q_i, which the building is required to resist at the strength level, and Q_{un}, which is a lower bound on the required ultimate strength of the building computed using plastic analysis.

The comparison of required lateral strengths of buildings in the United States (V/W) and Japan (Q_i/W) that follows ignores by necessity the effects of gravity loads on member sizes in a building frame. For selected framing systems, the seismic forces may not significantly influence member proportions, although this will be the exception rather than the rule. Recognizing the pitfalls associated with comparing directly the required lateral strengths of buildings in the United States and Japan, it is nonetheless useful to compare V/W and Q_i/W.

It is evident from the data presented in Table 6.8 that the force requirements of the Building Standard Law substantially exceed those of the *NEHRP Provisions* for reinforced concrete framing systems. For steel braced framing systems, the force requirements of the Building Standard Law and the *NEHRP Provisions* are similar; for steel moment frames, the member sizes would likely be similar after the substantial differences in drift limits between the Building Standard Law and the *NEHRP Provisions* are accounted for.

117

Seismic design for Q_{un} will generally control the proportioning of a building frame in Japan, especially for reinforced concrete buildings. Assuming this to be the case, it is clear that buildings designed in Japan will likely have greater strength than comparable buildings designed in the United States, especially for reinforced concrete buildings.

Table 6.8 - Comparison of Design Base Shears Normalized by Reactive Weight

Material	Stories	Frame Type	United States			Japan		
			T sec.	R	V/W	T sec.	Q_i/W	Q_{un}/W
RC	5	MRF	0.64	8	0.08	0.40	0.20	0.30
RC	10	MRF	1.09	8	0.06	0.80	0.16	0.24
RC	5	Wall	0.43	5.5	0.15	0.40	0.20	0.40
RC	10	Wall	0.72	5.5	0.11	0.80	0.16	0.32
Steel	5	MRF	0.75	8	0.07	0.60	0.19	0.24
Steel	10	MRF	1.26	8	0.05	1.20	0.11	0.14
Steel	5	BF	0.43	5	0.25	0.60	0.28	0.33
Steel	10	BF	0.72	5	0.18	1.20	0.17	0.19

The question remains "What are the implications, if any, of the Hyogoken-Nanbu earthquake for the seismic design of new buildings in the United States, and especially buildings in regions of high seismicity such as California?" Given that (a) modern Japanese buildings suffered some structural damage in the earthquake, (b) the duration of the earthquake was relatively short — perhaps one-third to one-quarter of that expected in the design earthquake in California, (c) Japanese buildings are typically stronger and stiffer than those constructed in the United States, and (d) Japanese buildings are generally more redundant than those in the United States, it is likely that modern buildings, located in regions of high seismicity, and designed per the NEHRP Provisions, will suffer significant damage in a design earthquake. Such damage may be avoided for new construction through calibration of current seismic design procedures (ostensibly calibration of response modification factors) so as to achieve the desired performance objectives with a high degree of reliability [ATC, 1995a; FEMA, 1995].

The response of the two seismically isolated buildings in the Kobe region was varied. The West Japan Post Office, an essential facility, performed extremely well. The measured floor accelerations were less than 40% of the peak ground acceleration. This reduction in floor accelerations permitted the facility to remain operational after the earthquake — testimony to the benefits afforded to low- and medium-rise buildings by seismic isolation. Increased use of this

118

innovative technology, especially for mission-critical buildings required to remain operational after a major earthquake, should be promoted.

There are many similarities between the Kobe region and seismically active regions in the United States. The city of Oakland, California, has much in common with Kobe, namely, its proximity to a major active fault, extensive deposits of soft soils and bay mud beneath many of the engineered buildings in the downtown area, and a significant inventory of non-ductile concrete, steel, and masonry buildings. If there is a lesson to be learned by policy makers from this earthquake, it is that if a severe earthquake strikes a major urban area in the United States, the social and economic losses will be huge, and the impact on the economy of the United States will be significant. Improvement in model seismic design codes and the timely introduction of mandatory requirements for seismic rehabilitation of vulnerable buildings are key steps in mitigating the risk posed to the built environment by earthquake shaking.

Acknowledgments

REFERENCES

[AIJ, 1960] *Illustration of Building Constructions in Japan*, Architectural Institute of Japan, Tokyo, 1960, 85 pp.

[AIJ, 1970] *Design Essentials in Earthquake Resistant Buildings*, (English translation of 1966 publication in Japanese), Architectural Institute of Japan, Tokyo, 1970, 295 pp.

[AIJ, 1979] *Design Standard for Steel Structures*, English translation of the 1970 Japanese publication, Architectural Institute of Japan, Tokyo, 1979, 113 pp.

[AIJ, 1995a] *Preliminary Reconnaissance Report of the 1995 Hyogoken-Nanbu Earthquake*, English Edition, Architectural Institute of Japan, Tokyo, 1995.

[AIJ, 1995b] *Reconnaissance Report on Damage to Steel Buildings Observed from the 1995 Hyogoken-Nanbu Earthquake*, Steel Committee of the Kinki Branch of the Architectural Institute of Japan, Osaka, 1995, (in Japanese).

[ATC, 1995] *Structural Response Modification Factors*, Report No. ATC-19, Applied Technology Council, Redwood City, California, 1994.

[Aoyama, 1981] H. Aoyama, "Outline of Earthquake Provisions in the Recently Revised Japanese Building Code," *Bulletin of the New Zealand Society for Earthquake Engineering*, Vol. 14, No. 2, June, 1981.

[Aoyama, 1993] H. Aoyama, "Outline of Earthquake Provisions in the Recently Revised Japanese Building Code," Japan International Cooperation Agency, Tsukuba International Center, Japan, 1993, 34 pp.

[BSSC, 1991] *NEHRP Recommended Provisions for the Development of Seismic Regulations for New Buildings*, Building Seismic Safety Council, Washington, D.C., 1991.

[Chiba, 1989] N. Chiba, "Building in Steel in Japan," *Proceedings from the International Symposium entitled "Building in Steel - the Way Ahead,"* British Constructional Steelwork Association, London, 1989.

[EERI, 1995] *The Hyogoken-Nanbu Earthquake: Great Hanshin Earthquake Disaster, January 17, 1995; Preliminary Reconnaissance Report*, Earthquake Engineering Research Institute, Oakland, California, 1995.

[FEMA, 1995] *Performance Based Seismic Design of Buildings*, Federal Emergency Management Agency, Washington, D.C., 1995.

[ICBO, 1994] *Uniform Building Code*, International Conference of Building Officials, Whittier, California, 1994.

[Ishiyama, 1989] Y. Ishiyama, "Aseismic Design Method and its History in Japan," summary of oral presentation, *Proceedings of the 3rd U.S.-Japan Workshop on the Improvement of Building Structural Design and Construction Practices*, ATC-15-2, Applied Technology Council, Redwood City, California, 1989.

[Ishiyama and Ohashi, 1990] Y. Ishiyama and Y. Ohashi, "History of Structural Regulations in Japanese Building Codes and Outline of Wind-Resistant and Seismic Regulations," *Wind and Seismic Effects*, Ed. N. Raufaste, NIST SP 776, NIST, Gaithersburg, Maryland, January 1990, pp. 335-347.

[Morino, Nishiyama, and Sakaguchi, 1994] S. Morino, I. Nishiyama, and N. Sakaguchi, "Hybrid Structures in Japan - Research and Practice," SSRC annual meeting, Lehigh University, Pennsylvania, 1994.

[Naka, Wakabayashi, and Murata, 1972] T. Naka, M. Wakabayashi, and J. Murata, "Steel-Reinforced Concrete Construction," IABSE preliminary report, 1972.5, Amsterdam, Holland, 1972.

[Naka, Wakabayashi, and Takada, 1960] T. Naka, M. Wakabayashi, S. Takada, "Quake Resisting Design of Composite Structures in Japan," *Proceedings of the Second World Conference on Earthquake Engineering*, V. 3, Tokyo, Japan, 1960, pp. 1811-1826.

[Nikkei, 1995] *Nikkei Architecture*, 27 March, 1995, Tokyo, Japan, 1995, (in Japanese).
[Otani, 1995] S. Otani, *Private Communication*.

[Otsuki, 1956] Y. Otsuki, "Development of Earthquake Resisting Building Construction in Japan," *Proceedings of the First World Conference on Earthquake Engineering*, Berkeley, California, 1956, pp. 16.1-16.17.

[RMS, 1995] *The Great Hanshin Earthquake, January 17, 1995*, Risk Management Solutions and Failure Analysis Associates, Menlo Park, California, 1995.
[Teran-Gilmore, 1995] A. Teran-Gilmore, *Private Communication*.
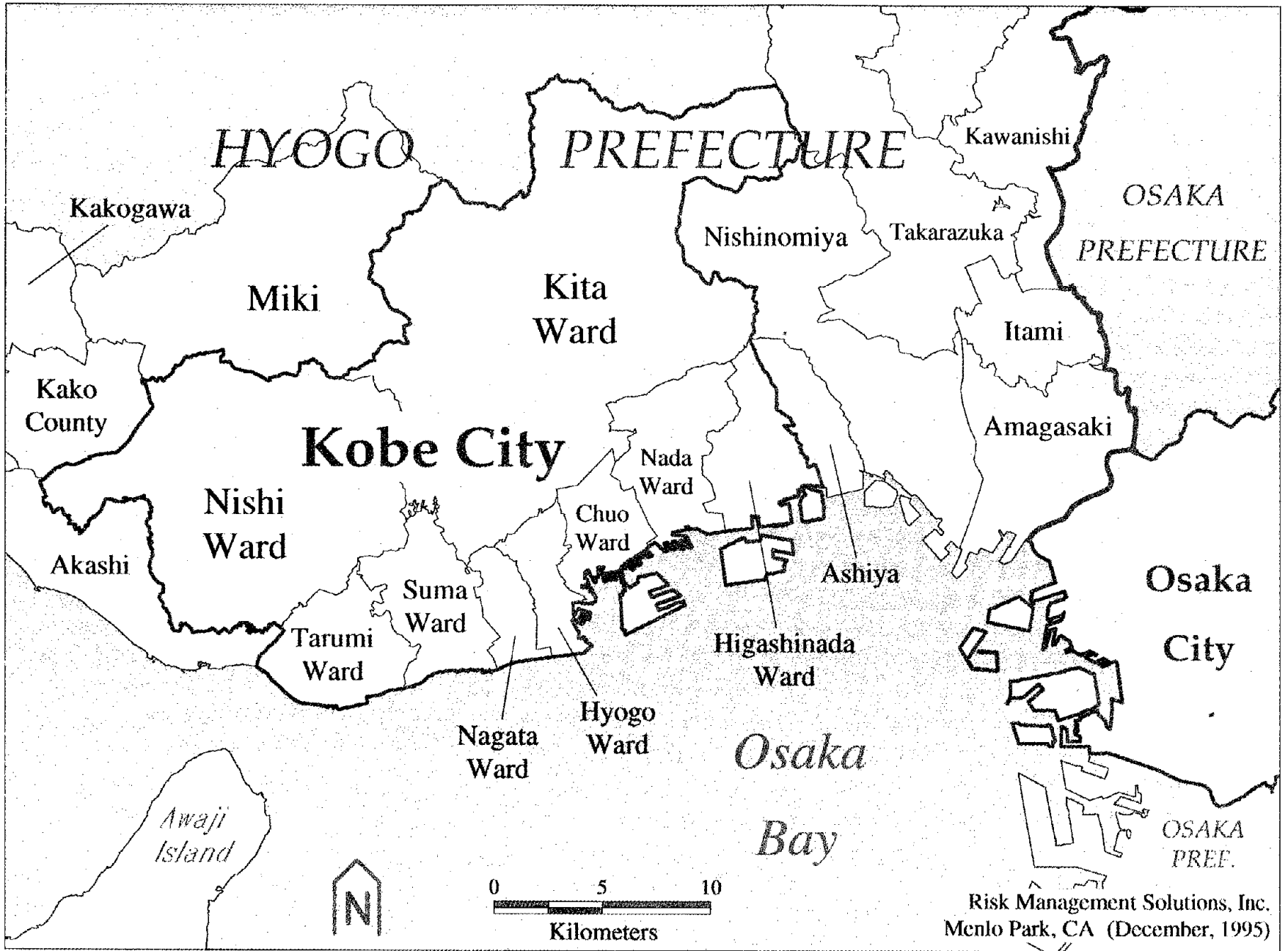
Fig. 6.1 Map of the Greater Kobe and Osaka region

122
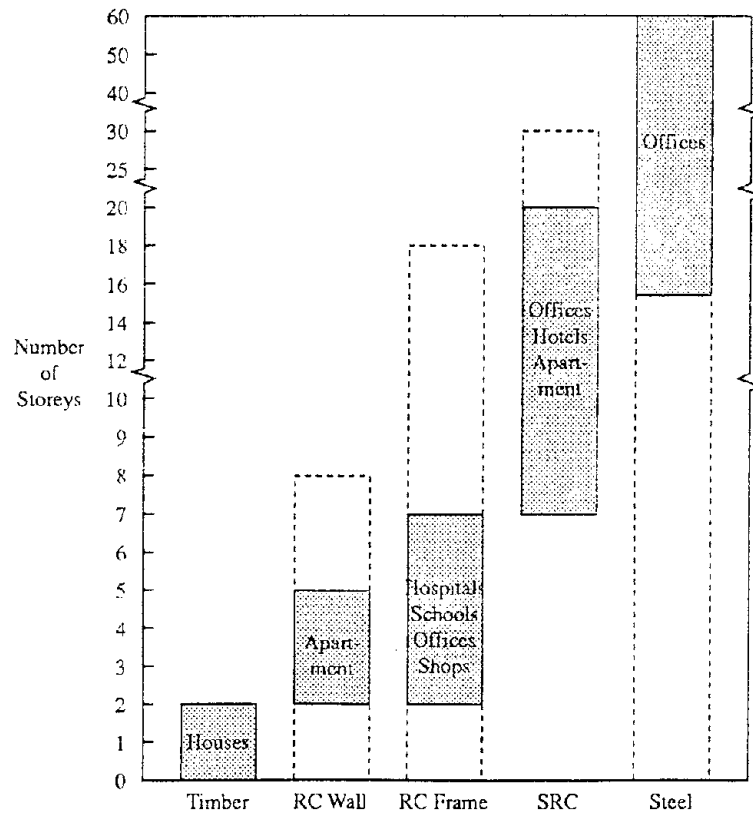
Fig. 6.2 Types of construction in Japan [Aoyama, 1993]
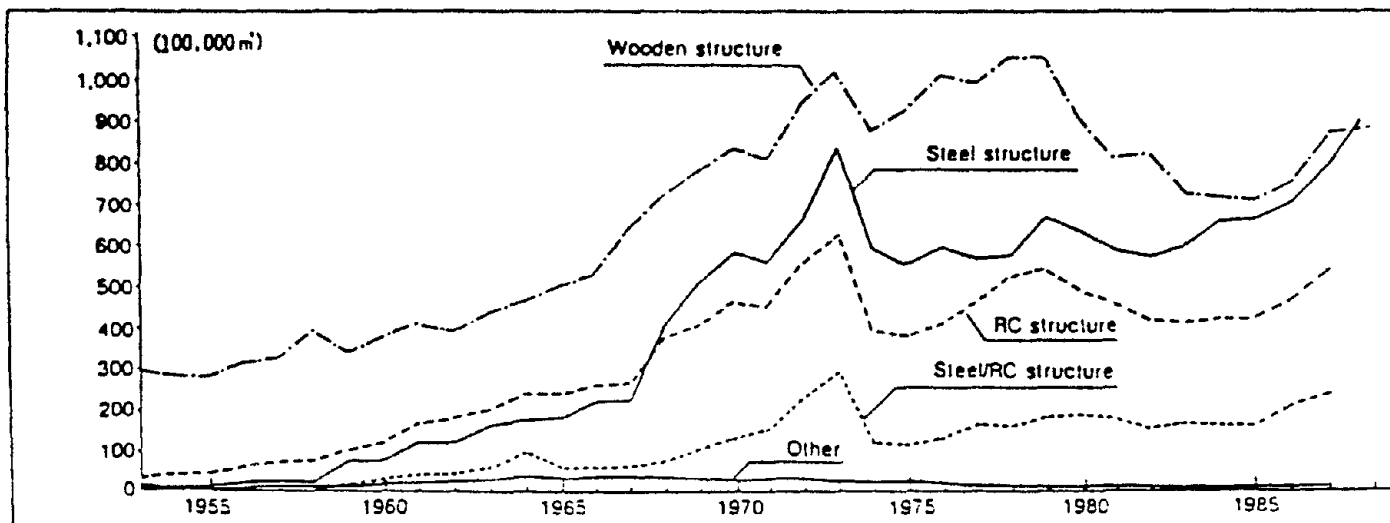
Fig. 6.3 Annual floor area in building construction [Chiba, 1989]
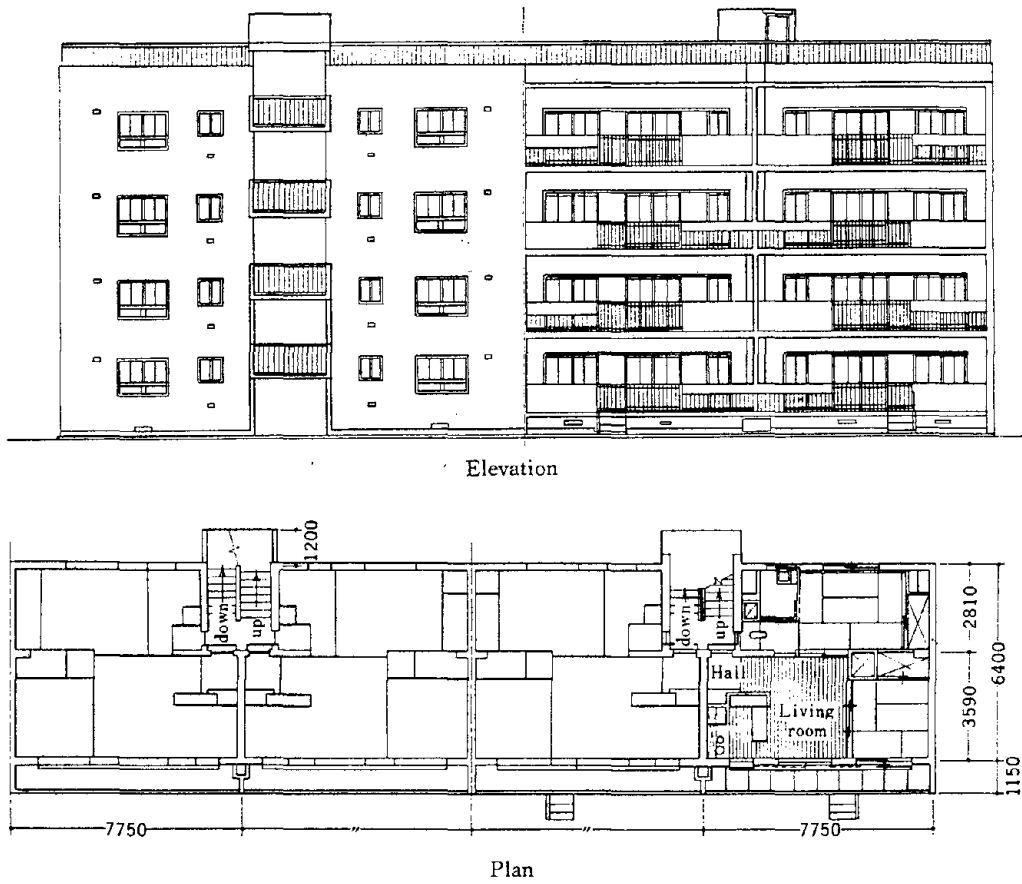
Fig. 6.4 Typical bearing wall construction geometry [AIJ, 1970]
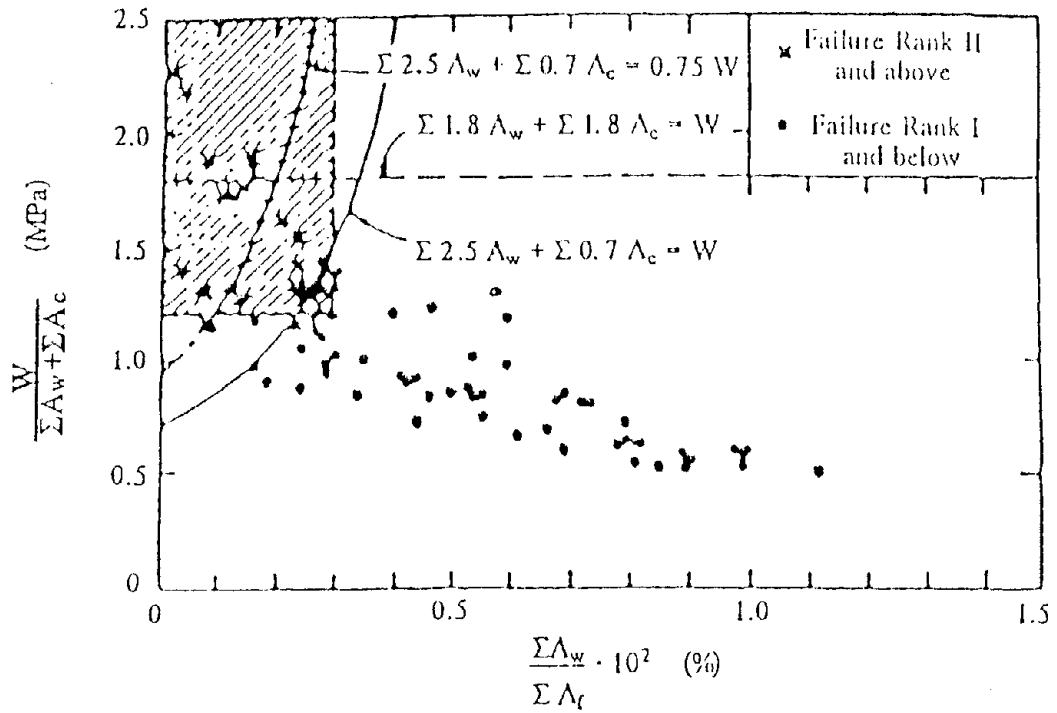
Fig. 6.5 Damage information for bearing wall construction [Aoyama, 1993]

125
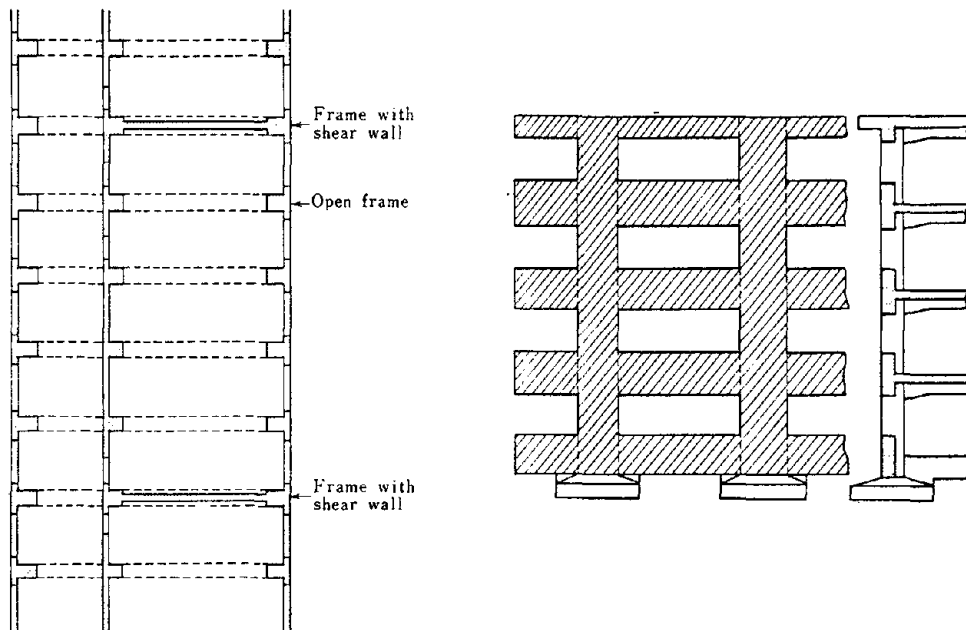
Fig. 6.6 Typical geometries for frame and frame-wall construction [AIJ, 1970]

Fig. 6.7 Reinforcement details for frame and frame-wall construction [AIJ, 1970]

126

Rectangular column

Section of column

Hoop
Diagonal hoop

Hoop 9 ᵐ

Longitudinal bars of column (d ≥ 16mm)

Lapped bar splices

Longitudinal bars of girder

Framework of reinforced concrete construction

Roof floor slab

Wall

Girder

Beam

Concrete block partition

Wall

Girder

Second floor slab

Beam

Column

Girder

Beam

Haunch

Wall girder

Girder

Wall

Column

Beam

Tie beam

Wall

Tie beam

Wall girder

Isolated footing

Column

Tie beam

Longitudinal bars of girder (d ≥ 16mm)

Stirrup (d ≥ 9mm)

Wall girder

Section at the end of wall girder

Section at the end of girder

Stirrup

Girder

Bend bars

Cantilever beam

Section at the center of girder

Section at the end of the beam

Section of the free end of the beam

Fig. 6.8 Reinforcement details for frame and frame-wall construction [AIJ, 1970]

127

Fig. 6.9 Steel usage in SRC construction [AIJ, 1970]
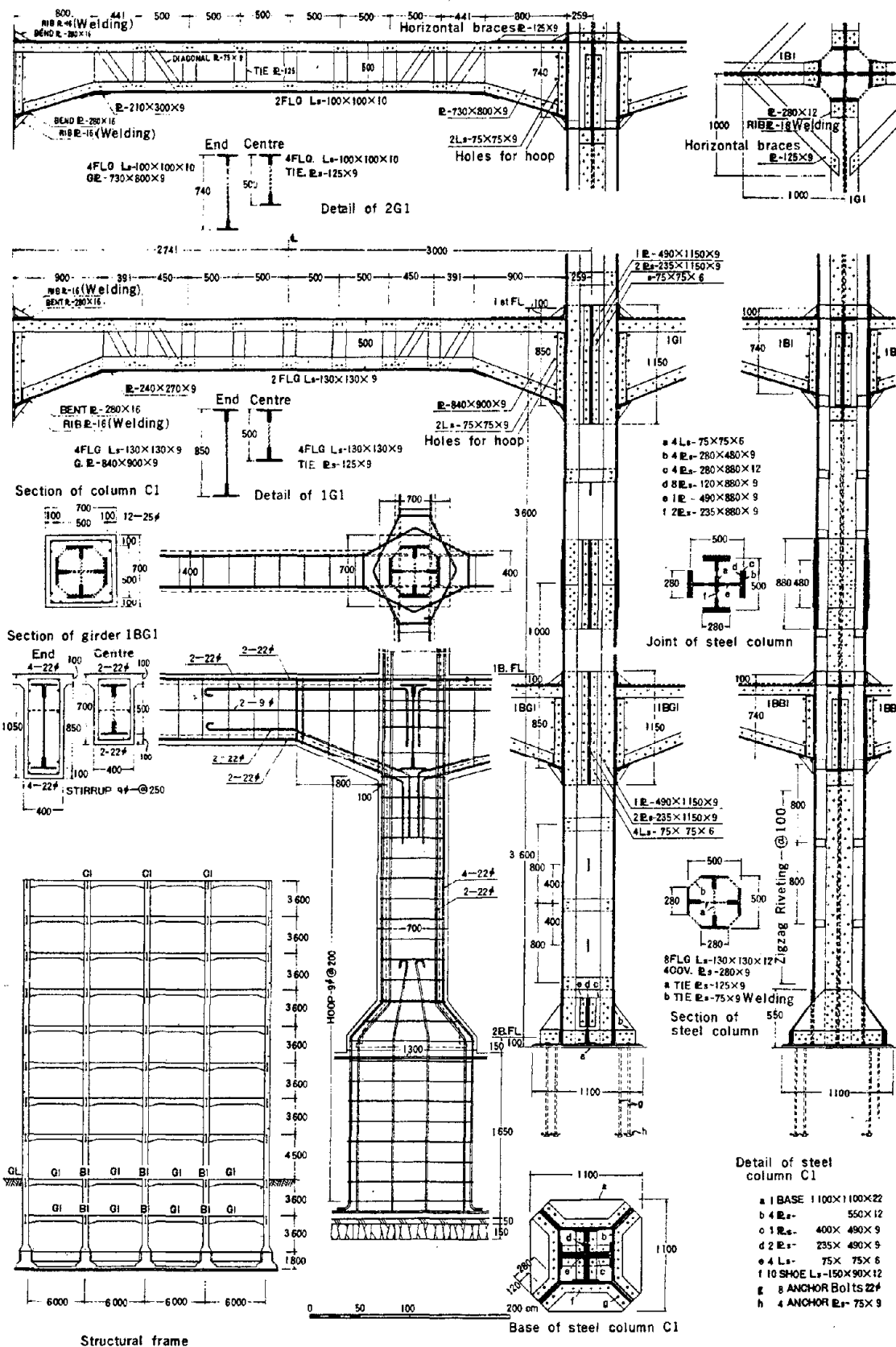
Fig. 6.10 Construction details for SRC [AIJ, 1960]

129
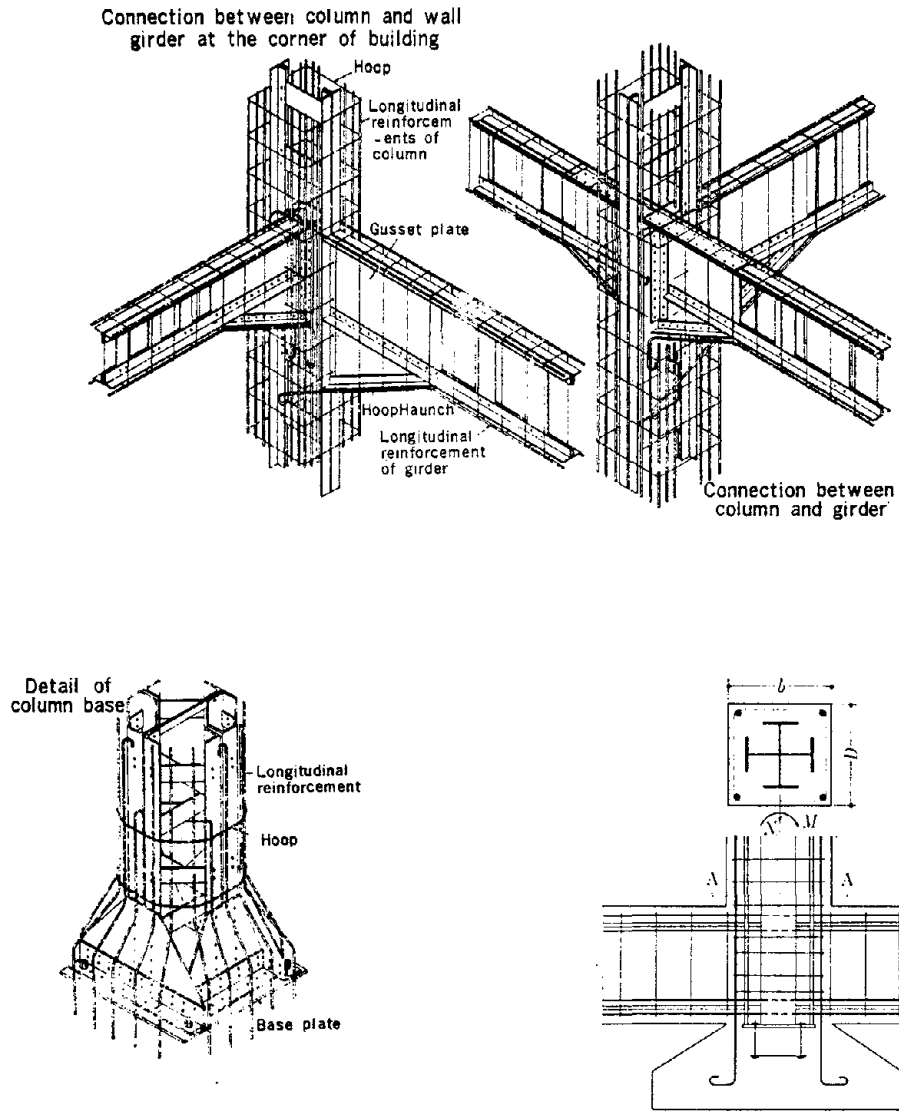
Fig. 6.11Construction details for SRC [upper and left drawings-AIJ, 1960; lower right drawing-AIJ, 1970; next page drawing-Chiba, 1989]

130

Cross-section of
SRC column

Steel
bar

concrete

Tie plate

Stub

Beam

Column

Plate girder

UB

Welded cruciform section

131
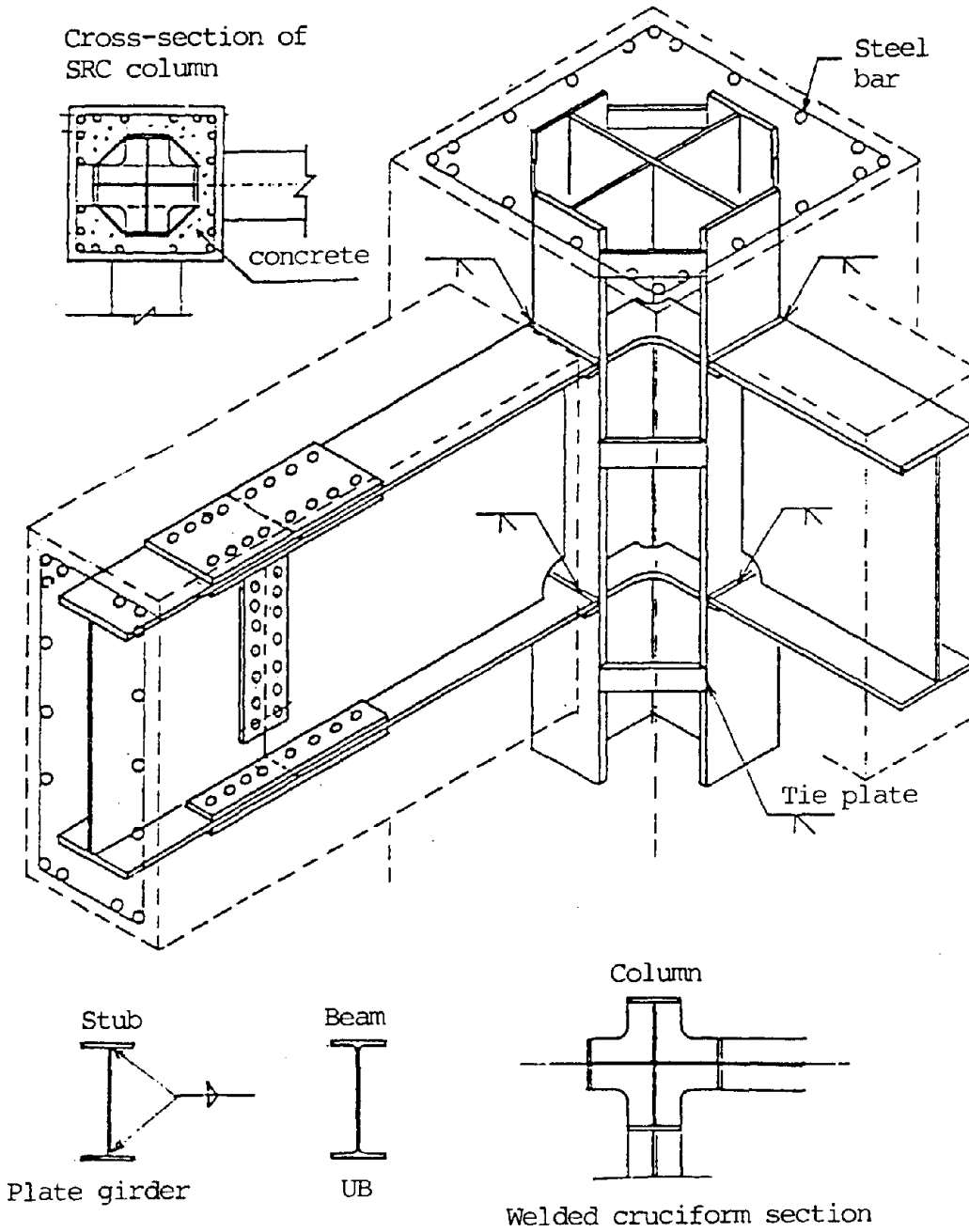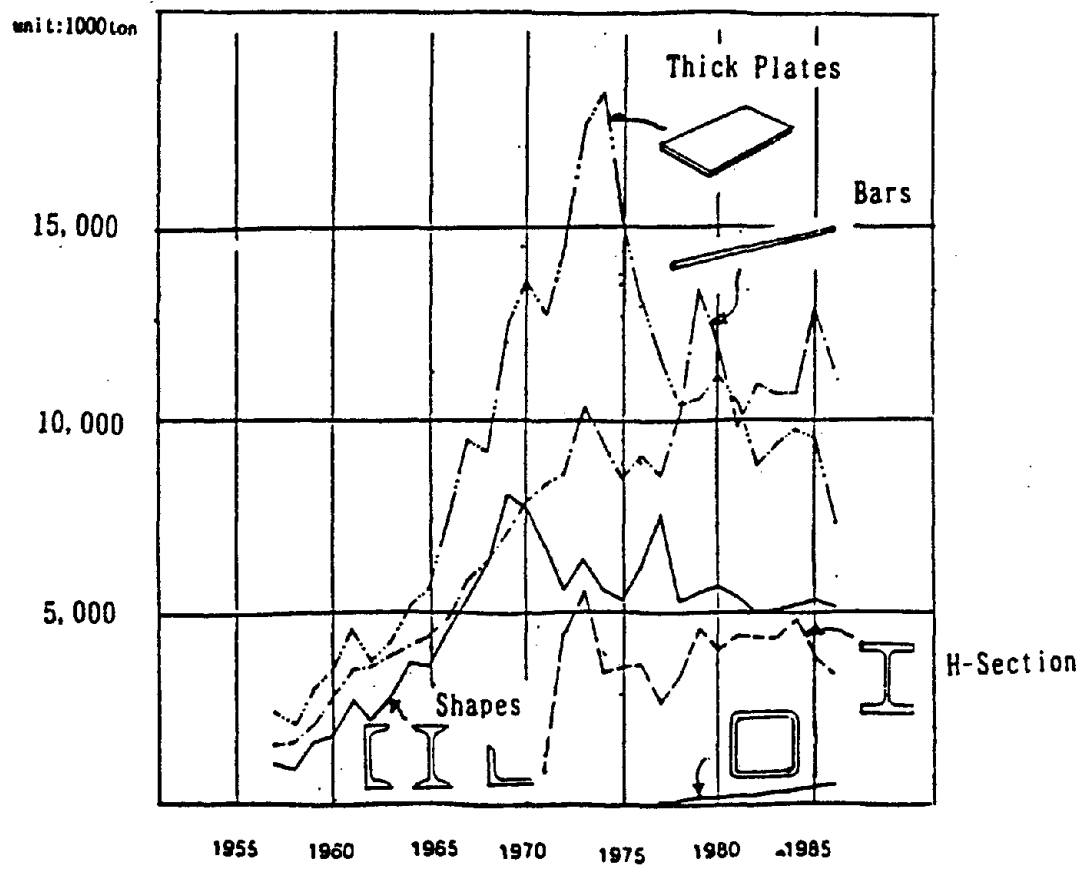
Fig. 6.12 Annual production of steel components in Japan [Chiba, 1989]
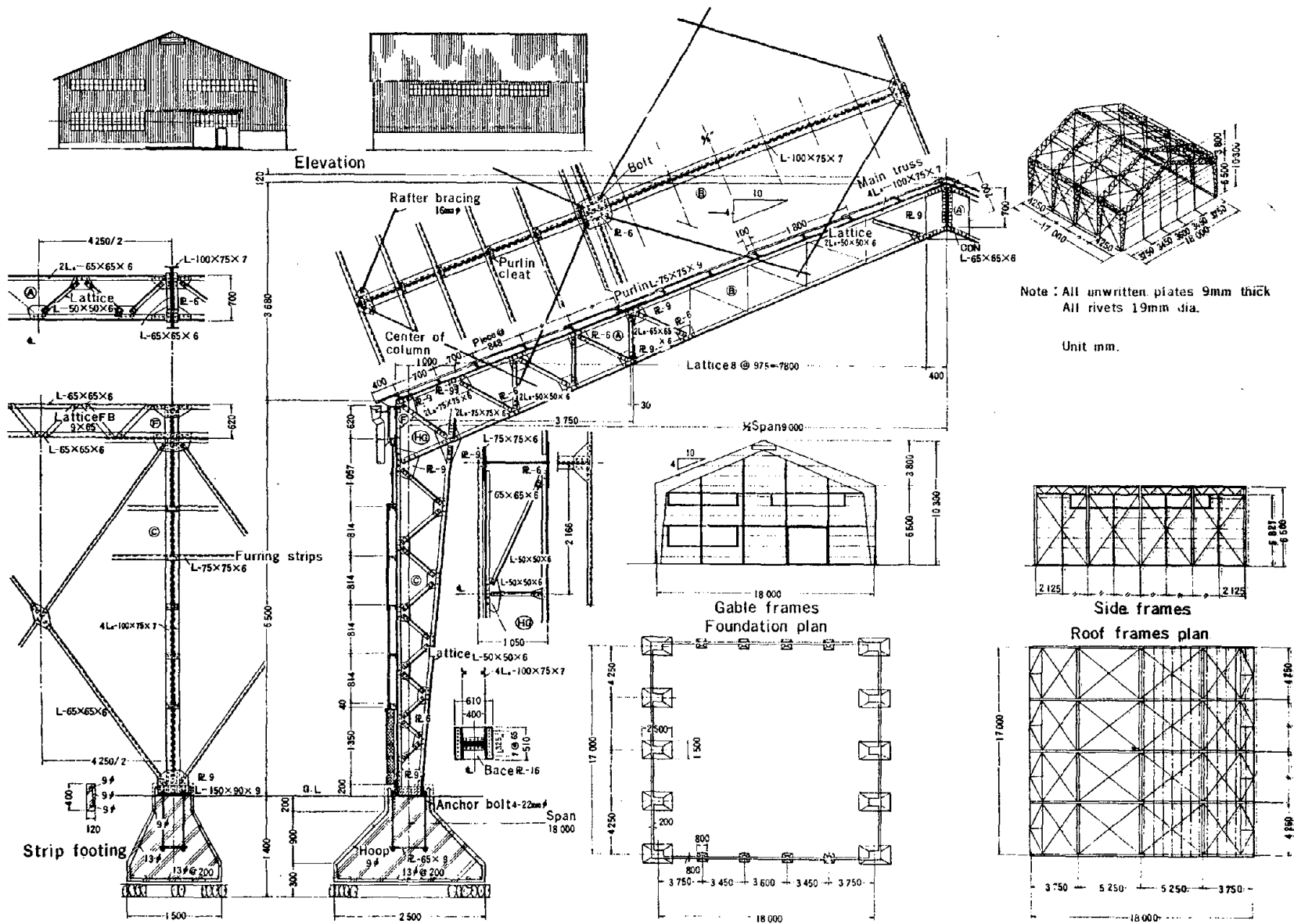
Fig. 6.13 Construction details for a 1950's steel industrial building [AIJ, 1960]

(a) Diaphragm-Type

(b) Vertical stiffener type

(c) Flat rib type
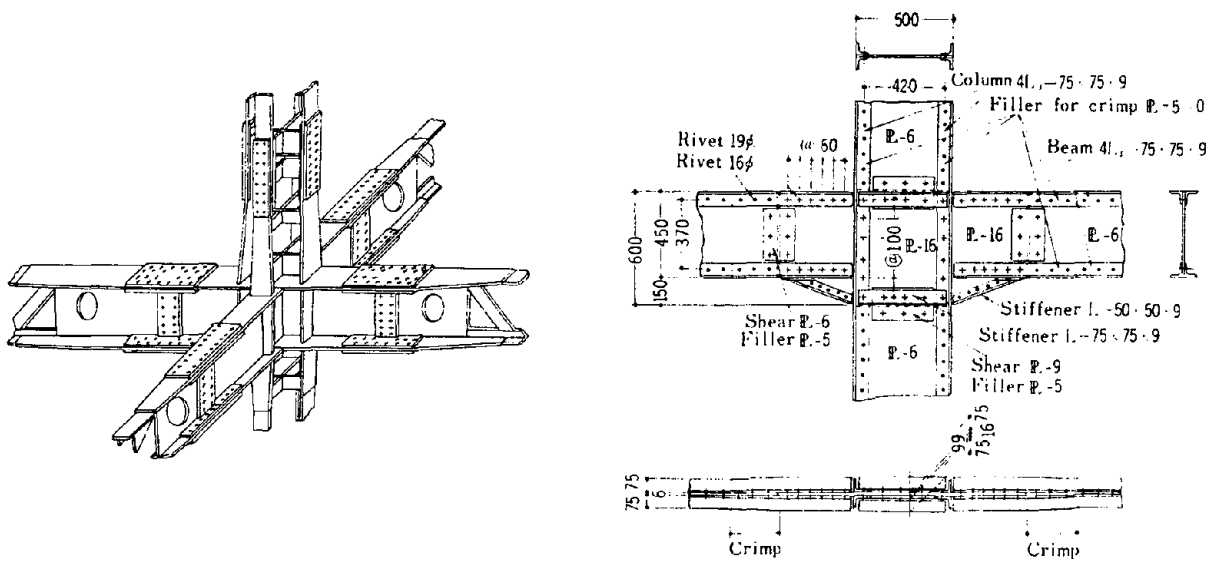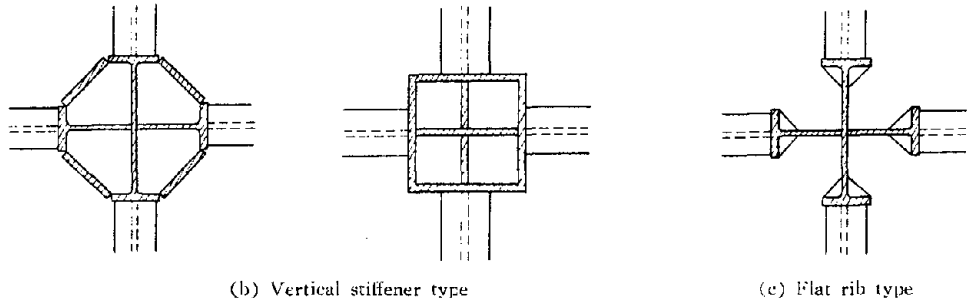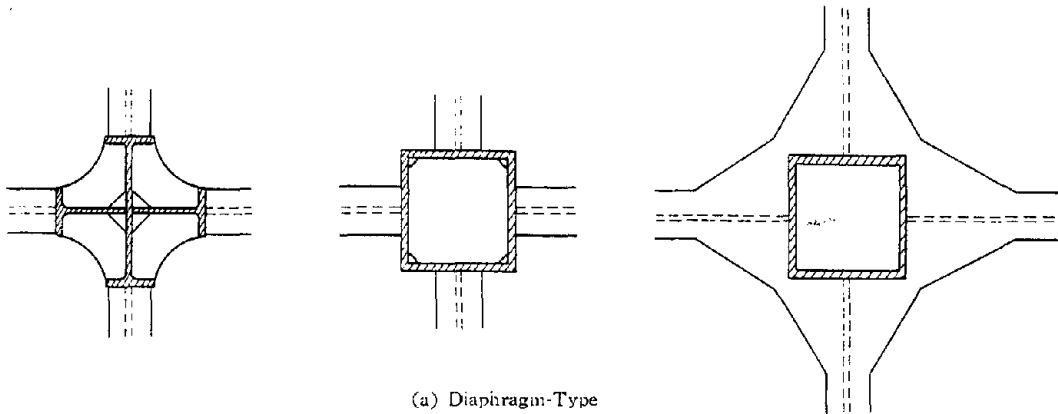
Fig. 6.14 Steel beam-column connection details [AIJ, 1970]

134
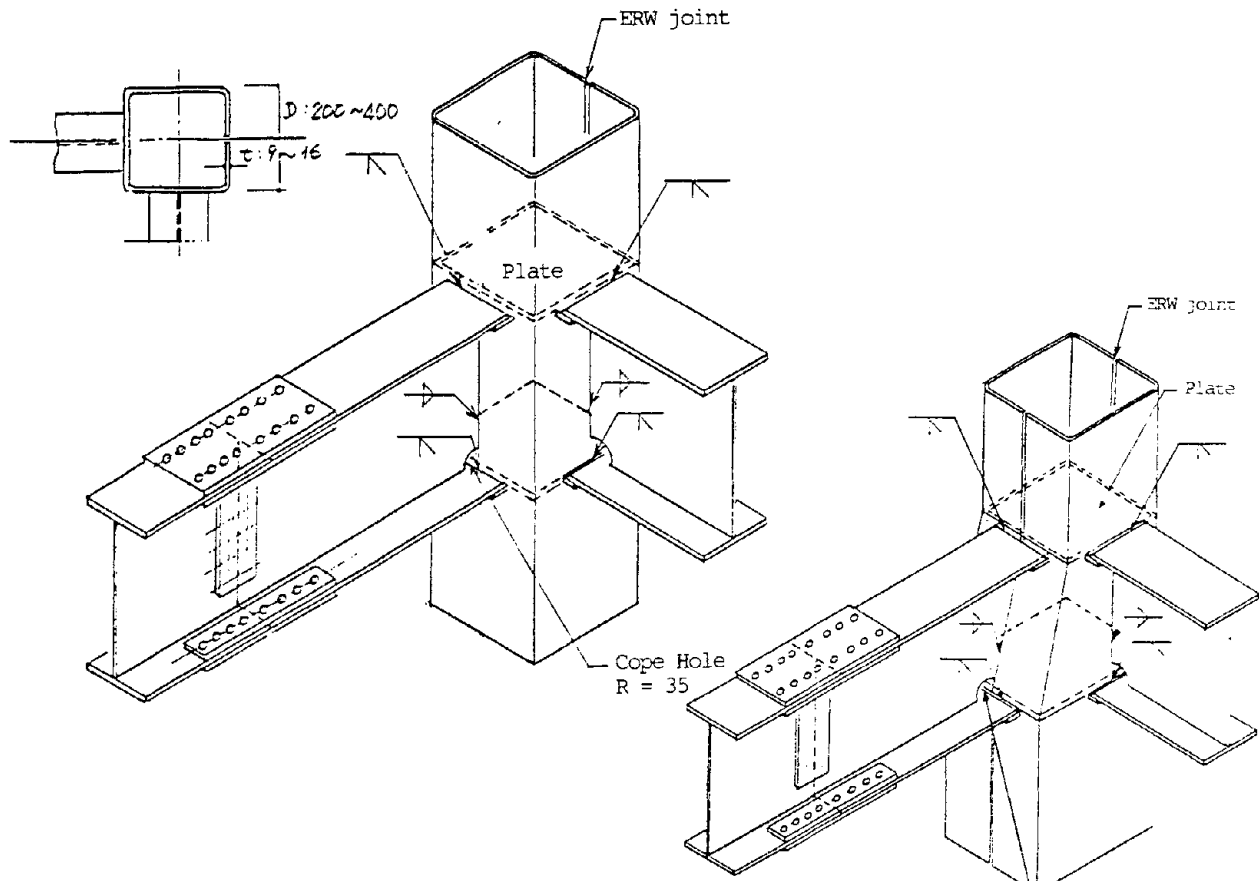
Fig. 6.15 Steel beam-box column connection details

[Chiba, 1989]

D : 200 ~ 400
τ : 9 ~ 16

Plate

ERW joint

Cope Hole
R = 35

ERW joint

Plate

Cope hole
R = 35

Stub

Beam

Plate girder

UB

D : 300 ~ 700
τ : 19 ~ 32

Double light gauge channels
or parallel flange channels

Welded box column

Plate

Cope hole R = 35

135

(a) through-diaphragm   (b) interior diaphragm   (c) exterior diaphragm
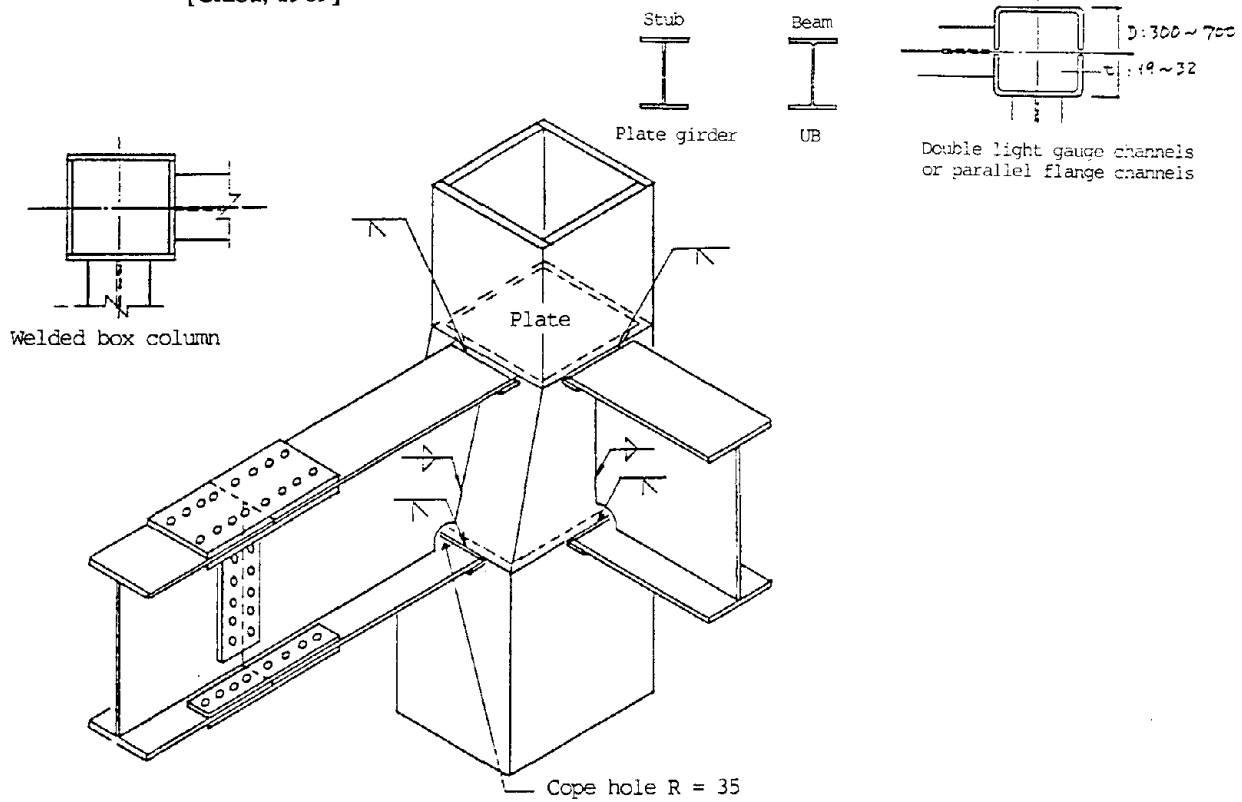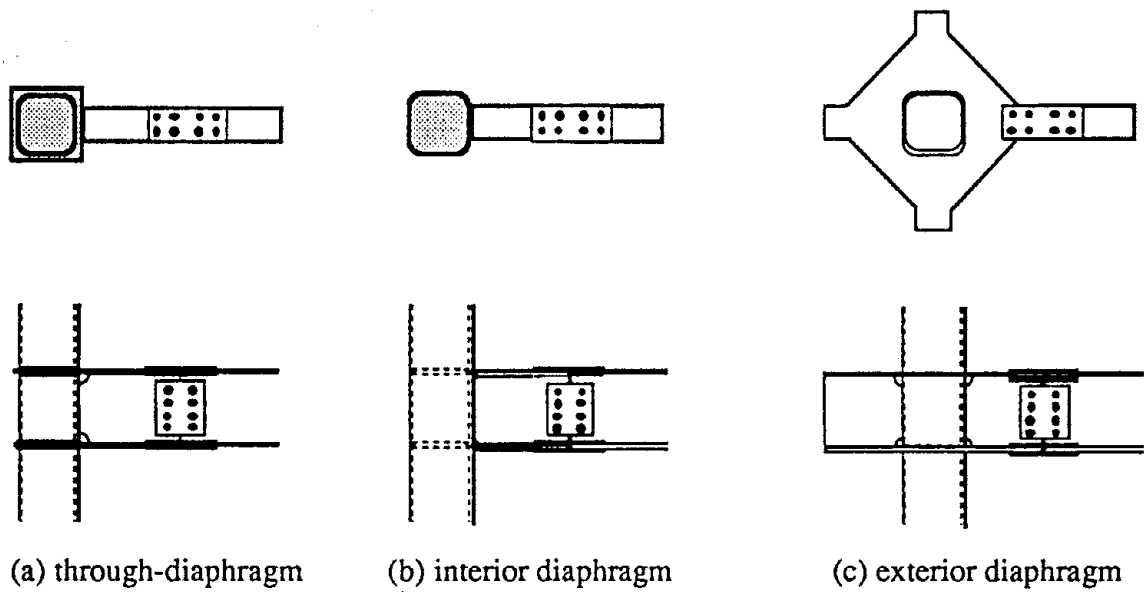
Fig. 6.16 Typical beam-box column connection details
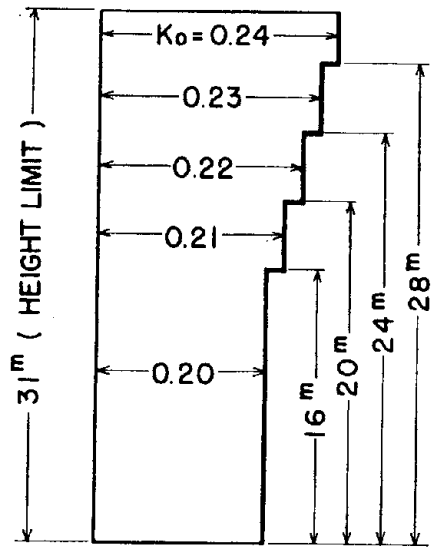
Fig. 6.17 Horizontal seismic coefficient from the 1951 Building Standard Law [Otsuki, 1956]

136

```
┌─────────────────────────┐ ┌──────────────┐ ┌──────────────┐     ┌──────────────┐
│ 1. Timber construction  │ │ 2. h ≦31m and│ │ 3.           │     │ 4.           │
│ Others, as specified by │ │ other than 1 │ │ 31m < h ≦60m │     │ h > 60m      │
│ Ministry of Construction│ │              │ │              │     │              │
└─────────────────────────┘ └──────────────┘ └──────────────┘     └──────────────┘
```

5. Conventional structural design including first phase design for earthquakes

6. Check for storey drift

Note:
h =height

Second phase design for earthquakes

7. Check for rigidity factor and eccentricity

8. Use of specifications of Ministry of Construction

9. Check ultimate capacity for lateral load

10. Approval by building officials of local government body

11. Special approval required

Fig. 6.18 Seismic design per the 1981 Building Standard law [Aoyama, 1993]

137
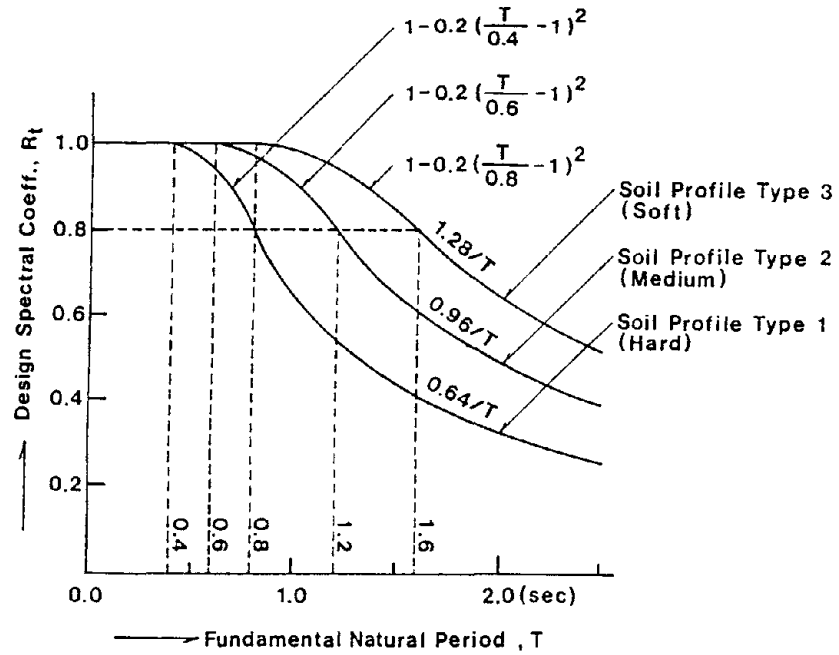
Fig. 6.19 Spectral ordinate factor Rt [Aoyama, 1993]
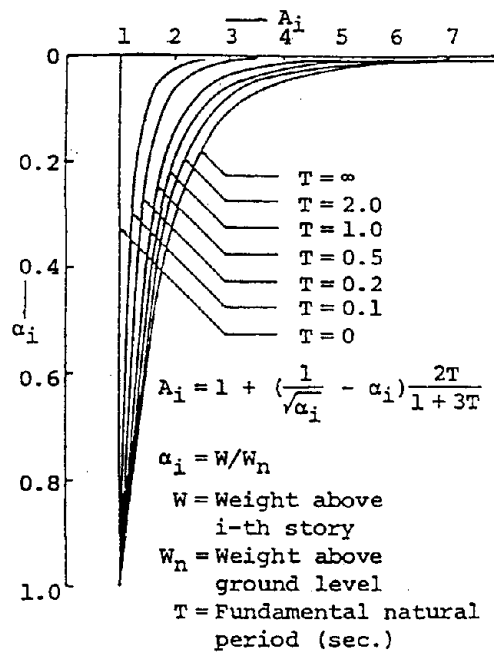
Fig. 6.20 Vertical distribution factor [Aoyama, 1993]

138
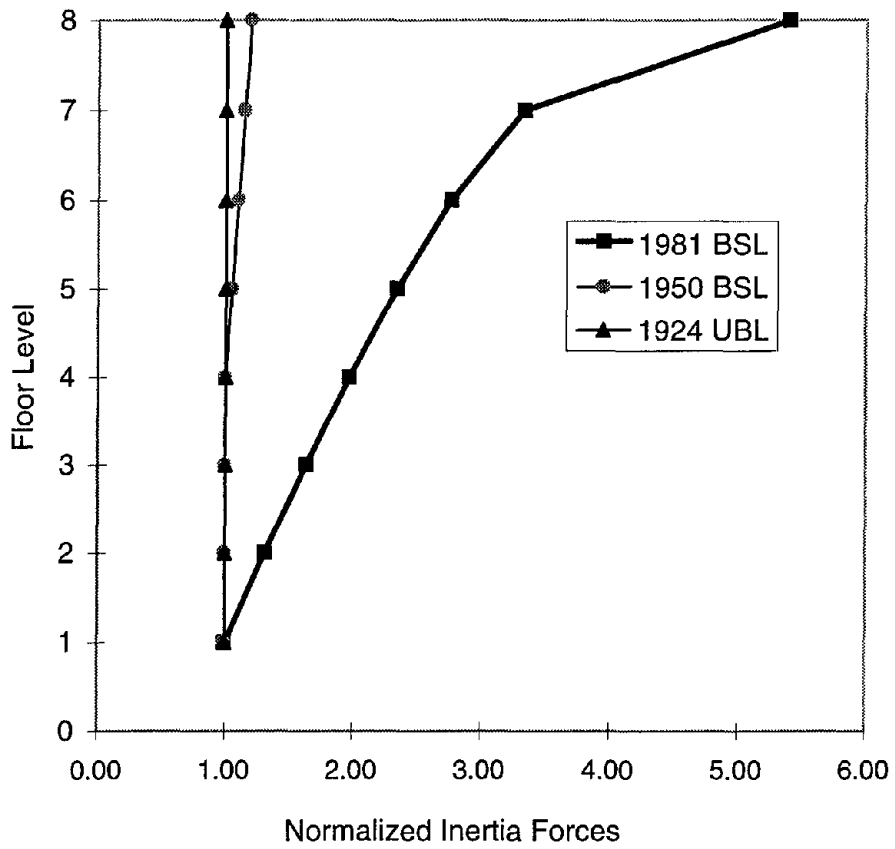
Fig. 6.21 Normalized inertia force profiles for the 1924 UBL, 1950 BSL, and 1981 BSL
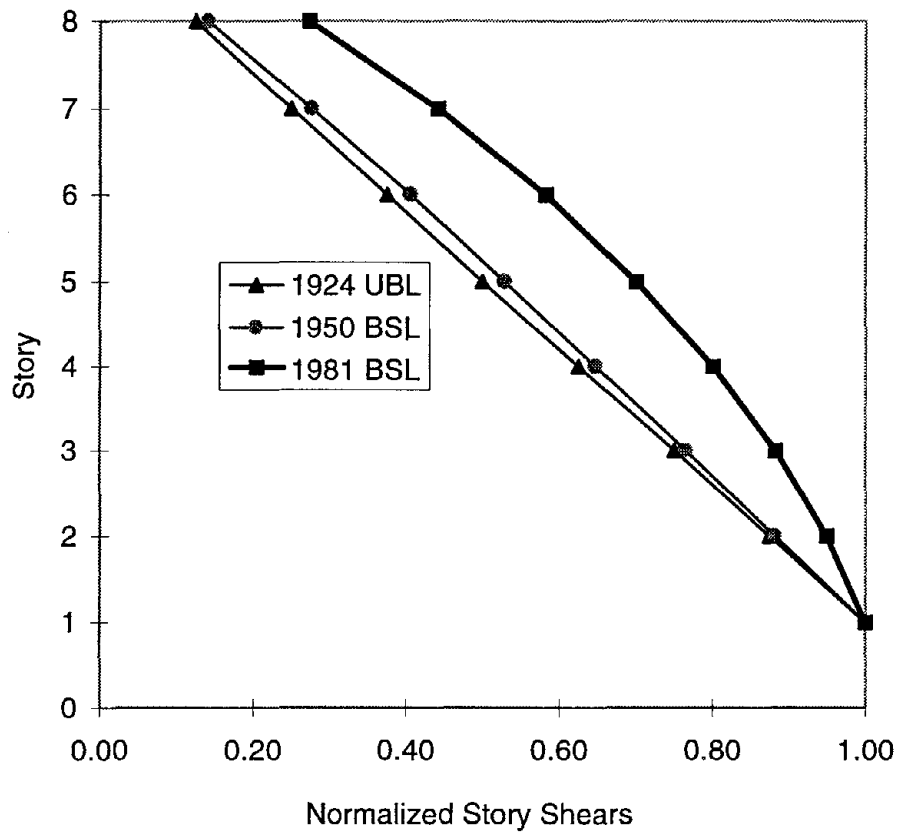
Fig. 6.22 Normalized story shear distributions for the 1924 UBL, 1950 BSL, and 1981 BSL

140
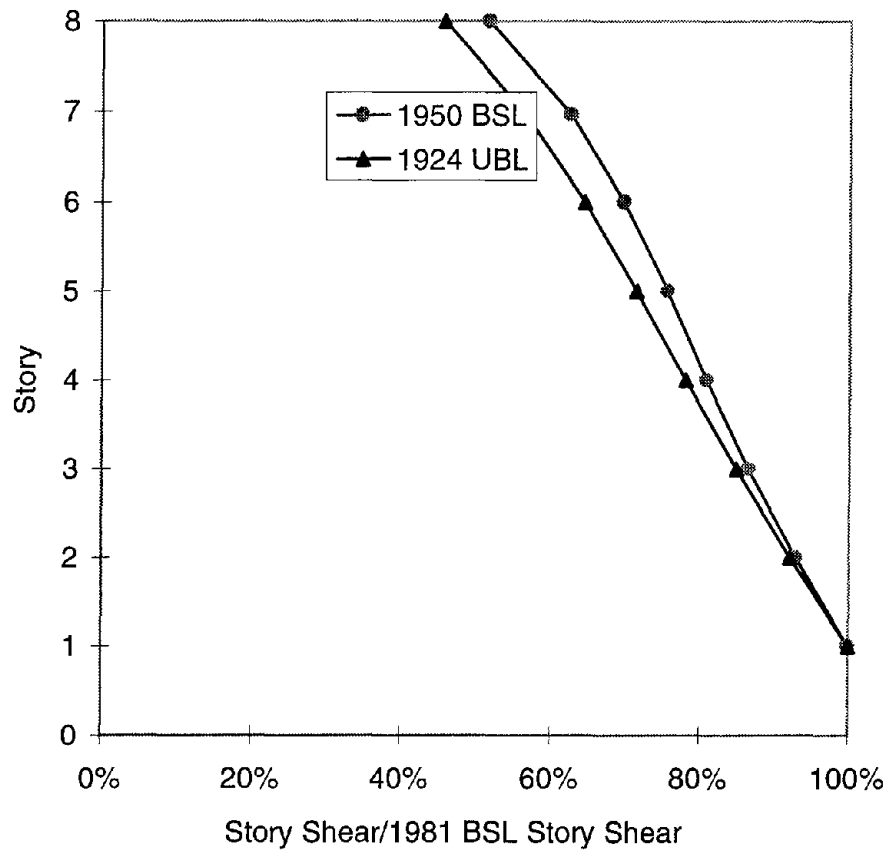
Fig. 6.23 Story shear distributions normalized to the 1981 BSL story shear distribution

JR 宝塚駅

NS	694
EW	587
UD	410

神戸大学

NS	270
EW	305
UD	

神戸海洋気象台

NS	818
EW	617
UD	332

JR 鷹取駅

NS	642
EW	666
UD	290

本山

NS	421
EW	775
UD	379

震央
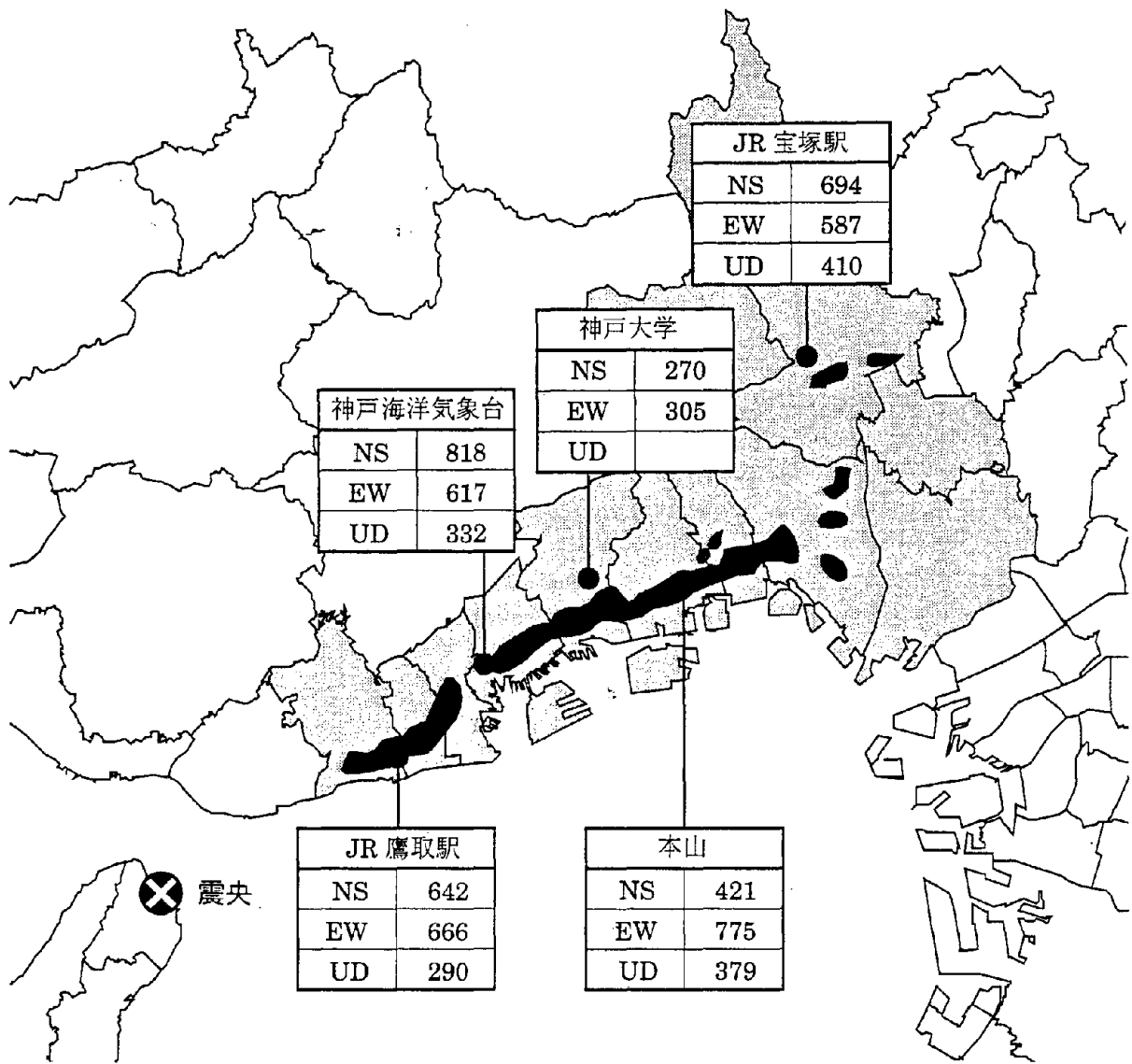
Fig. 6.24 Extent of intensity 7 shaking
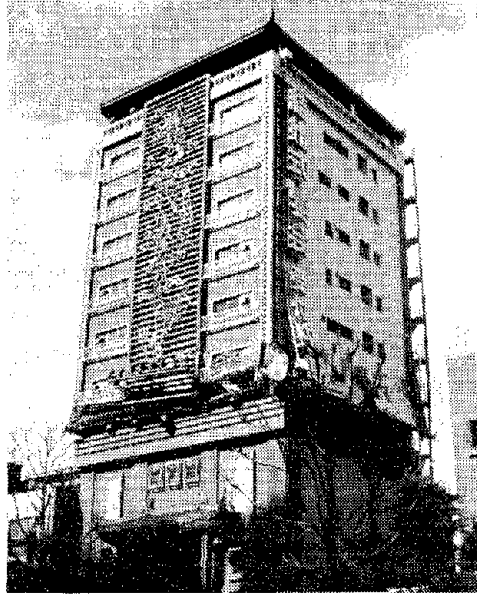
Fig. 6.25 Mid-height story collapse

Fig. 6.26 First story collapse
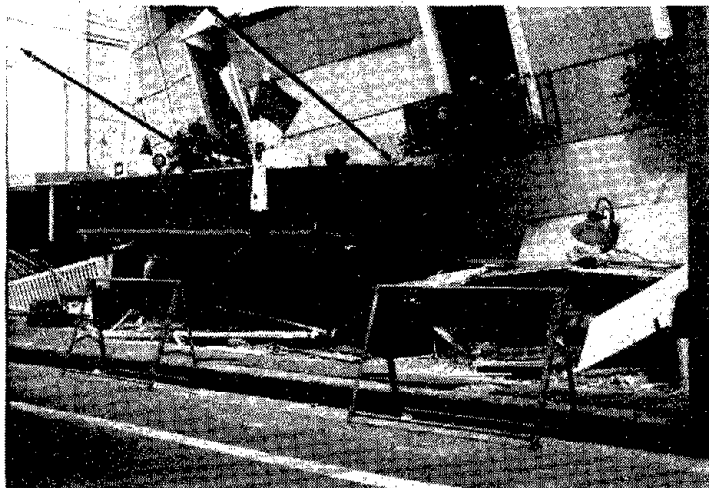
Fig. 6.27 First story collapse
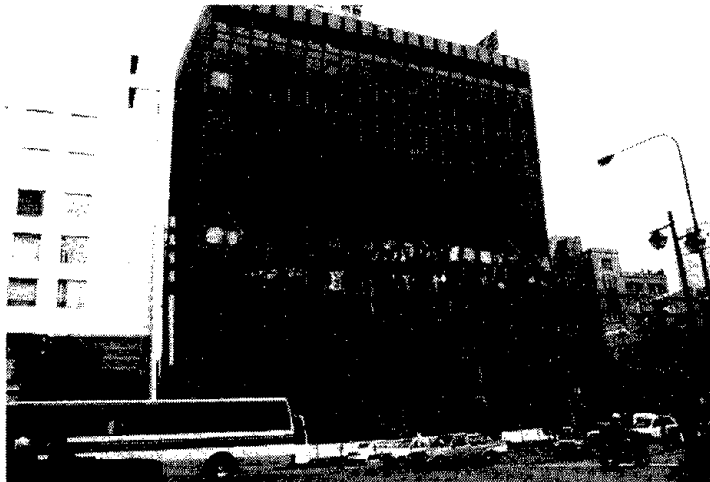
Fig. 6.28 Mid-height story collapse
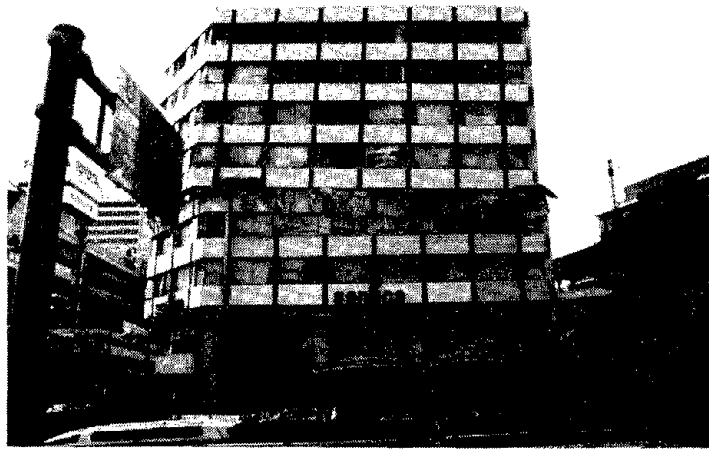
Fig. 6.29 Mid-height story collapse likely due to irregularity
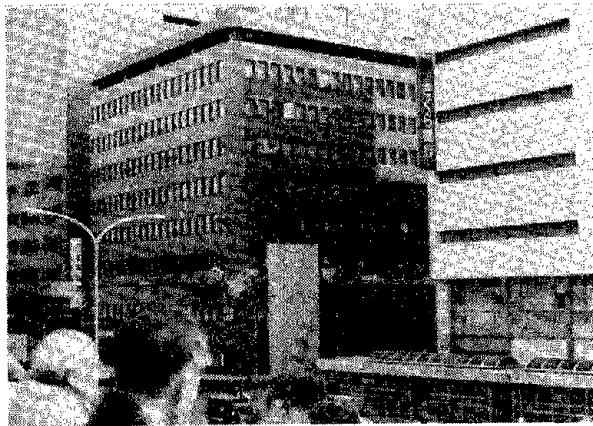
Fig. 6.30 Mid-height story collapse likely due to irregularity

144
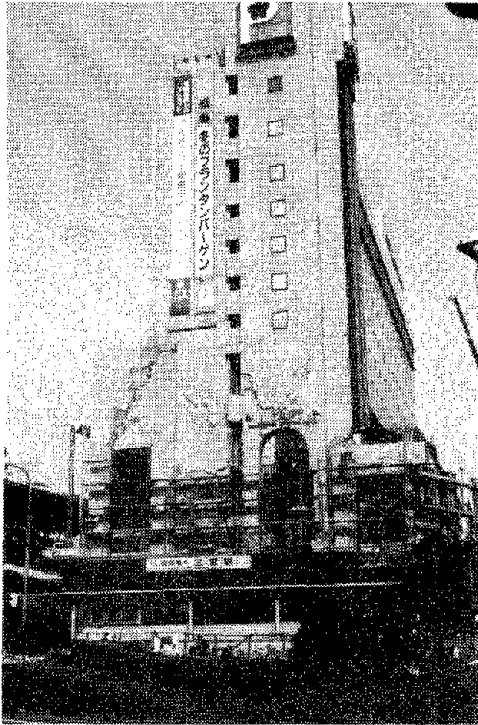
Fig. 6.31 Building damage likely due to irregularity

Fig. 6.32 Overturned nine-story building
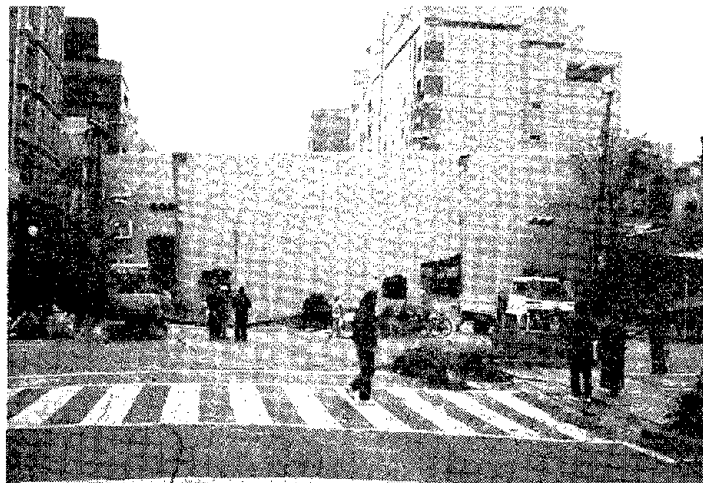
Fig. 6.33 Bearing wall details - overturned nine-story building

Fig. 6.34 Foundation details - overturned nine-story building
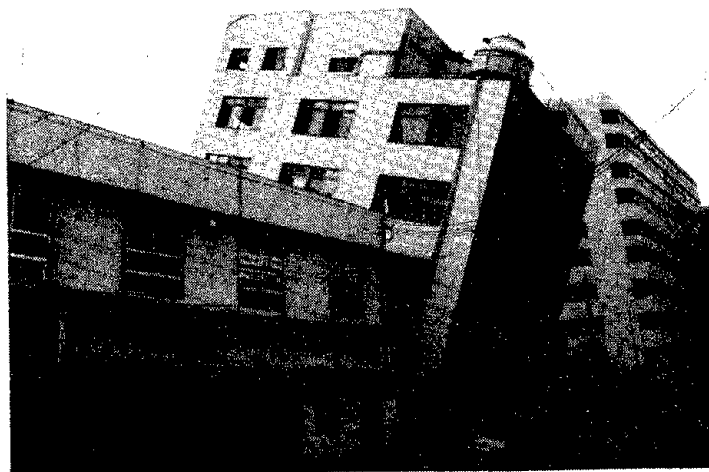
Fig. 6.35 Overturned six-story building

Fig. 6.36 Tension failure of frame-wall - overturned six-story building

146
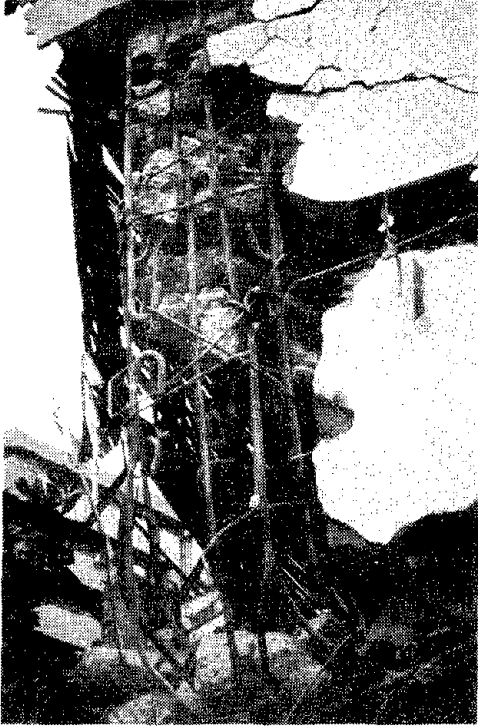
Fig. 6.37 Typical pre-1971 rebar details -
from overturned six-story building

Fig. 6.38 Post-1971 column rebar details

147

Fig. 6.39 Mid-height story collapse - West City Hospital

Fig. 6.40 Failed columns (piers) - West City Hospital

Fig. 6.41 Damage to shear-critical reinforced concrete columns; post-1981 construction

148
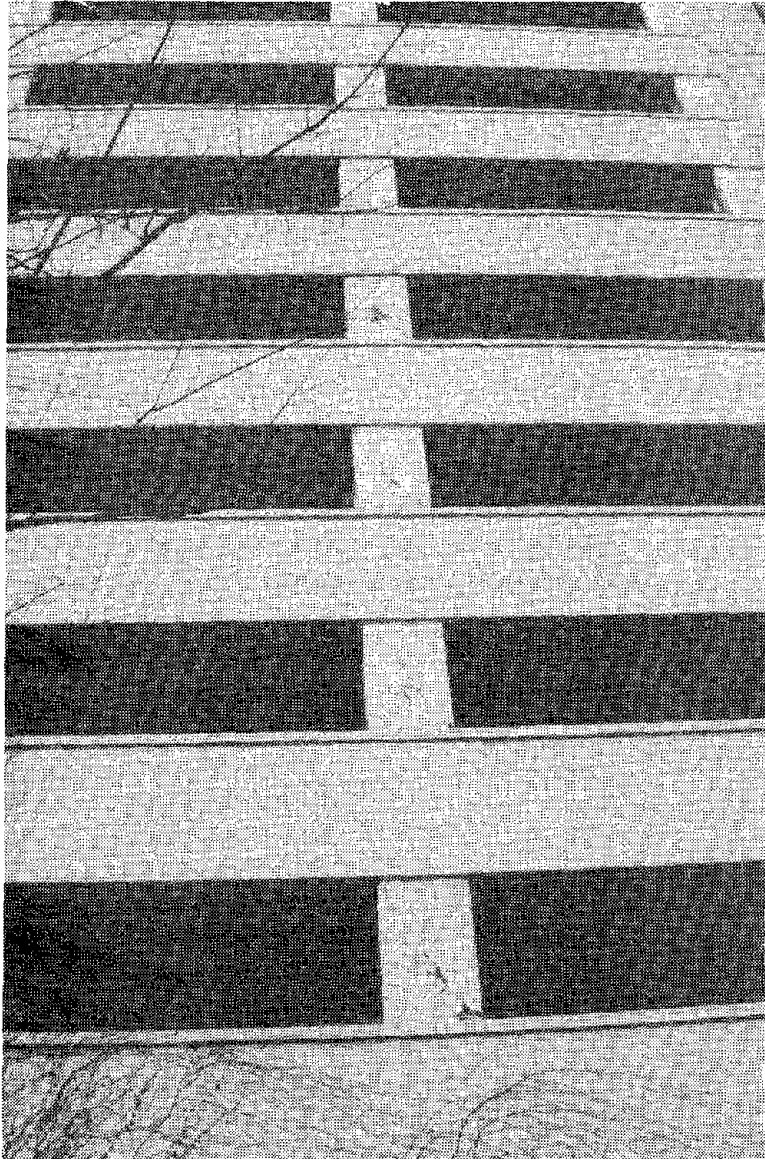
Fig. 6.42 Damage to shear-critical reinforced concrete columns
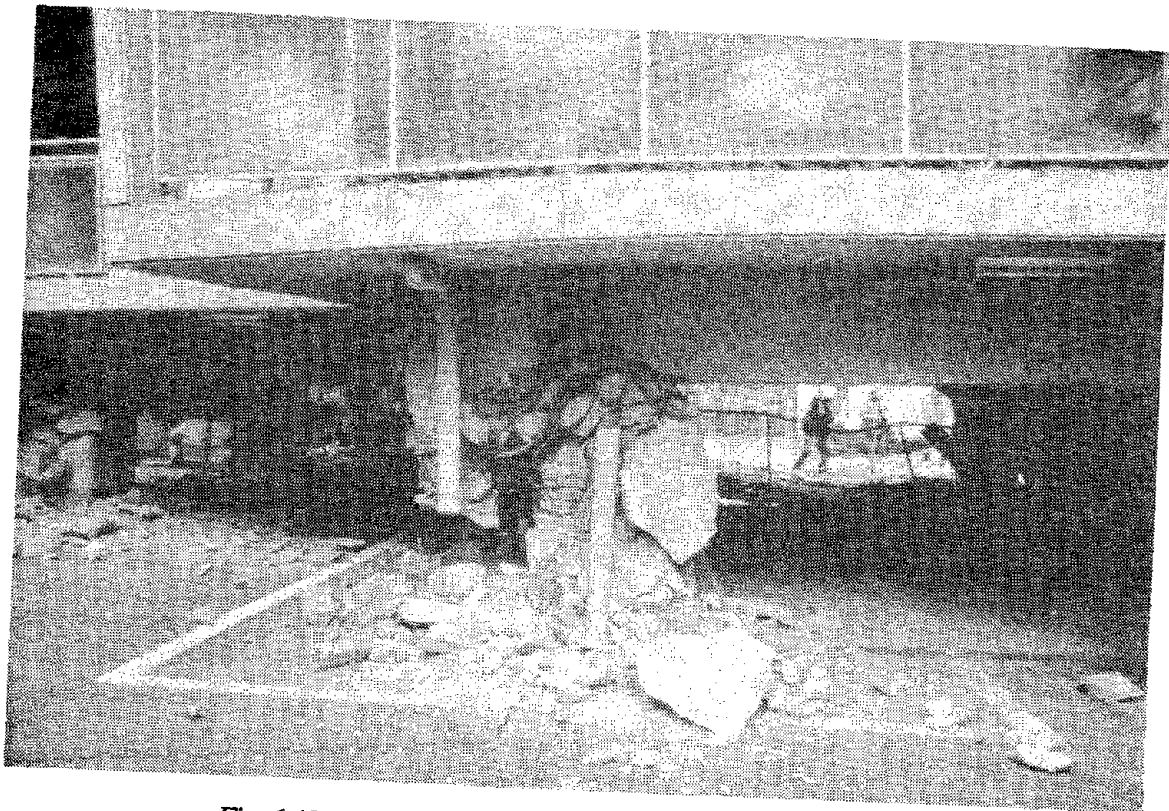
Fig. 6.43 Shear failure of first-story reinforced concrete columns

Fig. 6.44 Nine-story building with failed first-story columns

Fig. 6.45 Shear-cracking in a beam-column
joint; post-1981 construction
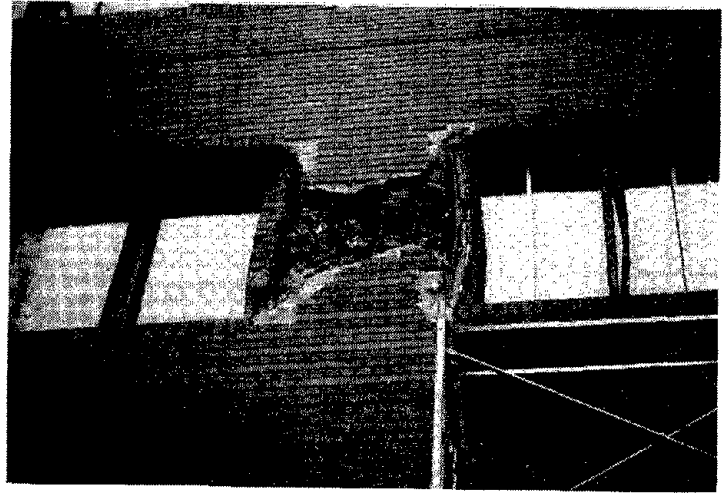
Fig. 6.46 Shear-failure of a short column (pier);
post-1981 construction
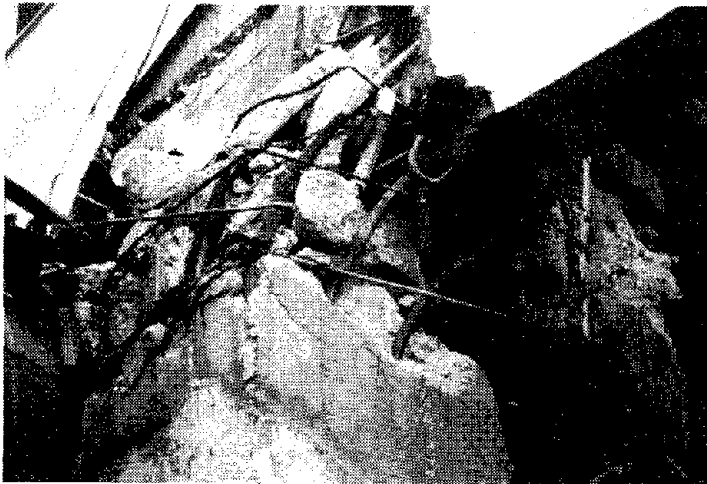
Fig. 6.47 Failed beam-column joint; pre-1971 construction

Fig. 6.48 Damage to a haunched beam-circular
column joint; pre-1971 construction

Fig. 6.49 Damage to a beam-column joint

Fig. 6.50 Damage to a modern beam-column joint

153

Fig. 6.51 Failure and collapse of precast concrete cladding
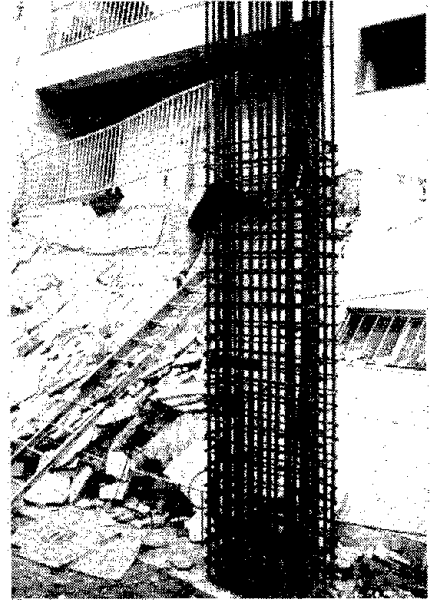
Fig. 6.52 Construction details for
a new reinforced concrete column
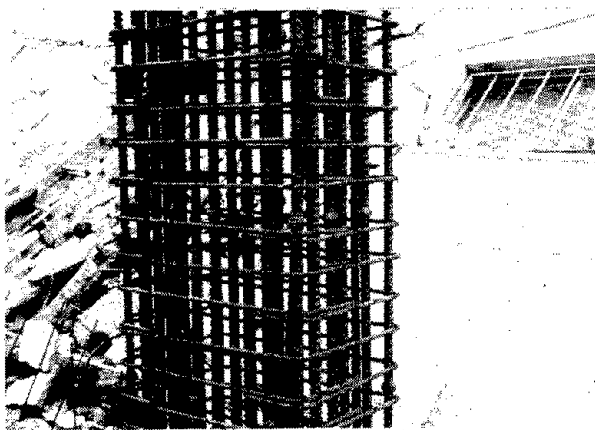
Fig. 6.53 Transverse reinforcement in
a new reinforced concrete column

Fig. 6.54 Complete collapse of
reinforced concrete building;
pre-1971 construction

154
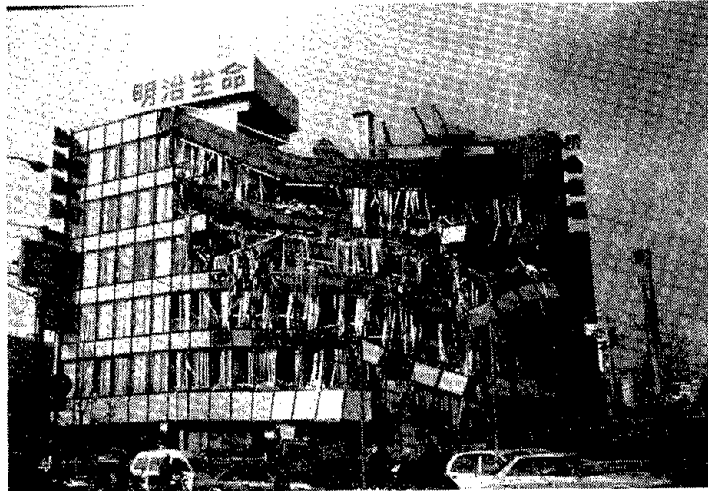
Fig. 6.55 Partial collapse of mid-rise reinforced concrete building

Fig. 6.56 Damage to a reinforced concrete structural wall
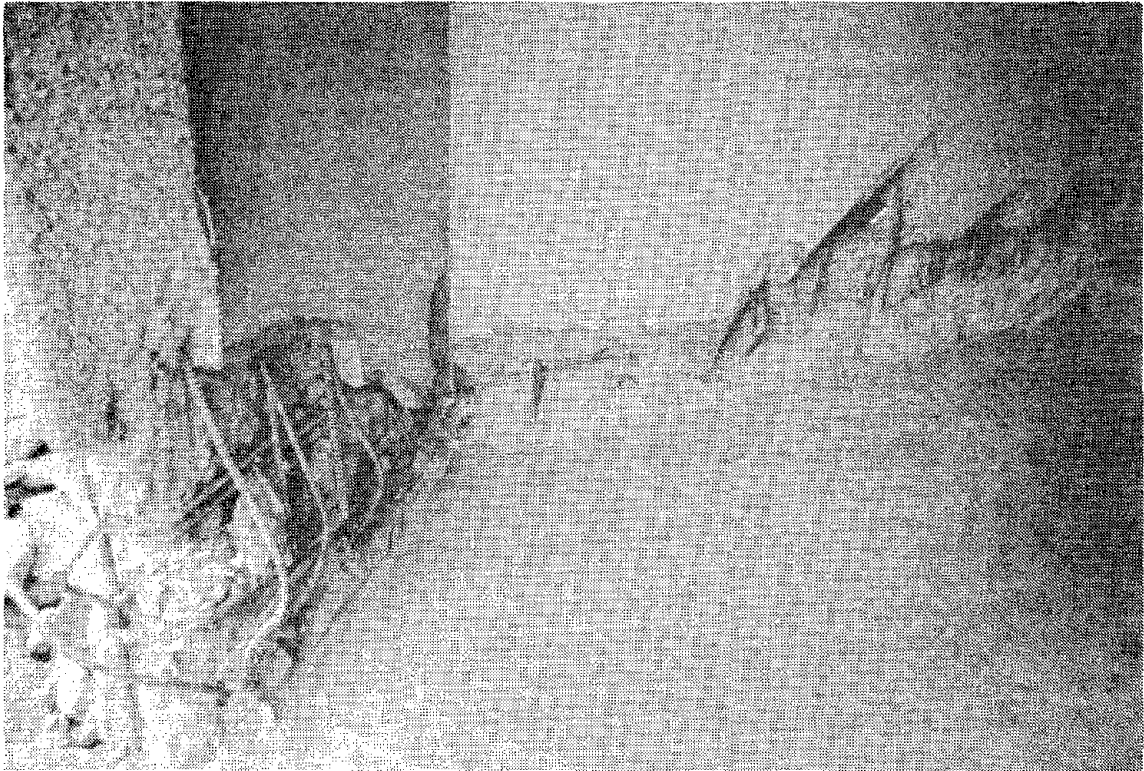
Fig. 6.57 Damage to a reinforced concrete structural wall
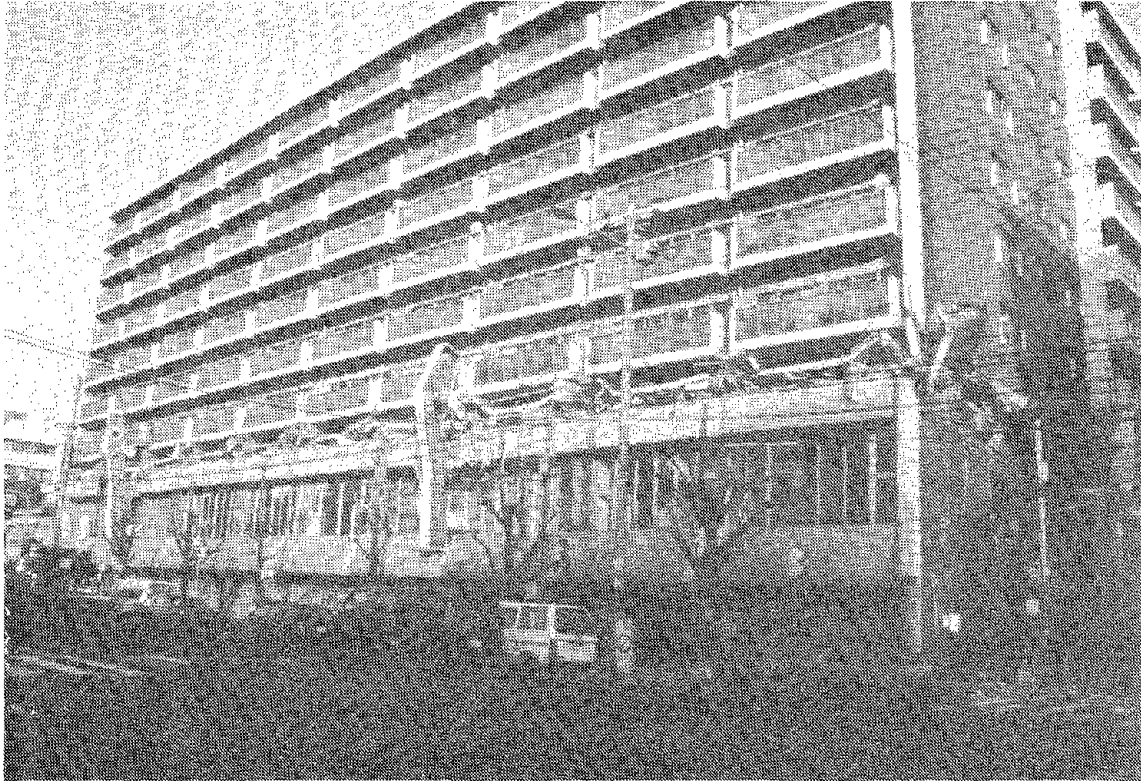
Fig. 6.58 South elevation of an irregular, U-shaped, reinforced concrete building

Fig. 6.59 Part-west elevation of the building shown in Figure 6.58
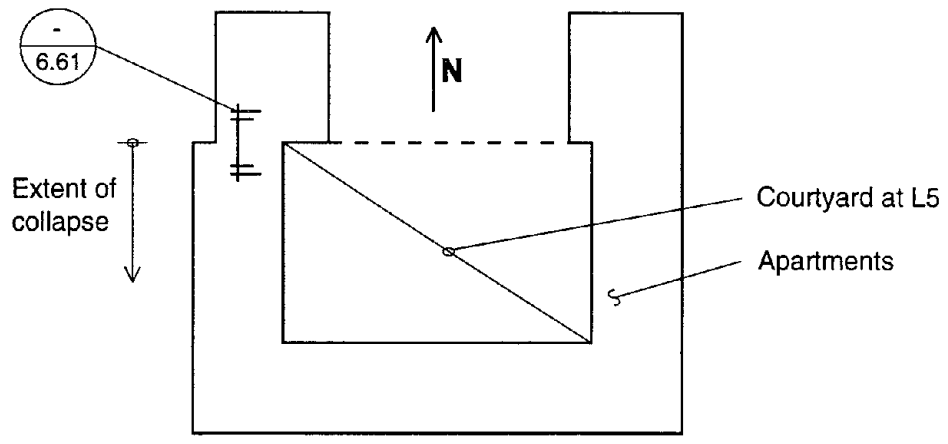
Plan Geometry above L5
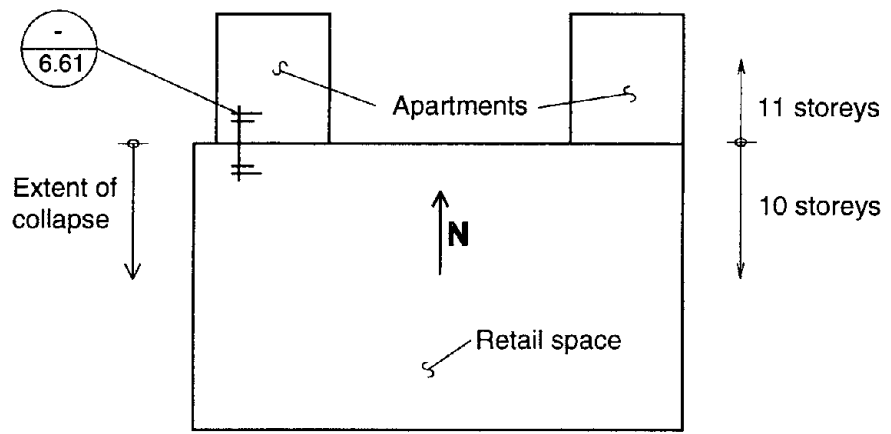
Plan Geometry at L1

Fig. 6.60 Schematic plans of collapsed building at Levels 1 and 5
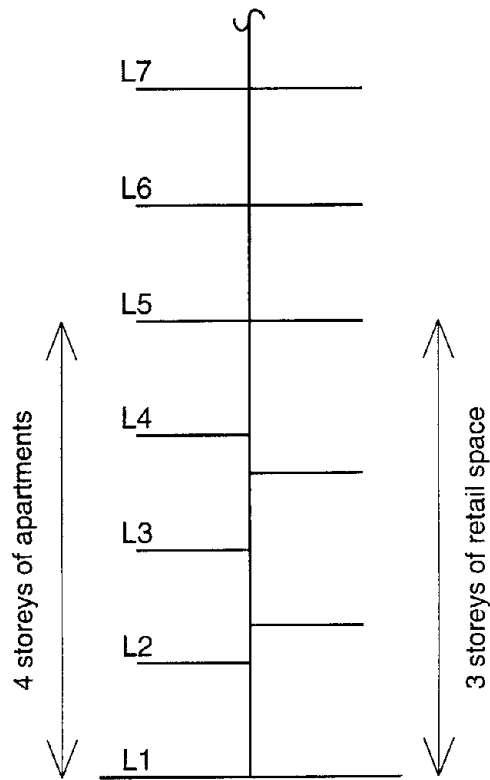
Cross section through building

Fig. 6.61 Schematic cross-section through the collapsed building

159
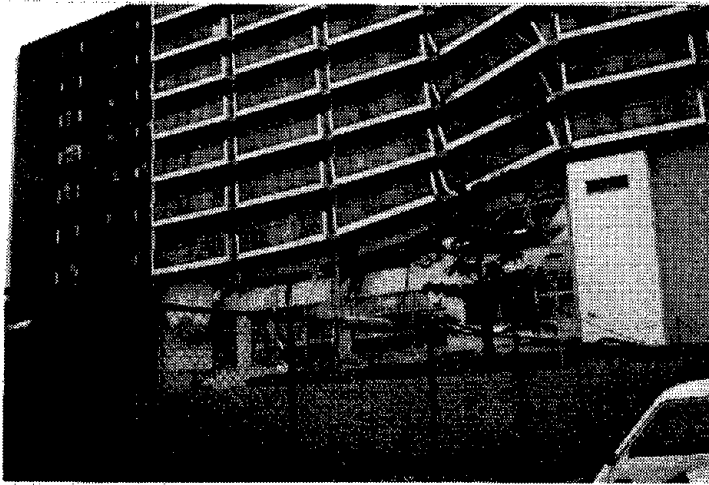
Fig. 6.62 East elevation of collapsed building
showing mid-height collapse

Fig. 6.63 Elevation of courtyard wall
in the collapsed building
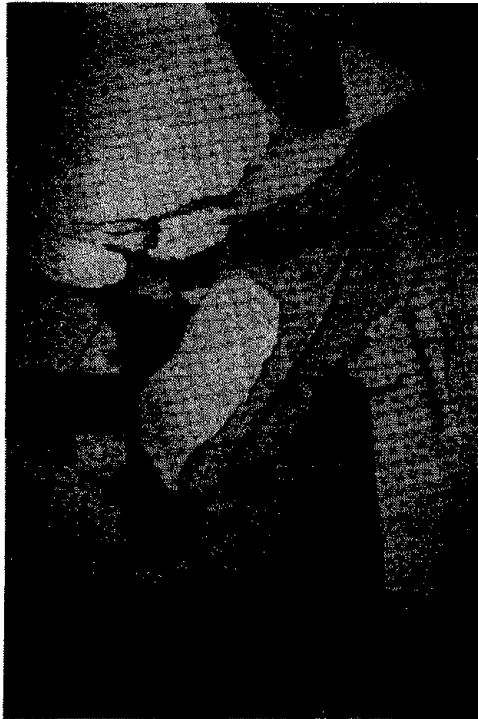
Fig. 6.64 Typical damage in collapsed story
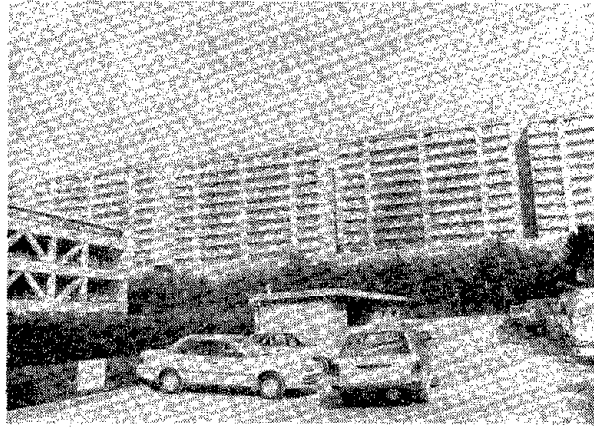
Fig. 6.65 Modern reinforced concrete frame-wall construction on Port Island

Fig. 6.66 Shear cracking in short wall piers; post-1981 construction
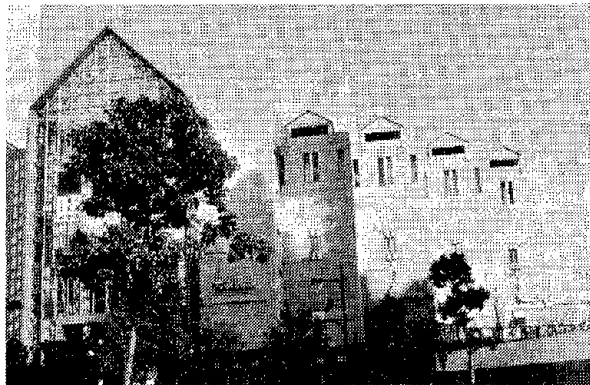
Fig. 6.67 Exterior view of a damaged building; post-1981 construction
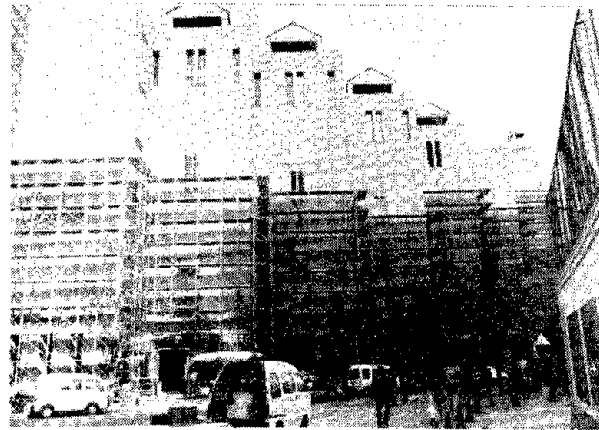
Fig. 6.68 Shear cracking in reinforced concrete walls (behind scaffolding)

Fig. 6.69 Heavy damage to reinforced concrete structural walls
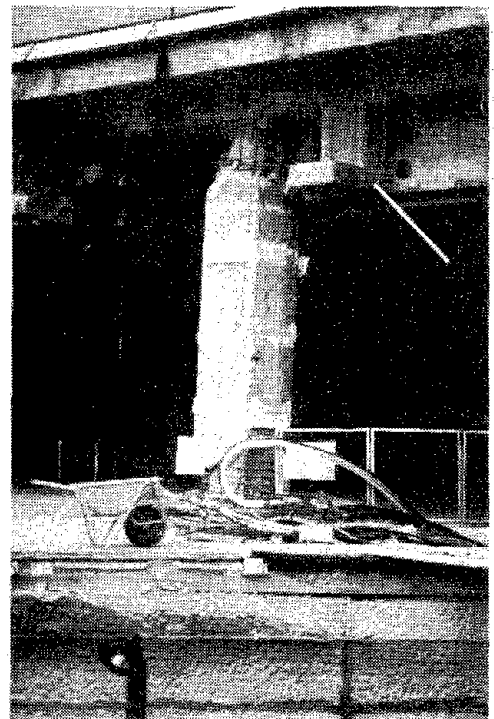
Fig. 6.70 Plastic hinging in a reinforced concrete column

162
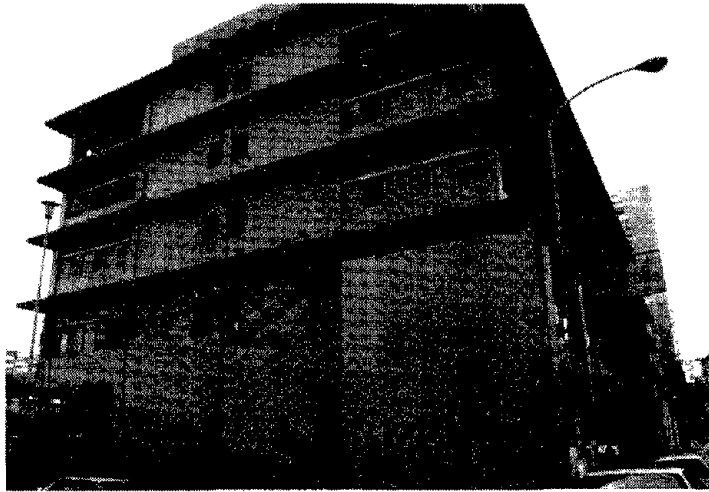
Fig. 6.71 Five-story Kobe-Chou Post Office
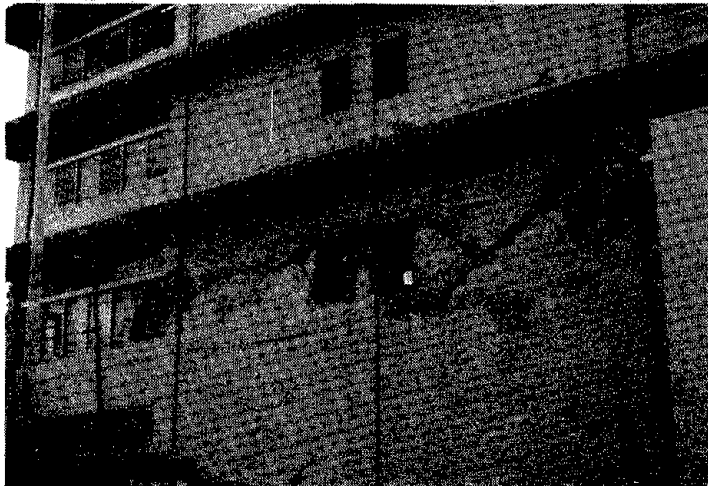
Fig. 6.72 Damage to the northern wall of the Post Office
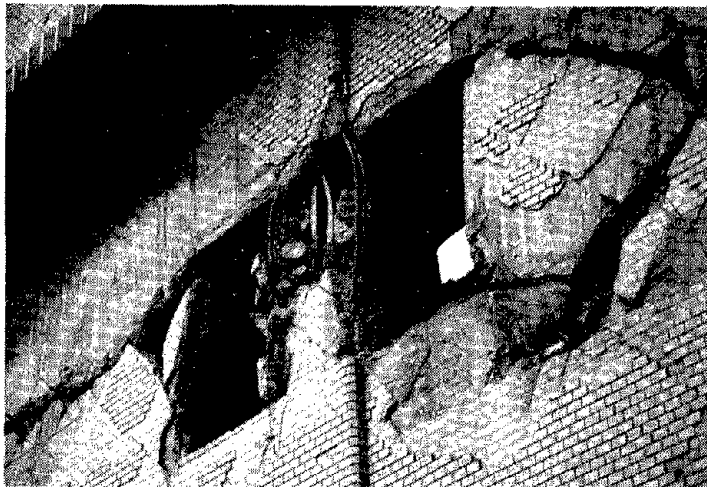
Fig. 6.73 Failed SRC column in the middle of the structural wall shown in Figure 6.72

Fig. 6.74 Failed SRC boundary element at the
edge of the wall shown in Figure 6.72
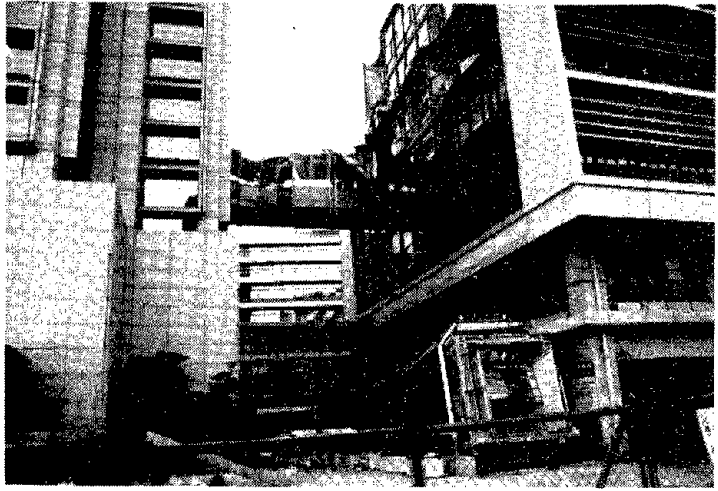
Fig. 6.75 Breezeway between buildings in
the Kobe City Hall complex
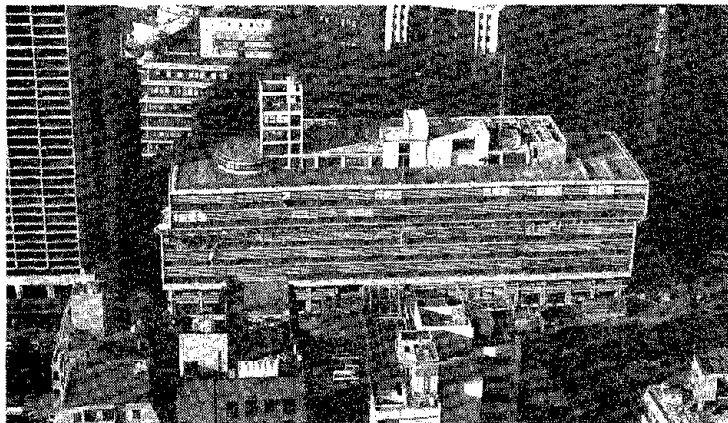
Fig. 6.76 Aerial view of the Kobe City Hall (Annex) following the earthquake
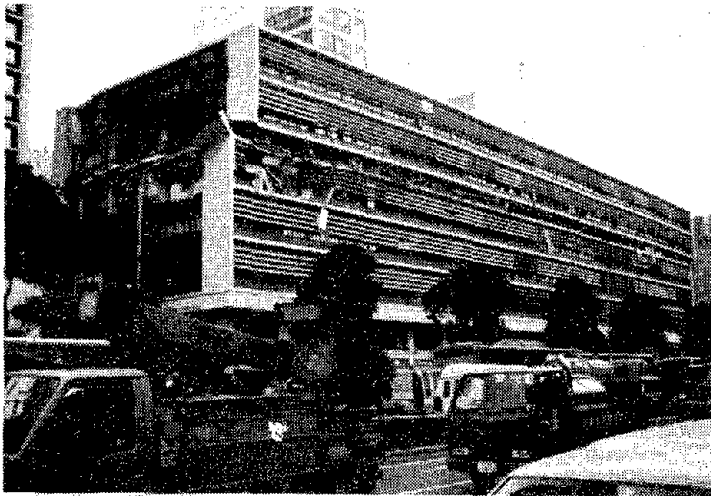
Fig. 6.77 End elevation of Annex building showing collapsed story

Fig. 6.78 View of end of Annex building
showing offset above collapsed story

Fig. 6.79 Shear failure of first-story, SRC columns
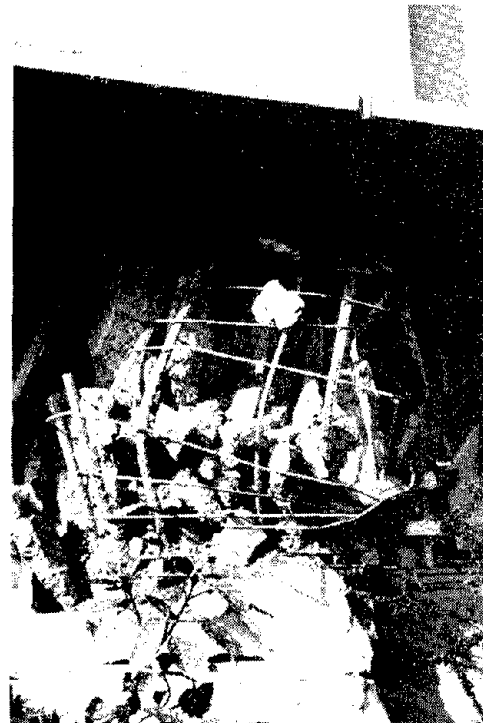
Fig. 6.80 Rebar details in the failed columns
of Figure 6.79
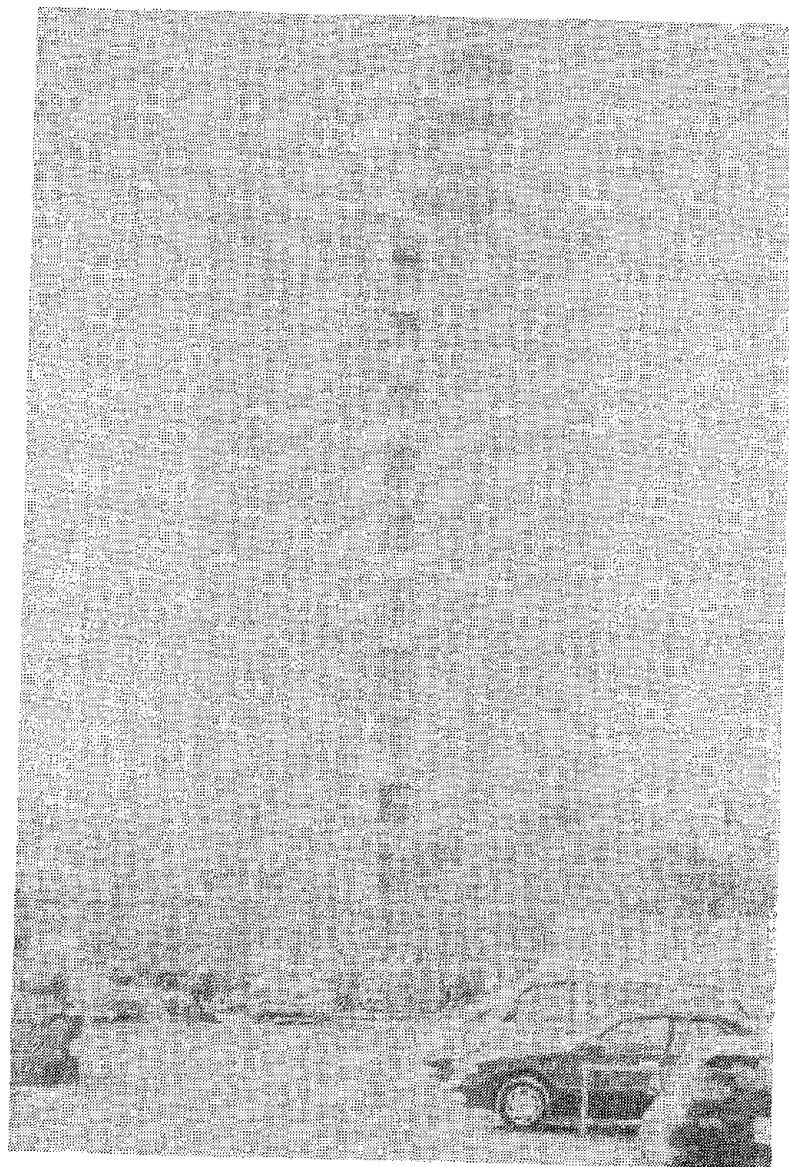
Fig. 6.81 Elevation of modern, damaged, SRC building
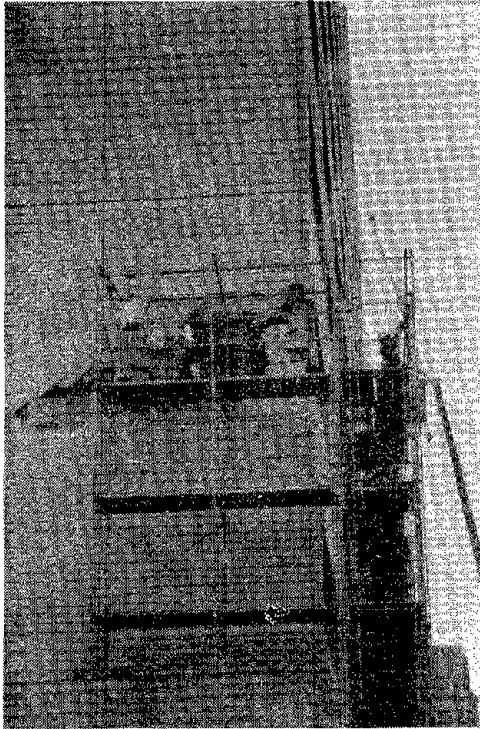
Fig. 6.82 Exterior view of damage to
an SRC boundary element
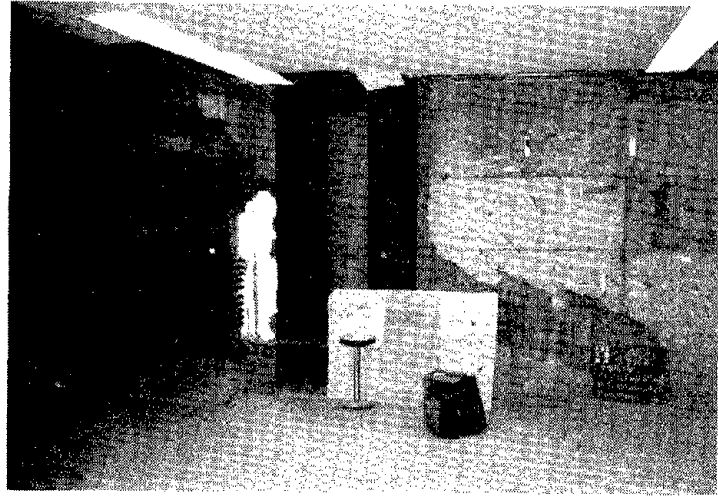
Fig. 6.83 Interior view of the damaged boundary element shown
in Figure 6.82

Fig. 6.84 Repair detail for a damaged boundary
element splice
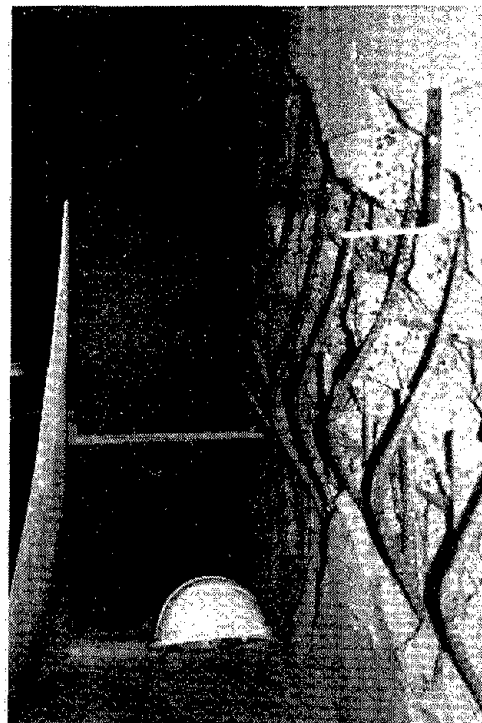
Fig. 6.85 Rebar buckling in the damaged SRC
structural wall
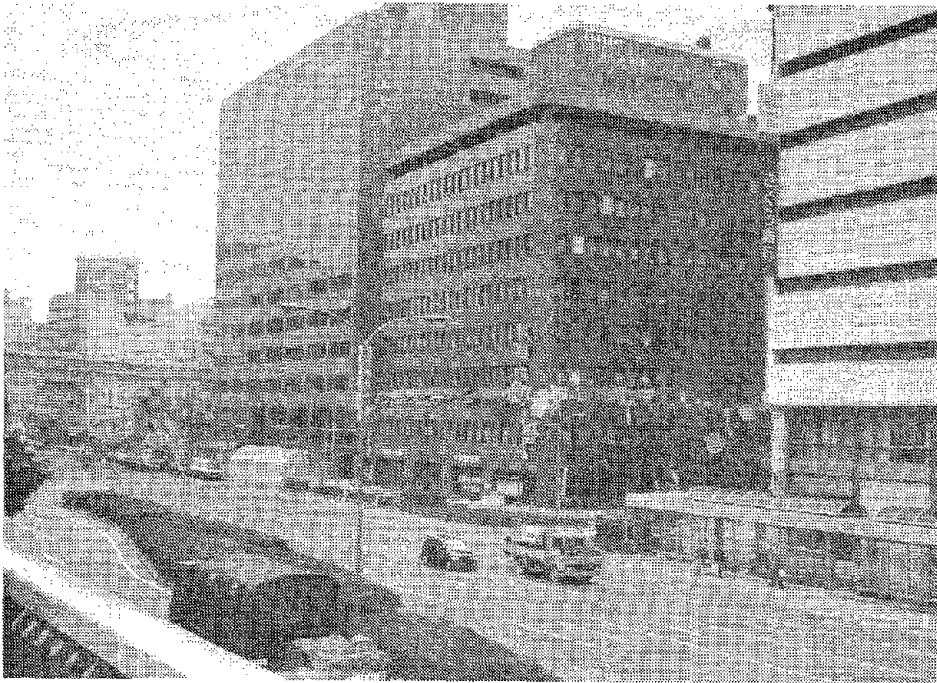
Fig. 6.86 View of two damaged SRC buildings
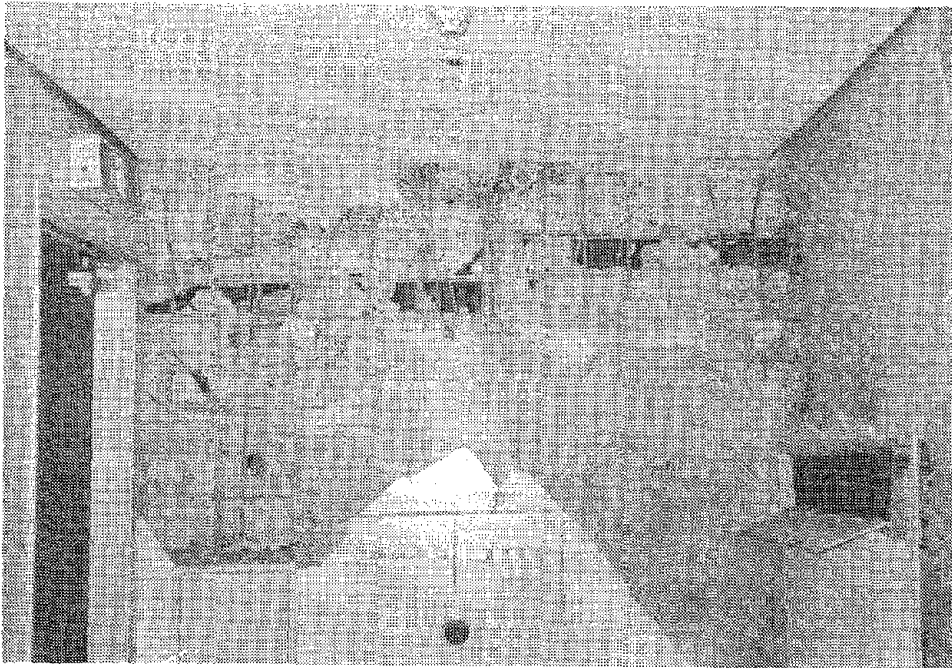
Fig. 6.87 Damage to a post-1981 SRC building incorporating structural walls

Fig. 6.88 Soft and weak story failure of
a steel moment frame building
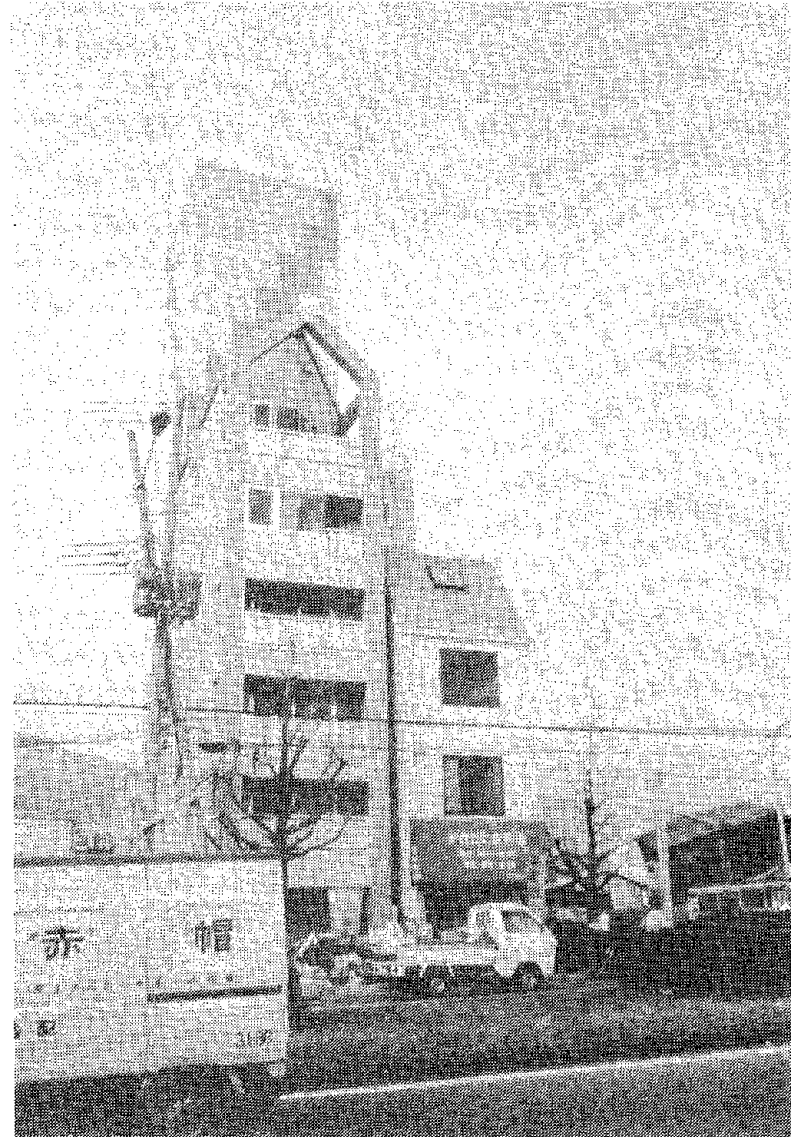
Fig. 6.89 High aspect ratio buildings
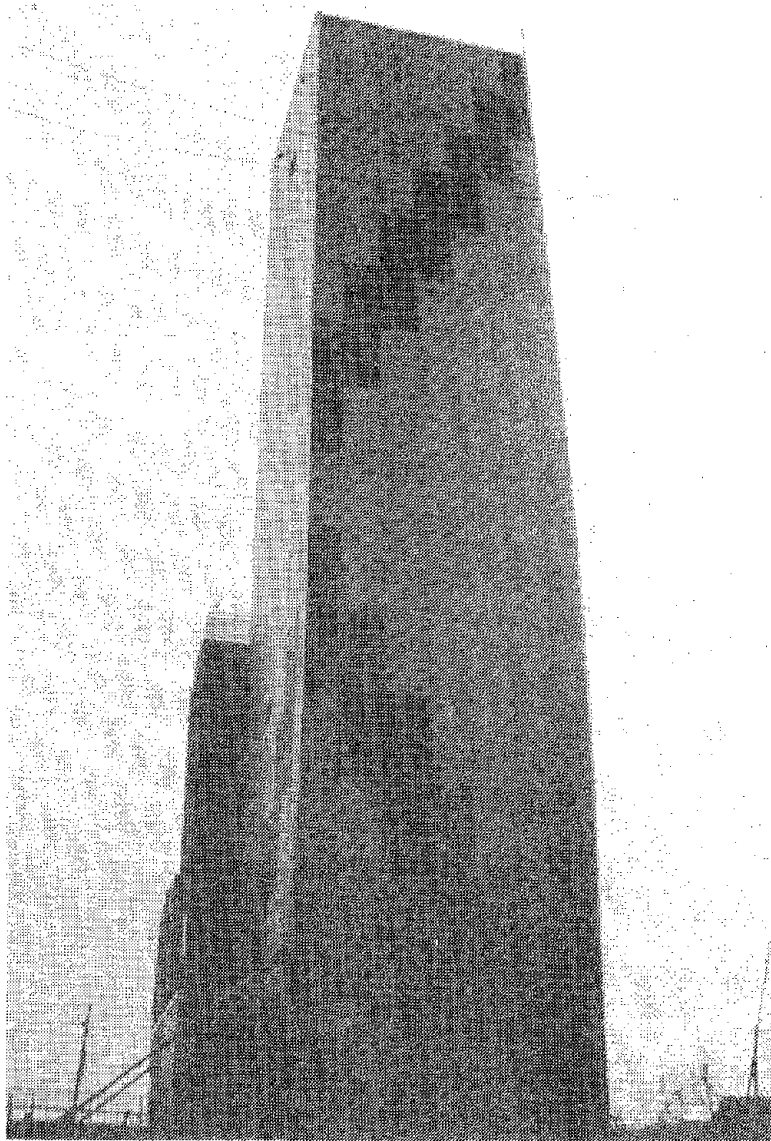
Fig. 6.90 Permanent torsional deformation of a high aspect ratio building

Fig. 6.91 Excessive sway due to fracture of slender braces

Fig. 6.92 Failed column-beam connection at continuity plate
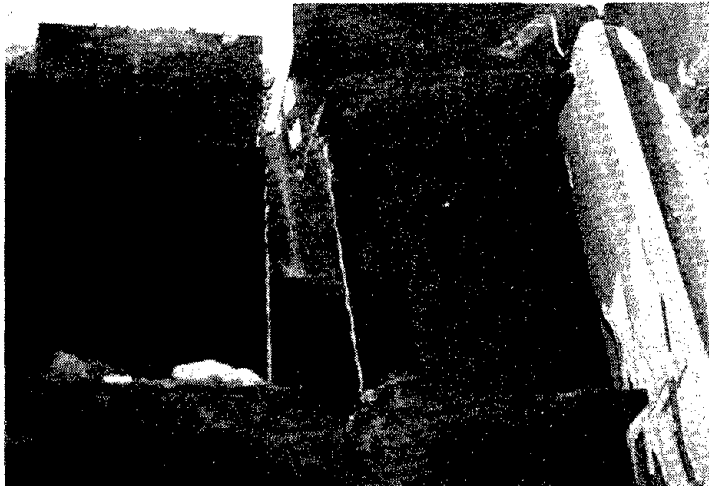
Fig. 6.93 Failed column-beam connection at face of column

Fig. 6.94 Failed baseplate connection

171
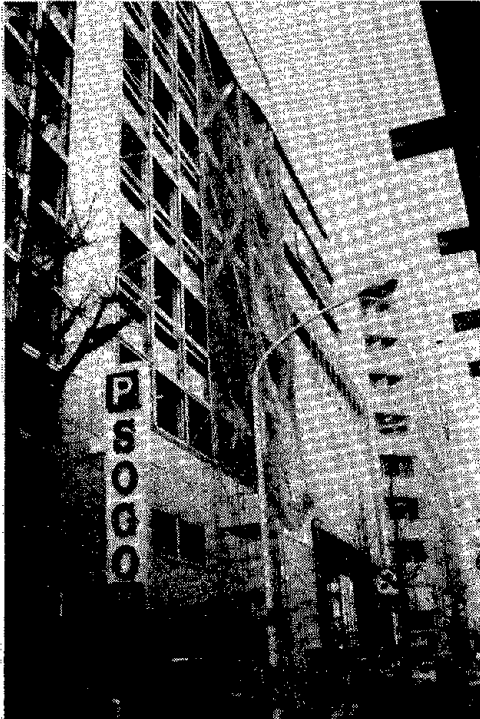
Fig. 6.95 View of damaged, modern, cross-braced, steel building

Fig. 6.96 Fracture of box column immediately above grade beam
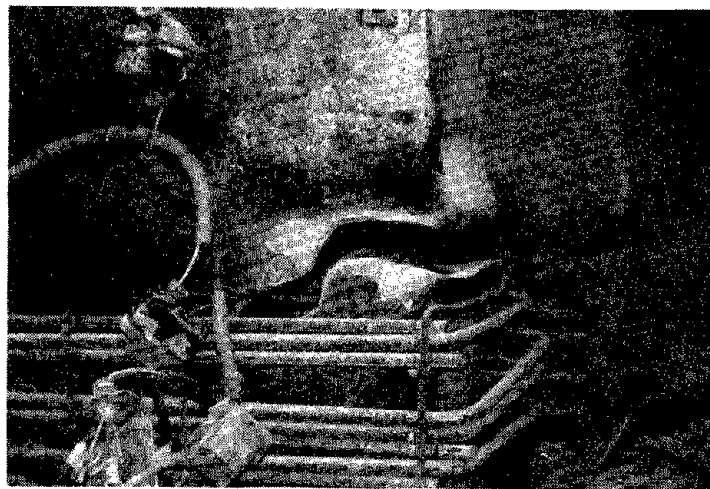
Fig. 6.97 View of fractured box column
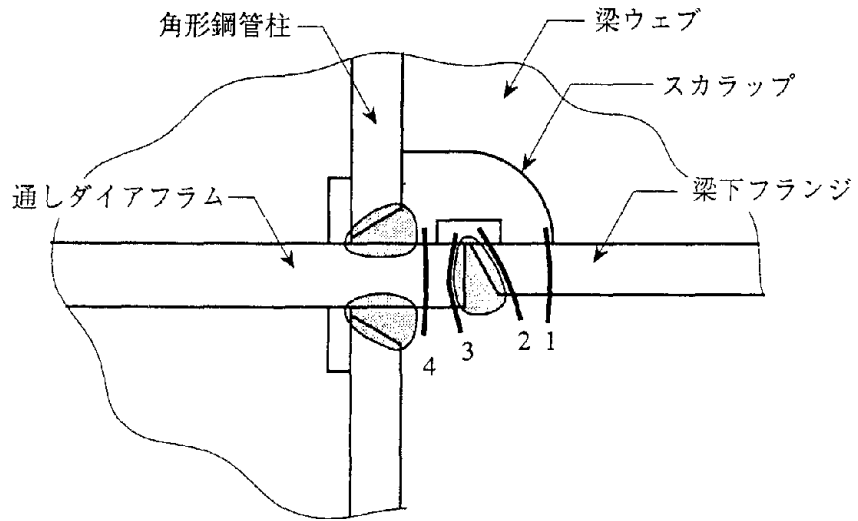
Fig. 6.98 Summary of observed failures in steel moment-frame connections
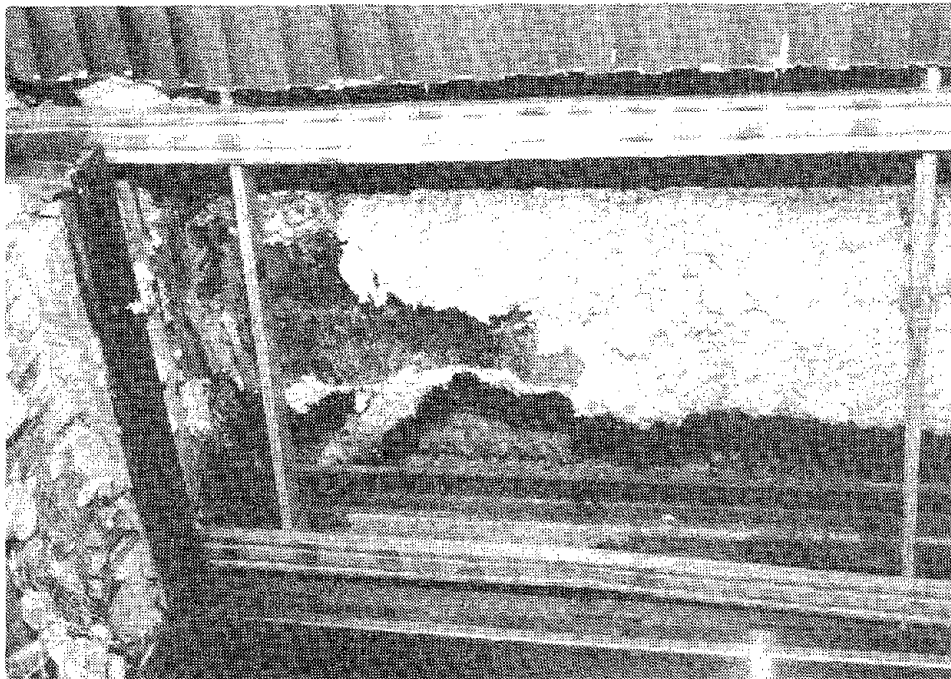
Fig. 6.99 Type 1 fracture of a moment-frame connection
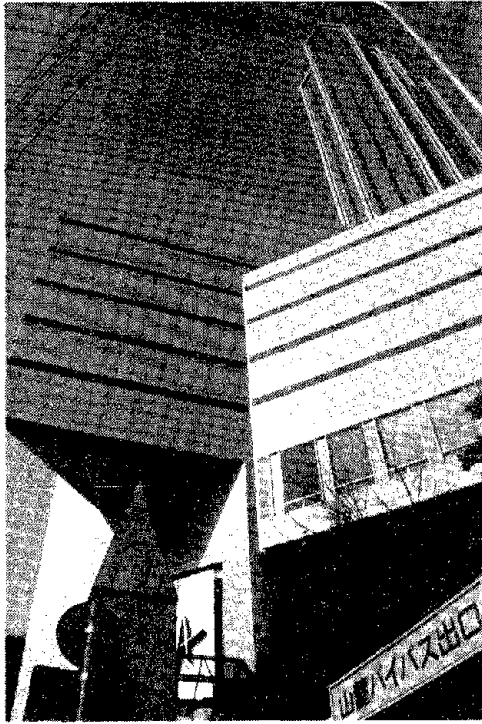
Fig. 6.100 View of modern steel moment-frame building

Fig. 6.101 Elevation of a high aspect ratio building

Fig. 6.102 Elongated bolts in a damaged baseplate connection

174

Fig. 6.103 Overturned steel moment-frame building
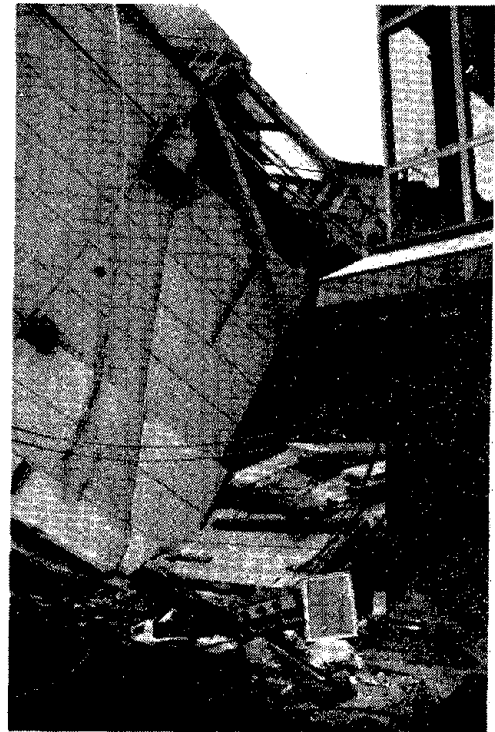
Fig. 6.104 Base of an overturned steel
moment-frame building

Fig. 6.105 View of a failed baseplate connection

175
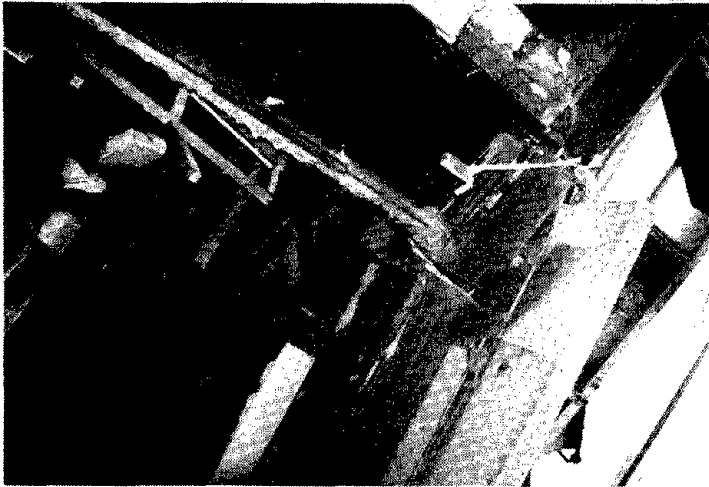
Fig. 6.106 Failed all-welded beam-column connection
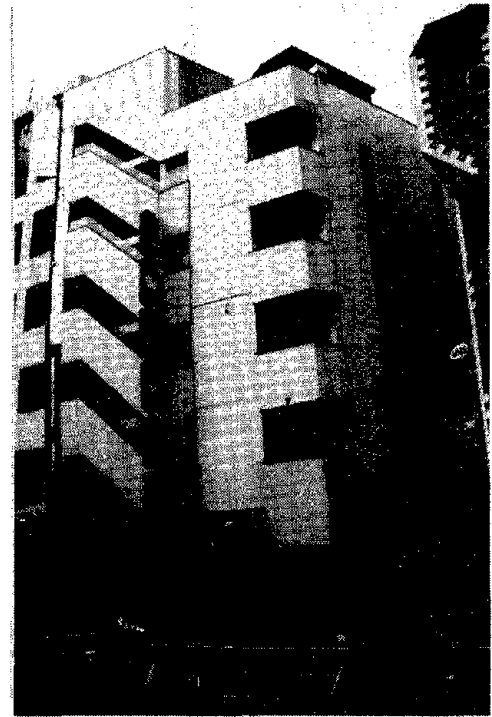
Fig. 6.107 View of a damaged, six-story,
steel moment-frame building

Fig. 6.108 Failed moment connection in
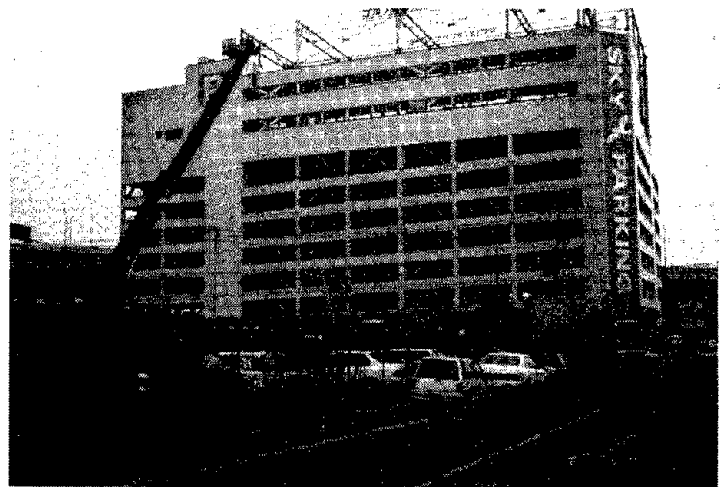building shown in Figure 6.107

Fig. 6.109 Elevation of a six-story, steel-braced parking structure
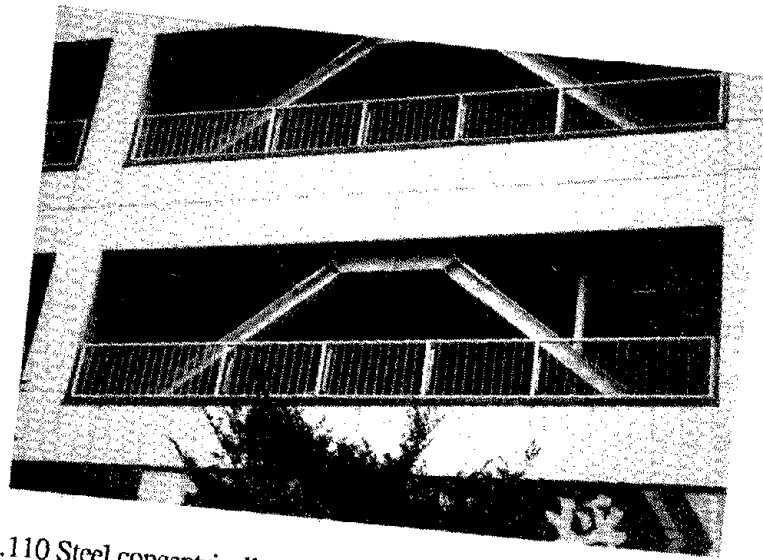
Fig. 6.110 Steel concentrically-braced frame in building shown in Figure 6.109
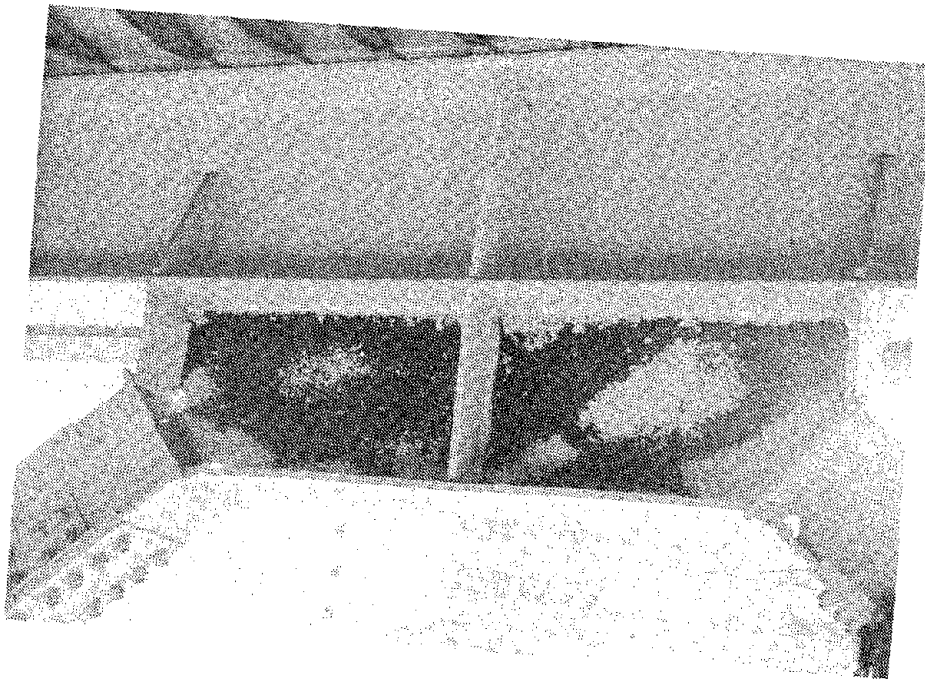

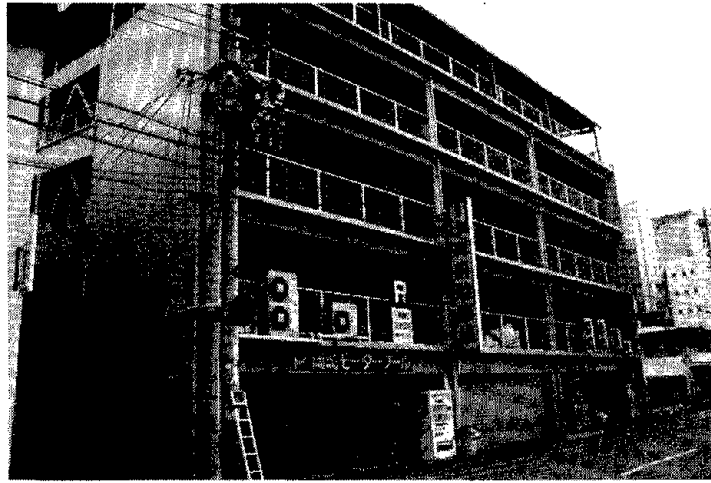Fig. 6.111 Shear yielding in braced frame gusset plate connections

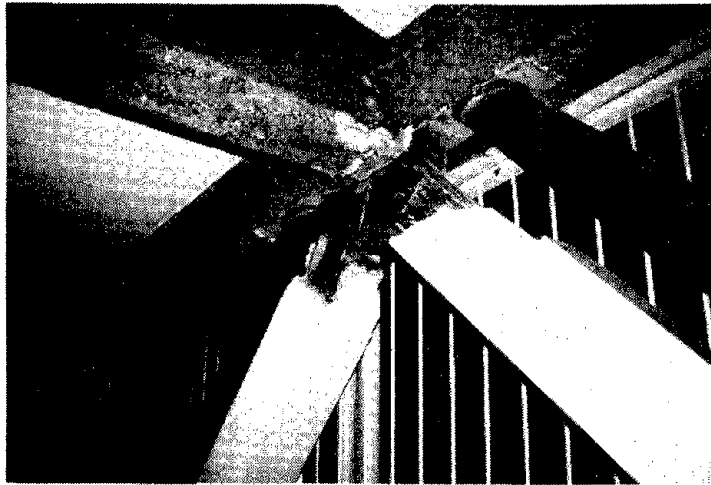Fig. 6.112 Elevation of a four-story, steel-braced parking structure

Fig. 6.113 View of failed brace-to-gusset plate connection

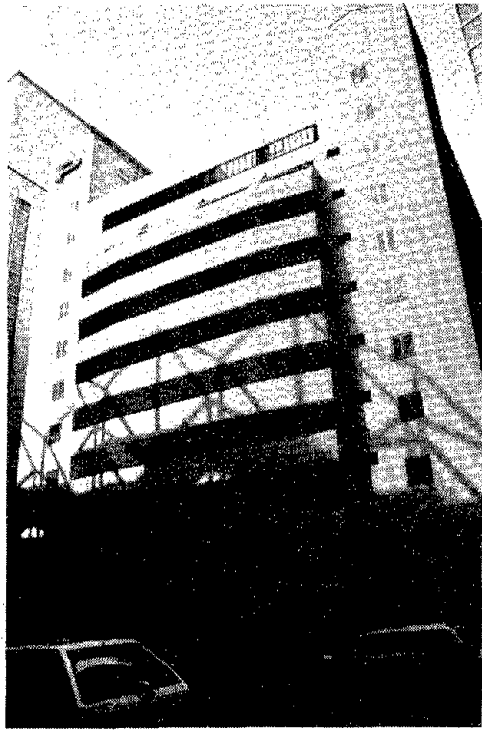Fig. 6.114 Detailed view of failed connection

178

Fig. 6.115 Elevation of a modern, six-story,
steel-braced parking structure

Fig. 6.116
Elevation of one bay of damaged concentrically-braced framing

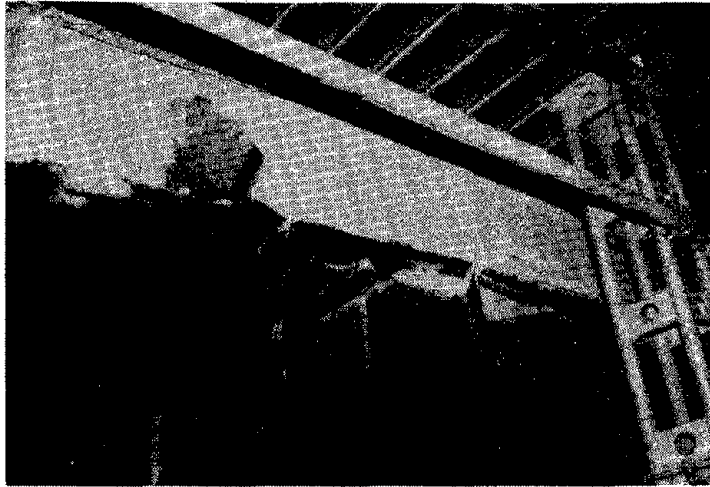Fig. 6.117 Failed beam-column connection

179

Fig. 6.118 Local buckling of floor beam indicating early hinge formation

Fig. 6.119 View of buckled concentric brace
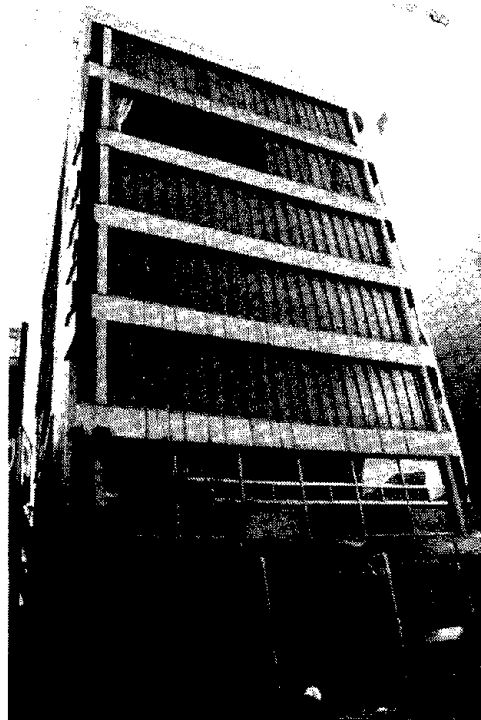
Fig. 6.120 Elevation of an eight-story, steel framed building
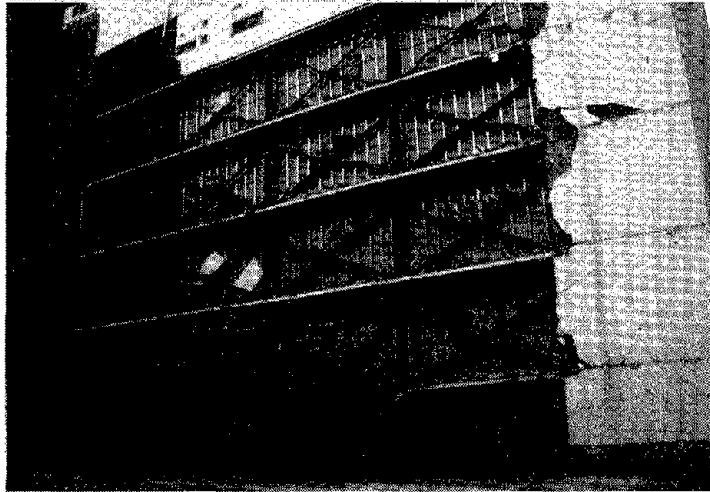
Fig. 6.121 Elevation of damaged X-braced steel frames
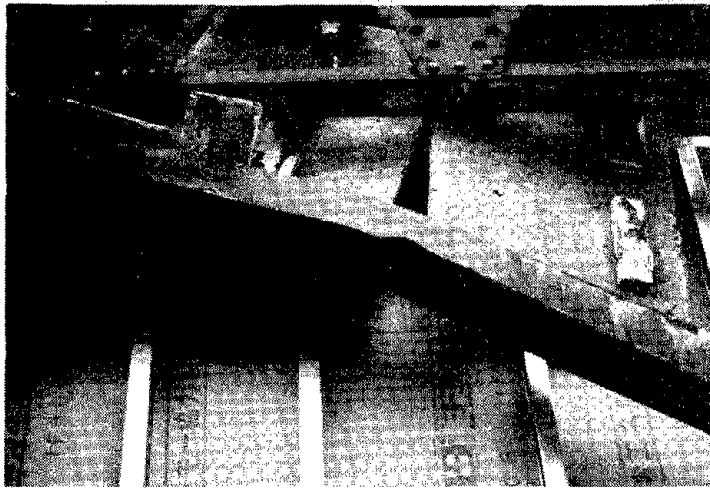
Fig. 6.122 Buckled H-section brace
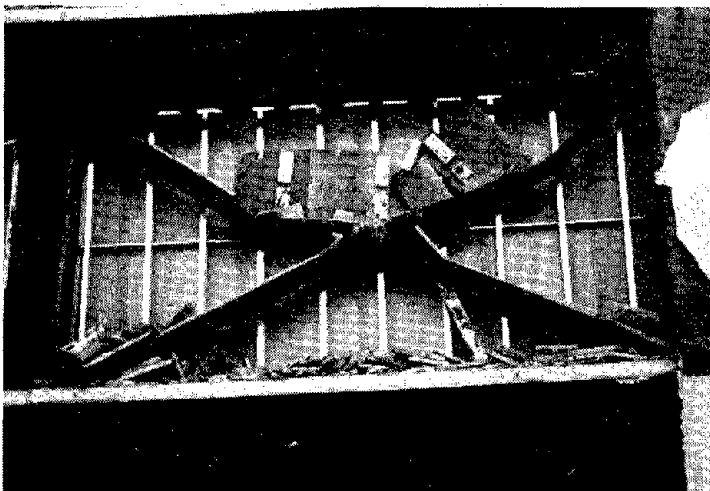
Fig. 6.123 Buckled braces in one bay of framing

Fig. 6.124 Failed brace-brace gusset plate connection
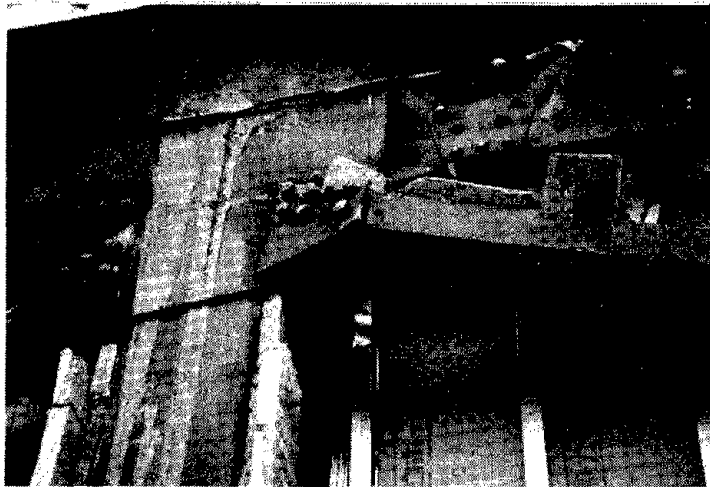
Fig. 6.125 Failed brace-column gusset plate connection

182
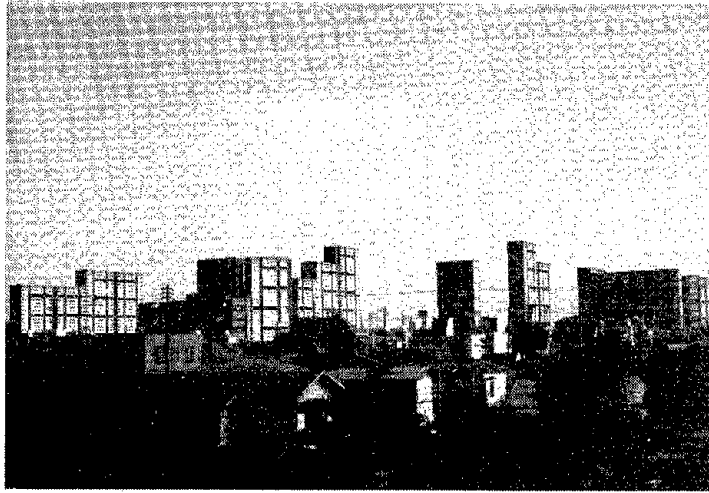
Fig. 6.126 View of Ashiyahama Seaside Town

Fig. 6.127 Elevation of typical apartment block in the Ashiyahama complex

183
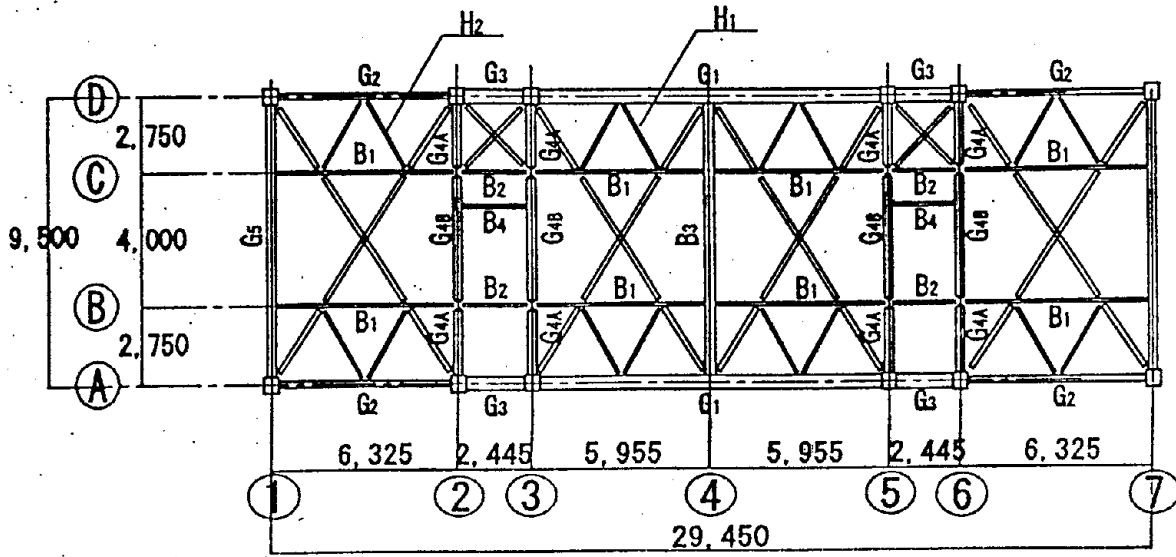
Fig. 6.128 Typical floor plan details
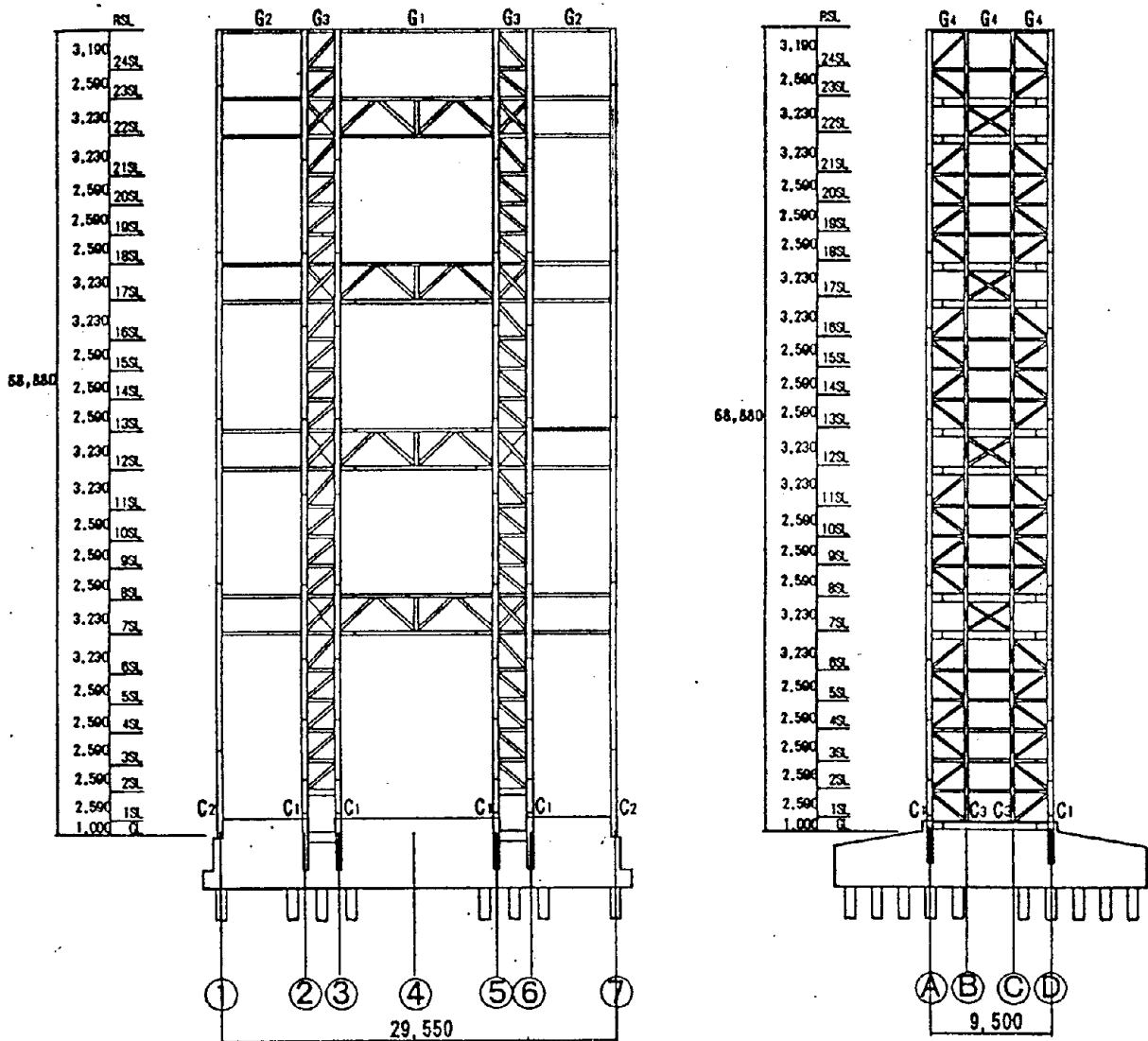
Fig. 6.129 Schematic elevation of 24-story apartment block

184

Fig. 6.130 Net-section tension failure in column at welded splice
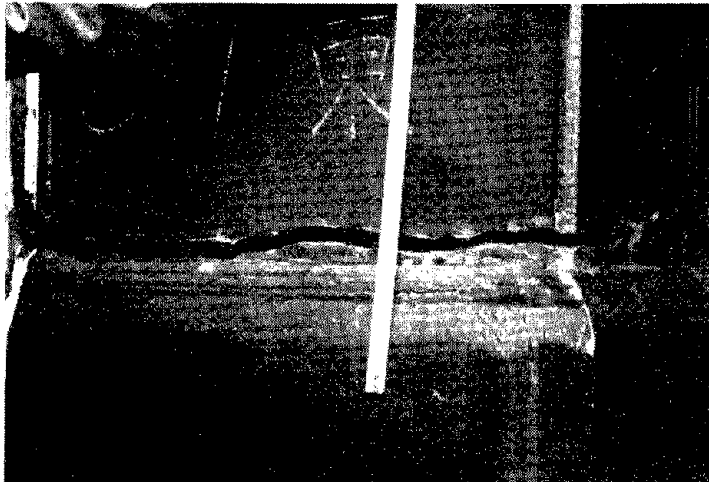
Fig. 6.131 Detail of connection failure shown in Figure 6.130

185

Fig. 6.132 Transition from steel braced frame to steel moment frame
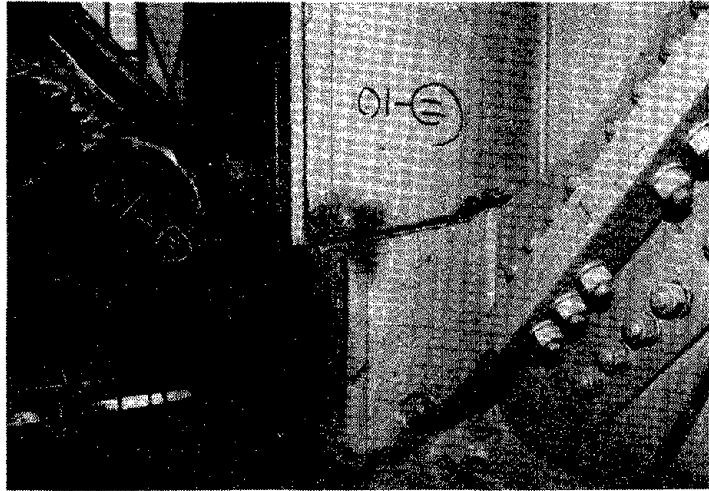
Fig. 6.133 Failed connection in braced tower

Fig. 6.134 Detail of column and brace failures
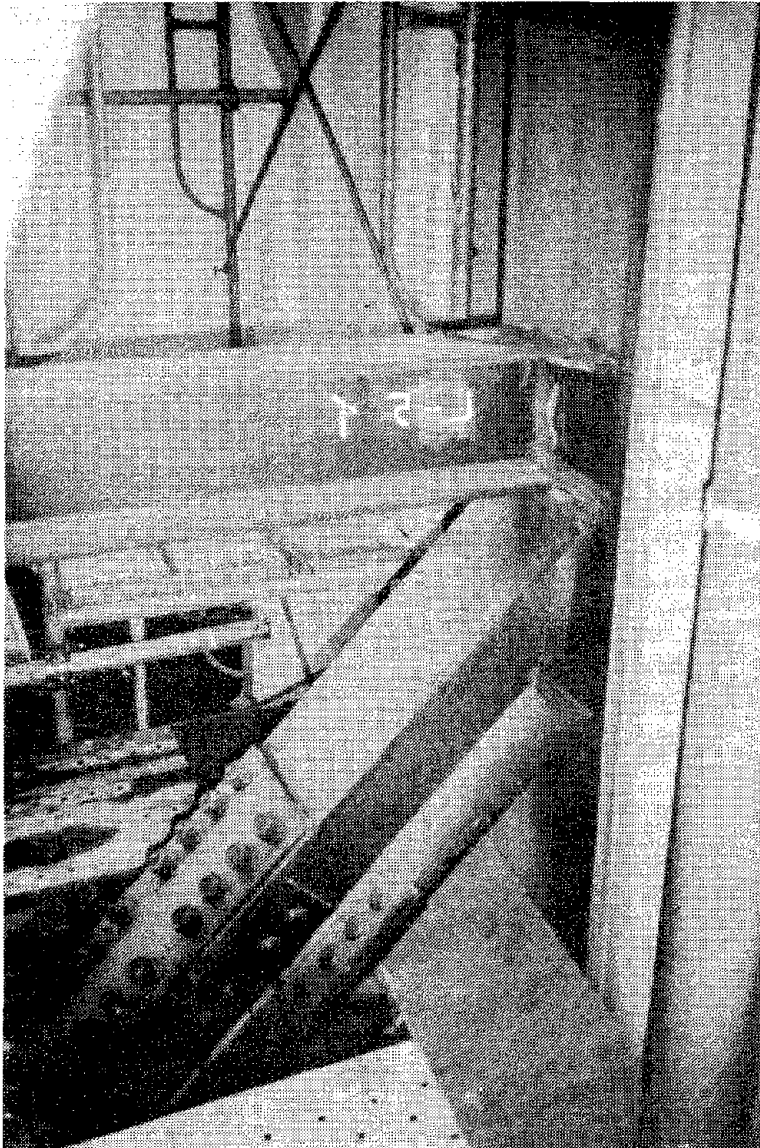
Fig. 6.135

Failed connection in braced tower
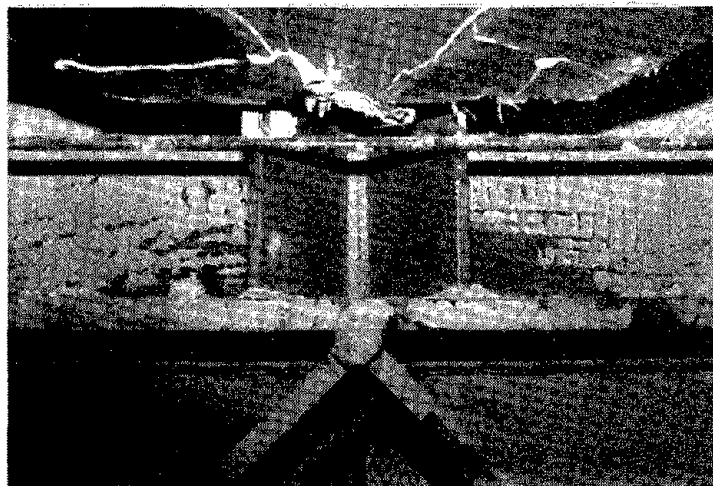
Fig. 6.136 Yielded panel-point connection in transfer truss

188

Fig. 6.137
Lightly-damaged precast cladding
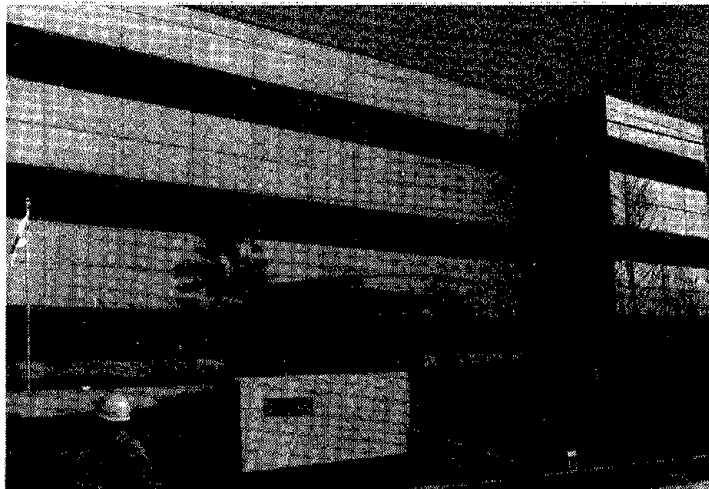
Fig. 6.138 Elevations of the Matsumura-Gumi buildings

189
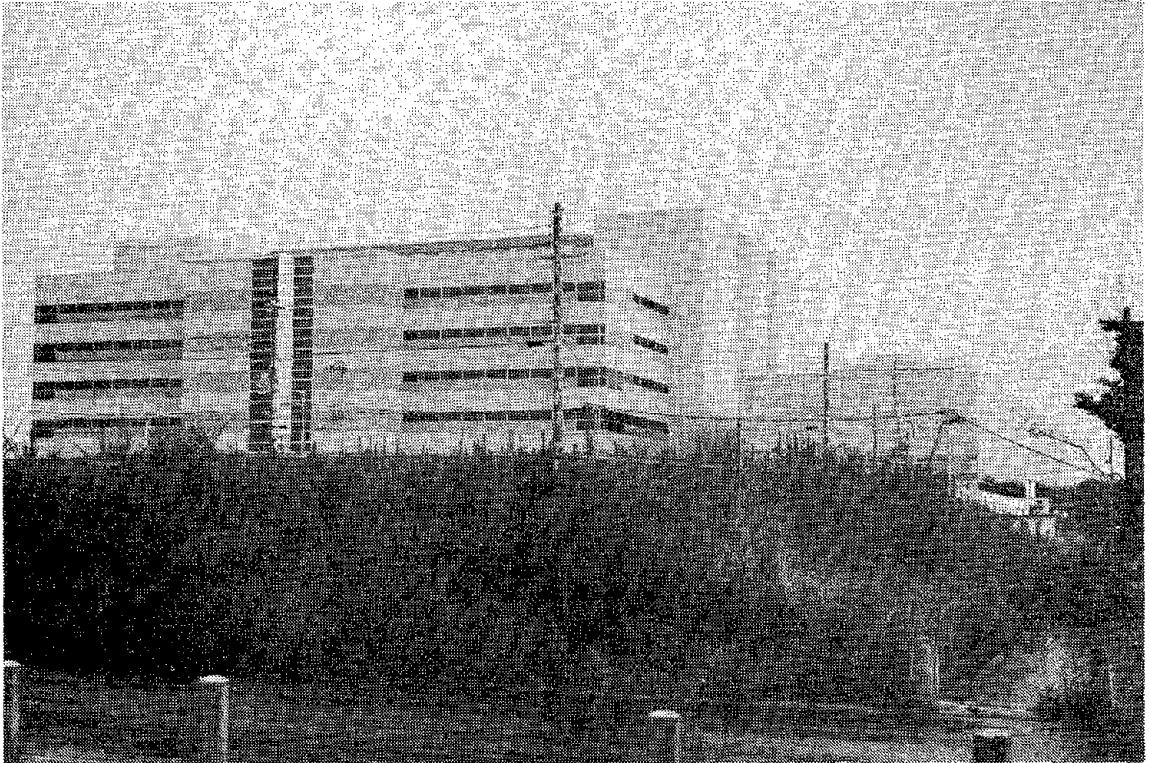
Fig. 6.139 View of the West Japan Postal Center
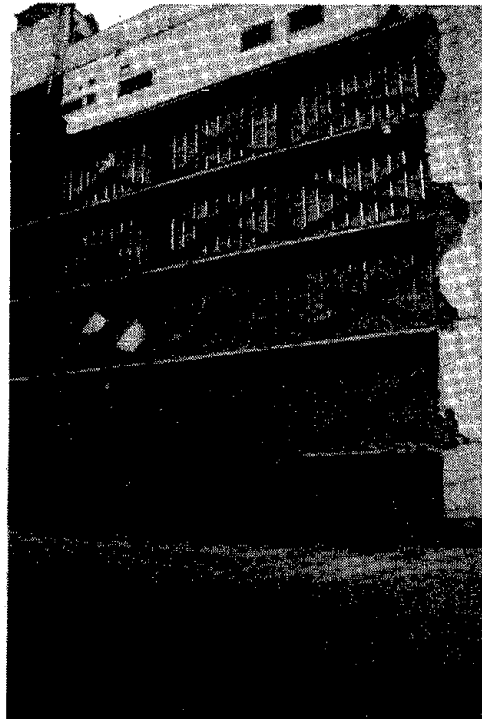
Fig. 6.140 Failure of lath-mortar cladding
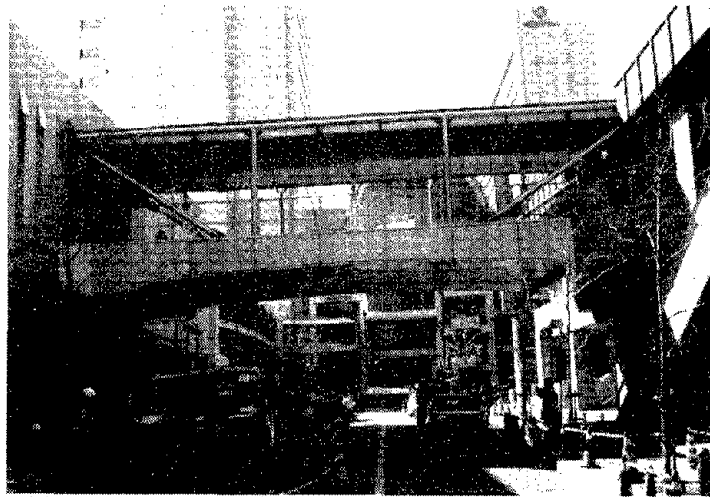
Fig. 6.141 Elevation of damage elevated walkway
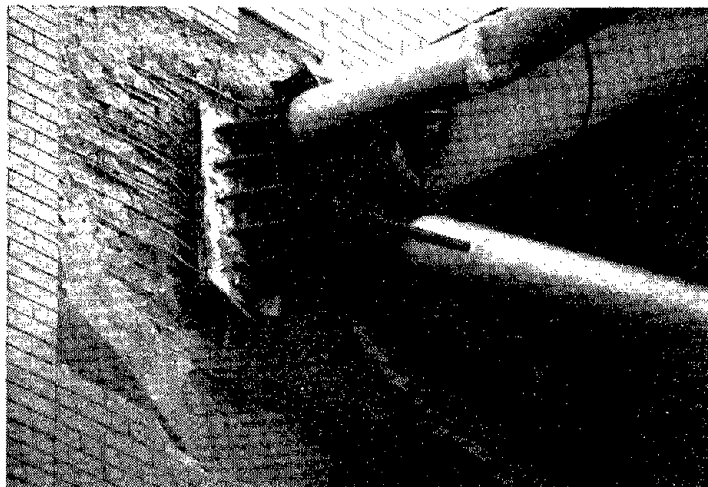
Fig. 6.142 Brace buckling and near-connection failure in damaged elevated walkway

Fig. 6.143 Collapse of elevated walkways connecting apartment blocks

CHAPTER 7

PERFORMANCE OF HIGHWAY BRIDGES

7.1 INTRODUCTION

Damage to bridges was widespread. Full or partial collapse occurred in highway bridges, railway bridges and train stations. Some sections of railway bridges located over 30 km (18 miles) from the epicenter collapsed while other bridges only a few km from the fault were only moderately damaged. Due to the large geographic area that was subjected to damage and the short time that the reconnaissance team had in the epicentral region, attention during reconnaissance was focused on areas where there was a concentration of damage and on areas where lessons for U.S. design practice would most likely result. Additional information was gathered separately from the reconnaissance effort.

Most of the bridges inspected immediately following the earthquake were components of two major elevated highways that connected the cities of Osaka and Kobe. These were the Hanshin Expressway Kobe Route, Highway 3, and the Wangan Route, Highway 5. These are identified in Figure 7.1, which is a map of the greater Kobe area. Both of these are elevated for essentially their entire lengths. The Kobe Route is over land along its length while the Wangan Route connects a series of man-made islands just off the coast. The Kobe Route was completed over 25 years ago, whereas the Wangan Route was completed within the last two or three years. The difference in seismic behavior was quite pronounced.

The collapsed portions of the Kobe Route were being removed at maximum speed at the time of the initial reconnaissance. Temporary repairs were being conducted on the severely and less severely damaged single-column piers that were still standing. Initial estimates suggest that close to 25% of the entire length of the expressway experienced some form of earthquake damage.

Additional information was obtained on other important bridges during subsequent reconnaissance and through publications and presentations at international meetings. These structures include the Meishin and Chugoku Highways (constructed in the 1960's) and the Akashi-Kaikyo Bridge (under construction at the time of the earthquake).

This chapter presents a brief history of bridge seismic design practice in Japan and describes important observations on bridge performance during the earthquake.

7.2 BRIDGE SEISMIC DESIGN PRACTICE IN JAPAN

In Japan, the design and construction practices for bridges and buildings are clearly divided into civil (doboku) engineering and architectural (kenchiku) engineering. Different design

codes are used in different fields. This section presents a brief overview of the development of bridge seismic design practice in Japan and a summary of the current design specifications. Chapter 6 provides similar discussion for building practice.

7.2.1 DEVELOPMENT OF BRIDGE SEISMIC DESIGN PRACTICE

The "seismic coefficient method", whereby the seismic design base shear is equal to the product of a seismic coefficient and the structure, was first introduced in Japan after the destructive 1923 Great Kanto Earthquake (M 7.9). In the 1926 "Road Law," the horizontal seismic coefficient was set as equal to or more than 0.1. This value was raised to 0.2 in the 1939 bridge design specifications. A more sophisticated representation of the seismic coefficient was implemented in 1956, with values of the coefficient ranging from 0.1 to 0.35 based on the seismicity and ground conditions. A standard vertical seismic coefficient of 0.1 was adopted in 1939. The collapsed bridges of the No. 3 Kobe Route of the Hanshin Expressway were completed between 1966 and 1969, and likely were designed based on the 1956 code.

After experiences gained in the 1964 Niigata earthquake (M 7.5), the 1968 Tokachi-oki earthquake (M 7.9), and the 1971 San Fernando earthquake (M 7.2), many changes were made in the bridge seismic design codes. The 1971 "Specifications for Highway Bridges" adopted a modified seismic coefficient method in which the horizontal seismic coefficient included the effect of structural period, but only for structures higher than 15m or with a period of greater than 0.5s. Therefore, the previous rigid assumption continued to apply to many elevated freeway structures. Improved seismic detailing appeared in this code as well as liquefaction checks. In 1980, a new code document incorporated research results as well as experience gained in the 1978 Miyagiken-oki earthquake (M 7.4). In the 1980 code, a strength level check was added together with provisions for shear strength checks in reinforced concrete structures.

The newest version of bridge seismic design provisions is the Japan Road Association (JRA) "Specifications for Highway Bridges - Volume V - Earthquake Resistant Design" published in February 1990. Hanshin Expressway Administration implemented these design guidelines for the construction of highway bridges in the Kansai area in June 1990. It is reported that existing bridges managed by the Hanshin Expressway Administration have been checked using the current design guidelines.

7.2.2 CURRENT BRIDGE SEISMIC DESIGN

Current Japanese design uses a two-level seismic coefficient approach with allowable stress design as the first level and an ultimate strength check as the second level design. For more complicated bridges, dynamic analyses based on spectral response or time history response are also conducted. In addition, support details are specified to prevent superstructure unseating.

7.2.2.1 Allowable Stress Design

In the first step of the design process, the structure is designed for an initial horizontal force (base shear) using allowable stress design methods. The horizontal seismic coefficient is calculated from the following equation.

$$k_h = c_Z c_G c_I c_T k_{ho} \qquad 7.1$$

where k_{ho} is the fundamental coefficient and equals to 0.2; c_Z is the seismic zone factor taken as 1.0, 0.85, and 0.7 for different regions; c_G is the ground soil factor ranging from 0.8 to 1.2; c_I is the importance factor taken as 1.0 or 0.8; and c_T is the modification factor based on different fundamental period of the structure. For Hanshin Expressway highway bridges, both the seismic zone factor and the importance factor are taken as 1.0, thus Equation 7.1 can be specifically written as Equation 7.2.

$$k_h = 0.2 c_G c_T k_{ho} \qquad 7.2$$

7.2.2.2 Ultimate Strength Check for Concrete Piers

The ultimate horizontal capacity, P_a, of concrete piers is checked for a lateral force equal to the product of a coefficient and the equivalent weight, as described by Equation 7.3.

$$P_a \geq k_{he} W \qquad 7.3$$

where P_a is the required ultimate horizontal strength, k_{he} is the equivalent horizontal seismic coefficient (based on Newmark's equal energy principle), and W is the equivalent weight. The calculations for the variables in Equation 7.3 are essentially based on two failure modes of the pier, these being flexural failure and shear failure.

For the flexural failure mode, the horizontal strength can be calculated by Equation 7.4.

$$P_a = P_y + (P_u - P_y)/\alpha \qquad 7.4$$

where P_y is the yield strength, P_u is the strength at flexural failure, and α is the safety factor taken as 1.5. If the failure strength P_u is larger than the shear strength, then a shear failure mode must be considered with the horizontal capacity calculated using Equation 7.5.

$$P_u = P_s = S_c + S_s \qquad 7.5$$

195

where P_s is the shear strength, S_c is the shear contribution of concrete, and S_s is the shear contribution of reinforcement.

The equivalent weight is calculated as

$$W = W_u + c_p W_p \qquad 7.6$$

where W_u is the superstructure weight, W_p is the pier weight, and c_p is taken as 0.5 for the flexural failure mode or 1.0 for the shear failure mode.

Based on the equivalent energy method, the equivalent ultimate horizontal seismic coefficient is determined using the following equation.

$$k_{he} = \frac{k_{he}}{\sqrt{2\mu - 1}} \qquad 7.7$$

where k_{hc} is the horizontal seismic coefficient for the second level check; μ is the allowable ductility factor, which can be taken as $\mu = 1.0$ for the shear failure mode and $\mu = 1 + (\delta_u - \delta_y)/(\alpha\delta_y)$ for the flexural failure mode, where δ_y and δ_u are the yield displacement and the failure displacement, respectively. The horizontal coefficient k_{hc} for the second level check is calculated by Equation 7.8.

$$k_{he} = c_z c_I c_R k_{hco} \qquad 7.8$$

where c_Z and c_I are defined above, c_R ranges from 0.3 to 1.0 depending on the equivalent fundamental period T_{eq} of the structure and soil, and k_{hco} is the standard value taken as 1.0. Thus, for Hanshin Expressway bridges, Equation 7.8 can be simplified as,

$$k_{he} = c_R . \qquad 7.9$$

The second level check is done for design ground accelerations from 0.3g to 0.4g that were considered as the range of peak ground accelerations in an earthquake as large as the 1923 Great Kanto earthquake. Since the elastic response acceleration of a bridge is about 1.0g for a ground acceleration of 0.3g to 0.4g, the standard value of the seismic coefficient, k_{hco} is taken as 1.0.

It is clear that the second level check is different from the capacity design approach that has been adopted in the second step capacity check in the current Japanese building design codes, as described in Chapter 6. The second level check used in bridge design essentially relies on

strength rather than ductility. For an earthquake where the ground acceleration is much higher than that considered in Equations 7.8 and 7.9, it is uncertain whether structures designed and checked based on this approach will possess sufficient reserve strength or ductility.

7.3 THE HANSHIN EXPRESSWAY VIADUCT KOBE ROUTE - ROUTE 3

7.3.1 DESCRIPTION OF THE ROUTE

The Osaka-Kobe area experienced a tremendous increase in traffic during the 1960's as a result of a significant economic expansion, together with post-war rehabilitation and the 1970 World's Fair in Osaka. To handle the increasing traffic demand, and to avoid conflicts of interest with already existing administrative units, the Hanshin Expressway Public Corporation (HEPC) was established in May 1962. It was created as an independent organization under special legislation. HEPC began construction of expressways in Osaka and Kobe in 1964, and by 1987, these expressways comprised over 138 km serving eleven cities. About 137 km of the expressway is elevated. When the Hanshin Expressway opened to traffic in 1965, the volume of vehicles per day was 7000. By 1994, this toll road serviced 910,000 vehicles per day. Table 7.1, taken from a 1987 report from the Hanshin Expressway Administration and Technology Center [HEPC, 1987], shows the different cities and length of expressway in service.

TABLE 7.1. Hanshin Expressway Lengths

CITY	OPERATED LENGTH, km
Osaka	72.6
Sakai	7.5
Higashi-Osaka	6.1
Toyonaka	7.4
Moriguchi	2.7
Matsubera	2.2
Ikeda	0.1
Kobe	27.2
Amagasaki	4.6
Nishinomiya	6.0
Ashiya	2.1
TOTAL	138.5

197

The Expressway runs in a one-way clockwise loop around the City of Osaka with a total length of 10.3 km and radial extensions linking Osaka with the cities of Kobe, Sakai, and others. The design speed is up to 80 km/hr and the number of lanes is either four or six (two or three in each direction). A typical elevation of the most damaged section of this expressway is shown in Figure 7.2. The standard 4-lane superstructure width prior to 1970 is shown in Figure 7.3 as the "Previous Spec." The standard 4-lane width after 1970 is also shown in Figure 7.3 as the "Current Spec." The several types of superstructure along the Hanshin Expressway are shown in Figure 7.4.

7.3.2 OBSERVED DAMAGE

The bridge team surveyed the portion of the expressway between the city of Nishinomiya and west of downtown Kobe city (Sannomiya area). In this portion of the expressway, the piers typically had square cross sections, up to 14 x 14 ft (4.5m x 4.5m), or circular cross sections, up to 10 ft (2.9m to 3.2m) diameter. Both steel and reinforced concrete piers were found in this area; however, the majority were reinforced concrete piers. In the area where the earthquake damage was most severe, the substructure consisted of single pier supports as shown in Figure 7.2. Initial estimates indicate that approximately 25 percent of this expressway suffered some form of damage. Table 7.2 [Iemura, et al., 1995] summarizes the extent of damage. According to Iemura, et al., damage to girders typically was caused by failure of bearings and piers. The reported number of elements requiring demolition is, of course, subjective.

Table 7.2 Approximate Damage Statistics for the Hanshin Expressway Kobe Route

Structural Elements	Total Number	Number Damaged	Number Requiring Demolition
Piers	1175	650	160
Bearings	1100[*]	700[*]	200[*]
Girders	1305[**]	1100[**]	100[**]

[*] Number of supporting lines [**] Number of spans

Typically, the larger square piers were located at the street intersections with circular piers in between. The typical pier spacing at the intersection was close to 240 ft (77m) with an average spacing of 180 ft (58m) between the circular piers. The superstructure types included: (a) steel plate girder, (b) steel box girder, and (c) precast prestressed girder (see Figure 7.4). Initial estimates put the average weight of the superstructure between 200 and 300 psf. The superstructure was non-continuous with the pier support, except for the section consisting of about 15 piers in the Fukae-Honmachi area that completely collapsed (see Figure 7.5). In this section of the expressway, the piers were monolithic with the superstructure (see Figure 7.6). As noted below, many bearings in other sections failed. Bearing failures probably limited the amount of shear transmitted down to the piers, and may have prevented collapse at many other locations.

Most of the damage observed by the reconnaissance team in the Kobe Route, between the Sannomiya and Nishinomiya areas, seemed to indicate a strong north-south pulse in the motion. The cracking and spalling patterns on all columns had most damage on the north and south faces

with less damage elsewhere. Furthermore, many columns shared the same permanent drift. Building failures near the expressway seemed to confirm this fact with more damage on north-south walls than on east-west walls.

Visual inspection of some spans showed partial failure of a number of restrainers. Loss of some spans seems to be attributable to inadequate restraint (see Figure 7.7). The restraint failure took many forms, from sheared bolts on the connector plates to failed pins in roller bearings.

Considerable distress was observed in the steel and concrete piers. Buckling of the steel piers was observed as shown in Figure 7.8. All significant forms of distress in the concrete piers apparently were associated with failure of the transverse reinforcement. The transverse reinforcement typically consisted of about 16 mm (0.6 in.) diameter bars at about 300 mm (12 in.) center to center spacing, configured as hoops or ties, with no additional transverse legs. The ties were anchored with 90-degree standard hooks with about 300 mm (12 in.) extensions at the free ends. The ends of the hoops were lapped approximately 20 bar diameters. Some of the circular piers had two layers of longitudinal and transverse reinforcement. This amount and detailing of reinforcement apparently proved to be insufficient to provide proper confinement to the massive concrete piers (see Figure 7.9).

Personal communications from PWRI representatives during a UJNR meeting indicated the following information about the single-column section that collapsed in the Fukae-Honmachi area. This section was constructed in 1969 according to the 1964 specification. The ground beneath the structures was identified as "sand." Concrete materials tests indicated concrete compressive strength of 421 kgf/cm^2 and modulus of 2.83 x 10^5 kgf/cm^2. Steel materials tests indicated yield stresses of 3,590 and 3,620 kgf/cm^2 and ultimate strengths of 5,600 and 5,793 kgf/cm^2 for longitudinal and transverse reinforcement, respectively.

Another common occurrence was the failure of gas pressure welded splices of longitudinal pier reinforcement (see Figure 7.10). In this type of splice, an arc is formed between the ends of the bars, melting the bar ends, which are then pushed together to create the weld. Most of the longitudinal steel was spliced by this procedure. Failure of this type of splice was observed at the base of the piers (see Figure 7.11), at mid-height of the piers (see Figure 7.12), and the top of the piers just below the pier cap (see Figure 7.13). This last observation is significant, because pier might normally be modeled as a cantilever due to the lack of continuity with the superstructure. According to some Japanese engineers, the gas pressure welding technique has been replaced by mechanical and "full-welded" splices. It is not clear at this time, when and if this practice ended. Further information on the reinforcing bar characteristics and welding process would be helpful to study this issue in more detail.

Failure of gas pressure welded splices in the longitudinal bars in many instances was accompanied by apparent shear failure of both square and circular concrete piers (see Figures 7.14 and 7.15). The longitudinal reinforcement in these piers consisted of the equivalent of #10 (32 mm) or #11 (35 mm) bars at 4 in. on centers in one or two exterior layers. In the case of only one layer, this resulted in longitudinal reinforcement ratios of less than 1% of the gross cross-sectional

area of the pier. Premature failure of the splices may have contributed to the shear failures in these columns.

7.4 THE HANSHIN EXPRESSWAY VIADUCT WANGAN ROUTE - ROUTE 5

7.4.1 GENERAL DESCRIPTION OF THE ROUTE AND DAMAGE OVERVIEW

The Wangan Route, Route 5, begins at the harbor on the southwest side of Osaka and traverses about 20 kilometers (12 miles) to the west where it ends on Rokko Island (see Figure 7.1). The expressway is an elevated viaduct that crosses water at many locations. The route connects many man-made islands with substantial bridges with different configurations. These spans include tied arch, arch, and cable stayed bridges. The route opened for traffic in April of 1994, with the bridges having been designed by the 1980 and 1990 earthquake design codes for highway bridges [Iemura, et al., 1995].

Unlike many of the spans of the older Kobe Route, the newer bridges of the Wangan Route performed exceptionally well in light of the large seismic demands including wide-spread liquefaction. There were, however, significant damage observations. Table 7.3 [Iemura, et al., 1995] summarizes the extent of damage.

Table 7.3 Approximate Damage Statistics for the Hanshin Expressway Wangan Route

Structural Elements	Total Number	Number Damaged	Number Requiring Demolition
Piers	366	57	0
Bearings	451[*]	180[*]	42[*]
Girders	462[**]	36[**]	1[**]

[*] Number of supporting lines [**] Number of spans

The following subsections briefly describe the major bridges and connecting roadways of this route. Performance observations are reported, as well.

7.4.2 NISHINOMIYA-KO BRIDGE

Reconnaissance of the Wangan Route began on the mainland near Koshien Island (Figure 7.1). The reconnaissance team crossed a small bridge to this island, and then traversed the island to Nishinomiya-Ko Bridge.

The Nishinomiya-Ko Bridge connects Koshien Island and Nishinomiya Island (Figure 7.1). The bridge structure is a tied arch with a 252 m span (780 ft) and steel deck. A striking architectural feature of the bridge is the "basket handle" shape of the non-parallel arches, that is, the arches are closer to each other at the top than at the bottom. Pneumatic caissons were used for the main piers in this area where liquefaction was expected [HEPC, 1994]. The bridge was

completed in 1993. Plan and elevation views are shown in Figure 7.21. **[Carol -These figure numbers are out of sequence. Be sure to get them in sequence.]**

The approach span on the Koshien Island side of the bridge had fallen off its support at the tied arch end, fracturing the restrainers (Figures 7.16 and 7.17). The steel box-girder span had been simply supported at pier 98 (opposite the arch end of the span). When the arch end of the span fell, the expansion joint was broken at pier 98 and the girder nearly dropped at that end also (Figures 7.18 and 7.19). The Hanshin Expressway Public Corporation reported that a fixed bearing at pier 100 on the opposite side of the channel had also broken.

A large amount of liquefaction occurred in the area around this bridge. A 6 in. (150 mm) thick asphalt pavement near the collapsed span was broken into several large pieces with multiple cracks. All around the base of pier 98, liquefaction caused the soil to settle about one meter (Figure 7.20). The pile driving process probably compacted the soil within the boundary of the foundation, effectively eliminating liquefaction in this zone. Pier 98 appeared to be perfectly plumb. Under the viaduct on Koshien Island, evidence of wide-spread liquefaction included areas of subsidence and numerous sand boils. There was also evidence of longitudinal movement of the box girders, including parts of restrainers and bearings lying on the ground.

7.4.3 BRIDGE CONNECTING THE MAINLAND AND NISHINOMIYA ISLAND

A large plate girder bridge connected the mainland to Nishinomiya Island (B2 in Figure 7.1) near the Kobe-end of the island. The first water pier suffered major failure (Figure 7.22) that appeared to have initiated at a construction joint. A wide crack extended from the construction joint down through the pier to below the water line. This resulted in a large separation between the parts of the pier. Large cracks in the asphalt evinced the occurrence of liquefaction, but the land pier was almost plumb. (Bridge closure prevented the reconnaissance team from crossing over to Nishinomiya Island.)

7.4.4 SHUKUGAWA BRIDGE

At the west side of Nishinomiya Island was the Shukugawa Bridge, a large three-span continuous haunched plate girder bridge (B3 in Figure 7.1) that connected this island to a long, narrow man-made island. Unfortunately, the reconnaissance team was unable to cross to the island. From the mainland, however, we could see that the approach to the west connecting this bridge to the far island shifted off its bearings to the west and nearly fell off the pier (see Figure 7.23). The Hanshin Expressway Public Corporation reported that the pier shifted seaward, the bearing had been broken, and the bridge almost came off the seat.

7.4.5 SHIN-ASHIYAGAWA BRIDGE

The Shin-Ashiyagawa Bridge (B3 in Figure 7.1) is a steel girder bridge with 175 m (540 ft) center span. The reconnaissance team was unable to access this bridge. According to the Hanshin Expressway Public Corporation, the bridge suffered damage at a land pier located on the Osaka side of the bridge and at a pier in the water near midspan. The land pier is reported to

have shifted seaside, and the bearing broke, resulting in near unseating. At the water pier a bearing had been broken.

7.4.6 HIGASHI-KOBE BRIDGE

The Higashi-Kobe Bridge connects Fukae Island and Uozaki Island (B4 in Figure 7.1, and Figure 7.24). The bridge is a three-span cable stayed bridge spanning 885 m (2,750 ft) with center span of 485 m (1,500 ft). Construction of this 13.5 (42 ft) wide bridge was begun in 1985 and completed in 1992. The towers are 150 m (465 ft) high and are founded on pneumatic caissons. The pier and caisson were constructed together. The land-based piers were cast-in-place concrete piles. To extend the longitudinal period of the bridge, and thereby reduce seismic force, the supports of the main girder were designed to be moveable. Plan and elevation views are shown in Figure 7.27 [HEPC, 1994].

The land surrounding this bridge showed evidence of significant liquefaction. Near the shore closest to the east tower of the bridge, there was massive subsidence that failed asphalt pavement. Numerous sand boils were evident. Lateral spreading moved the sea wall several feet toward the water, creating a zone about 100 meters (310 ft) long where the subsidence was approximately two meters (6.2 ft) deep by eight meters wide (24.8 ft) (Figure 7.25). This zone extended to the edge of the water and possibly to the east tower of the cable stayed bridge (Figure 7.26). The tower was not observed from close-range because it was in the water about 40 meters (125 ft) from the shore. From that distance, there appeared to be no damage. However, the Hanshin Expressway Public Corporation reported damage to pendulum supports, wind shoes, and damper shoes at pier 187, as well as local buckling of the pier.

7.4.7 ROKKO ISLAND BRIDGE

The Rokko Island Bridge carries two levels of traffic between Uozaki Island and Rokko Island (B5 in Figure 7.1). The bridge structure is a steel tied arch that measures 217 meters (670 ft) from end to end. The bridge structure was completely fabricated on land, floated to the site on barges, and lifted to the piers with large floating cranes [HEPC, 1994]. It is founded on pneumatic caissons. Construction was completed in 1992. Plan and elevation views are shown in Figure 7.27.

The south end of the bridge had shifted about 300 mm (12 in.) toward the east, resulting unseating, and resulting in the east-most arch hanging in the air (Figure 7.28). Six of the lateral bracing members connecting the two arches near their tops had buckled (Figure 7.29), possibly as a consequence of this movement.

7.4.8 KOBE OHASHI BRIDGE

The Kobe Ohashi Bridge is an arch bridge that carries two levels of automobile traffic between Kobe and Port Island (B6 in Figure 7.1). Figure 7.30 is a photograph taken from the west side of the bridge.

The spans south of the arch (Port Island side) consist of large box girder spans at each elevation. At the third pier south of the arch the restrainer connecting two girders fractured in the lower level; relative movement between the two girders was evident (Figure 7.31). Apparent liquefaction resulted in about 50 cm (20 in.) of settlement around this double-decker pier (Figure 7.32).

The fourth pier south of the arch is a two-column double-decker bent carrying steel box girders at both levels. As shown in Figure 7.33, the two spans at the upper level of the roadway separated by several inches and the restrainers connecting them were broken. A short wall at the lower level of the pier dropped about 30 cm (12 in.) as shown in Figure 7.34. A second bridge that is not in operation runs along the east side of this roadway. It may be for a future transit system. One of the spans shifted 15 to 20 cm (6 to 8 in.) and was resting on another span (Figure 7.35).

Figure 7.36 shows the effects of liquefaction near the south abutment of the arch. About one meter of settlement occurred all around the abutment. However, it appeared that the abutment had not moved. One of the cross beams carrying the roadway had a large shear crack. It appears that a bearing fractured, allowing the span to move in the longitudinal direction. It appeared that some restraint in the transverse direction may have led to the shear crack.

An expansion joint separates the approach roadway span and the arch truss section. A permanent deformation of almost 25 cm (10 in.) between the two spans closed the expansion joint (Figure 7.37). One side of the joint yielded and was forced under the joint on the other side. At the other end of the bridge, a permanent gap resulted, indicating that the center section of the roadway translated to the south (toward Port Island).

From the bridge, it appeared that there was also a large amount of liquefaction on the Kobe (north) side of the arch bridge. Settlement of up to one meter or more was observed in some places (Figure 7.38). Concrete pavement and sidewalks had cracked and been displaced in various directions. Parts of a parking structure had separated by about 50 cm (20 in.) (Figure 7.39).

The girders that carry the deck of the bridge extend beyond the arch and rest on a separate abutment. The seats on this pier had broken and the concrete was fractured due to the movement of the deck. Both spans of a two-level ramp leading to the arch bridge had fallen from their piers and dropped to the roadway below (Figure 7.40).

The approach spans on the Kobe-side experienced some damage. Broken restrainers were common. At another location, the upper column of a double-decker bent failed and buckled, and fractured longitudinal bars were evident. Further toward Kobe there were several other bents with failed columns. The transit bridge running next to the arch (mentioned above) had several steel piers that were tilted by about 5/8 in. per ft (50 mm per meter) (Figure 7.41). At one location where the approach to the arch transitions from a continuous span to a simple span, restrainers were broken and pounding had clearly occurred. Further towards Kobe were four double-deck reinforced concrete bents; both columns had failed in all of these bents failed, with

evidence of buckled and fractured longitudinal reinforcement and fractured transverse hoops. All of these columns had failed in the middle-third of the column supporting the lower level roadway.

Also at the Kobe end of the approach spans, several highways came together creating a complex set of intersections at several elevations. One of the circular cross section columns of a steel bent displayed evidence of yielding and local buckling (Figure 7.42). One circular cross section concrete column of another bent had a flexural failure at mid-height that apparently resulted from fracture of the longitudinal steel at welded splices (Figure 7.43). Another steel column buckled about 2.4 meters (7.5 ft) above a one-meter high concrete pedestal (Figure 7.44).

Liquefaction was evident throughout this area. The roadway and sidewalks had settled all around these piers except for the zone immediately adjacent to the piers. Further north toward the center of Kobe, other concrete piers had mid-height failures similar to the one described previously.

7.5 THE MEISHIN AND CHUGOKU HIGHWAYS

These highways were both built in the 1960's, and are operated by the Japan Highway Corporation. The routes are identified in Figure 7.1. The reconnaissance team was unable to view the sites of these highways. Detailed information provided to the team by the Japan Highway Corporation [JHC; 1995] forms the basis of the discussion below.

The bridges along the Meishin Highway consist of a series of relatively short span bridges supported on piers. Superstructures comprise either hollow reinforced concrete slabs or continuous steel bridges. Supports include reinforced concrete columns and wall piers. Damage was observed in columns, piers, and rocker bearings of several of the bridges. Figure 7.45 displays the typical failure modes of the Ohnishi Bridge, Suidoh Bridge, and Moribe Bridge. Ties through the wall thickness appeared to be absent, and at least in some cases the longitudinal reinforcement apparently was discontinuous near the midheight, factors which may have contributed to some of the failures. The Kawaragi-nish Bridge had 66-degree skewed supports, with pin-ended interior columns; failure included twisting in plan, span collapse, and torsional cracking of a pier wall (Figure 7.46).

The bridges along the Chugoku Highway consist of a similar series of relatively short span bridges supported on piers. Figure 7.47 shows the Takarazuka Bridge. This five-span continuous bridge was fixed at two points with three pairs of piers. Typical shear failures are shown.

Table 7.4 [Iemura, et al., 1995] summarizes the extent of damage along the Meishin and Chugoku routes.

Table 7.4 Approximate Damage Statistics for the Meishin and Chugoku Highways

Structural Elements	Total Number	Number Damaged	Number Requiring Demolition
Piers	1673	299	56
Bearings	2310[*]	56[*]	150[*]
Girders	571[**]	13[**]	2[**]

[*] Number of supporting lines [**] Number of spans

7.6 AKASHI KAIKYO BRIDGE

The Akashi Kaikyo Bridge is designed to be a 3-span, 2-hinged stiffening truss suspension bridge that will span the Akashi Straits and link Awaji Island and the Hyogo Prefecture (see Figure 6.1). When completed the bridge will be 3,910 meters (12,100 ft) long with a center span of 1990 meters (6,170 ft). Construction was begun in May 1988 and is scheduled to be complete in 1998. At the time of the earthquake, the bridge was at the stage of suspension cable squeezing. Figure 7.48 depicts selected bridge plans.

Nitta [1995] describes the topography, geology, siting considerations, and seismic design of the bridge. According to Nitta, the foundations were chosen so as to avoid the vicinity of the several known faults under the strait. Design considered a magnitude 8.5 at an epicentral distance of 150 km (90 miles), and response spectra for past earthquakes (of magnitude 6 or more occurring within 300 km (180 miles)) evaluated from theory of probability for a recurrence interval of 150 years.

Nitta [1995] also describes the condition of the structures following the earthquake. According to the report, no damage was apparent in the anchorages, main towers, cables, or catwalks. Surveys following the earthquake indicated the foundation displacements shown in Figure 7.49. The effect on the skeleton of the bridge is shown in Figure 7.50.

7.7 SUMMARY AND CONCLUSIONS

The performance of the highway bridges during the Hyogoken-Nanbu Earthquake provided a vivid reminder of past failures as well as new insights that will help designers in the future. Prominent observations and implications include the following:

- Many of the older reinforced concrete columns contained widely spaced transverse reinforcement. The wide spacing is likely to have resulted in insufficient confinement and shear strength. Numerous apparent shear failures and flexural failures were likely to have been a direct consequence of inadequate transverse reinforcement. Many of the failed columns had relatively large cross sections. The behavior of columns with large cross sections has not been adequately investigated in laboratory studies.

205

- Several reinforced concrete pier walls failed during the earthquake, apparently due primarily to loading out of the plane of the wall. Contributing factors may include (a) lack of ties through the thickness of the wall, (b) discontinuous longitudinal reinforcement, (c) generally inadequate shear strength and flexural confinement. Studies of behavior of walls loaded out of their plane appear to be warranted.

- Many of the reinforced concrete columns and piers contained longitudinal reinforcement that had been spliced using the gas pressure welding technique. Many of these fractured during the earthquake. Fracture of the welded splices appears to have been a major contributor to failure of several columns. This splicing technique has not been widely used in the United States. Nonetheless, the effectiveness of this and other splicing techniques should be further studied.

- Distress and failure were observed in numerous steel columns. Common forms of distress included apparent yielding, local buckling, and tearing (usually at buckled sections). Distress often was observed along the column length at locations where steel plate thickness changed or concrete infills terminated. Techniques for evaluating existing steel columns, retrofitting existing steel columns, and designing new steel columns should be investigated.

- Fractured longitudinal restrainers and bearings were observed for several spans, including some that had become unseated. Failures were observed in both the older Hanshin Expressway Kobe Route 3 and the newer Wangan Route 5. Studies are needed to compare U.S. and Japanese restrainer and bearing design procedures, to improve bearing designs, and to determine the efficacy of restrainers in modifying response of bridges.

- Bridge foundations, including those located in areas of widespread liquefaction, performed remarkably well. Studies should be carried out to further evaluation performance of bridge foundations in this earthquake, and to compare US and Japanese foundation design and construction practices.

- Although failures were observed on both the older Hanshin Expressway Kobe Route 3 and the newer Wangan Route 5, the degree of damage on the older route far exceeded that on the newer route. This later observation likely demonstrates the effect of improvements in bridge engineering and construction practices in Japan over the intervening years. Comparative studies of U.S. and Japanese bridge designs should be carried out to identify similarities and differences in engineering and construction practices. Improvements in design and construction practices should be pursued through cooperative studies.

206

REFERENCES

[HEPC, 1987] "Deterioration and Repair of Bridge Structure in Hanshin Expressway," a report by the Hanshin Expressway Administration and Technology Center, Hanshin Expressway Public Corporation, October 1987.

"ACI 318 (92)," Building Code and Commentary, American Concrete Institute, Detroit, MI, 1992, 347 pp.

[HEPC, 1994] "Way to the 21st Century: Structures and Techniques of Wangan Route," Hanshin Expressway Public Corporation, Osaka, Japan, 1994.

[Kuroda, 1993] "Short Cuts of Hyogo Road," Shobunsha Publications, Inc., Tokyo, Japan, (January 1993), p. 99.

[Iemura, et al., 1995] Hirokazu Iemura, Susumu Inoue, Kazuyuki Izuno, and Akira Igarashi, "Engineering Features of Damage on Highway Bridges Due to the Hyogoken-Nanbu Earthquake," Department of Civil Engineering, Kyoto University, 1995.

[Nitta, 1995] Atsushi Nitta, "Effect of the Southern Hyogo Earthquake on the Akashi-Kaikyo Bridge," Honshu-Shikoku Bridge Authority, April 18, 1995.

[HEPC, 1994]"Techno Gallery: Structures and Technologies of the Hanshin Expressway," Hanshin Expressway Public Corporation, Osaka, Japan, Sept 1994.

[JHC, 1995]

I1 Koshien Island
I2 Nishinomiya Island
I3 Fukae Island
I4 Hozaki Island
I5 Rocco Island
I6 Port Island

B1 Nishinomiya ko Bridge
B2
B3 Shukugawa Bridge
B4 Higashi-Kobe Bridge
B5 Rocco Island Bridge
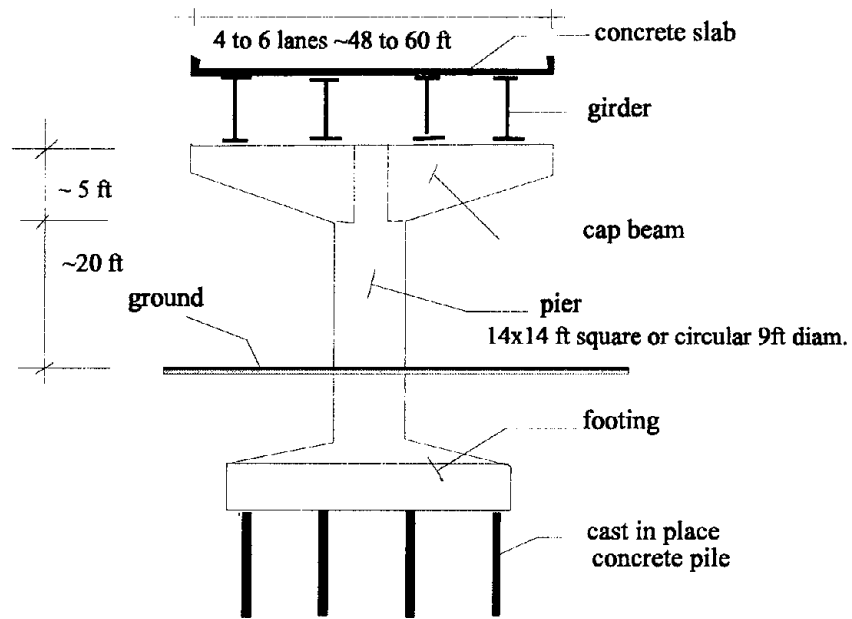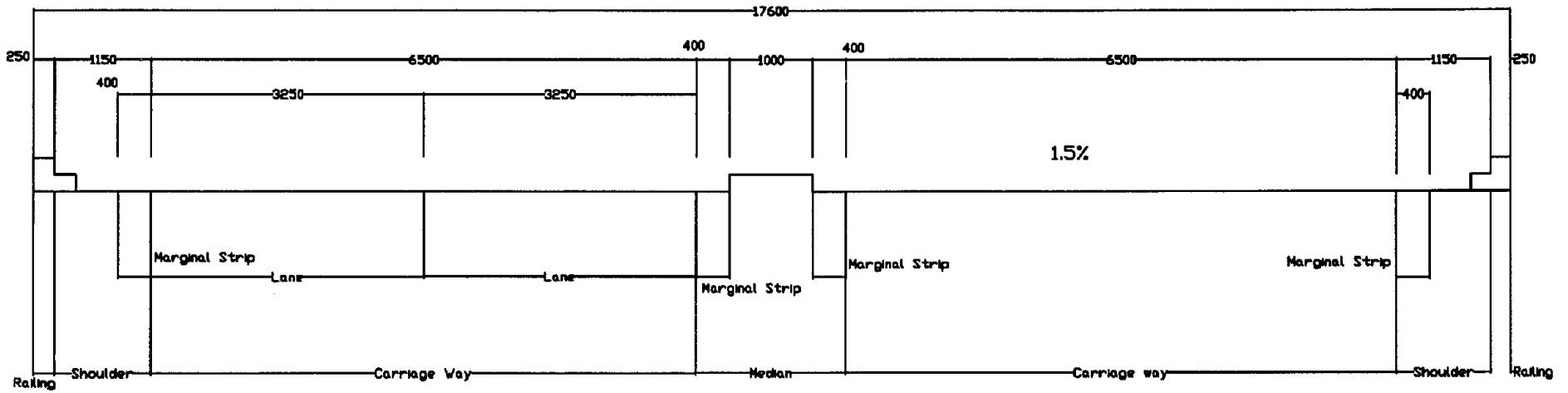B6 Kobe Ohashi Bridge
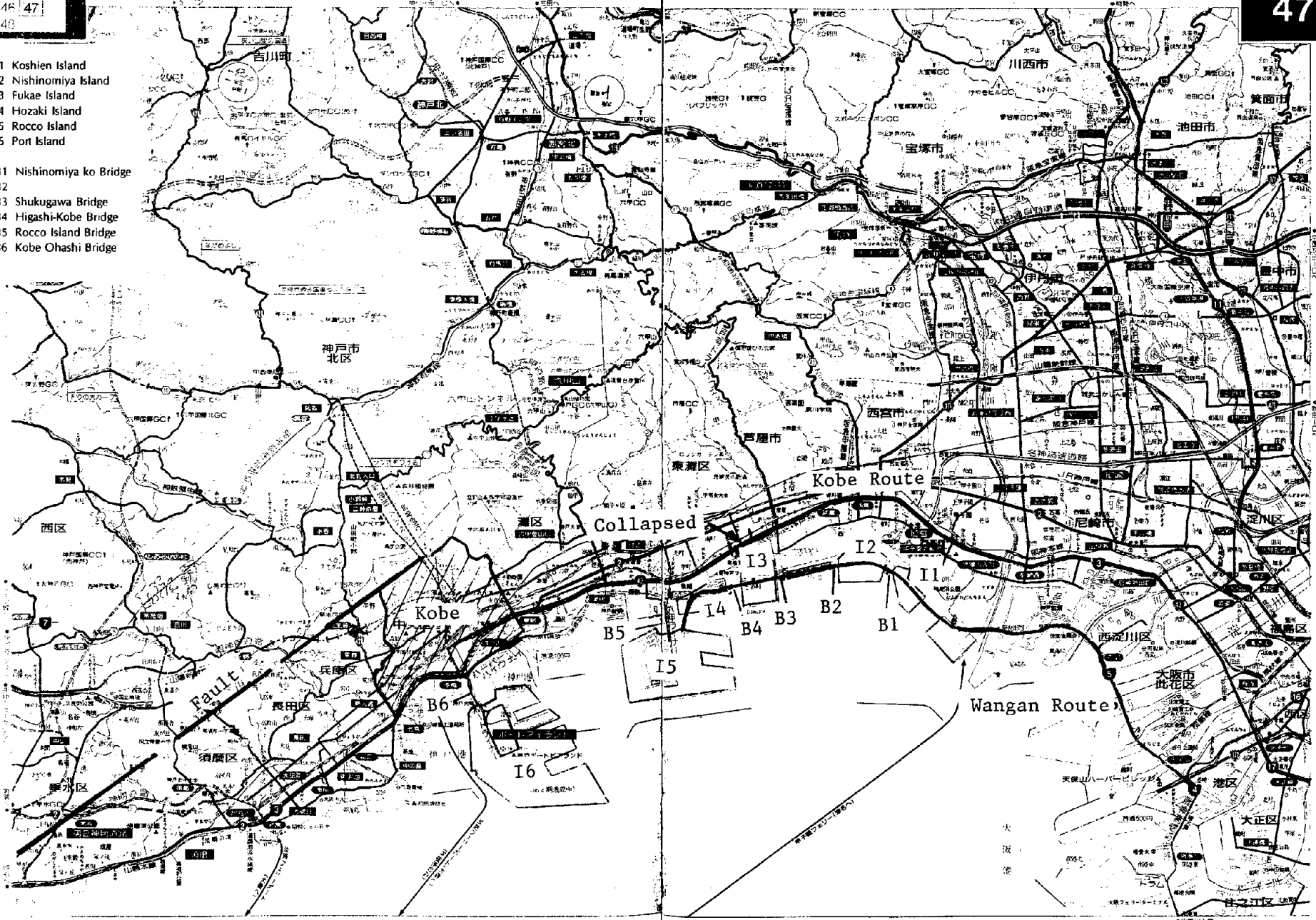
Fig. 7.1 Map of Greater Kobe-Osaka Area

Fig. 7.2 Typical section of a pier in the most damaged portions of the Hanshin Expressway Kobe Route
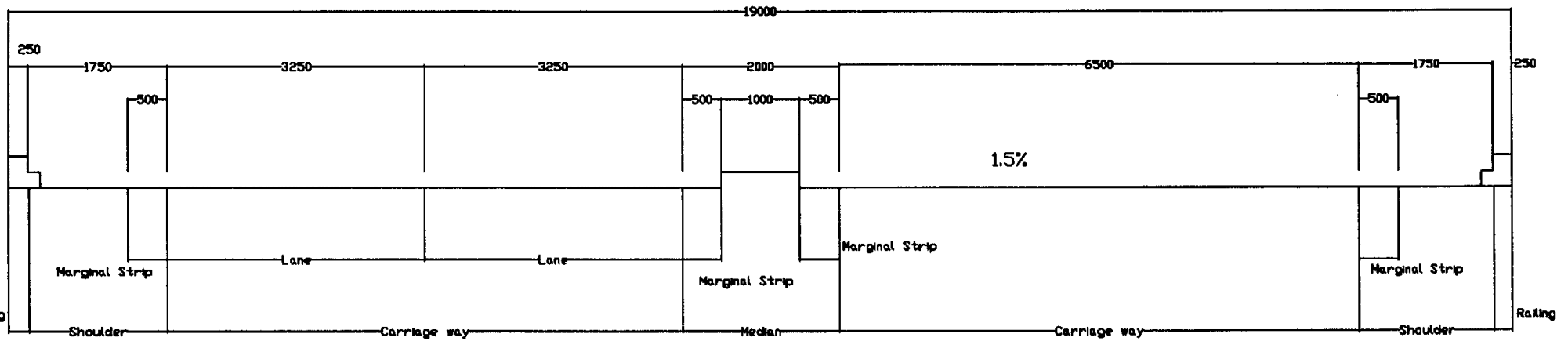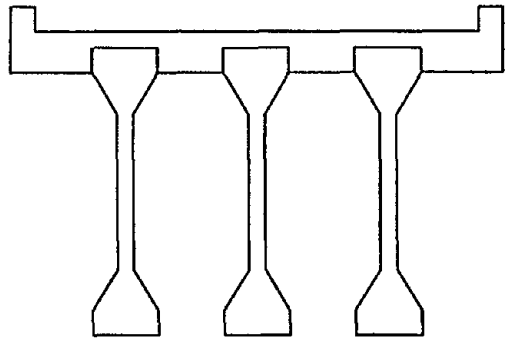
Previous Spec
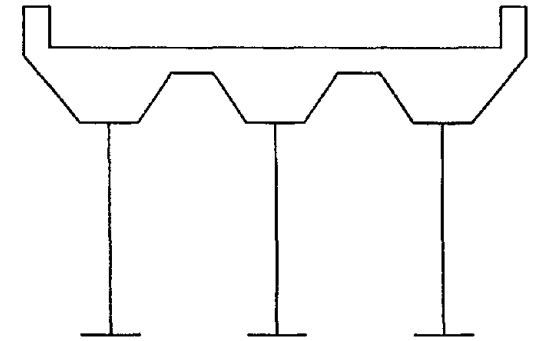

Current Spec

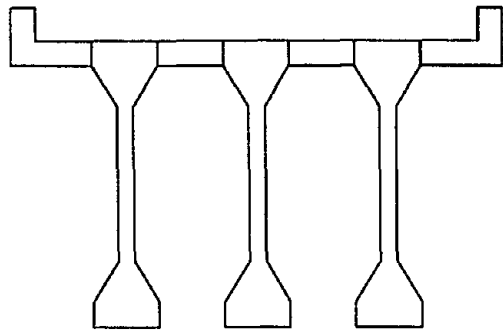Fig. 7.3 Typical section of four-lane section of Kobe Route after 1970
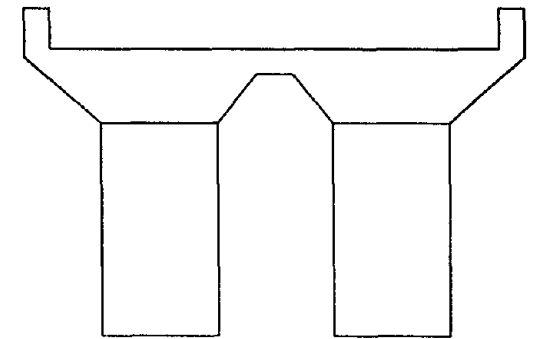
210

PC Bridge
Composite l-type girder

Steel Bridge
Composite l-type girder

211

PC Bridge
T-type girder

Steel Bridge
Composite box-type girder

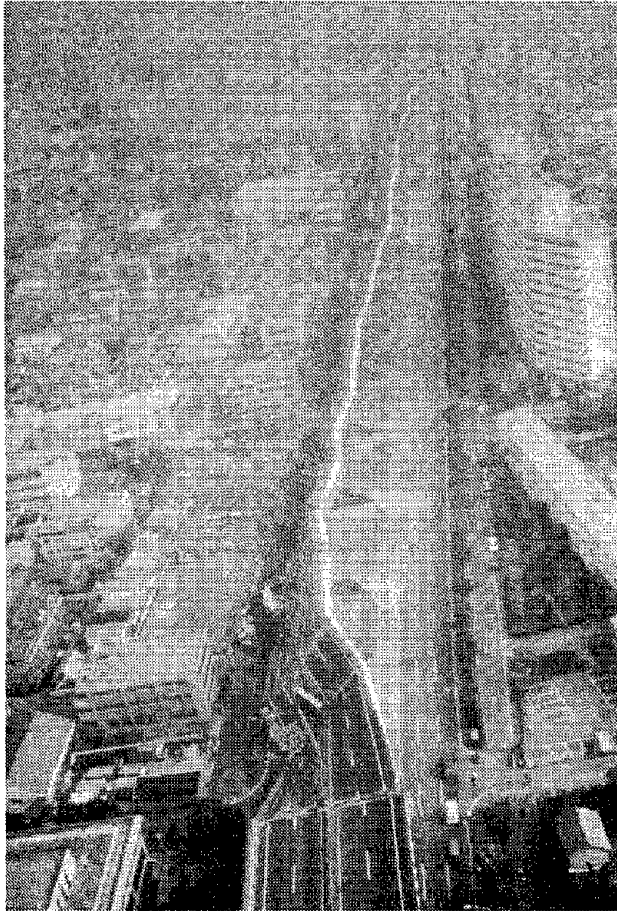Fig. 7.4 Superstructure types along Kobe Route

Fig. 7.5 Collapsed portion of Kobe Route in the Fukae-Honma-chi area

Fig. 7.6 Monolithic portion of Kobe Route in the Fukae-Honma-chi area
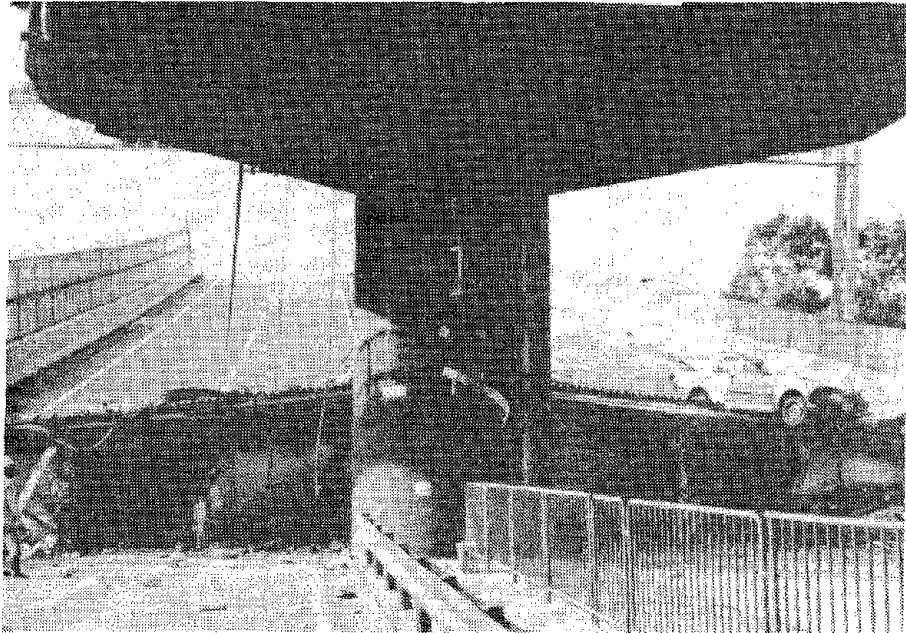
212

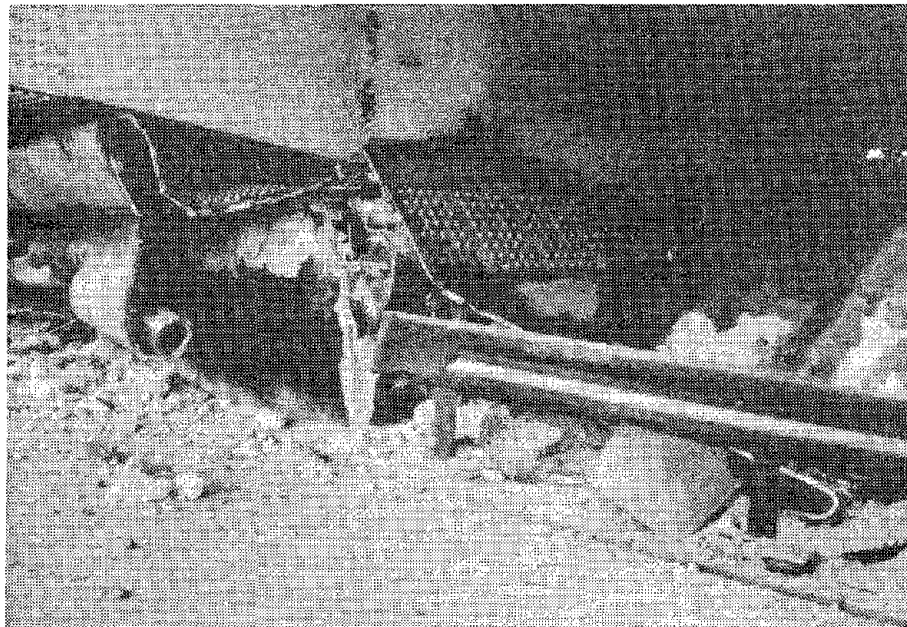Fig. 7.7 Restrainer failure in Kobe Route

Fig. 7.8 Failure of steel piers
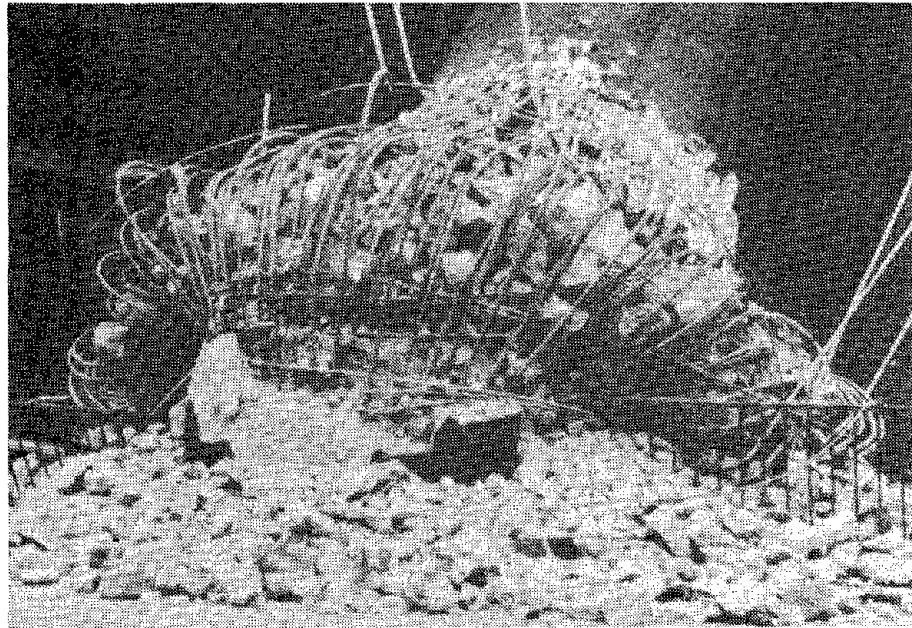
Fig. 7.9 Failure from insufficient confinement steel
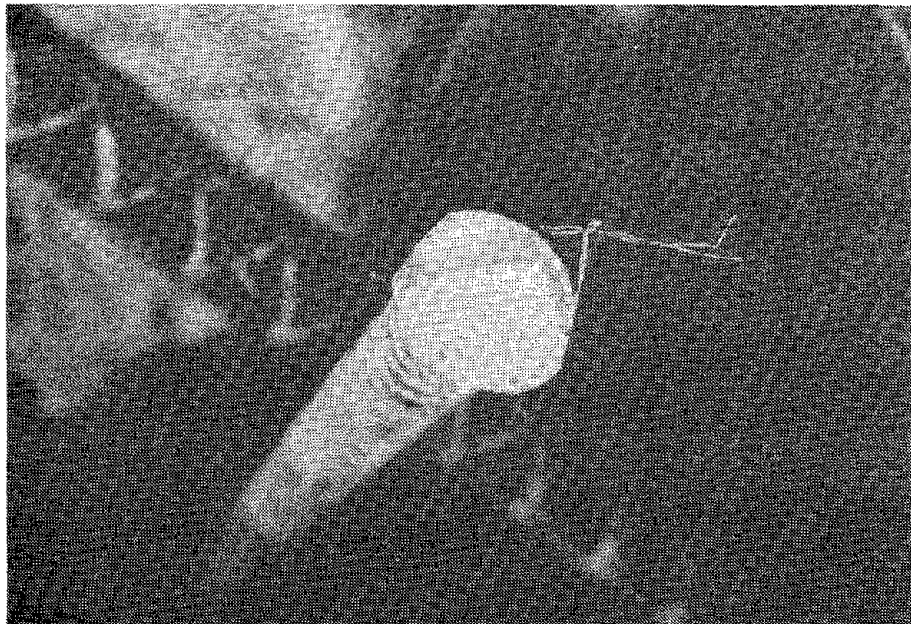
Fig. 7.10 Close-up of gas pressure weld splice failure
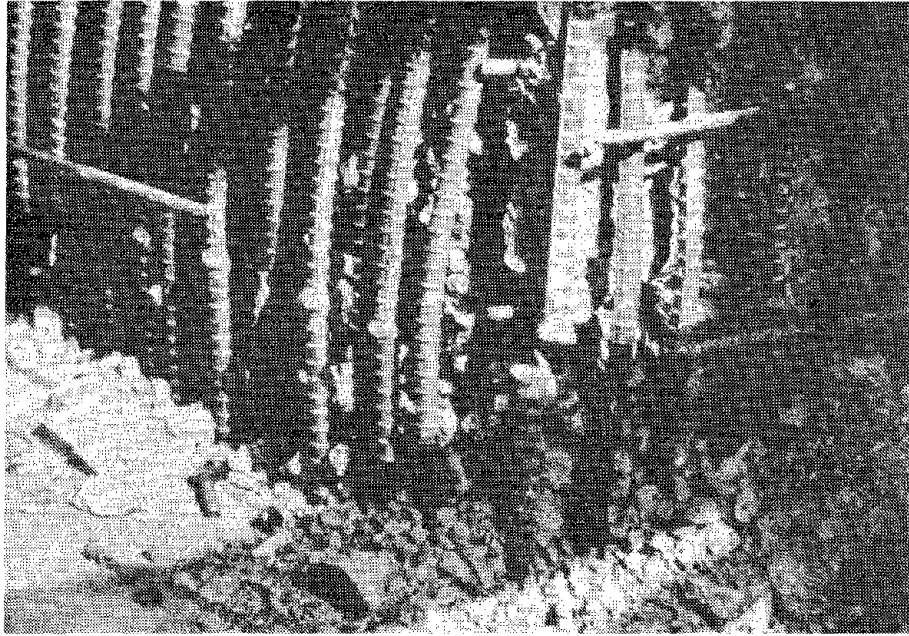
Fig. 7.11 Splice failure at the base of a pier
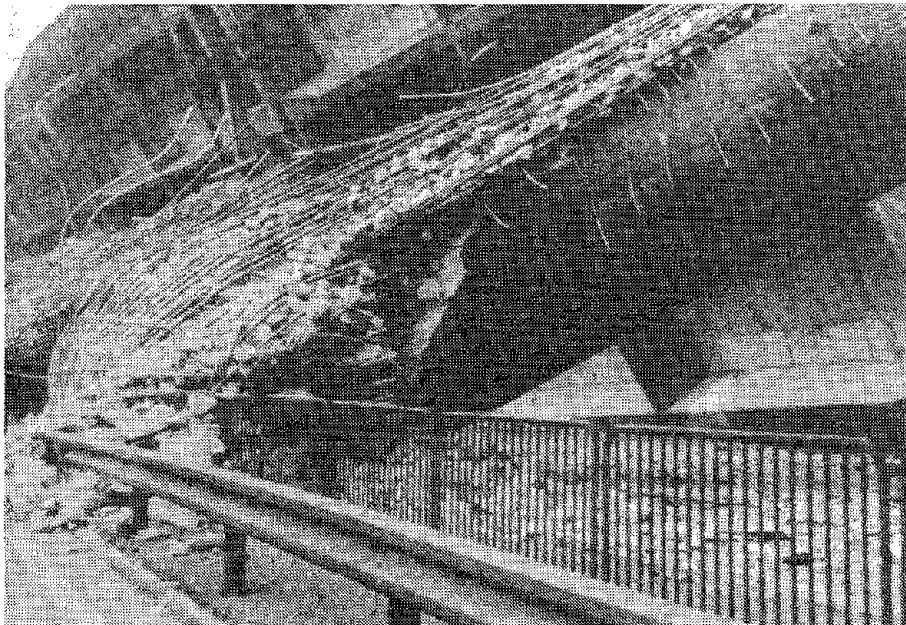
Fig. 7.12 Splice failure at mid-height of pier

Fig. 7.13 Splice failure just under pier cap
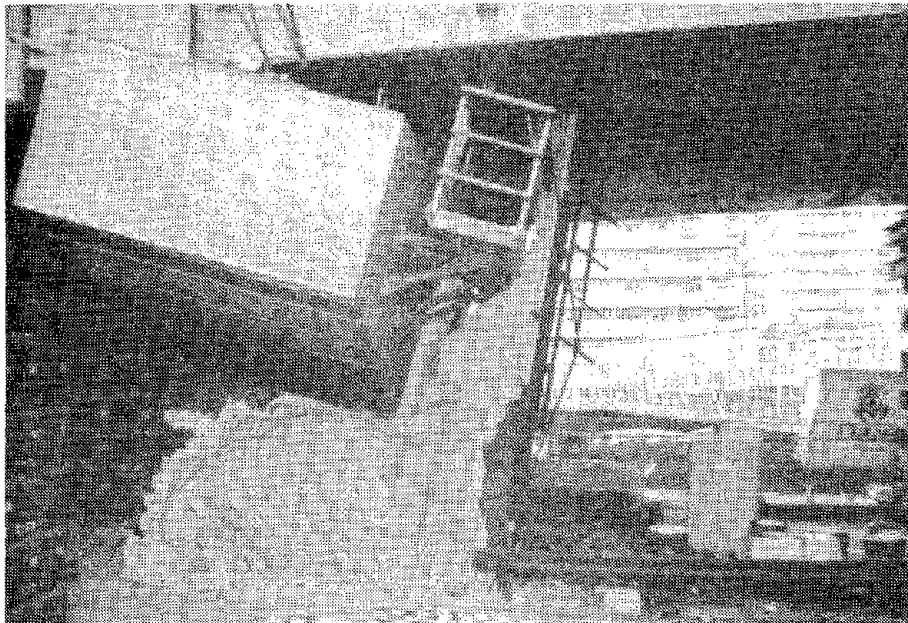
Fig. 7.14 Splice failure followed by shear failure of square pier

216

Fig. 7.15 Splice failure followed by shear failure of circular pier

NISHINOMIYA KO BRIDGE

● Side View
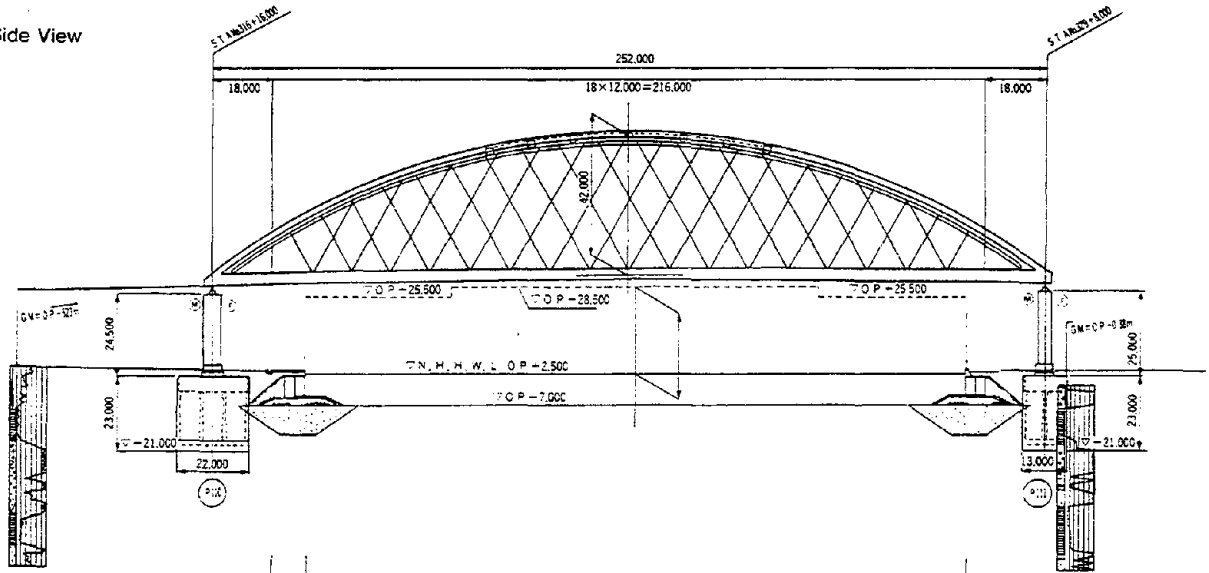
● Plan View
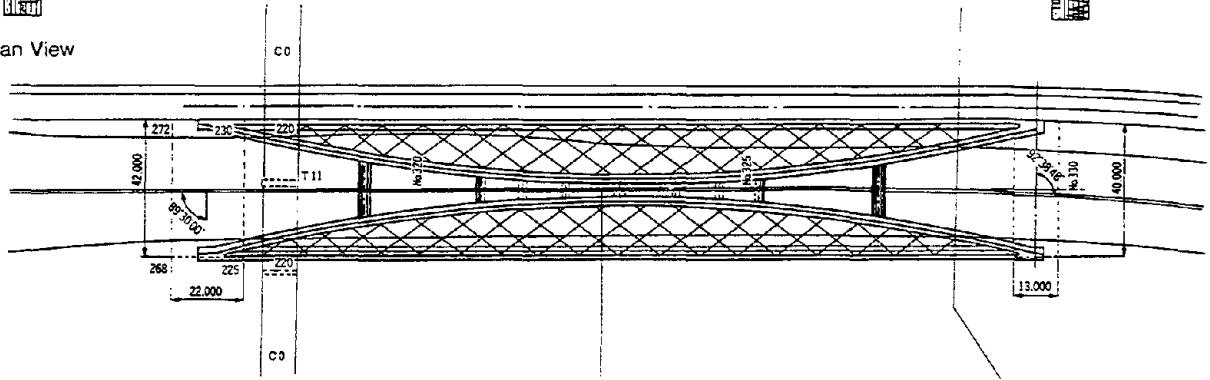
● Sectional View
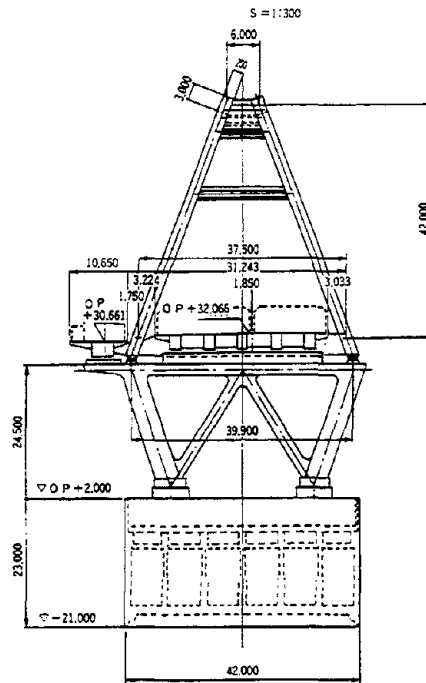
Fig. 7.16 Plan and elevation views of the Nishnomiya Ko tied arch bridge

218

Fig. 7.17 Restrainer failure in approach span to Nishnomiya Ko tied arch bridge

Fig. 7.18 View of collapsed span from the south
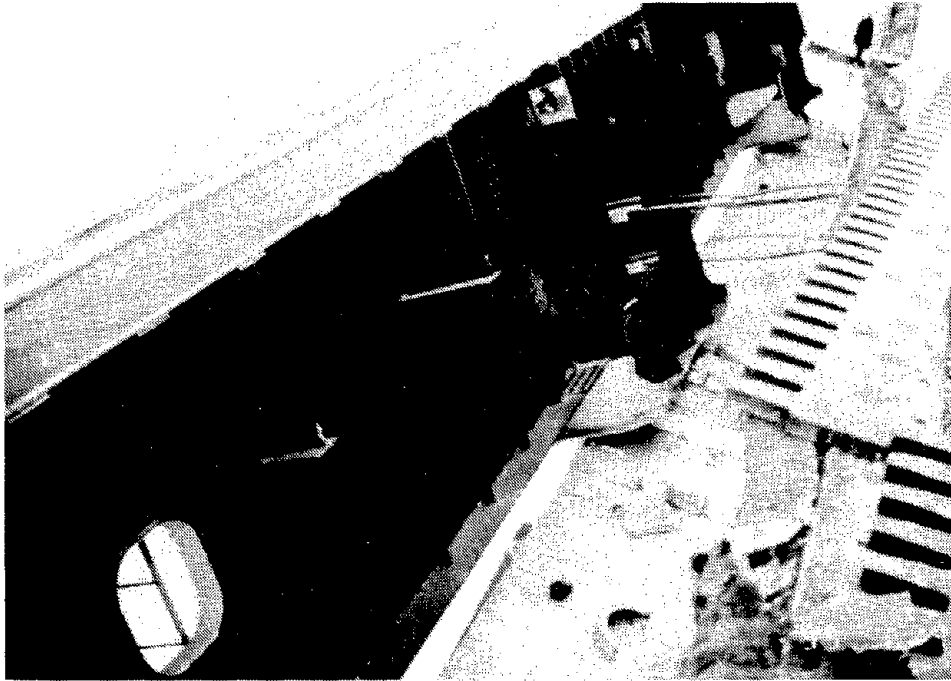
Fig. 7.19 Details of the top edge of collapsed span
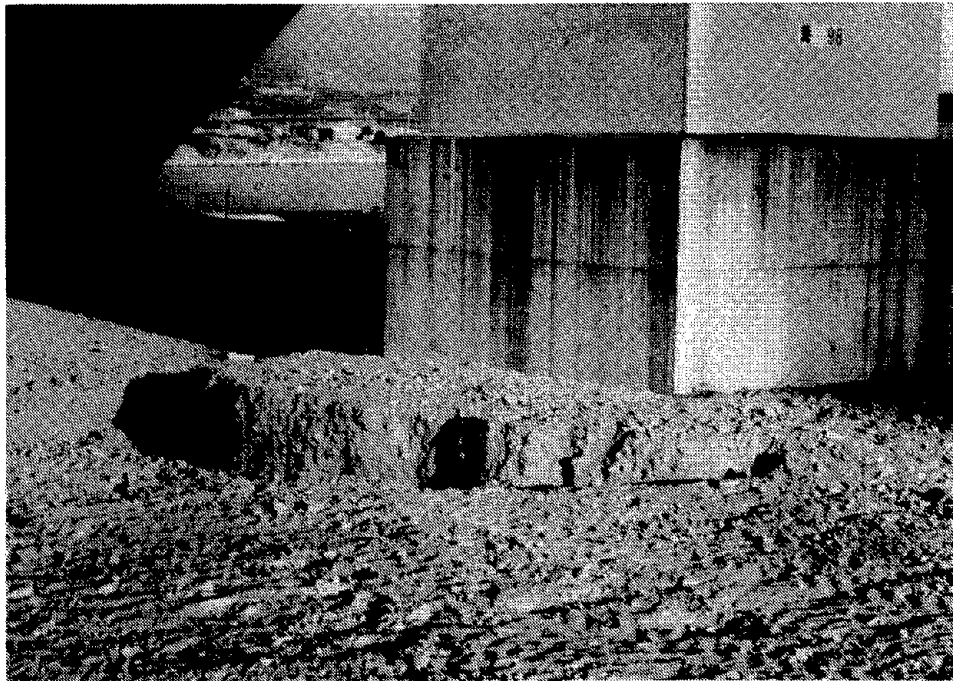
Fig. 7.20 Settlement around pier at east end of dropped span
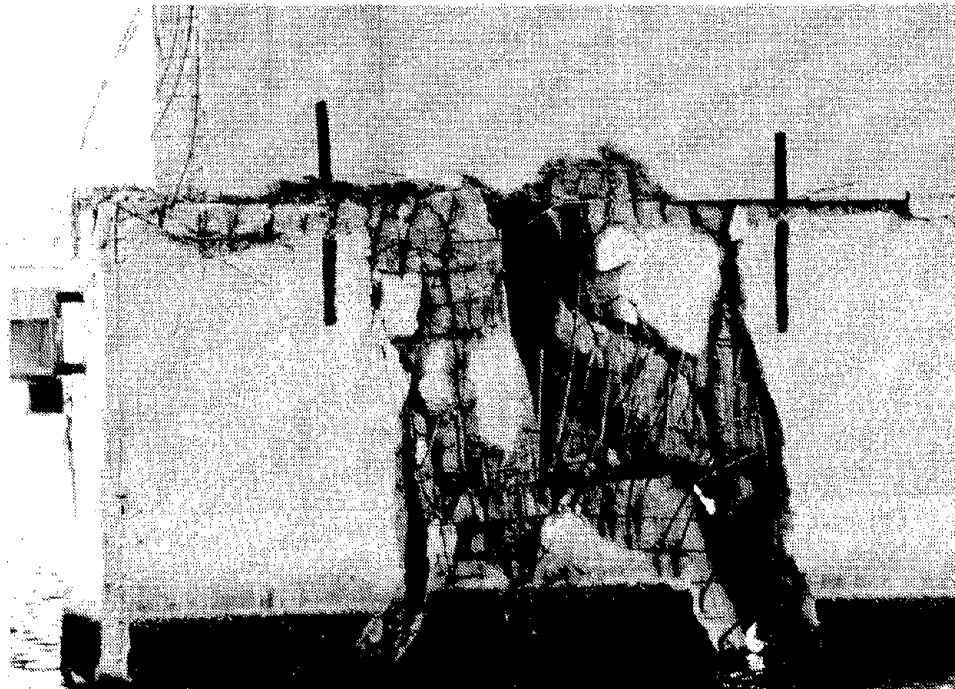
Fig. 7.21 Close-up of pier damage

Fig. 7.22 Superstructure movement

221
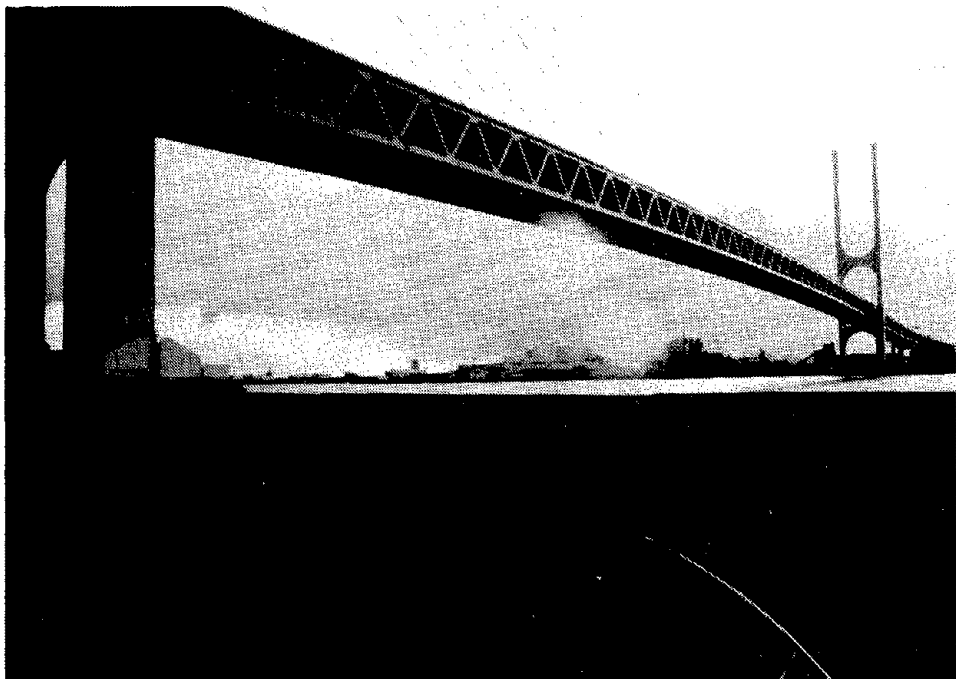
Fig. 7.23 Higashi Kobe bridge

HIGASHI KOBE BRIDGE

● Side View
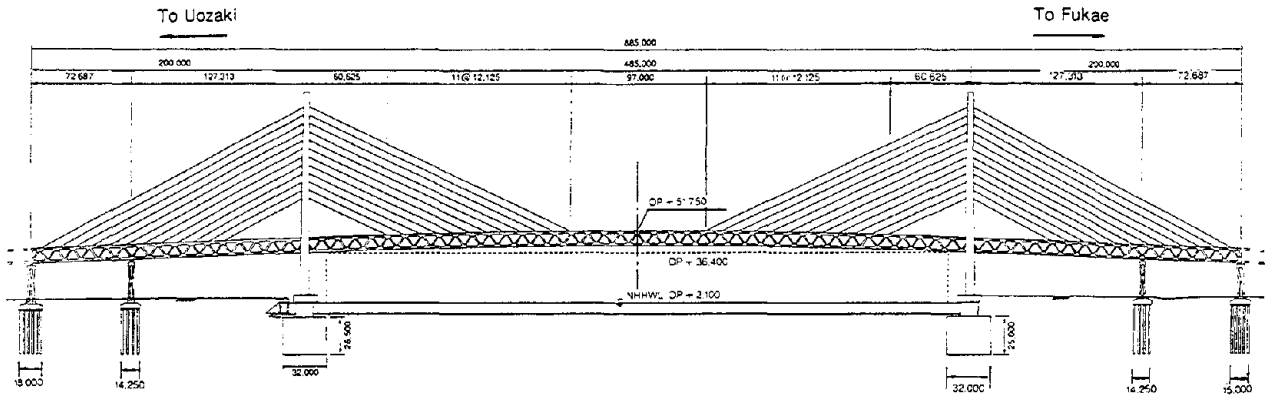
● Plan View
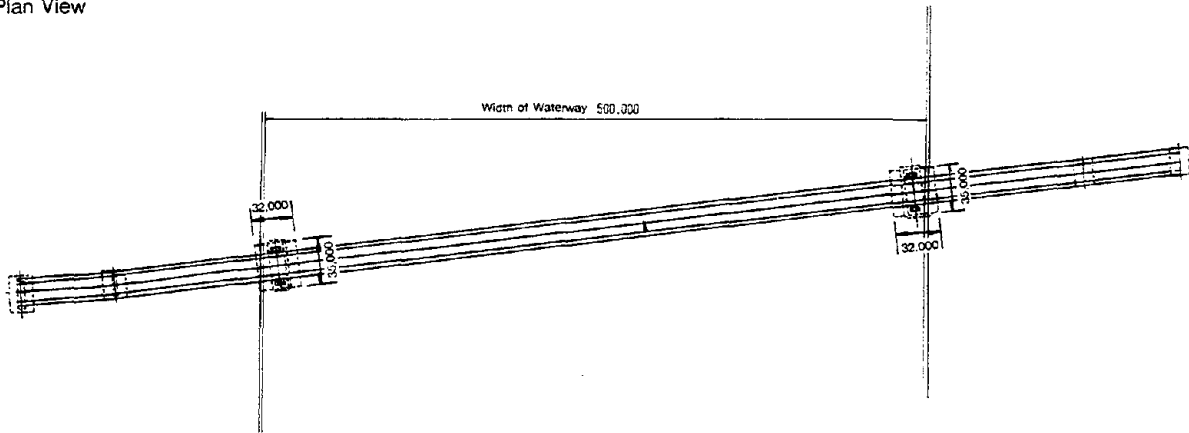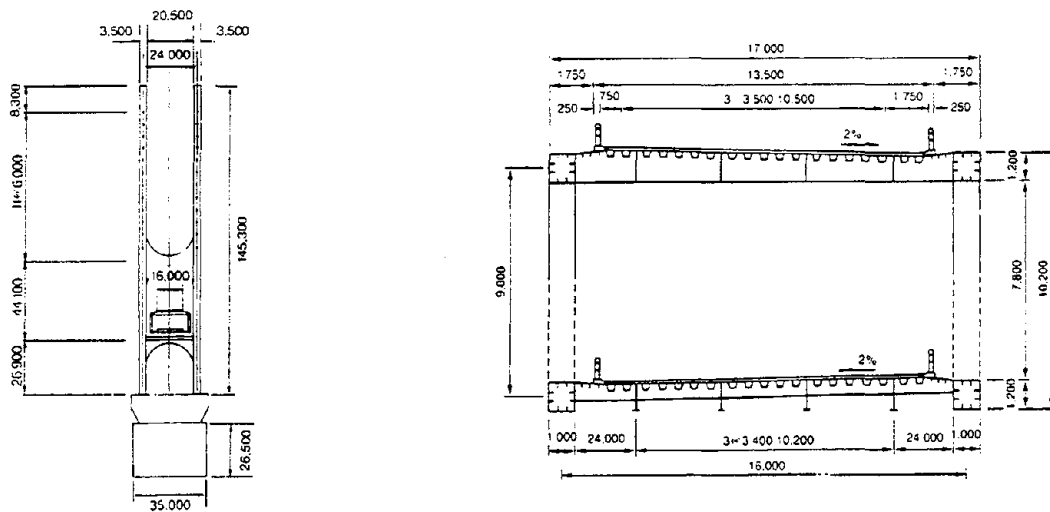
● Sectional View

Fig. 7.24 Higashi Kobe bridge (from Reference 4)

223
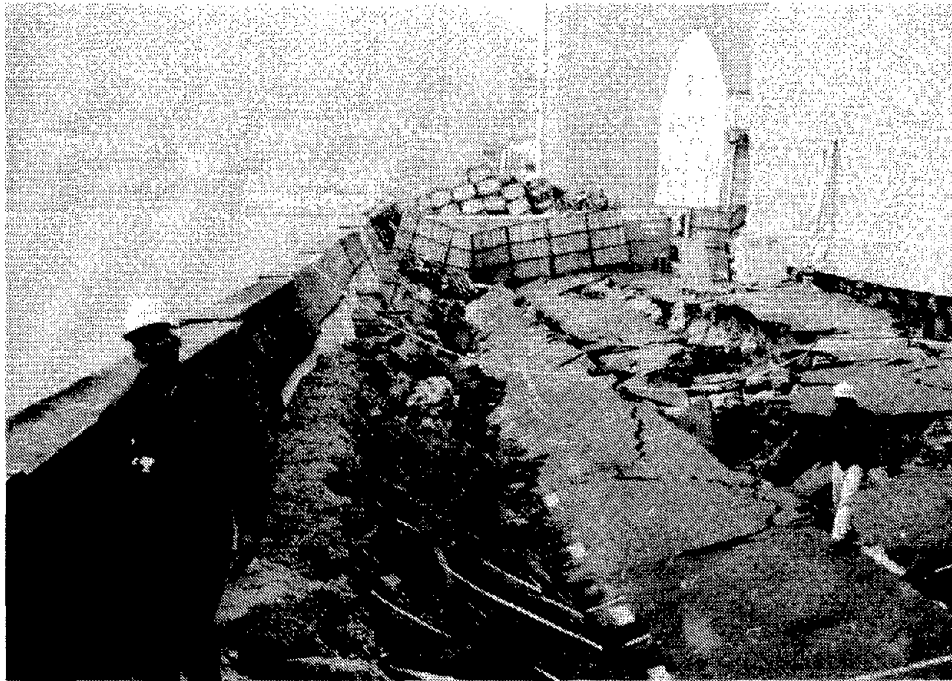
Fig. 7.25 Lateral spreading near the Higashi Kobe bridge
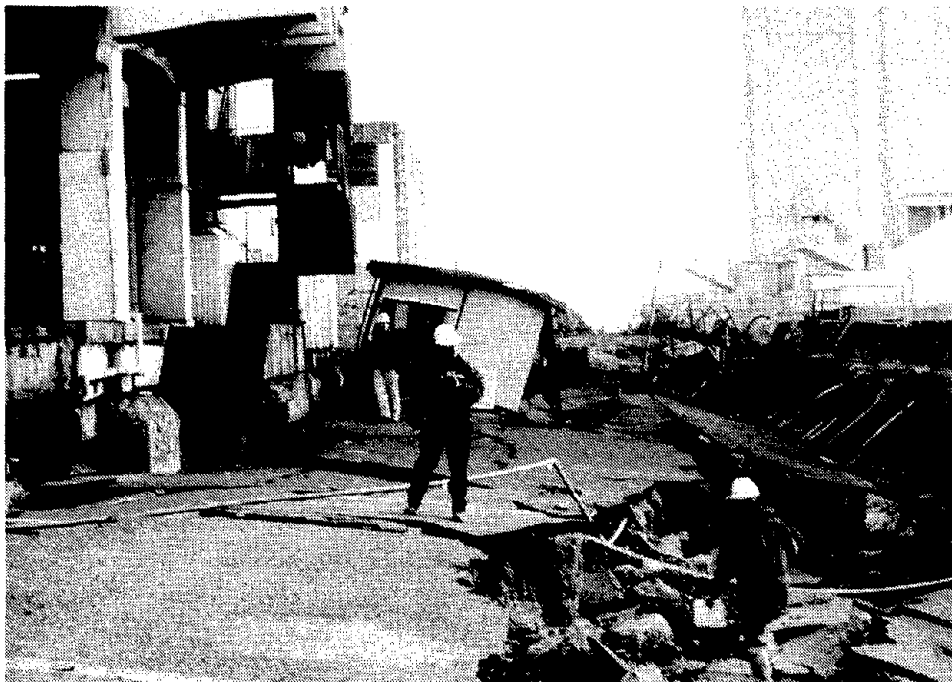
Fig. 7.26 Lateral spreading at the Higashi Kobe bridge

ROKKO ISLAND BRIDGE

●Side View
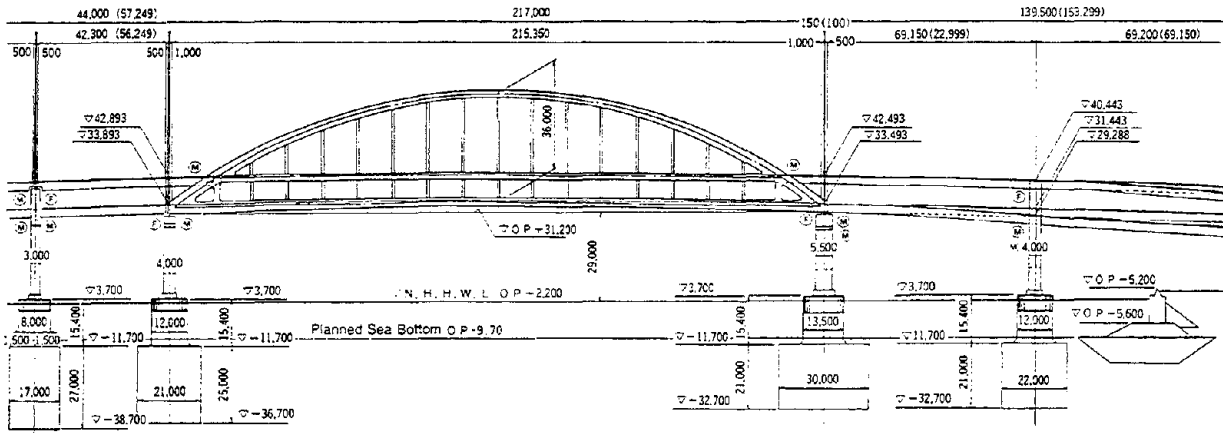
●Plan View
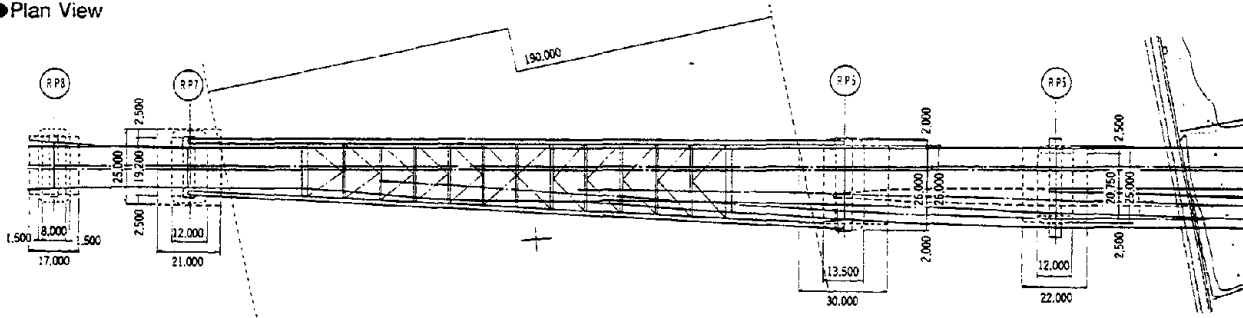
●Sectional View
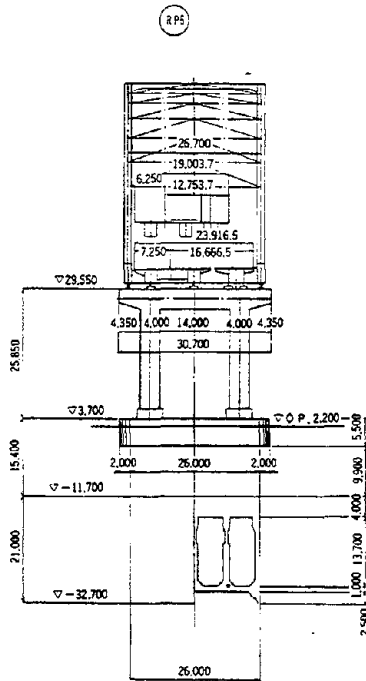
Fig. 7.27 Rokko Island bridge (from Reference 4)
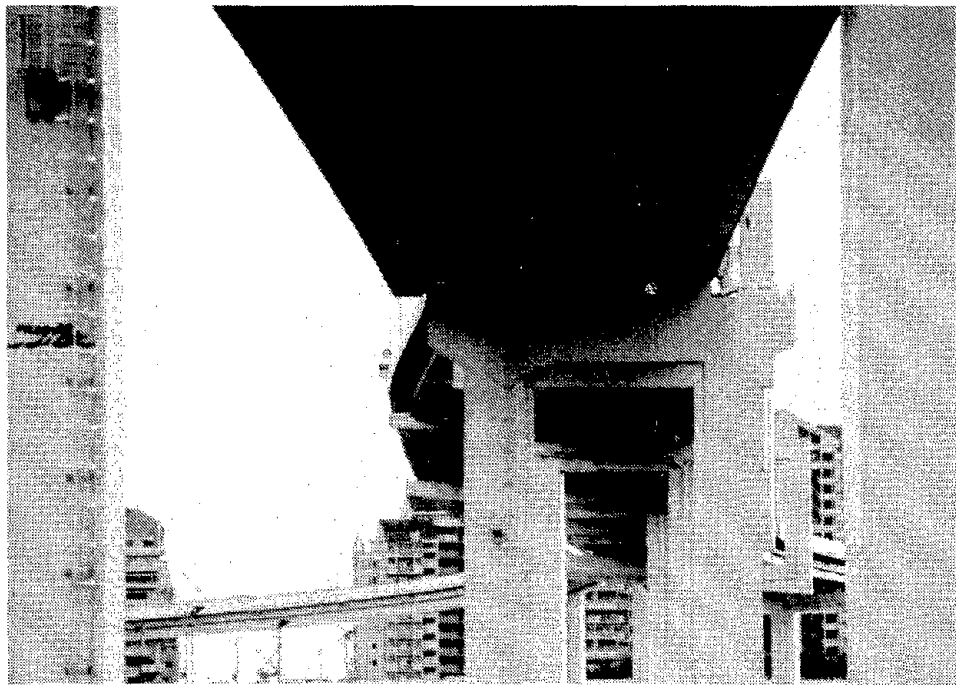
Fig. 7.28 South end of span shifted to the east
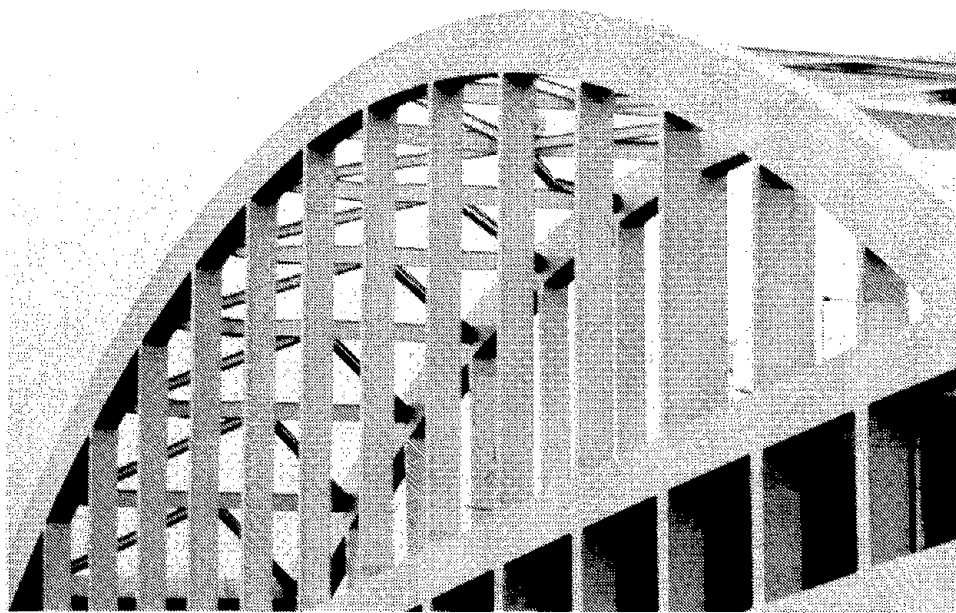
Fig. 7.29 Buckled brace at top of arch

226
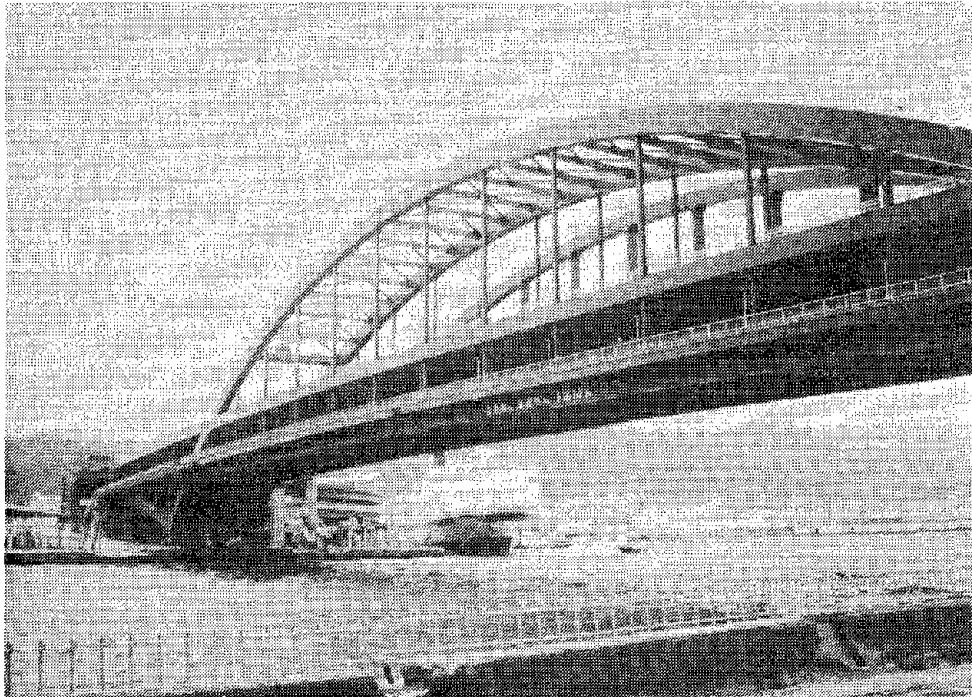
Fig. 7.30 Port Island bridge
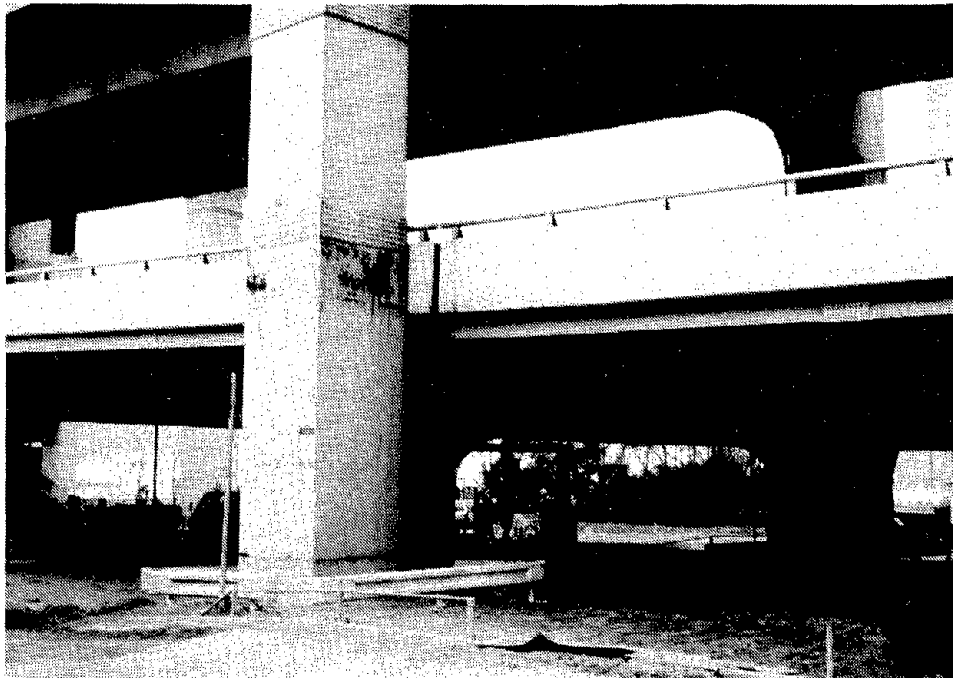
Fig. 7.31 South end of Port Island bridge

227

Fig. 7.32 Settlement around piers at south end of Port Island bridge
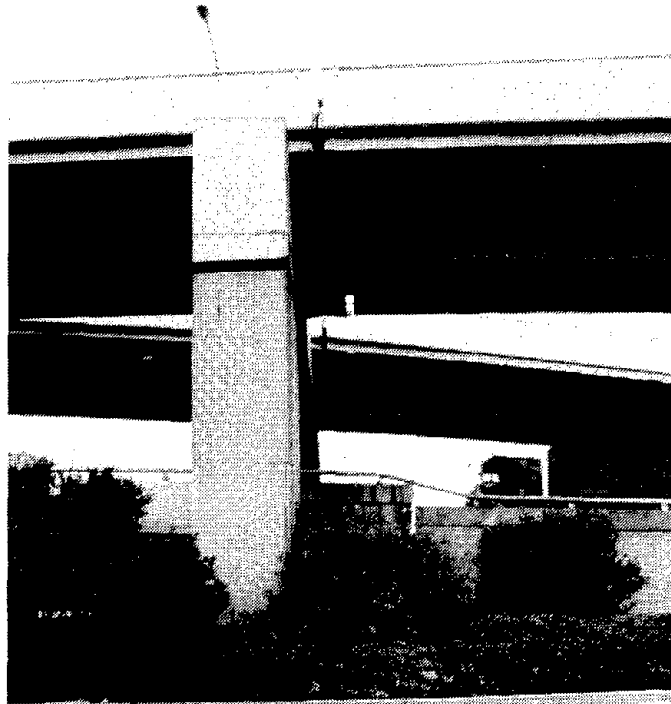
Fig. 7.33 Opening of expansion joint

228

Fig. 7.34 Abutment settlement

Fig. 7.35 Transverse superstructure movement

229
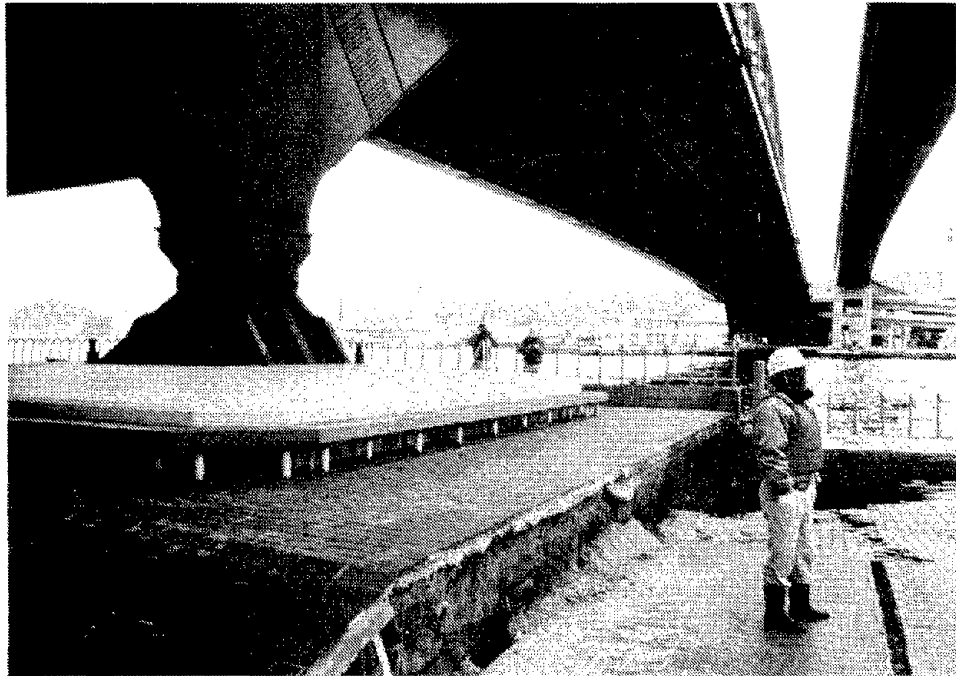
Fig. 7.36 Settlement at south end of Port Island bridge
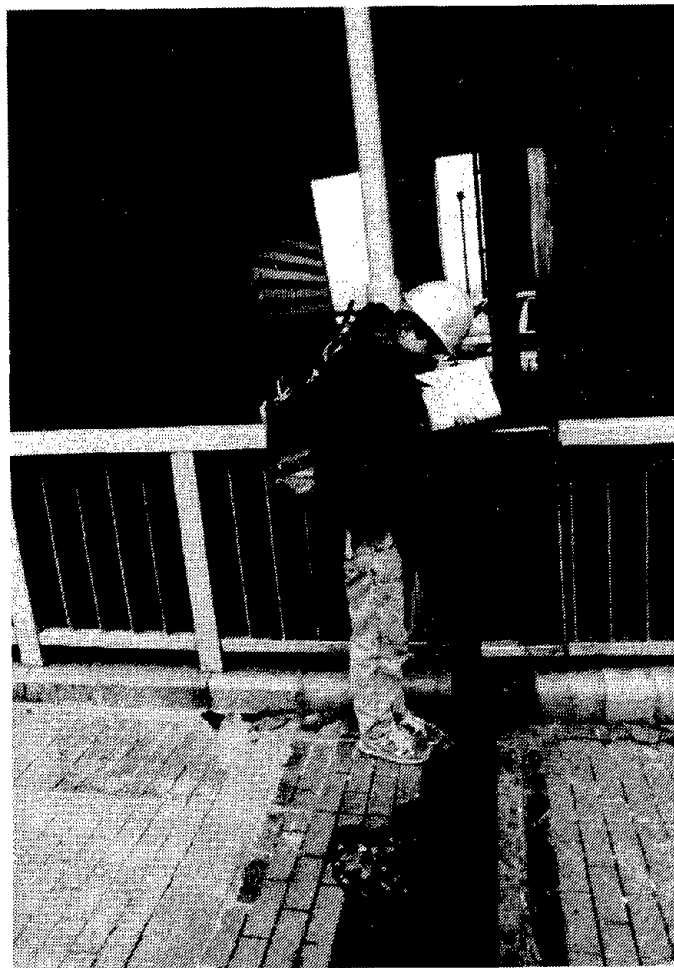
Fig. 7.37 Expansion joint opening on Port Island bridge

230

Fig. 7.38 Settlement on northeast side of Port Island bridge
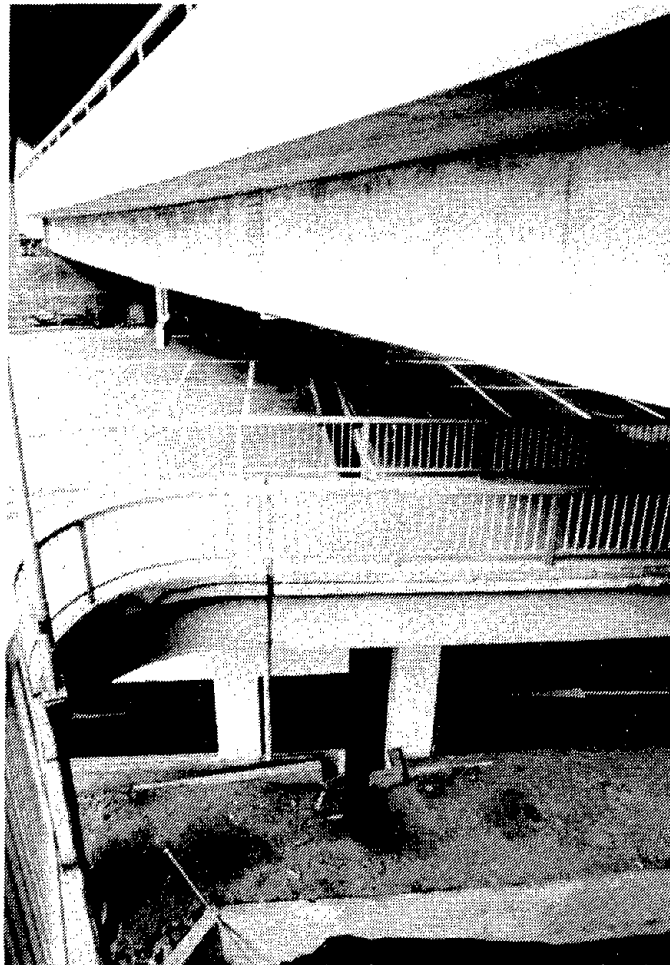
Fig. 7.39 Damaged parking facilities

Fig. 7.40 Dropped span in parking structure at north end of Port Island bridge

Fig. 7.41 Inclined piers on elevated railway

Fig. 7.42 Buckling at base of steel column

Fig. 7.43 Spalling in large modern column

234

Fig. 7.44 Buckled steel column
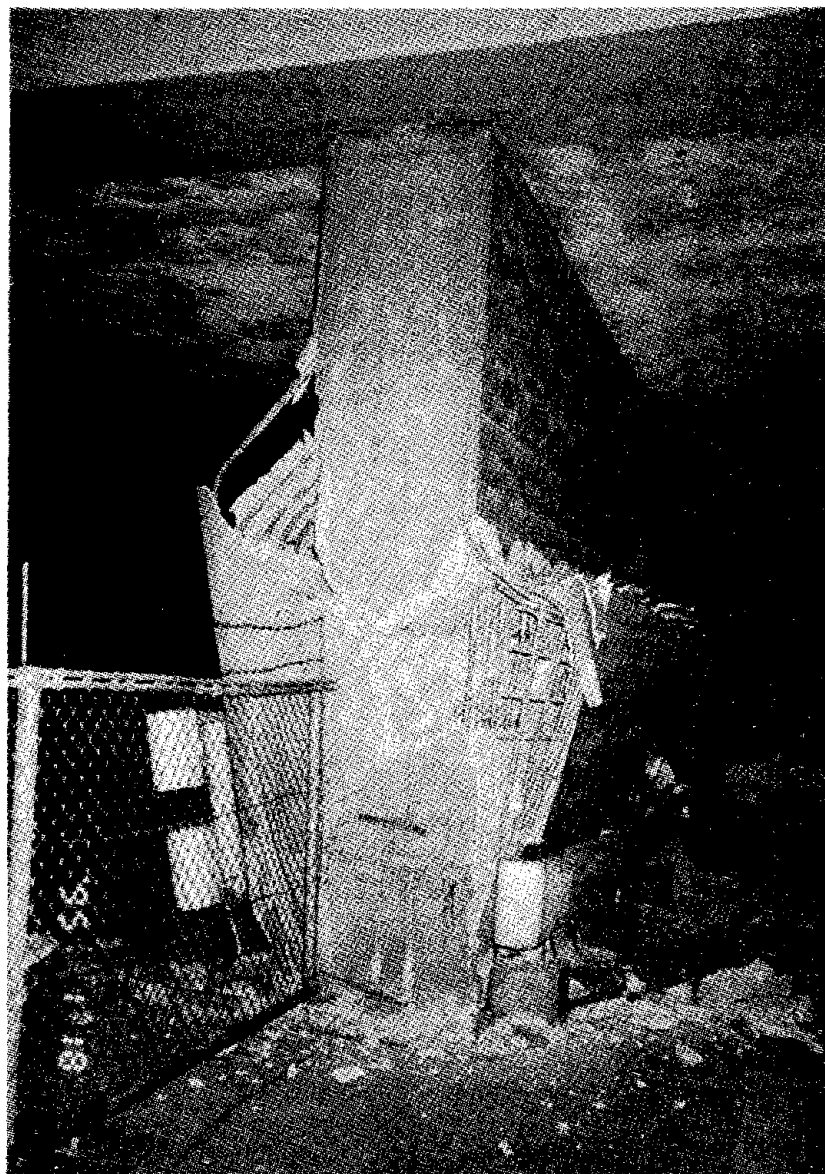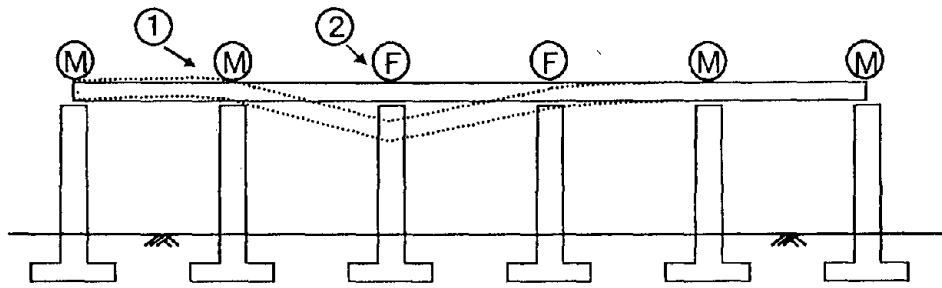
Fig. 7.45 Typical failure modes of the Ohnishi, Suidoh, and Moribe Bridges [JHC, 1995]

Fig. 7.45 (continued)

Fig. 7.45 (continued)

（a）側 面 図

（b）平 面 図

（c）正 面 図

上り線

下り線

P24 P25 P26 P27
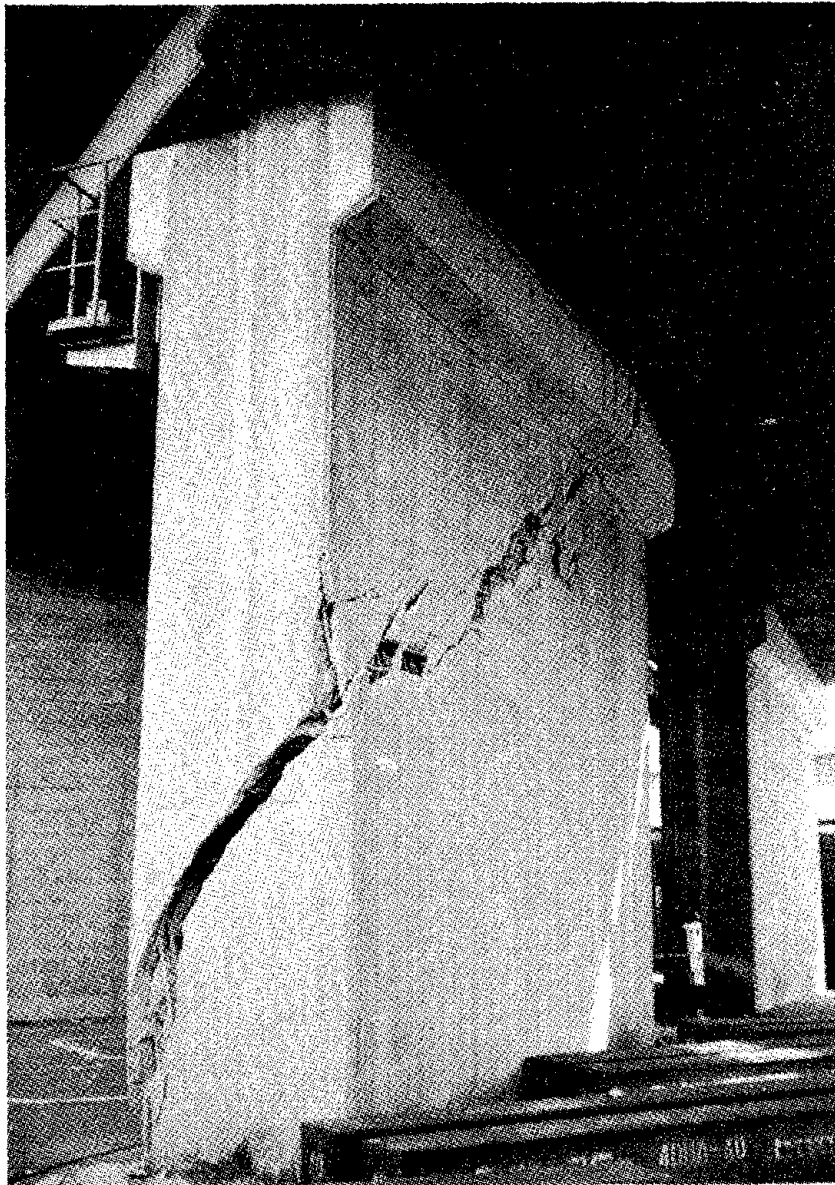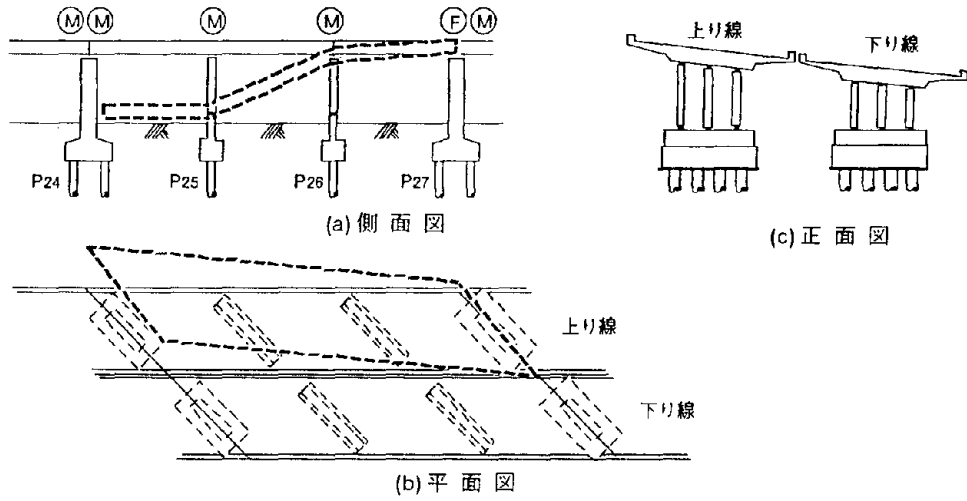
Fig. 7.46 Damage to the Kawaragi-nish Bridge [JHC, 1995]

239
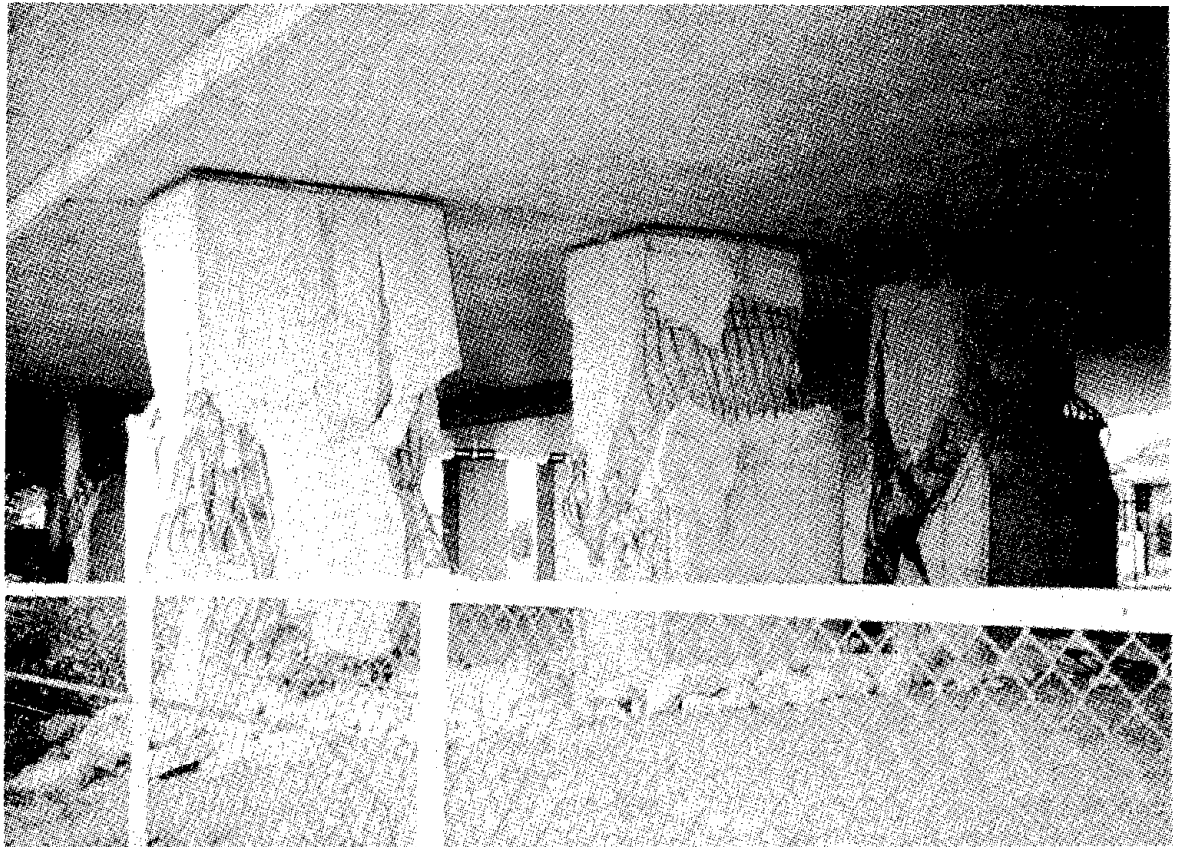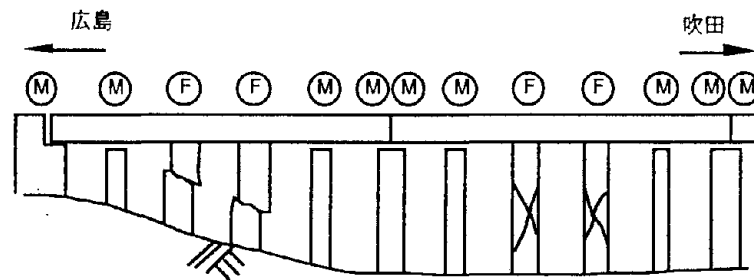
Fig. 7.47 Damage to the Takarazuka Bridge [JHC, 1995]

Main Tower

35.5

T.P.+297.2
(Theoretical apex
of cables)

282.8

T.P.+81
(Height of road
surface)

Cross-Section of
Suspended Structure

35.50

2.50 10.75 3.50 10.75 2.50

Grating As Pavement
and steel deck

14.00

T.P.+10

6.6

46.5   14.8

Akashi Kaikyo Bridge   Matsuho Viaduct

3910   300

960   1990   960

3.0% linear grade   1.5% parabolic grade   3.0% linear grade

Kobe side   Awaji side

T.P.+297.2

Height of road surface
T.P.+96

Height of road surface
T.P.+53   T.P.+53

T.P.+10
N.H.H.W.L (T.P.+0.9)   T.P.+10

P.-61   T.P.-50   T.P.-57

Height of road surface   Height of road surface
T.P.+81

Side View   1 A   2 P   3 P   4 A

T.P.······Mean sea level of Tokyo Bay   N.H.H.W.L······Nearly highest high water level (unit : m)

-25   -50   -75 -100   -100 -75 -50   -25

Plane View

Fig. 7.48 Details of the Akashi- Kaikyo Bridge [Nitta, 1995]

Δx	0
Δy	0
Δz	0

Δx	+ 11
Δy	0
Δz	- 40

Δx	単位
Δy	mm
Δz	

Δx	+ 880
Δy	+ 936
Δz	- 239

Δx	+1,123
Δy	+ 838
Δz	+ 157

center line of eastern main cable

$\begin{cases} \theta\ x = 0 \\ \theta\ y = 0 \\ \theta\ z = 0 \end{cases}$ rad
rad
rad

$\begin{cases} \theta\ x = -8.5520 \times 10^{-6} \text{rad} \\ \theta\ y = +6.4690 \times 10^{-5} \text{rad} \\ \theta\ z = 0 \qquad \text{rad} \end{cases}$

$\begin{cases} \theta\ x = -7.6920 \times 10^{-5} \text{rad} \\ \theta\ y = +1.1580 \times 10^{-3} \text{rad} \\ \theta\ z = +2.3944 \times 10^{-3} \text{rad} \end{cases}$

$\begin{cases} \theta\ x = +3.6508 \times 10^{-4} \text{rad} \\ \theta\ y = +4.3125 \times 10^{-4} \text{rad} \\ \theta\ z = -3.9437 \times 10^{-4} \text{rad} \end{cases}$

center line of western main cable

Δx	0
Δy	0
Δz	0

Δx	+ 11
Δy	0
Δz	- 40

Δx	+ 795
Δy	+ 936
Δz	- 241

Δx	+1,137
Δy	+ 836
Δz	+ 170

(1 A) (2 P) (3 P) (4 A)

direction of X-axsis: 1A→2P

Fig. 7.49 Earthquake-induced foundation displacements - Akashi-Kaikyo Bridge [Nitta, 1995]

242

(vertical and horizontal displacement)

(displacement of main cable at the direction perpendicular to the bridge)

Fig. 7.50 Earthquake-induced skeletal displacements - Akashi-Kaikyo Bridge [Nitta, 1995]

243

EARTHQUAKE ENGINEERING RESEARCH CENTER REPORT SERIES

EERC reports are available from the National Information Service for Earthquake Engineering (NISEE) and from the National Technical Information Service (NTIS). Numbers in parentheses are Accession Numbers assigned by the National Technical Information Service; these are followed by a price code. Contact NTIS, 5285 Port Royal Road, Springfield Virginia, 22161 for more information. Reports without Accession Numbers were not available from NTIS at the time of printing. For a current complete list of EERC reports (from EERC 67-1) and availablity information, please contact University of California, EERC, NISEE, 1301 South 46th Street, Richmond, California 94804-4698.

UCB/EERC-84/01   "Pseudodynamic Test Method for Seismic Performance Evaluation: Theory and Implementation," by Shing, P.-S.B. and Mahin, S.A., January 1984, (PB84 190 644)A08.

UCB/EERC-84/02   "Dynamic Response Behavior of Kiang Hong Dian Dam," by Clough, R.W., Chang, K.-T., Chen, H.-Q. and Stephen, R.M., April 1984, (PB84 209 402)A08.

UCB/EERC-84/03   "Refined Modelling of Reinforced Concrete Columns for Seismic Analysis," by Kaba, S.A. and Mahin, S.A., April 1984, (PB84 234 384)A06.

UCB/EERC-84/04   "A New Floor Response Spectrum Method for Seismic Analysis of Multiply Supported Secondary Systems," by Asfura, A. and Der Kiureghian, A., June 1984, (PB84 239 417)A06.

UCB/EERC-84/05   "Earthquake Simulation Tests and Associated Studies of a 1/5th-scale Model of a 7-Story R/C Frame-Wall Test Structure," by Bertero, V.V., Aktan, A.E., Charney, F.A. and Sause, R., June 1984, (PB84 239 409)A09.

UCB/EERC-84/06   "Unassigned," by Unassigned, 1984.

UCB/EERC-84/07   "Behavior of Interior and Exterior Flat-Plate Connections Subjected to Inelastic Load Reversals," by Zee, H.L. and Moehle, J.P., August 1984, (PB86 117 629/AS)A07.

UCB/EERC-84/08   "Experimental Study of the Seismic Behavior of a Two-Story Flat-Plate Structure," by Moehle, J.P. and Diebold, J.W., August 1984, (PB86 122 553/AS)A12.

UCB/EERC-84/09   "Phenomenological Modeling of Steel Braces under Cyclic Loading," by Ikeda, K., Mahin, S.A. and Dermitzakis, S.N., May 1984, (PB86 132 198/AS)A08.

UCB/EERC-84/10   "Earthquake Analysis and Response of Concrete Gravity Dams," by Fenves, G.L. and Chopra, A.K., August 1984, (PB85 193 902/AS)A11.

UCB/EERC-84/11   "EAGD-84: A Computer Program for Earthquake Analysis of Concrete Gravity Dams," by Fenves, G.L. and Chopra, A.K., August 1984, (PB85 193 613/AS)A05.

UCB/EERC-84/12   "A Refined Physical Theory Model for Predicting the Seismic Behavior of Braced Steel Frames," by Ikeda, K. and Mahin, S.A., July 1984, (PB85 191 450/AS)A09.
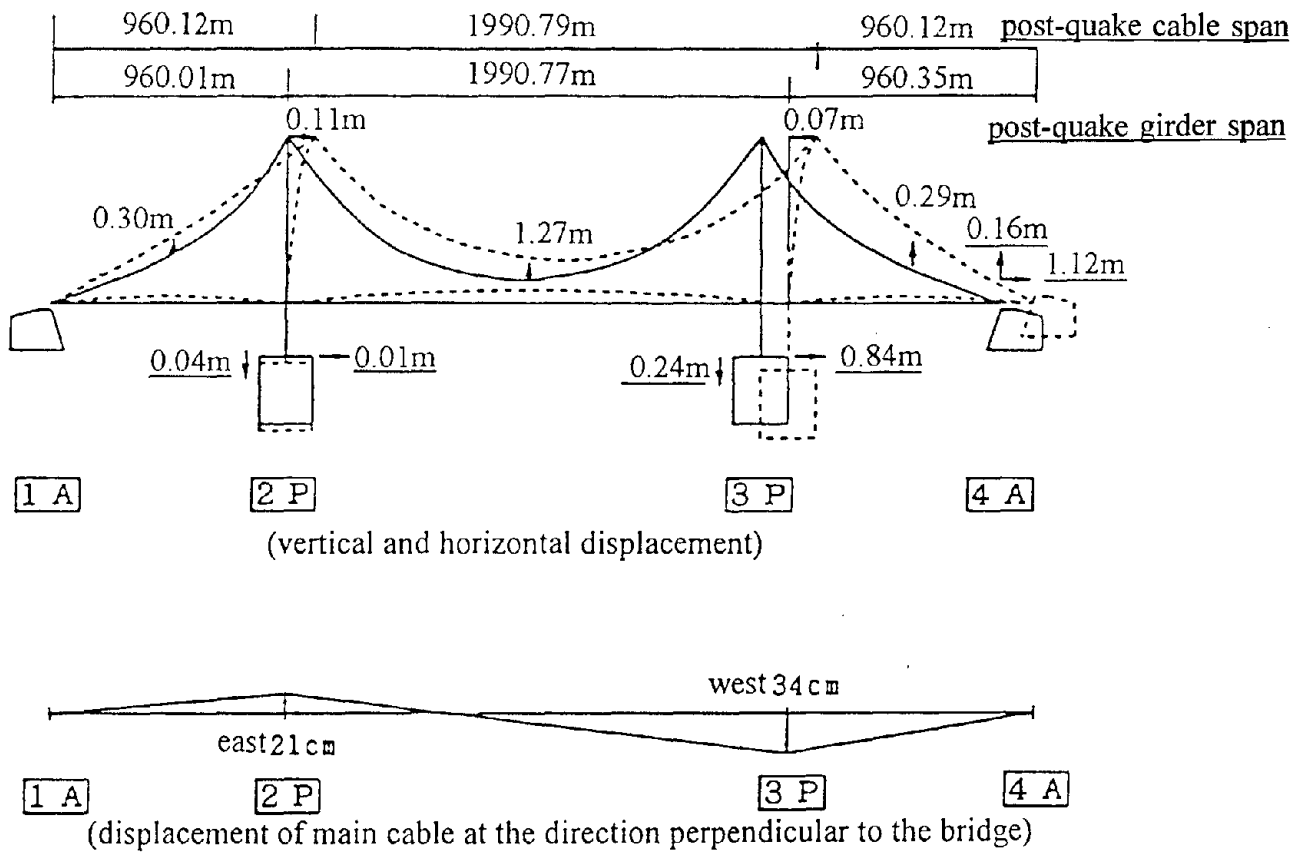
UCB/EERC-84/13   "Earthquake Engineering Research at Berkeley - 1984," by EERC, August 1984, (PB85 197 341/AS)A10.

UCB/EERC-84/14   "Moduli and Damping Factors for Dynamic Analyses of Cohesionless Soils," by Seed, H.B., Wong, R.T., Idriss, I.M. and Tokimatsu, K., September 1984, (PB85 191 468/AS)A04.

UCB/EERC-84/15   "The Influence of SPT Procedures in Soil Liquefaction Resistance Evaluations," by Seed, H.B., Tokimatsu, K., Harder, L.F. and Chung, R.M., October 1984, (PB85 191 732/AS)A04.

UCB/EERC-84/16   "Simplified Procedures for the Evaluation of Settlements in Sands Due to Earthquake Shaking," by Tokimatsu, K. and Seed, H.B., October 1984, (PB85 197 887/AS)A03.

UCB/EERC-84/17   "Evaluation of Energy Absorption Characteristics of Highway Bridges Under Seismic Conditions - Volume I (PB90 262 627)A16 and Volume II (Appendices) (PB90 262 635)A13," by Imbsen, R.A. and Penzien, J., September 1986.

UCB/EERC-84/18   "Structure-Foundation Interactions under Dynamic Loads," by Liu, W.D. and Penzien, J., November 1984, (PB87 124 889/AS)A11.

UCB/EERC-84/19   "Seismic Modelling of Deep Foundations," by Chen, C.-H. and Penzien, J., November 1984, (PB87 124 798/AS)A07.

UCB/EERC-84/20   "Dynamic Response Behavior of Quan Shui Dam," by Clough, R.W., Chang, K.-T., Chen, H.-Q., Stephen, R.M., Ghanaat, Y. and Qi, J.-H., November 1984, (PB86 115177/AS)A07.

UCB/EERC-85/01   "Simplified Methods of Analysis for Earthquake Resistant Design of Buildings," by Cruz, E.F. and Chopra, A.K., February 1985, (PB86 112299/AS)A12.

UCB/EERC-85/02   "Estimation of Seismic Wave Coherency and Rupture Velocity using the SMART 1 Strong-Motion Array Recordings," by Abrahamson, N.A., March 1985, (PB86 214 343)A07.

UCB/EERC-85/03   "Dynamic Properties of a Thirty Story Condominium Tower Building," by Stephen, R.M., Wilson, E.L. and Stander, N., April 1985, (PB86 118965/AS)A06.

UCB/EERC-85/04   "Development of Substructuring Techniques for On-Line Computer Controlled Seismic Performance Testing," by Dermitzakis, S. and Mahin, S., February 1985, (PB86 132941/AS)A08.

UCB/EERC-85/05   "A Simple Model for Reinforcing Bar Anchorages under Cyclic Excitations," by Filippou, F.C., March 1985, (PB86 112 919/AS)A05.

UCB/EERC-85/06   "Racking Behavior of Wood-framed Gypsum Panels under Dynamic Load," by Oliva, M.G., June 1985, (PB90 262 643)A04.

244

UCB/EERC-85/07   "Earthquake Analysis and Response of Concrete Arch Dams," by Fok, K.-L. and Chopra, A.K., June 1985, (PB86 139672/AS)A10.

UCB/EERC-85/08   "Effect of Inelastic Behavior on the Analysis and Design of Earthquake Resistant Structures," by Lin, J.P. and Mahin, S.A., June 1985, (PB86 135340/AS)A08.

UCB/EERC-85/09   "Earthquake Simulator Testing of a Base-Isolated Bridge Deck," by Kelly, J.M., Buckle, I.G. and Tsai, H.-C., January 1986, (PB87 124 152/AS)A06.

UCB/EERC-85/10   "Simplified Analysis for Earthquake Resistant Design of Concrete Gravity Dams," by Fenves, G.L. and Chopra, A.K., June 1986, (PB87 124 160/AS)A08.

UCB/EERC-85/11   "Dynamic Interaction Effects in Arch Dams," by Clough, R.W., Chang, K.-T., Chen, H.-Q. and Ghanaat, Y., October 1985, (PB86 135027/AS)A05.

UCB/EERC-85/12   "Dynamic Response of Long Valley Dam in the Mammoth Lake Earthquake Series of May 25-27, 1980," by Lai, S. and Seed, H.B., November 1985, (PB86 142304/AS)A05.

UCB/EERC-85/13   "A Methodology for Computer-Aided Design of Earthquake-Resistant Steel Structures," by Austin, M.A., Pister, K.S. and Mahin, S.A., December 1985, (PB86 159480/AS)A10 .

UCB/EERC-85/14   "Response of Tension-Leg Platforms to Vertical Seismic Excitations," by Liou, G.-S., Penzien, J. and Yeung, R.W., December 1985, (PB87 124 871/AS)A08.

UCB/EERC-85/15   "Cyclic Loading Tests of Masonry Single Piers: Volume 4 - Additional Tests with Height to Width Ratio of 1," by Sveinsson, B., McNiven, H.D. and Sucuoglu, H., December 1985, (PB87 165031/AS)A08.

UCB/EERC-85/16   "An Experimental Program for Studying the Dynamic Response of a Steel Frame with a Variety of Infill Partitions," by Yanev, B. and McNiven, H.D., December 1985, (PB90 262 676)A05.

UCB/EERC-86/01   "A Study of Seismically Resistant Eccentrically Braced Steel Frame Systems," by Kasai, K. and Popov, E.P., January 1986, (PB87 124 178/AS)A14.

UCB/EERC-86/02   "Design Problems in Soil Liquefaction," by Seed, H.B., February 1986, (PB87 124 186/AS)A03.

UCB/EERC-86/03   "Implications of Recent Earthquakes and Research on Earthquake-Resistant Design and Construction of Buildings," by Bertero, V.V., March 1986, (PB87 124 194/AS)A05.

UCB/EERC-86/04   "The Use of Load Dependent Vectors for Dynamic and Earthquake Analyses," by Leger, P., Wilson, E.L. and Clough, R.W., March 1986, (PB87 124 202/AS)A12.

UCB/EERC-86/05   "Two Beam-To-Column Web Connections," by Tsai, K.-C. and Popov, E.P., April 1986, (PB87 124 301/AS)A04.

UCB/EERC-86/06   "Determination of Penetration Resistance for Coarse-Grained Soils using the Becker Hammer Drill," by Harder, L.F. and Seed, H.B., May 1986, (PB87 124 210/AS)A07.

UCB/EERC-86/07   "A Mathematical Model for Predicting the Nonlinear Response of Unreinforced Masonry Walls to In-Plane Earthquake Excitations," by Mengi, Y. and McNiven, H.D., May 1986, (PB87 124 780/AS)A06.

UCB/EERC-86/08   "The 19 September 1985 Mexico Earthquake: Building Behavior," by Bertero, V.V., July 1986.

UCB/EERC-86/09   "EACD-3D: A Computer Program for Three-Dimensional Earthquake Analysis of Concrete Dams," by Fok, K.-L., Hall, J.F. and Chopra, A.K., July 1986, (PB87 124 228/AS)A08.

UCB/EERC-86/10   "Earthquake Simulation Tests and Associated Studies of a 0.3-Scale Model of a Six-Story Concentrically Braced Steel Structure," by Uang, C.-M. and Bertero, V.V., December 1986, (PB87 163 564/AS)A17.

UCB/EERC-86/11   "Mechanical Characteristics of Base Isolation Bearings for a Bridge Deck Model Test," by Kelly, J.M., Buckle, I.G. and Koh, C.-G., November 1987, (PB90 262 668)A04.

UCB/EERC-86/12   "Effects of Axial Load on Elastomeric Isolation Bearings," by Koh, C.-G. and Kelly, J.M., November 1987, PB88-179015(A06).

UCB/EERC-87/01   "The FPS Earthquake Resisting System: Experimental Report," by Zayas, V.A., Low, S.S. and Mahin, S.A., June 1987, (PB88 170 287)A06.

UCB/EERC-87/02   "Earthquake Simulator Tests and Associated Studies of a 0.3-Scale Model of a Six-Story Eccentrically Braced Steel Structure," by Whittaker, A., Uang, C.-M. and Bertero, V.V., July 1987, (PB88 166 707/AS)A18.

UCB/EERC-87/03   "A Displacement Control and Uplift Restraint Device for Base-Isolated Structures," by Kelly, J.M., Griffith, M.C. and Aiken, I.D., April 1987, (PB88 169 933)A04.

UCB/EERC-87/04   "Earthquake Simulator Testing of a Combined Sliding Bearing and Rubber Bearing Isolation System," by Kelly, J.M. and Chalhoub, M.S., December 1990, PB92-192962(A09).

UCB/EERC-87/05   "Three-Dimensional Inelastic Analysis of Reinforced Concrete Frame-Wall Structures," by Moazzami, S. and Bertero, V.V., May 1987, (PB88 169 586/AS)A08.

UCB/EERC-87/06   "Experiments on Eccentrically Braced Frames with Composite Floors," by Ricles, J. and Popov, E., June 1987, (PB88 173 067/AS)A14.

UCB/EERC-87/07   "Dynamic Analysis of Seismically Resistant Eccentrically Braced Frames," by Ricles, J. and Popov, E., June 1987, (PB88 173 075/AS)A16.

UCB/EERC-87/08   "Undrained Cyclic Triaxial Testing of Gravels-The Effect of Membrane Compliance," by Evans, M.D. and Seed, H.B., July 1987, (PB88 173 257)A19.

245

UCB/EERC-87/09   "Hybrid Solution Techniques for Generalized Pseudo-Dynamic Testing," by Thewalt, C. and Mahin, S.A., July 1987, (PB 88 179 007)A07.

UCB/EERC-87/10   "Ultimate Behavior of Butt Welded Splices in Heavy Rolled Steel Sections," by Bruneau, M., Mahin, S.A. and Popov, E.P., September 1987, (PB90 254 285)A07.

UCB/EERC-87/11   "Residual Strength of Sand from Dam Failures in the Chilean Earthquake of March 3, 1985," by De Alba, P., Seed, H.B., Retamal, E. and Seed, R.B., September 1987, (PB88 174 321/AS)A03.

UCB/EERC-87/12   "Inelastic Seismic Response of Structures with Mass or Stiffness Eccentricities in Plan," by Bruneau, M. and Mahin, S.A., September 1987, (PB90 262 650/AS)A14.

UCB/EERC-87/13   "CSTRUCT: An Interactive Computer Environment for the Design and Analysis of Earthquake Resistant Steel Structures," by Austin, M.A., Mahin, S.A. and Pister, K.S., September 1987, (PB88 173 339/AS)A06.

UCB/EERC-87/14   "Experimental Study of Reinforced Concrete Columns Subjected to Multi-Axial Loading," by Low, S.S. and Moehle, J.P., September 1987, (PB88 174 347/AS)A07.

UCB/EERC-87/15   "Relationships between Soil Conditions and Earthquake Ground Motions in Mexico City in the Earthquake of Sept. 19, 1985," by Seed, H.B., Romo, M.P., Sun, J., Jaime, A. and Lysmer, J., October 1987, (PB88 178 991)A06.

UCB/EERC-87/16   "Experimental Study of Seismic Response of R. C. Setback Buildings," by Shahrooz, B.M. and Moehle, J.P., October 1987, (PB88 176 359)A16.

UCB/EERC-87/17   "The Effect of Slabs on the Flexural Behavior of Beams," by Pantazopoulou, S.J. and Moehle, J.P., October 1987, (PB90 262 700)A07.

UCB/EERC-87/18   "Design Procedure for R-FBI Bearings," by Mostaghel, N. and Kelly, J.M., November 1987, (PB90 262 718)A04.

UCB/EERC-87/19   "Analytical Models for Predicting the Lateral Response of R C Shear Walls: Evaluation of their Reliability," by Vulcano, A. and Bertero, V.V., November 1987, (PB88 178 983)A05.

UCB/EERC-87/20   "Earthquake Response of Torsionally-Coupled Buildings," by Hejal, R. and Chopra, A.K., December 1987, PB90-208638(A15).

UCB/EERC-87/21   "Dynamic Reservoir Interaction with Monticello Dam," by Clough, R.W., Ghanaat, Y. and Qiu, X-F., December 1987, (PB88 179 023)A07.

UCB/EERC-87/22   "Strength Evaluation of Coarse-Grained Soils," by Siddiqi, F.H., Seed, R.B., Chan, C.K., Seed, H.B. and Pyke, R.M., December 1987, (PB88 179 031)A04.

UCB/EERC-88/01   "Seismic Behavior of Concentrically Braced Steel Frames," by Khatib, I., Mahin, S.A. and Pister, K.S., January 1988, (PB91 210 898/AS)A11.

UCB/EERC-88/02   "Experimental Evaluation of Seismic Isolation of Medium-Rise Structures Subject to Uplift," by Griffith, M.C., Kelly, J.M., Coveney, V.A. and Koh, C.G., January 1988, (PB91 217 950/AS)A09.

UCB/EERC-88/03   "Cyclic Behavior of Steel Double Angle Connections," by Astaneh-Asl, A. and Nader, M.N., January 1988, (PB91 210 872)A05.

UCB/EERC-88/04   "Re-evaluation of the Slide in the Lower San Fernando Dam in the Earthquake of Feb. 9, 1971," by Seed, H.B., Seed, R.B., Harder, L.F. and Jong, H.-L., April 1988, (PB91 212 456/AS)A07.

UCB/EERC-88/05   "Experimental Evaluation of Seismic Isolation of a Nine-Story Braced Steel Frame Subject to Uplift," by Griffith, M.C., Kelly, J.M. and Aiken, I.D., May 1988, (PB91 217 968/AS)A07.

UCB/EERC-88/06   "DRAIN-2DX User Guide.," by Allahabadi, R. and Powell, G.H., March 1988, (PB91 212 530)A12.

UCB/EERC-88/07   "Theoretical and Experimental Studies of Cylindrical Water Tanks in Base-Isolated Structures," by Chalhoub, M.S. and Kelly, J.M., April 1988, (PB91 217 976/AS)A05.

UCB/EERC-88/08   "Analysis of Near-Source Waves: Separation of Wave Types Using Strong Motion Array Recording," by Darragh, R.B., June 1988, (PB91 212 621)A08.

UCB/EERC-88/09   "Alternatives to Standard Mode Superposition for Analysis of Non-Classically Damped Systems," by Kusainov, A.A. and Clough, R.W., June 1988, (PB91 217 992/AS)A04.

UCB/EERC-88/10   "The Landslide at the Port of Nice on October 16, 1979," by Seed, H.B., Seed, R.B., Schlosser, F., Blondeau, F. and Juran, I., June 1988, (PB91 210 914)A05.

UCB/EERC-88/11   "Liquefaction Potential of Sand Deposits Under Low Levels of Excitation," by Carter, D.P. and Seed, H.B., August 1988, (PB91 210 880)A15.

UCB/EERC-88/12   "Nonlinear Analysis of Reinforced Concrete Frames Under Cyclic Load Reversals," by Filippou, F.C. and Issa, A., September 1988, (PB91 212 589)A07.

UCB/EERC-88/13   "Implications of Recorded Earthquake Ground Motions on Seismic Design of Building Structures," by Uang, C.-M. and Bertero, V.V., November 1988, (PB91 212 548)A06.

UCB/EERC-88/14   "An Experimental Study of the Behavior of Dual Steel Systems," by Whittaker, A.S., Uang, C.-M. and Bertero, V.V., September 1988, (PB91 212 712)A16.

UCB/EERC-88/15   "Dynamic Moduli and Damping Ratios for Cohesive Soils," by Sun, J.I., Golesorkhi, R. and Seed, H.B., August 1988, (PB91 210 922)A04.

| UCB/EERC-88/16 | "Reinforced Concrete Flat Plates Under Lateral Load: An Experimental Study Including Biaxial Effects," by Pan, A. and Moehle, J.P., October 1988, (PB91 210 856)A13. |
| | |

UCB/EERC-88/16   "Reinforced Concrete Flat Plates Under Lateral Load: An Experimental Study Including Biaxial Effects," by Pan, A. and Moehle, J.P., October 1988, (PB91 210 856)A13.

UCB/EERC-88/17   "Earthquake Engineering Research at Berkeley - 1988," by EERC, November 1988, (PB91 210 864)A10.

UCB/EERC-88/18   "Use of Energy as a Design Criterion in Earthquake-Resistant Design," by Uang, C.-M. and Bertero, V.V., November 1988, (PB91 210 906/AS)A04.

UCB/EERC-88/19   "Steel Beam-Column Joints in Seismic Moment Resisting Frames," by Tsai, K.-C. and Popov, E.P., November 1988, (PB91 217 984/AS)A20.

UCB/EERC-88/20   "Base Isolation in Japan, 1988," by Kelly, J.M., December 1988, (PB91 212 449)A05.

UCB/EERC-89/01   "Behavior of Long Links in Eccentrically Braced Frames," by Engelhardt, M.D. and Popov, E.P., January 1989, (PB92 143 056)A18.

UCB/EERC-89/02   "Earthquake Simulator Testing of Steel Plate Added Damping and Stiffness Elements," by Whittaker, A., Bertero, V.V., Alonso, J. and Thompson, C., January 1989, (PB91 229 252/AS)A10.

UCB/EERC-89/03   "Implications of Site Effects in the Mexico City Earthquake of Sept. 19, 1985 for Earthquake-Resistant Design Criteria in the San Francisco Bay Area of California," by Seed, H.B. and Sun, J.I., March 1989, (PB91 229 369/AS)A07.

UCB/EERC-89/04   "Earthquake Analysis and Response of Intake-Outlet Towers," by Goyal, A. and Chopra, A.K., July 1989, (PB91 229 286/AS)A19.

UCB/EERC-89/05   "The 1985 Chile Earthquake: An Evaluation of Structural Requirements for Bearing Wall Buildings," by Wallace, J.W. and Moehle, J.P., July 1989, (PB91 218 008/AS)A13.

UCB/EERC-89/06   "Effects of Spatial Variation of Ground Motions on Large Multiply-Supported Structures," by Hao, H., July 1989, (PB91 229 161/AS)A08.

UCB/EERC-89/07   "EADAP - Enhanced Arch Dam Analysis Program: Users's Manual," by Ghanaat, Y. and Clough, R.W., August 1989, (PB91 212 522)A06.

UCB/EERC-89/08   "Seismic Performance of Steel Moment Frames Plastically Designed by Least Squares Stress Fields," by Ohi, K. and Mahin, S.A., August 1989, (PB91 212 597)A05.

UCB/EERC-89/09   "Feasibility and Performance Studies on Improving the Earthquake Resistance of New and Existing Buildings Using the Friction Pendulum System," by Zayas, V., Low, S., Mahin, S.A. and Bozzo, L., July 1989, (PB92 143 064)A14.

UCB/EERC-89/10   "Measurement and Elimination of Membrane Compliance Effects in Undrained Triaxial Testing," by Nicholson, P.G., Seed, R.B. and Anwar, H., September 1989, (PB92 139 641/AS)A13.

UCB/EERC-89/11   "Static Tilt Behavior of Unanchored Cylindrical Tanks," by Lau, D.T. and Clough, R.W., September 1989, (PB92 143 049)A10.

UCB/EERC-89/12   "ADAP-88: A Computer Program for Nonlinear Earthquake Analysis of Concrete Arch Dams," by Fenves, G.L., Mojtahedi, S. and Reimer, R.B., September 1989, (PB92 139 674/AS)A07.

UCB/EERC-89/13   "Mechanics of Low Shape Factor Elastomeric Seismic Isolation Bearings," by Aiken, I.D., Kelly, J.M. and Tajirian, F.F., November 1989, (PB92 139 732/AS)A09.

UCB/EERC-89/14   "Preliminary Report on the Seismological and Engineering Aspects of the October 17, 1989 Santa Cruz (Loma Prieta) Earthquake," by EERC, October 1989, (PB92 139 682/AS)A04.

UCB/EERC-89/15   "Experimental Studies of a Single Story Steel Structure Tested with Fixed, Semi-Rigid and Flexible Connections," by Nader, M.N. and Astaneh-Asl, A., August 1989, (PB91 229 211/AS)A10.

UCB/EERC-89/16   "Collapse of the Cypress Street Viaduct as a Result of the Loma Prieta Earthquake," by Nims, D.K., Miranda, E., Aiken, I.D., Whittaker, A.S. and Bertero, V.V., November 1989, (PB91 217 935/AS)A05.

UCB/EERC-90/01   "Mechanics of High-Shape Factor Elastomeric Seismic Isolation Bearings," by Kelly, J.M., Aiken, I.D. and Tajirian, F.F., March 1990.

UCB/EERC-90/02   "Javid's Paradox: The Influence of Preform on the Modes of Vibrating Beams," by Kelly, J.M., Sackman, J.L. and Javid, A., May 1990, (PB91 217 943/AS)A03.

UCB/EERC-90/03   "Earthquake Simulator Testing and Analytical Studies of Two Energy-Absorbing Systems for Multistory Structures," by Aiken, I.D. and Kelly, J.M., October 1990, (PB92 192 988)A13.

UCB/EERC-90/04   "Unassigned," by Unassigned, 1990.

UCB/EERC-90/05   "Preliminary Report on the Principal Geotechnical Aspects of the October 17, 1989 Loma Prieta Earthquake," by Seed, R.B., Dickenson, S.E., Riemer, M.F., Bray, J.D., Sitar, N., Mitchell, J.K., Idriss, I.M., Kayen, R.E., Kropp, A., Harder, L.F., Jr. and Power, M.S., April 1990, (PB 192 970)A08.

UCB/EERC-90/06   "Models of Critical Regions in Reinforced Concrete Frames Under Seismic Excitations," by Zulfiqar, N. and Filippou, F.C., May 1990.

UCB/EERC-90/07   "A Unified Earthquake-Resistant Design Method for Steel Frames Using ARMA Models," by Takewaki, I., Conte, J.P., Mahin, S.A. and Pister, K.S., June 1990, PB92-192947(A06).

UCB/EERC-90/08   "Soil Conditions and Earthquake Hazard Mitigation in the Marina District of San Francisco," by Mitchell, J.K., Masood, T., Kayen, R.E. and Seed, R.B., May 1990, (PB 193 267/AS)A04.

247

UCB/EERC-90/09   "Influence of the Earthquake Ground Motion Process and Structural Properties on Response Characteristics of Simple Structures," by Conte, J.P., Pister, K.S. and Mahin, S.A., July 1990, (PB92 143 064)A15.

UCB/EERC-90/10   "Experimental Testing of the Resilient-Friction Base Isolation System," by Clark, P.W. and Kelly, J.M., July 1990, (PB92 143 072)A08.

UCB/EERC-90/11   "Seismic Hazard Analysis: Improved Models, Uncertainties and Sensitivities," by Araya, R. and Der Kiureghian, A., March 1988, PB92-193010(A08).

UCB/EERC-90/12   "Effects of Torsion on the Linear and Nonlinear Seismic Response of Structures," by Sedarat, H. and Bertero, V.V., September 1989, (PB92 193 002/AS)A15.

UCB/EERC-90/13   "The Effects of Tectonic Movements on Stresses and Deformations in Earth Embankments," by Bray, J. D., Seed, R. B. and Seed, H. B., September 1989, PB92-192996(A18).

UCB/EERC-90/14   "Inelastic Seismic Response of One-Story, Asymmetric-Plan Systems," by Goel, R.K. and Chopra, A.K., October 1990, (PB93 114 767)A11.

UCB/EERC-90/15   "Dynamic Crack Propagation: A Model for Near-Field Ground Motion.," by Seyyedian, H. and Kelly, J.M., 1990.

UCB/EERC-90/16   "Sensitivity of Long-Period Response Spectra to System Initial Conditions," by Blasquez, R., Ventura, C. and Kelly, J.M., 1990.

UCB/EERC-90/17   "Behavior of Peak Values and Spectral Ordinates of Near-Source Strong Ground-Motion over a Dense Array," by Niazi, M., June 1990, (PB93 114 833)A07.

UCB/EERC-90/18   "Material Characterization of Elastomers used in Earthquake Base Isolation," by Papoulia, K.D. and Kelly, J.M., 1990, PB94-190063(A08).

UCB/EERC-90/19   "Cyclic Behavior of Steel Top-and-Bottom Plate Moment Connections," by Harriott, J.D. and Astaneh-Asl, A., August 1990, (PB91 229 260/AS)A05.

UCB/EERC-90/20   "Seismic Response Evaluation of an Instrumented Six Story Steel Building," by Shen, J.-H. and Astaneh-Asl, A., December 1990, (PB91 229 294/AS)A04.

UCB/EERC-90/21   "Observations and Implications of Tests on the Cypress Street Viaduct Test Structure," by Bollo, M., Mahin, S.A., Moehle, J.P., Stephen, R.M. and Qi, X., December 1990, (PB93 114 775)A13.

UCB/EERC-91/01   "Experimental Evaluation of Nitinol for Energy Dissipation in Structures," by Nims, D.K., Sasaki, K.K. and Kelly, J.M., 1991.

UCB/EERC-91/02   "Displacement Design Approach for Reinforced Concrete Structures Subjected to Earthquakes," by Qi, X. and Moehle, J.P., January 1991, (PB93 114 569/AS)A09.

UCB/EERC-91/03   "A Long-Period Isolation System Using Low-Modulus High-Damping Isolators for Nuclear Facilities at Soft-Soil Sites," by Kelly, J.M., March 1991, (PB93 114 577/AS)A10.

UCB/EERC-91/04   "Dynamic and Failure Characteristics of Bridgestone Isolation Bearings," by Kelly, J.M., April 1991, (PB93 114 528)A05.

UCB/EERC-91/05   "Base Sliding Response of Concrete Gravity Dams to Earthquakes," by Chopra, A.K. and Zhang, L., May 1991, (PB93 114 544/AS)A05.

UCB/EERC-91/06   "Computation of Spatially Varying Ground Motion and Foundation-Rock Impedance Matrices for Seismic Analysis of Arch Dams," by Zhang, L. and Chopra, A.K., May 1991, (PB93 114 825)A07.

UCB/EERC-91/07   "Estimation of Seismic Source Processes Using Strong Motion Array Data," by Chiou, S.-J., July 1991, (PB93 114 551/AS)A08.

UCB/EERC-91/08   "A Response Spectrum Method for Multiple-Support Seismic Excitations," by Der Kiureghian, A. and Neuenhofer, A., August 1991, (PB93 114 536)A04.

UCB/EERC-91/09   "A Preliminary Study on Energy Dissipating Cladding-to-Frame Connection," by Cohen, J.M. and Powell, G.H., September 1991, (PB93 114 510)A05.

UCB/EERC-91/10   "Evaluation of Seismic Performance of a Ten-Story RC Building During the Whittier Narrows Earthquake," by Miranda, E. and Bertero, V.V., October 1991, (PB93 114 783)A06.

UCB/EERC-91/11   "Seismic Performance of an Instrumented Six-Story Steel Building," by Anderson, J.C. and Bertero, V.V., November 1991, (PB93 114 809)A07.

UCB/EERC-91/12   "Performance of Improved Ground During the Loma Prieta Earthquake," by Mitchell, J.K. and Wentz, Jr., F.J., October 1991, (PB93 114 791)A06.

UCB/EERC-91/13   "Shaking Table - Structure Interaction," by Rinawi, A.M. and Clough, R.W., October 1991, (PB93 114 917)A13.

UCB/EERC-91/14   "Cyclic Response of RC Beam-Column Knee Joints: Test and Retrofit," by Mazzoni, S., Moehle, J.P. and Thewalt, C.R., October 1991, (PB93 120 277)A03.

UCB/EERC-91/15   "Design Guidelines for Ductility and Drift Limits: Review of State-of-the-Practice and State-of-the-Art in Ductility and Drift-Based Earthquake-Resistant Design of Buildings," by Bertero, V.V., Anderson, J.C., Krawinkler, H., Miranda, E. and The CUREe and The Kajima Research Teams, July 1991, (PB93 120 269)A08.

UCB/EERC-91/16   "Evaluation of the Seismic Performance of a Thirty-Story RC Building," by Anderson, J.C., Miranda, E., Bertero, V.V. and The Kajima Project Research Team, July 1991, (PB93 114 841)A12.

248

UCB/EERC-91/17   "A Fiber Beam-Column Element for Seismic Response Analysis of Reinforced Concrete Structures," by Taucer, F., Spacone, E. and Filippou, F.C., December 1991, (PB94 117 629AS)A07.

UCB/EERC-91/18   "Investigation of the Seismic Response of a Lightly-Damped Torsionally-Coupled Building," by Boroschek, R. and Mahin, S.A., December 1991, (PB93 120 335)A13.

UCB/EERC-92/01   "Studies of a 49-Story Instrumented Steel Structure Shaken During the Loma Prieta Earthquake," by Chen, C.-C., Bonowitz, D. and Astaneh-Asl, A., February 1992, (PB93 221 778)A08.

UCB/EERC-92/02   "Response of the Dumbarton Bridge in the Loma Prieta Earthquake," by Fenves, G.L., Filippou, F.C. and Sze, D.T., January 1992, (PB93 120 319)A09.

UCB/EERC-92/03   "Models for Nonlinear Earthquake Analysis of Brick Masonry Buildings," by Mengi, Y., McNiven, H.D. and Tanrikulu, A.K., March 1992, (PB93 120 293)A08.

UCB/EERC-92/04   "Shear Strength and Deformability of RC Bridge Columns Subjected to Inelastic Cyclic Displacements," by Aschheim, M. and Moehle, J.P., March 1992, (PB93 120 327)A06.

UCB/EERC-92/05   "Parameter Study of Joint Opening Effects on Earthquake Response of Arch Dams," by Fenves, G.L., Mojtahedi, S. and Reimer, R.B., April 1992, (PB93 120 301)A04.

UCB/EERC-92/06   "Seismic Behavior and Design of Semi-Rigid Steel Frames," by Nader, M.N. and Astaneh-Asl, A., May 1992, PB93-221760(A17).

UCB/EERC-92/07   "A Beam Element for Seismic Damage Analysis," by Spacone, E., Ciampi, V. and Filippou, F.C., August 1992, (PB95-192126)A06.

UCB/EERC-92/08   "Nonlinear Static and Dynamic Analysis of Reinforced Concrete Subassemblages," by Filippou, F.C., D'Ambrisi, A. and Issa, A., August 1992, PB95-192175(A09).

UCB/EERC-92/09   "Evaluation of Code Accidental-Torsion Provisions Using Earthquake Records from Three Nominally Symmetric-Plan Buildings," by De la Llera, J.C. and Chopra, A.K., September 1992, (PB94 117 611)A08.

UCB/EERC-92/10   "Slotted Bolted Connection Energy Dissipators," by Grigorian, C.E., Yang, T.-S. and Popov, E.P., July 1992, (PB92 120 285)A03.

UCB/EERC-92/11   "Mechanical Characteristics of Neoprene Isolation Bearings," by Kelly, J.M. and Quiroz, E., August 1992, (PB93 221 729)A07.

UCB/EERC-92/12   "Application of a Mass Damping System to Bridge Structures," by Hasegawa, K. and Kelly, J.M., August 1992, (PB93 221 786)A06.

UCB/EERC-92/13   "Earthquake Engineering Research at Berkeley - 1992," by EERC, October 1992, PB93-223709(A10).

UCB/EERC-92/14   "Earthquake Risk and Insurance," by Brillinger, D.R., October 1992, (PB93 223 352)A03.

UCB/EERC-92/15   "A Friction Mass Damper for Vibration Control," by Inaudi, J.A. and Kelly, J.M., October 1992, (PB93 221 745)A04.

UCB/EERC-92/16   "Tall Reinforced Concrete Buildings: Conceptual Earthquake-Resistant Design Methology," by Bertero, R.D. and Bertero, V.V., December 1992, (PB93 221 695)A12.

UCB/EERC-92/17   "Performance of Tall Buildings During the 1985 Mexico Earthquakes," by Terán-Gilmore, A. and Bertero, V.V., December 1992, (PB93 221 737)A11.

UCB/EERC-92/18   "Dynamic Analysis of Nonlinear Structures using State-Space Formulation and Partitioned Integration Schemes," by Inaudi, J.A. and De la Llera, J.C., December 1992, (PB94 117 702/AS/A05.

UCB/EERC-93/01   "Seismic Performance of an Instrumented Six-Story Reinforced-Concrete Building," by Anderson, J.C. and Bertero, V.V., 1993.

UCB/EERC-93/02   "Evaluation of an Active Variable-Damping-Structure," by Polak, E., Meeker, G., Yamada, K. and Kurata, N., 1993, (PB93 221 711)A05.

UCB/EERC-93/03   "An Experimental Study of Flat-Plate Structures under Vertical and Lateral Loads," by Hwang, S.-H. and Moehle, J.P., February 1993, (PB94 157 690/AS)A13.

UCB/EERC-93/04   "Seismic Performance of a 30-Story Building Located on Soft Soil and Designed According to UBC 1991," by Terán-Gilmore, A. and Bertero, V.V., 1993, (PB93 221 703)A17.

UCB/EERC-93/05   "Multiple-Support Response Spectrum Analysis of the Golden Gate Bridge," by Nakamura, Y., Der Kiureghian, A. and Liu, D., May 1993, (PB93 221 752)A05.

UCB/EERC-93/06   "On the Analysis of Structures with Viscoelastic Dampers," by Inaudi, J.A., Zambrano, A. and Kelly, J.M., August 1993, PB94-165867(A06).

UCB/EERC-93/07   "Earthquake Analysis and Response of Concrete Gravity Dams Including Base Sliding," by Chávez, J.W. and Fenves, G.L., December 1993, (PB94 157 658/AS)A10.

UCB/EERC-93/08   "Model for Anchored Reinforcing Bars under Seismic Excitations," by Monti, G., Spacone, E. and Filippou, F.C., December 1993, PB95-192183(A05).

UCB/EERC-93/09   "A Methodology for Design of Viscoelastic Dampers in Earthquake-Resistant Structures," by Abbas, H. and Kelly, J.M., November 1993, PB94-190071(A10).

UCB/EERC-93/10   "Tuned Mass Dampers Using Viscoelastic Dampers," by Inaudi, J.A., Lopez-Almansa, F. and Kelly, J.M., December 1993.

UCB/EERC-93/11 "Nonlinear Homogeneous Dynamical Systems," by Inaudi, J.A. and Kelly, J.M., December 1993.

UCB/EERC-93/12 "Synthesized Strong Ground Motions for the Seismic Condition Assessment of the Eastern Portion of the San Francisco Bay Bridge," by Bolt, B.A. and Gregor, N.J., December 1993, PB94-165842(A10).

UCB/EERC-93/13 "On the Analysis of Structures with Energy Dissipating Restraints," by Inaudi, J.A., Nims, D.K. and Kelly, J.M., December 1993, PB94-203619(A07).

UCB/EERC-94/01 "Preliminary Report on the Seismological and Engineering Aspects of the January 17, 1994 Northridge Earthquake," by EERC, January 1994, (PB94 157 666/AS)A05.

UCB/EERC-94/02 "Energy Dissipation with Slotted Bolted Connections," by Grigorian, C.E. and Popov, E.P., February 1994, PB94-164605.

UCB/EERC-94/03 "The Influence of Plate Flexibility on the Buckling Load of Elastomeric Isolators," by Kelly, J.M., March 1994, PB95-192134(A04).

UCB/EERC-94/04 "Insitu Test Results from Four Loma Prieta Earthquake Liquefaction Sites: SPT, CPT, DMT and Shear Wave Velocity," by Mitchell, J.K., Lodge, A.L., Coutinho, R.Q., Kayen, R.E., Seed, R.B., Nishio, S. and Stokoe II, K.H., April 1994, PB94-190089(A09).

UCB/EERC-94/05 "Seismic Response of Steep Natural Slopes," by Sitar, N. and Ashford, S.A., May 1994, PB94-203643(A10).

UCB/EERC-94/06 "Small-Scale Testing of a Self-Centering Friction Energy Dissipator for Structures," by Nims, D.K. and Kelly, J.M., August 1994.

UCB/EERC-94/07 "Accidental and Natural Torsion in Earthquake Response and Design of Buildings," by De la Llera, J.C. and Chopra, A.K., June 1994, PB94-203627(A14).

UCB/EERC-94/08 "Preliminary Report on the Principal Geotechnical Aspects of the January 17, 1994 Northridge Earthquake," by Stewart, J.P., Bray, J.D., Seed, R.B. and Sitar, N., June 1994, PB94203635(A12).

UCB/EERC-94/09 "Performance of Steel Building Structures During the Northridge Earthquake," by Bertero, V.V., Anderson, J.C. and Krawinkler, H., August 1994, PB95-112025(A10).

UCB/EERC-94/10 "Manual for Menshin Design of Highway Bridges: Ministry of Construction, Japan," by Sugita, H. and Mahin, S., August 1994, PB95-192100(A08).

UCB/EERC-94/11 "Earthquake Analysis and Response of Two-Level Viaducts," by Singh, S.P. and Fenves, G.L., October 1994, (A09).

UCB/EERC-94/12 "Response of the Northwest Connector in the Landers and Big Bear Earthquakes," by Fenves, G.L. and Desroches, R., December 1994, PB95-192001(A08).

UCB/EERC-95/01 "Geotechnical Reconnaissance of the Effects of the January 17, 1995, Hyogoken-Nanbu Earthquake, Japan," by , August 1995.

UCB/EERC-95/02 "The Attenuation of Strong Ground Motion Displacement," by Gregor, N.J., June 1995.

UCB/EERC-95/03 "Upgrading Bridge Outrigger Knee Joint Systems," by Stojadinovic, B. and Thewalt, C.R., June 1995.

UCB/EERC-95/04 "Earthquake Hazard Reduction in Historical Buildings Using Seismic Isolation," by Garevski, M., June 1995.

UCB/EERC-95/05 "Final Report on the International Workshop on the Use of Rubber-Based Bearings for the Earthquake Protection of Building," by Kelly, J.M., May 1995.

UCB/EERC-95/06 "Seismic Rehabilitation of Framed Buildings Infilled with Unreinforced Masonry Walls Using Post-Tensioned Steel Braces," by Terán-Gilmore, A., Bertero, V.V. and Youssef, N., June 1995.

UCB/EERC-95/07 "Earthquake Analysis and Response of Concrete Arch Dams," by Tan, H. and Chopra, A.K., August 1995.

UCB/EERC-95/08 "Behavior of Pre-Northridge Moment Resisting Steel Connections," by Yang, T.-S. and Popov, E.P., August 1995.

UCB/EERC-95/09 "Seismic Behavior and Retrofit of Older Reinforced Concrete Bridge T-Joints," by Lowes, L.N. and Moehle, J.P., September 1995.

UCB/EERC-95/10 "Seismological and Engineering Aspects of the 1995 Hyogoken-Nanbu (Kobe) Earthquake," by EERC, November 1995.

Reproduced by NTIS

National Technical Information Service
Springfield, VA 22161

*This report was printed specifically for your order
from nearly 3 million titles available in our collection.*

For economy and efficiency, NTIS does not maintain stock of its vast collection of technical reports. Rather, most documents are printed for each order. Documents that are not in electronic format are reproduced from master archival copies and are the best possible reproductions available. If you have any questions concerning this document or any order you have placed with NTIS, please call our Customer Service Department at (703) 487-4660.

About NTIS

NTIS collects scientific, technical, engineering, and business related information — then organizes, maintains, and disseminates that information in a variety of formats — from microfiche to online services. The NTIS collection of nearly 3 million titles includes reports describing research conducted or sponsored by federal agencies and their contractors; statistical and business information; U.S. military publications; audiovisual products; computer software and electronic databases developed by federal agencies; training tools; and technical reports prepared by research organizations worldwide. Approximately 100,000 *new* titles are added and indexed into the NTIS collection annually.

For more information about NTIS products and services, call NTIS at (703) 487-4650 and request the free *NTIS Catalog of Products and Services*, PR-827LPG, or visit the NTIS Web site
http://www.ntis.gov.

NTIS
*Your indispensable resource for government-sponsored
information—U.S. and worldwide*
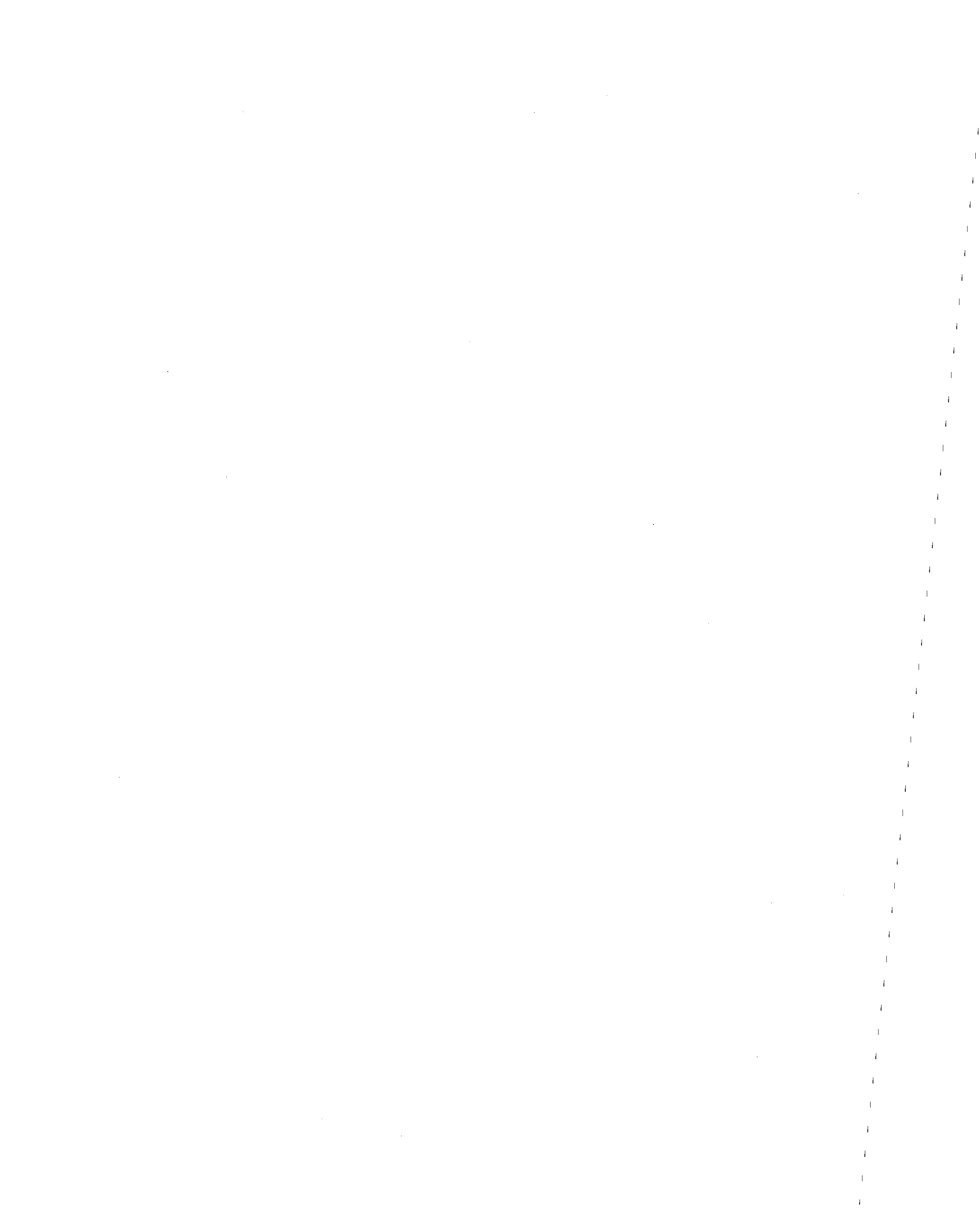
U.S. DEPARTMENT OF COMMERCE
Technology Administration
National Technical Information Service
Springfield, VA 22161   (703) 487-4650